Journal of Medicinal Chemistry

pubs.acs.org/jmc Article

Potent Antimalarials with Development Potential Identified by Structure-Guided Computational Optimization of a Pyrrole-Based Dihydroorotate Dehydrogenase Inhibitor Series

Michael J. Palmer, Xiaoyi Deng, Shawn Watts, Goran Krilov, Aleksey Gerasyuto, Sreekanth Kokkonda, Farah El Mazouni, John White, Karen L. White, Josefine Striepen, Jade Bath, Kyra A. Schindler, Tomas Yeo, David M. Shackleford, Sachel Mok, Ioanna Deni, Aloysus Lawong, Ann Huang, Gong Chen, Wen Wang, Jaya Jayaseelan, Kasiram Katneni, Rahul Patil, Jessica Saunders, Shatrughan P. Shahi, Rajesh Chittimalla, Iñigo Angulo-Barturen, María Belén Jiménez-Díaz, Sergio Wittlin, Patrick K. Tumwebaze, Philip J. Rosenthal, Roland A. Cooper, Anna Caroline Campos Aguiar, Rafael V. C. Guido, Dhelio B. Pereira, Nimisha Mittal, Elizabeth A. Winzeler, Diana R. Tomchick, Benoît Laleu, Jeremy N. Burrows, Pradipsinh K. Rathod, David A. Fidock, Susan A. Charman, and Margaret A. Phillips*

Cite This: *J. Med. Chem.* 2021, 64, 6085−6136 Read Online

ACCESS | Metrics & More | Article Recommendations | Supporting Information

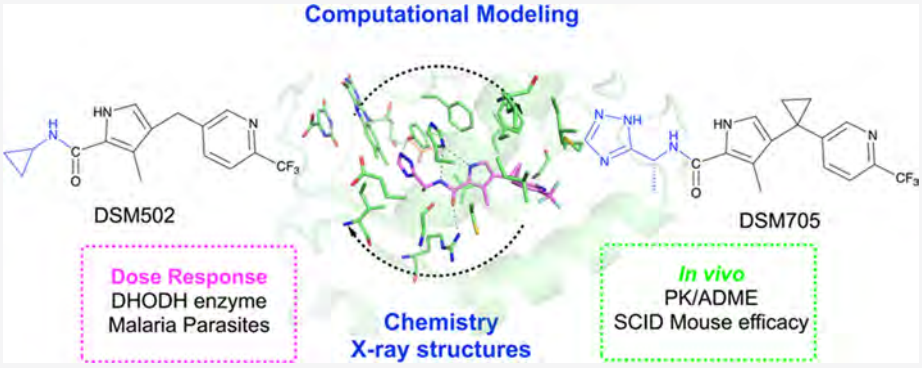

ABSTRACT: Dihydroorotate dehydrogenase (DHODH) has been clinically validated as a target for the development of new antimalarials. Experience with clinical candidate triazolopyrimidine DSM265 (**1**) suggested that DHODH inhibitors have great potential for use in prophylaxis, which represents an unmet need in the malaria drug discovery portfolio for endemic countries, particularly in areas of high transmission in Africa. We describe a structure-based computationally driven lead optimization program of a pyrrole-based series of DHODH inhibitors, leading to the discovery of two candidates for potential advancement to preclinical development. These compounds have improved physicochemical properties over prior series frontrunners and they show no time-dependent CYP inhibition, characteristic of earlier compounds. Frontrunners have potent antimalarial activity *in vitro* against blood and liver schizont stages and show good efficacy in *Plasmodium falciparum* SCID mouse models. They are equally active against *P. falciparum* and *Plasmodium vivax* field isolates and are selective for *Plasmodium* DHODHs versus mammalian enzymes.

INTRODUCTION

Malaria is one of the most widespread and ancient infectious diseases of humanity.[1] Five species of the single-celled eukaryote *Plasmodium* genus are responsible for the disease. *Plasmodium falciparum* causes the most deaths, while *Plasmodium vivax* has a wider global distribution and a dormant liver stage that can reactivate years after the primary infection. Despite the strong implementation of malaria control programs, progress toward reducing the global incidence of malaria and deaths has stalled in recent years.[2] Malaria, which is transmitted by the *Anopheles* mosquito causes a febrile illness, the severity of which depends on both the *Plasmodium* species and host factors such as immunity. In 2020, the World Health Organization estimated

Received: January 30, 2021
Published: April 20, 2021

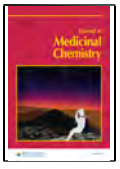

https://doi.org/10.1021/acs.jmedchem.1c00173
J. Med. Chem. 2021, 64, 6085−6136

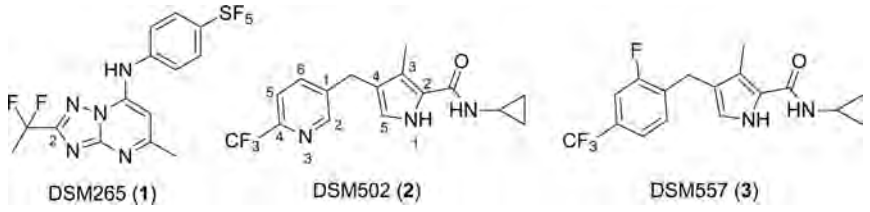

Figure 1. *P. falciparum* DHODH inhibitors from the triazolopyrimidine (**1**)[15] and pyrrole (**2**, **3**)[20] structural classes.

that malaria infected 229 million people worldwide, 93% in Africa, leading to over 0.4 million deaths, of which two-thirds were children under 5 years old.[2]

Malaria control and prevention has relied on drug therapy and vector control. A wide range of effective antimalarials has been used clinically; however, resistance to robust therapies such as chloroquine left a gap in treatment options until the discovery of the current gold standard two-drug artemisinin-based combination therapies (ACTs).[1,3] Emergence of ACT treatment failures in the Greater Mekong subregion has raised concerns that resistance to all ACTs could jeopardize malaria control programs.[4,5] These failures are in part associated with mutations in Kelch13, which cause a delayed parasite clearance time after treatment with artemisinins.[4−6] Fueled by the reduced activity of artemisinins, resistance to partner compounds, particularly piperaquine, has also emerged in southeast Asia.[7] However, artemether-lumefantrine and pyronaridine-artesunate currently remain efficacious in all regions. Efforts to validate triple-drug ACTs are underway to combat resistance until drugs with novel mechanisms of action can be deployed.[8,9]

In the past decade, a number of high-throughput screening campaigns against either intraerythrocytic parasites or *P. falciparum* enzymes have led to the identification of several novel chemical entities that reached clinical development and to the validation of a number of new parasite targets providing different mechanisms of action from previously used antimalarials.[1,10] The most advanced of these include two compounds in late-stage Phase II clinical studies: KAF156 (combination therapy with lumefantrine) for uncomplicated malaria[11,12] and spiroindolone KAE609, a fast-acting ATP4 inhibitor being developed for severe malaria.[3,13] Additional candidates to reach Phase II clinical development include the pyrimidine biosynthetic enzyme dihydroorotate dehydrogenase (DHODH) inhibitor DSM265 (**1**)[14,15] (Figure 1) and the PI4 kinase inhibitor MMV390048.[16] These Phase II development candidates have been instrumental in work to develop new strategies and assays to support malaria drug discovery programs.[17] These include the policy to introduce drugs as combinations to combat resistance and the desirability of targeting all *Plasmodium* species[18] and life cycle stages (blood, liver, and sexual stages).[1] While many new candidates have been advanced for malaria treatment, with the exception of tafenoquine (primarily developed to prevent relapse of dormant stages of *P. vivax* and *Plasmodium ovale*),[19] no new prophylaxis compounds have reached advanced clinical development since atovaquone/proguanil more than 20 years ago. The goal of current programs would be to deliver a candidate that could ideally be dosed orally as infrequently as once monthly and, at a minimum, no more frequently than weekly and that would have acceptable tolerability and a low cost of goods.[1,17]

Through our work on **1**, DHODH emerged as a strong target for malaria prophylaxis. In human Phase IIa clinical studies, **1**, which has a long human half-life,[21] was able to provide single-dose cures of *P. falciparum* malaria in patients in Peru.[22] However, it showed lower efficacy against *P. vivax*, and resistant parasites that mapped to mutations in DHODH were identified in two relapsing *P. falciparum* patients. Importantly, **1** has both potent blood and liver-stage antischizontal activity,[15,23] which supports the use of DHODH inhibitors for prophylaxis and provides superiority over compounds with only blood-stage activity for this indication. Human sporozoite challenge studies showed that **1** prevented the emergence of *P. falciparum* infection if dosed a day prior to infection, providing a clinical proof of concept supporting the DHODH target for this indication.[24,25] Despite its good efficacy, **1** was shown to be both teratogenic and to result in testicular toxicity in certain preclinical species (unpublished) and thus was unable to meet the safety bar required for continued clinical development, particularly for use as a prophylactic over months during the transmission season in Africa, or in pregnant women. While clinical development of **1** has been terminated, the clinical data obtained on **1** has validated DHODH as a strong target for malaria prophylaxis.

As the current clinical malaria portfolio now lacks a DHODH inhibitor, there is strong justification to identify new DHODH inhibitors from a different chemical class that will combine the good efficacy of **1** with a safety profile that can support its development. Importantly, there are no current drugs in use for malaria treatment that inhibit DHODH, which supports a strategy where different drugs will be used for treatment than for prophylaxis. This strategy mitigates the risk that resistance will be selected during treatment and then compromise the prophylactic indication where the low parasite burden presents a low risk for resistance to develop. Furthermore, DHODH is a well-characterized target, and the ability to directly test compounds for mammalian DHODH inhibition provides a mechanism to ensure that any selected clinical candidate does not inhibit DHODH, thus, dramatically reducing the risk of mechanism-based toxicity.

With the goal of identifying a new compound that could move forward to clinical development for malaria prophylaxis, we continued lead optimization of a pyrrole series of DHODH inhibitors that we previously reported had potent DHODH and *P. falciparum* inhibitory activity.[20] The strongest candidate to emerge from the earlier work, **2** (Figure 1), showed *in vivo* efficacy in the *P. falciparum* SCID mouse model but was less potent than **1**, it was predicted to have a shorter human half-life based on reduced metabolic stability, and it was a time-dependent CYP inhibitor raising potential safety concerns. To improve the properties of this series, we expanded our lead optimization program to include structure-based computational methods. Through this effort, we report herein on compounds with improved potency, better physicochemical properties, and for which we have eliminated the liability of time-dependent CYP inhibition. These next-generation pyrroles retain the desirable properties of **2**, including strong species selectivity

https://doi.org/10.1021/acs.jmedchem.1c00173
J. Med. Chem. 2021, 64, 6085−6136

against mammalian enzymes, equivalent and potent activity against both *P. falciparum* and *P. vivax* parasites, activity on both blood and liver stages blocking schizont formation, and good *in vivo* activity in SCID mouse models.

RESULTS

The goals of our pyrrole lead optimization program were to improve the properties of **2**[20] by identifying compounds with greater potency versus *P. falciparum* parasites, to achieve better metabolic stability and plasma exposure profiles that would be consistent with a frequency of no more than weekly dosing for prophylaxis, and to eliminate the risk of time-dependent CYP inhibition. Identified liabilities in **1** included inhibition of rodent DHODH, which complicated the development by making it more difficult to determine whether toxicities associated with **1** in preclinical rodent studies were due to on- or off-target effects, and poor solubility that required complex and costly formulations to obtain good oral bioavailablility.[15] Thus, based on our experience with **1**,[15] we sought to identify compounds with good solubility to enable simple formulation approaches while maintaining strong species selectivity against mammalian enzymes.

Computational Approaches to Compound Design. Focusing on potency as the initial goal, X-ray structures of DHODH bound to previously described pyrroles[20] were used as a starting point for computational predictions as detailed in the Experimental Section. We sought first to explore the potential to replace either the benzyl group or the cyclopropylamide with more potent substituents. To that end, programmatically enumerated libraries of commercially available precursors (eMolecules Building Blocks 2015) were docked with WScore into the binding site and WaterMap was used to assess areas of the binding pocket where potency gains could be made through the displacement of water molecules. Docked compounds providing the best scores were then analyzed using the free-energy perturbation (FEP+) method to predict *Pf*DHODH potency (Supporting Information Tables S1 and S2). A selection of previously reported pyrrole-based DHODH inhibitors[20] were studied to test the accuracy of predictions (retrospective validation) and refine the models (Figure 2A and Supporting Information Table S1 and S2). This work was aided by new X-ray structures as they became available, which were used to refine predictions during the course of the program. In total, 7 new pyrrole analogue-*Pf*DHODH structures were solved and are reported herein (Supporting Information Table S3 and Figures S1 and S2). The computational modeling effort supported the prioritization of compounds for synthesis (Tables 1−7).

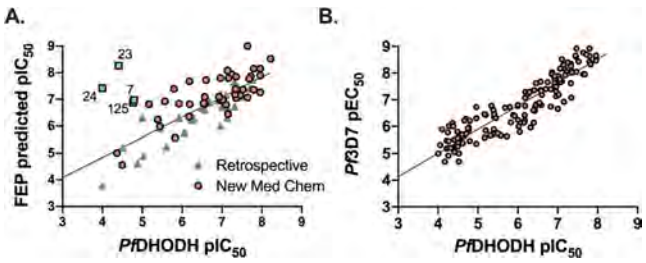

Figure 2. Structure−activity relationships. (A) Correlation between FEP+ predicted and measured *Pf*DHODH pIC_{50} values. Retrospective analysis of previously reported pyrrole-based compounds used as a validation set to test predictions are shown as light green triangles and compounds from this paper are shown as red circles. Both sets were included in the linear regression analysis (R^2 = 0.58). Outliers (shown as green squares) with their compound ID displayed were not included in the regression analysis. Data are provided in Supporting Information Tables S1 and S2. (B) Correlation between *Pf*DHODH pIC_{50} values and *P. falciparum* 3D7 cell pEC_{50} values. All data were included in the regression analysis (R^2 = 0.84). Data were taken from Tables 1−7.

Compounds were synthesized based on our previously described strategies,[20] with modifications as detailed in Schemes 1−8 and Supporting Information Schemes S1−S10. Compounds were first evaluated for activity against recombinant DHODH from *P. falciparum* (*Pf*DHODH) (IC_{50} < 0.03 μM) and *P. vivax* (*Pv*DHODH) (IC_{50} < 0.03 μM), for selectivity versus human DHODH (*h*DHODH) (IC_{50} > 30 μM) and for efficacy against *P. falciparum* 3D7 asexual blood stage (EC_{50} < 0.015 μM), with our target values for an optimized late lead shown in parentheses (Tables 1−7). Liver-stage assays were conducted later in the program because of their more limited availability. Compounds with good potency in enzyme and parasite assays were tested in human and mouse liver microsomes to assess metabolic stability and kinetic solubility at pH 6.5 to reflect the approximate pH of the upper small intestine in the fasted state (Supporting Information Table S4A). Our target for *in vitro* intrinsic clearance (CL_{int}) was <10 μL/min/mg microsomal protein, as experience suggested this level of stability would be required to translate to a sufficiently long half-life to support clinical development in humans. Compounds with the best combined properties were advanced to more detailed pharmacologic assays, pharmacokinetic studies, and additional parasitology.

Chemistry: Compound Synthesis and Structure−Activity Relationships (SARs) of Pyrrole-Based Compounds Versus DHODH and *P. falciparum* 3D7. *Nonchiral Amide and Benzyl Variations.* A series of analogues (**4**−**21**) that varied either the amide or benzyl group were synthesized primarily as shown in Scheme 1, plus variations as shown in Scheme 2 and Supporting Information Schemes S1, S2, and S4. The chemistry detailed in Scheme 1 and Supporting Information Schemes S1 and S2 constructed the pyrrole from a but-2-yn-1-one intermediate, Scheme 2 used a Weinreb amide variation to access the but-2-yn-1-one, and S4 used Friedel−Crafts methodology. A small set of nonchiral cyclic amides (**4**−**6**) were also made to further probe the cyclopropylamide binding pocket, with the addition of an ether linkage expected to improve on the poor potency of prior 4−6-membered cyclic rings in this position.[20] Additionally, we tested the ability of linker methylene to improve the geometry of a pyrazole ring (**7**) in this position and to promote binding. With the exception of the 3-methyloxetane **4**, all of the remaining compounds (**5**−**7**) had poor activity (Table 1).

Benzyl replacements added either an ortho fluoro to the 4-CF_3-pyridinyl ring (**8**−**10**), replaced the 4-CF_3 with S(O_2)N-($Me)_2$ (**11**), or replaced 4-CF_3-pyridinyl with isoquinoline (**12**−**17**) or benzoxazole (**18**−**21**) heteroatom aromatic ring systems, as several of these compounds were predicted to improve potency to <0.01 μM based on FEP+ calculation (Supporting Information Table S2). The 4-CF_3,2-F-pyridinyls and isoquinolines were made in the context of the cyclopropylamide, CH_2CF_3, or difluoroazetidine, all groups were previously shown to exhibit good activity in this position.[20] The addition of ortho F improved potency versus *P. falciparum* 3D7 by up to 6-fold (**8** and **10** versus **2**), while replacement of 4-CF_3 with S(O_2)N-($Me)_2$ (**11**) led to a 5−10-fold reduction in potency against

https://doi.org/10.1021/acs.jmedchem.1c00173
J. Med. Chem. 2021, 64, 6085−6136

Scheme 1

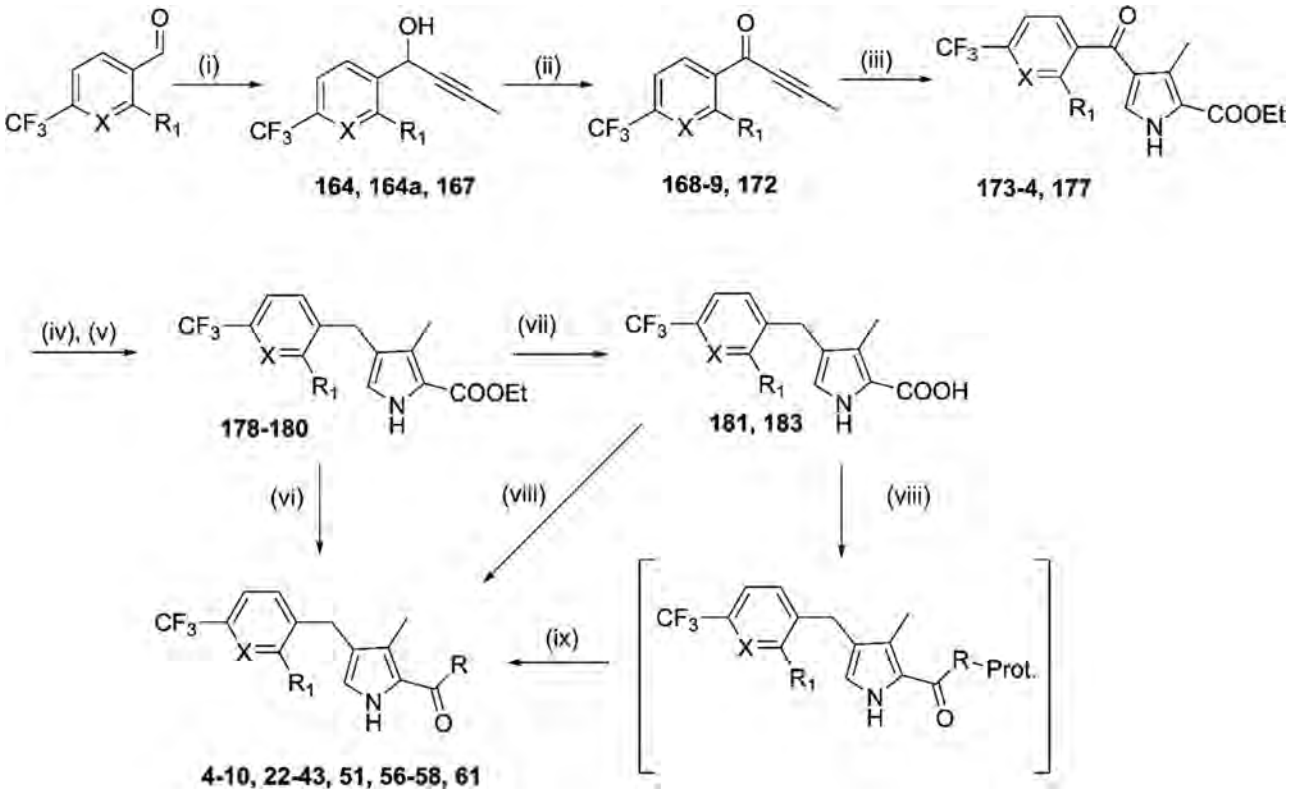

[a]Reagents and conditions: (i) 1-propynylmagnesium bromide, tetrahydrofuran (THF), 0 °C−room temperature (RT), 2−6 h; (ii) Dess−Martin, CH_2CI_2, RT, 2−4 h; (iii) ethyl isocyanoacetate, Ag_2CO_3, *N*-methyl-2-pyrrolidinone (NMP), 80 °C, 3−6 h; (iv) $NaBH_4$, EtOH, 0 °C−RT, 1 h; (v) trifluoroacetic acid (TFA), triethylsilane, CH_2CI_2, 50 °C, 1 h; (vi) amine, Me_3AI, THF, MW, 100 °C, 1 h; (vii) NaOH, EtOH, RT−80 °C, 2 h; (viii) amine, HATU, Et_3N, CH_2CI_2, RT, 4 h; (ix) TFA, triethylsilane, CH_2CI_2, RT, 1 h or amine, Me_3AI, THF, MW, 100 °C, 1 h or TBAF, THF, RT, 2 h.

Scheme 2

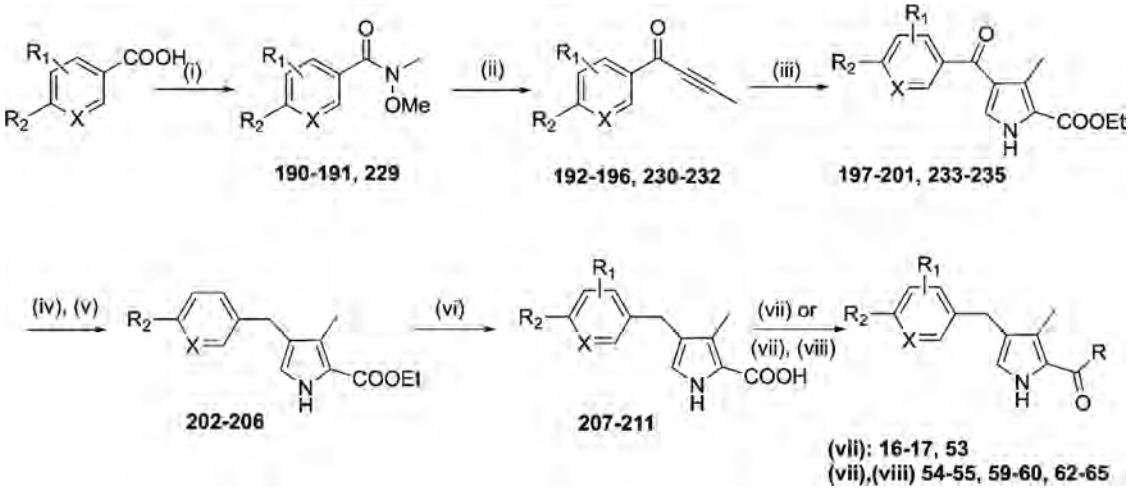

[a]Reagents and conditions: (i) CDI, *N*,*O*-dimethylhydroxylamine·HCl, DMF, 5 h; (ii) 1-propynylmagnesium bromide, THF, 0 °C−RT, 2 h; (iii) ethyl isocyanoacetate, Ag_2CO_3, NMP, RT−80 °C, 2 h; (iv) $NaBH_4$, EtOH, 0 °C−RT, 1 h; (v) TFA, triethylsilane, CH_2CI_2, 0 °C, 1 h; (vi) NaOH, EtOH/H_2O, RT−80 °C, 2 h; (vii) amine, HATU, Et_3N, CH_2CI_2, RT, 4 h; and (viii) TFA, triethylsilane, CH_2CI_2, RT, 1 h.

*Pf*DHODH and *Pf*3D7-infected cells relative to **2** (Table 1). The isoquinolines had excellent potency as predicted by FEP+; the best analogue **16** contained a cyclopropylamide and showed a potency boost against *Pf*3D7 of 15-fold relative to **2**. With sub-nM activity, this compound was the most potent in the pyrrole series (Table 1). The synthesis of the benzoxazoles was challenging and those with the preferred 7-methyl linkage could only be made in the context of an ethylester (**18**−**20**), and while **18** was potent it would not be expected to be metabolically stable. The 2-methyl linkage (**21**) could be made as an amide but lacked potency.

https://doi.org/10.1021/acs.jmedchem.1c00173
J. Med. Chem. 2021, 64, 6085−6136

Table 1. Nonchiral Amide and Benzyl Variations

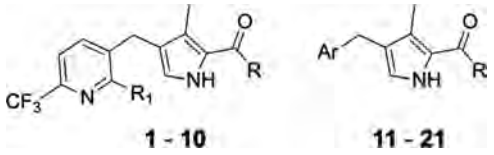

cmpd	cmpd ID	R	R1 or Ar	IC_{50} (μM)			EC_{50} (μM)
				*Pf*DHODH	*Pv*DHODH	*h*DHODH	*Pf*3D7
1	DSM265	NA	NA	0.030*	0.072*	>100*	0.0060*
2	DSM502	NA	NA	0.020*	0.014*	>100*	0.014*
3	DSM557	NA	NA	0.044*	0.015*	>100*	0.016*
4	DSM582	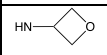	H	0.11	nd	nd	0.074
5	DSM586	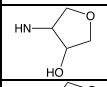	H	61	nd	nd	6.4
6	DSM594	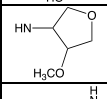	H	17	nd	nd	1.1 (0.9-1.3)
7	DSM595	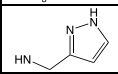	H	17	nd	nd	1.4
8	DSM580		F	0.011	0.0054	>100	0.0031
9	DSM592	$NHCH_2CF_3$	F	0.079	0.053	>100	0.020
10	DSM593	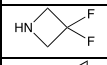	F	0.016	0.012	>100	0.0026 ± 0.00042 (2)
11	DSM600		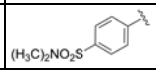	1.5	nd	nd	0.70
12	DSM601		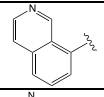	0.011	0.016	>100	0.0022
13	DSM611	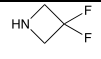	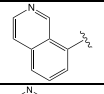	0.016	0.0077	>100	0.0038 ± 0.0025 (2)
14	DSM612	$NHCH_2CF_3$		0.035	0.017	>100	0.0096 ± 0.0091 (2)
15	DSM618		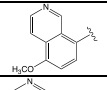	0.023	0.021	>50	0.0017
16	DSM623			0.0061	0.0040	>100	0.00092 ± 0.00029 (3)
17	DSM624	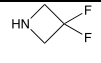	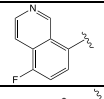	0.011	0.0065	>100	0.0034 ± 0.00085 (2)
18	DSM589	OEt	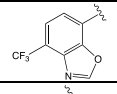	0.047	0.016	>100	0.024
19	DSM572	OEt		0.10	0.013	>100	0.22
20	DSM568	OEt		0.90	nd	>100	1.6
21	DSM569		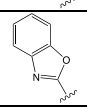	0.67	nd	>100	0.60

[a]*Pf*, *P. falciparum*; *Pv*, *P. vivax*; and *h*, human. Triplicate data were collected at each inhibitor concentration (3-fold dilution series for DHODH and 3−4-fold series for 3D7) for each EC_{50} or IC_{50} determination. Multiple biological replicates were performed for key compounds, and for these studies, data represent mean ± standard deviation with the number of independent experiments in parenthesis. *Data were taken from ref 20 and included in the table.

https://doi.org/10.1021/acs.jmedchem.1c00173
J. Med. Chem. 2021, 64, 6085−6136

Table 2. Chiral Amides

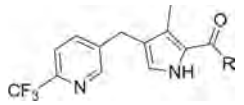

	Cmpd ID	stereo chem	R	IC_{50} (μM)			EC_{50} (μM)
				*Pf*DHODH	*Pv*DHODH	*h*DHODH	*Pf*3D7
22	DSM583	NA		2.7	nd	nd	2.1
23	DSM587	NA		39	nd	nd	8.9
24	DSM588	NA		>100	nd	nd	>10
25	DSM590	rac		0.034	0.030	>100	0.0090
26	DSM597	*ent1*	as above	0.020 ± 0.010 (7)	0.0072 ± 0.0068 (2)	>100	0.0093 ± 0.0047 (8)
27	DSM598	*ent2*	as above	3.9	nd	nd	0.45
28	DSM596	rac		0.27	nd	nd	0.043
29	DSM606	rac		0.26	0.12	>100	0.16
30	DSM690	*ent1*	as above	0.25	0.11	>100	0.066
31	DSM691	*ent2*	as above	>100	nd	nd	16
32	DSM607	rac		0.061	0.048	>100	0.0090 ± 0.0028 (2)
33	DSM629	*ent1*	as above	0.047 ± 0.0079 (5)	0.043	>100	0.0045 ± 0.00071 (2)
34	DSM630	*ent2*	as above	6.4	nd	nd	0.37
35	DSM608	rac		0.047	0.062	>100	0.0055 ± 0.0013 (3)
36	DSM632	*ent1*	as above	0.046 ± 0.0061 (6)	0.039 ± 0.0035 (2)	>100	0.0082 ± 0.0067 (3)
37	DSM633	*ent2*	as above	6.8	nd	nd	0.35
38	DSM628	rac		4.0	nd	nd	1.3 ± 0.0 (2)
39	DSM667	rac		0.37	0.10	>100	0.19
40	DSM739	rac		0.68 ± 0.18 (2)	0.32	>100	0.38 ± 0.24 (3)
41	DSM740	rac		1.3 ± 0.46 (2)	0.5	>100	0.38 ± 0.22 (2)
42	DSM756	*ent1*		0.10 ± 0.036 (2)	0.069	>100	0.020 ± 0.0057 (5)
43	DSM757	*ent2*	as above	68	nd	nd	>10 (3)
44	DSM760	*ent1*		0.12 ± 0.033 (3)	0.083	>100	0.017 ± 0.0074 (6)
45	DSM761	*ent2*	as above	54 ± 11 (2)	nd	nd	6.1 ± 2.5 (3)
46	DSM758	rac		0.65	0.43	>100	0.051 ± 0.036 (3)
47	DSM784	*ent1*	as above	0.35 ± 0.028 (2)	0.23	>100	0.024 ± 0.017 (5)
48	DSM785	*ent2*	as above	33 ± 9.9 (2)	nd	nd	1.6
49	DSM893	*ent1*		1.0	nd	nd	0.17
50	DSM894	*ent2*	as above	89	nd	nd	4.8
51	DSM764	rac		0.070	0.020	>100	0.12

[a]Rac, racemic; ent1, enantiomer 1; and ent2, enantiomer 2. See Table 1 footnote for other abbreviations and error analysis information.

Despite showing reasonably low Log $D_{7.4}$ values (<3.4), none of the highly potent isoquinoline compounds (**12**−**17**) from Table 1 had good metabolic stability (Supporting Information Table S4A). Compounds containing an ortho fluoro to the 4-

https://doi.org/10.1021/acs.jmedchem.1c00173
J. Med. Chem. 2021, 64, 6085−6136

Table 3. Chiral Amides with Variation of the Aryl group

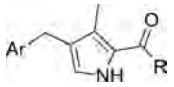

Cmpd	Cmpd ID	stereo chem	R	Ar	IC_{50} (μM)			EC_{50} (μM)
					*Pf*DHODH	*Pv*DHODH	*h*DHODH	*Pf*3D7
52	DSM617	rac	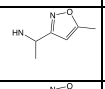	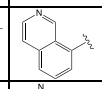	0.030	0.021	>100	0.0037
53	DSM625	rac	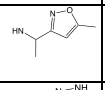	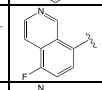	0.036	0.048	>100	0.0022 ± 0.00021 (2)
54	DSM832	*ent1*	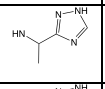	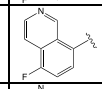	0.044	0.029	>100	0.0095 ± 0.0021 (2)
55	DSM833	*ent2*	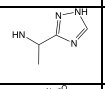	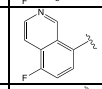	23	nd	nd	2.3
56	DSM634	*ent1*	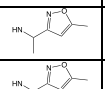	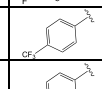	0.046	0.013	>100	0.17 ± 0.042 (2)
57	DSM635	*ent2*	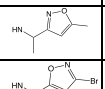	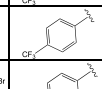	48	nd	nd	6.2
58	DSM765	rac	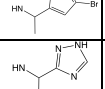	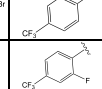	0.38	0.039	>100	0.26
59	DSM723	*ent1*	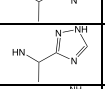	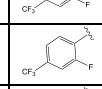	0.35	0.073	>100	0.15
60	DSM724	*ent2*	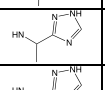	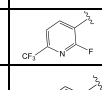	36	nd	nd	5.8
61	DSM744	rac	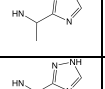	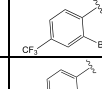	0.99 ± 0.014 (2)	0.73	>100	0.58 ± 0.2 (3)
62	DSM754	rac	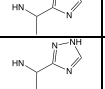	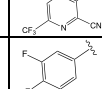	0.95	0.26	>100	0.99 ± 0.46 (3)
63	DSM767	rac	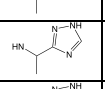	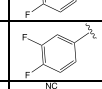	1.9	nd	nd	2.3
64	DSM836	*ent1*	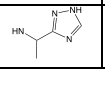	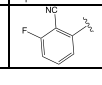	0.40	nd	nd	0.72
65	DSM837	*ent2*	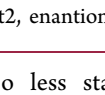	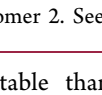	>100	nd	nd	>10
66	DSM850	rac	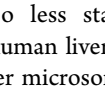	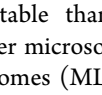	0.48	nd	nd	1.1

[a]Rac, racemic; ent1, enantiomer 1; and ent2, enantiomer 2. See Table 1 footnote for other abbreviations and error analysis information.

CF_3-pyridinyl ring (**8**–**10**) were also less stable than **2**. Benzoxazole **21** had good stability in human liver microsomes (HLM) but was unstable in mouse liver microsomes (MLM). With the exception of **21**, compounds in this set had relatively poor aqueous solubility at intestinal pH. Thus, these compounds lacked the physicochemical and metabolic characteristics to support progression.

Replacement of Cyclopropyl with Chiral Amides. Computational modeling suggested that substitution of the cyclopropylamide with chiral amides, particularly those with 5-membered heterocyclic rings could improve potency (Table S2). Using the chemistry described in Scheme 1 and Supporting Information Scheme S3, compounds **22**–**52** were synthesized and evaluated (Table 2). Three chiral amides with simple alcohol (**22** CH_2OH) or amines (**23** and **24**) ($NHCH_3$ and NH_2) groups were tested first, but these were poorly active and represented the compounds with the largest discrepancy between the predicted and observed potency in this study (Figure 2A and Supporting Information Table S2).

We next synthesized and tested isoxazole (**25**–**27**, **51**), pyrazole (**28**, **32**–**37**, **42**–**50**), triazole (**29**–**31**, **38**, **40**), oxadiazole (**39**), and imidazole (**41**) derivatives, which also varied by the addition of methyl groups to the rings. Key compounds were analyzed as both racemic mixtures and purified enantiomers early in the program, demonstrating that DHODH binding activity resided primarily in only one of the two enantiomer pairs (Table 2). Later compounds were often only evaluated as pure enantiomer pairs. Because of concerns that undecorated pyrazole analogues would show CYP inhibition, we also made a number of 5-substituted 3-methylpyrazole analogues, including 5-methyl (**42**, **43**), 5-CN (**44**, **45**), 5-$CONH_2$ (**46**–**47**), and 5-$COHNHCH_3$ (**49**, **50**) derivatives, all of which were predicted to bind well (Supporting Information Table S2). The most potent analogues were the active stereoisomers of the isoxazole (**26**), 4-methylpyrazole (**33**), 1,3 dimethylpyrazole (**36**), 3,5-dimethylpyrazole (**42**), 3-methyl, 5-carbonitrile pyrazole (**44**), and 3-methyl, 5-carboxamide pyrazole (**47**) derivatives, with all meeting potency criteria on *Pf*DHODH (IC_{50} < 0.030 μM) and *P. falciparum*

https://doi.org/10.1021/acs.jmedchem.1c00173
J. Med. Chem. 2021, 64, 6085−6136

Table 4. Single *R* Group Substitutions on the Bridging Carbon

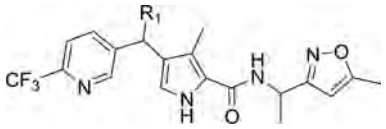

				IC_{50} (μM)			EC_{50} (μM)
cmpd	cmpd ID	Stereo chem	R1	*Pf*DHODH	*Pv*DHODH	*h*DHODH	*Pf*3D7
67	DSM619	rac	CH_3	0.079	0.074	>100	0.0030
68	DSM626	rac	OH	0.18	0.13	>100	0.022 ± 0.0049 (2)
69	DSM627	rac	OCH_3	0.15	0.10	>100	0.040 ± 0.0021 (2)
70	DSM631	rac	CN	0.27	0.41	>100	0.021
71	DSM644	*ent1*	D, D[a]	0.015	0.0091	>100	0.0047
72	DSM645	*ent2*	D, D[a]	63	nd	nd	>10

[a]Both methylene protons were replaced with deuterium.

Scheme 3

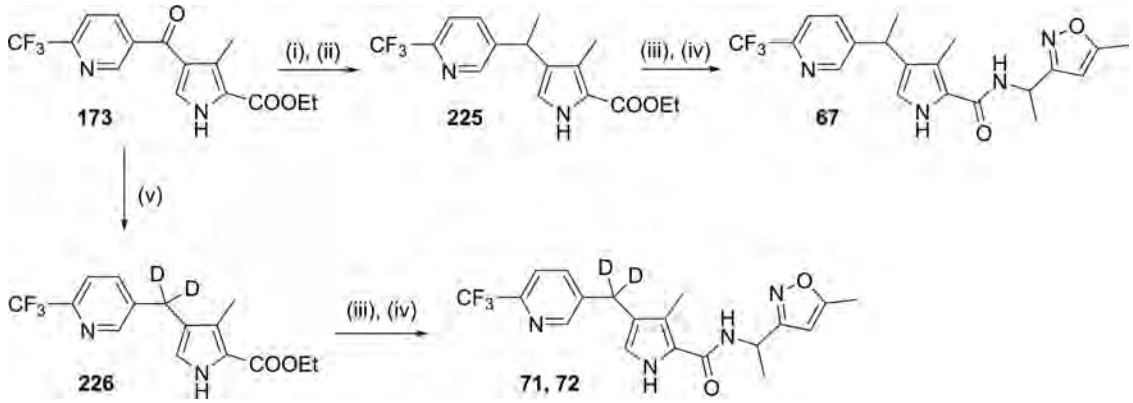

[a]Reagents and conditions: (i) methylmagnesium bromide, THF, 0 °C−RT, 4 h; (ii) TFA, triethylsilane, CH_2Cl_2, 0−85 °C, 1 h; (iii) NaOH, EtOH/H_20, RT−80 °C, 2 h; (iv) amine, HATU, Et_3N, CH_2Cl_2, RT, 3−4 h; and (v) $NaBD_4$, TFA−D, $CHCl_3$, 0 °C−RT, 16 h.

3D7 (EC_{50} < 0.020 μM) (Table 2). The triazole derivative **30** was also reasonably active (EC_{50} 0.066 μM), and because this group lowered Log *P* and improved metabolic stability, it was also incorporated into additional analogues that combined chiral amides with changes elsewhere in the molecule. When comparing enantiomer pairs, we found that the less active stereoisomer typically showed >100-fold lower potency against both *Pf*DHODH and *Pf*3D7-infected cells throughout the series. All active compounds also showed equal to more potent activity against *Pv*DHODH, and none of the analogues had any detectable activity (up to 100 μM) against *h*DHODH (Table 2).

For compounds containing 4-CF_3-pyridinyl in the aryl position (Table 2), the only compounds with a human CL_{int} within the target range contained either the triazole (the racemic **29** and its active enantiomer **30**) or the carboxamide pyrazole **47** (Supporting Information Table S4A). Four additional compounds, including the 4-methyl pyrazoles **28** and **33**, the dimethylpyrazole **36**, and the cyanopyrazole **44**, had CL_{int} values of <20 μL/min/mg, with **33** and **36** also meeting our *Pf*3D7 potency criteria.

Combining Chiral Amides with Variation of the Aryl Group. To further optimize both potency and absorption, distribution, metabolism, and excretion (ADME) properties, the more potent chiral amide substituents were combined with variations of the more potent isoquinolines (**52**−**55**) plus a set of additionally substituted benzyl (**56**−**60**, **62**, **64**−**66**) or pyridinyl rings (**61**, **63**) (Table 3). Additionally, we sought to determine whether the beneficial properties of the triazole (low LogP) could be paired with an aryl group that could boost potency in the combined molecule. Compounds were synthesized based on the chemistry depicted in Schemes 1, 2, and Supporting Information Scheme S4. Two compounds (**52** and **53**) that combined the most potent chiral amide (isoxazole) with isoquinoline showed excellent potency (*Pf*3D7 EC_{50} 0.002−0.004 μM), although they were 2−4-fold less potent than **16** (cyclopropylamide combined with the isoquinoline). However, both **52** and **53** were rapidly metabolized and poorly soluble (Supporting Information Table S4A). Combining the triazole with isoquinoline (**54**) improved potency by 7-fold over **30** (4-CF_3 pyridinyl), leading to potency in the target range for development (*Pf*3D7 EC_{50} < 0.015 μM), but metabolic stability of **54** was not sufficient for advancement. Combining the isoxazole with 4-CF_3 benzyl (**56**) reduced potency over **26** (4-CF_3 pyridinyl) by 2-fold and had minimal impact on metabolic stability but led to a compound that was amenable to crystallography as **26** had failed to cocrystallize with *Pf*DHODH (Table S3 and Supporting Information Figures S1 and S2). None of the ortho- or meta-substituted benzyl (**59**, **62**, **64**, **66**) or pyridinyl (**61**, **63**) rings provided good potency in the context of the triazole, regardless of the presence of a CF_3 or halogen in the 4 position, although the most active of this set was the 4-CF_3, 2-F-benzyl derivative **59**.

Substitutions on the Bridging Carbon. To explore the potential of bridging carbon modifications to impact both

https://doi.org/10.1021/acs.jmedchem.1c00173
J. Med. Chem. 2021, 64, 6085−6136

Scheme 4

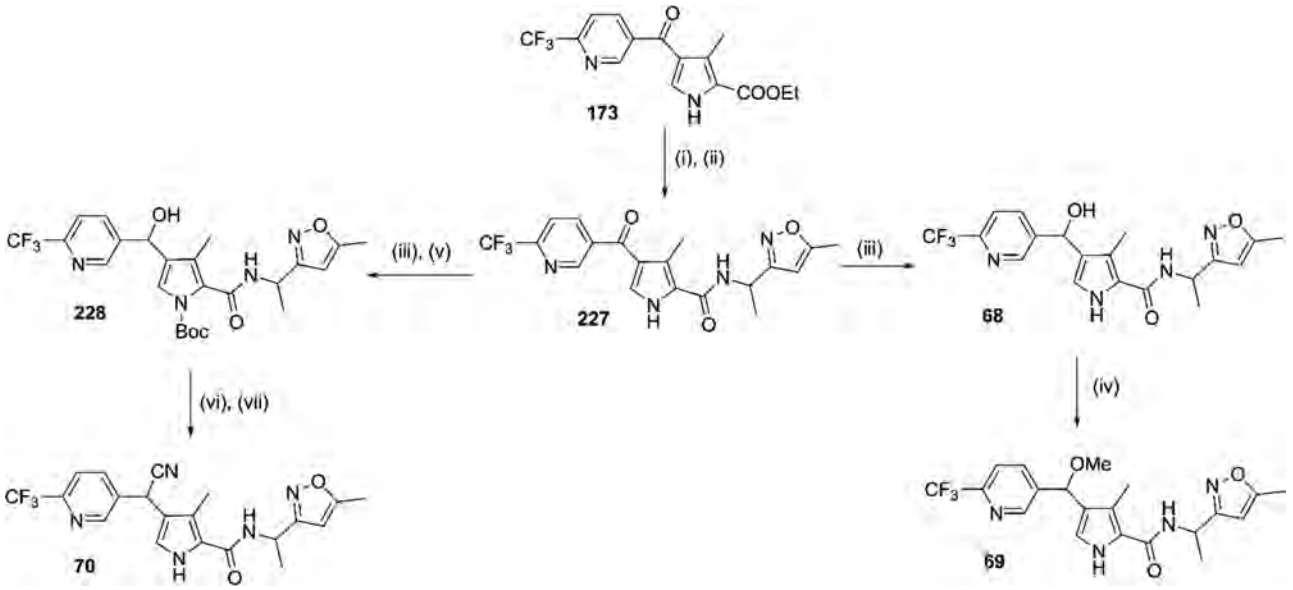

[a]Reagents and conditions: (i) NaOH, EtOH/H_2O, RT−80 °C, 2 h; (ii) amine, HATU, Et_3N, CH_2CI_2, RT, 16 h; (iii) $NaBH_4$, EtOH, 0 °C−RT, 1 h; (iv) MeI, THF, 0 °C−RT, 16 h; (v) $(Boc)_2O$, Et_3N, DMAP, CH_2CI_2, RT, 4 h; (vi) TMSCN, $(C_6F_5)_3B$, MeCN, RT, 8 h; (vii) HCI in dioxane, RT, 2 h.

potency and metabolic stability, we synthesized a series of analogues containing single *R* group substitutions on this carbon (**67**−**72**) (Table 4). The decision to make this set of compounds was done primarily with the goal of blocking a potential metabolic hotspot and one that might contribute to the time-dependent CYP inhibition of some compounds in the series. FEP+ predictions for the methyl analogue **67** suggested that it would have up to 6-fold improved potency versus **26** (FEP+ predicted IC_{50} for the pure *R*, *R* diastereomer was 0.013 μM), supporting the approach. The compound set was made in the context of the isoxazole amide group (**25**, **26**) that showed comparable potency to the best of the chiral amides. The synthesis of these analogues was achieved as shown in Schemes 3 and 4. The addition of a methyl to the bridging carbon (**67**) increased potency versus *Pf* 3D7-infected cells by 3-fold relative to the racemic **25** as predicted by FEP+. Compound **67** also showed equivalent IC_{50} values versus *Pf* and *Pv*DHODH compared to **25**/**26**; however, it was less metabolically stable and less soluble than **25** (Supporting Information Table S4A). Given the additional chiral center, **67** would be predicted to be 4-fold more active than measured if tested as the purified active diastereomer, demonstrating that the modification provided a potency boost. The addition of OH (**68**), OCH_3 (**69**), or CN (**70**) to the bridging methyl resulted in racemic compounds that were 2−3-fold less potent than **25**/**26**; therefore, the expectation is that the most active diastereomer would have an equivalent activity to **26**. Thus, all four substitutions were well tolerated. The addition of a cyano group to the bridging methyl led to an improvement in metabolic stability within the context of the isoxazole chiral amide (**70** vs **26**). Finally, we tested the effects of deuterating the bridging carbon (**71** and **72**) as a tool to determine if an isotope effect could reduce metabolism at this position, but it had no impact (see below).

Addition of Cyclopropyl to the Bridging Carbon. We next synthesized a set of analogues containing a cyclopropyl on the bridging carbon (**73**−**102**) (Table 5) since this functional group did not add an additional chiral center (e.g., **67** and **70**) but might yield the benefits of improved potency and/or metabolic stability that were observed for the single *R* group substitutions on the bridging carbon (above). Compounds were synthesized as shown in Scheme 5 and Supporting Information Schemes S5 and S6. The bridging cyclopropyl was tested in combination with a range of both nonchiral and chiral amides, combined with either 4-CF_3-pyridinyl or a handful of closely related substituted benzyl rings. As previously observed, compounds with cyclopropyl (**73**), difluoroazetidine (**74**), isoxazole (**75**), pyrazole (1*H*-4-yl) (**77**), and substituted pyrazoles (1*H*-3-yl) (**81**, **86**) at the amide position led to the best potency against *Pf*DHODH and *Pf* 3D7-infected cells, with all compounds in this set showing <0.005 μM potency against *Pf* 3D7. A potency gain of 3−10-fold for *Pf* 3D7-infected cells was observed for these compounds (**2** vs **73**, **26** vs **75**, **32** vs **77**, **42** vs **81**, **44** vs **86**). The triazole **79** also showed good potency (*Pf* 3D7 EC_{50} = 0.013 μM), which represents a 5-fold improvement over **30**, the analogue without the cyclopropyl on the bridge. While generally, the cyclopropyl bridge substitution improved potency, this was not the case for the 5-carboxamide pyrazole amide, where **47** was 2-fold more potent than **83** against *Pf* 3D7 cells. Of the compounds in this set, FEP+ calculations were only performed for **30** and **79**, and for this pair, FEP+ predicted that **30** would be more potent than **79**, while the opposite was observed experimentally (Table S2).

Combinations of the beneficial triazole with different benzyl groups (**92**−**102**) were synthesized to determine if more potent analogues could be identified (Table 5). The 2-F, 4-CF_3-benzyl analogue (**92**), was 12−40-fold less potent than **79** (4-CF_3-pyridinyl) against *Pf*DHODH and *Pf* 3D7-infected cells, respectively, mimicking the reduced activity observed for **59**−**61**. In contrast, the addition of *meta*-fluorine (**94**) yielded compounds that were ∼2-fold less potent than **79**, while the addition of *meta*-cyano improved potency by 2-fold (**98** and **99**). The active enantiomer containing 3-CF_3-benzyl (**96**) instead of 4-CF_3-benzyl was nearly 4-fold less potent than **79**. Replacement of 4-CF_3-pyridinyl with 4-CF_2-pyridinyl also led to a 10-fold drop in potency (**101** versus **79**).

https://doi.org/10.1021/acs.jmedchem.1c00173
J. Med. Chem. 2021, 64, 6085−6136

Table 5. Cyclopropyl Addition to the Bridging Carbon[a]

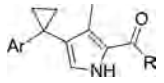

Cmpd	Cmpd ID	stereo chem	R	Ar	IC_{50} (μM)			EC_{50} (μM)
					*Pf*DHODH	*Pv*DHODH	*h*DHODH	*Pf*3D7
73	DSM650	NA			0.019 ± 0.010 (3)	0.011	>100	0.0020 ± 0.0013 (3)
74	DSM651	NA			0.021	0.017	>100	0.011 ± 0.0078 (2)
75	DSM653	*ent1*			0.016 ± 0.0028 (2)	0.030	>100	0.0012 ± 0.0010 (3)
76	DSM654	*ent2*	As above		80	nd	nd	1.3
77	DSM687	*ent1*			0.034	0.032	>100	0.0012 ±0.00014 (2)
78	DSM688	*ent2*	As above		4.6	nd	nd	0.17
79	DSM705	*ent1*			0.095 ± 0.040 (11)	0.052 ± 0.032 (4)	>100 (4)	0.012 ± 0.0050 (11)
80	DSM706	*ent2*	As above		61 ± 20 (5)	nd	nd	3.3 ± 0.28 (2)
81	DSM778	*ent1*			0.057 ± 0.00071 (2)	0.041	>100	0.0040 ± 0.0015 (4)
82	DSM779	*ent2*	As above		39 ± 1.4 (2)	nd	nd	3.0 ± 0.071 (2)
83	DSM780	rac			0.26	0.18	>100	0.046 ± 0.028 (3)
84	DSM844	*ent1*	As above		0.14 ± 0.058 (3)	0.17	>100	0.0094 ± 0.00085 (2)
85	DSM845	*ent2*	As above		57 ± 5.7 (2)	nd	nd	1.7
86	DSM782	*ent1*			0.073 ± 0.018 (2)	0.043	>100	0.0052 ± 0.0024 (3)
87	DSM783	*ent2*	As above		11 ± 3.0 (2)	nd	nd	4.3 ± 2.0 (2)
88	DSM797	*ent1*			0.086 ± 0.013 (2)	0.041	>100	0.022 ± 0.013 (3)
89	DSM798	*ent2*	As above		20 ± 16 (2)	nd	nd	0.52 (0.46 - 0.56)
90	DSM890	*ent1*			0.39	nd	nd	0.044 ± 0.0071 (3)
91	DSM891	*ent2*	As above		55	nd	nd	12
92	DSM790	*ent1*			1.2	nd	nd	0.41 ± 0.24 (2)
93	DSM791	*ent2*	As above		>100	nd	nd	nd
94	DSM809	*ent1*	As above		0.11	0.061	>100	0.029
95	DSM810	*ent2*	As Above		34	nd	nd	5.4
96	DSM811	*ent1*	As above		0.11	0.040	>100	0.048
97	DSM812	*ent2*	As Above		30	nd	nd	2.8
98	DSM846	rac	As above		0.14	0.26	>100	0.011
99	DSM873	*ent1*	As above		0.069 ± 0.028 (7)	0.064 ± 0.020 (4)	>100 (4)	0.0053 ± 0.0037 (10)
100	DSM874	*ent2*	As above		4.2 ± 0.071 (2)	nd	nd	1.9 ± 0.64 (2)
101	DSM964	*ent1*	As above		0.15	nd	nd	0.18
102	DSM965	*ent2*	As above		>30	nd	nd	>20

[a]Rac, racemic; ent1, enantiomer 1; and ent2, enantiomer 2. See Table 1 footnote for other abbreviations and error analysis information.

https://doi.org/10.1021/acs.jmedchem.1c00173
J. Med. Chem. 2021, 64, 6085−6136

Scheme 5

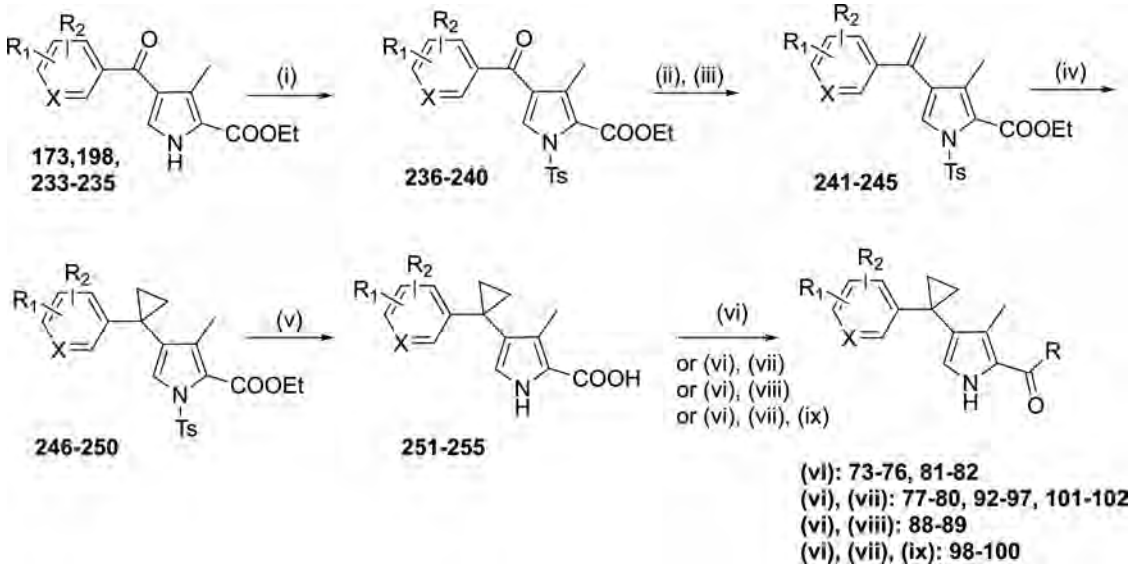

[a]Reagents and conditions: (i) a: NaH, TsCl, DMF, 0 °C−RT, 4.5 h or b: DMAP, Et_3N, TsCl, CH_2Cl_2, 0 °C−RT, 2 h; (ii) methylmagnesium bromide, THF, 0 °C−RT, 2−4 h; (iii) I2, toluene, RT−115 °C, 16 h; (iv) trimethylsulfoxonium iodide, ^{t}BuOK, THF, DMSO, 0 °C−RT, 4 h; (v) NaOH, EtOH/H_2O, RT−80 °C, 2 h; (vi) amine, HATU, Et_3N, CH_2Cl_2, RT, 4−5 h; (vii) trityl: TFA, triethylsilane, CH_2Cl_2, RT, 1 h; (viii) tosyl: TBAF, THF, RT−50 °C, 2 h; (ix) KCN, DMSO, RT−130 °C, 20 h.

The addition of the cyclopropyl to the bridging carbon improved potency in most, but not all cases, but had little impact on metabolic stability (Supporting Information Table S4A). The overall properties were best for the triazoles; for example, **79** compared favorably to **30** was more potent while retaining similar metabolic stability. Similar effects were observed for the carboxamide pyrazole **84** versus **47**, although solubility was better for **47**. While the isoxazole **75** with the bridging cyclopropyl was highly potent and improved over **26**, it was less metabolically stable, particularly versus MLM. The cyclopropyl analogue **73** had good metabolic stability in HLM and had an improved potency over **2**, but **73** showed a large species effect in MLM, suggesting that the development of this compound would be challenging. Replacement of 4-CF_3 of **79** with 4-CF_2H (**101**) improved metabolic stability but led to reduced potency. Replacement of 4-CF_3-pyridinyl of **73** with 3-cyano, 4-CF_3 (**99**) improved both potency and metabolic stability. Within the Table 5 series of compounds (cyclopropyl on the bridging carbon), the kinetic solubility was the best for compounds containing triazole (**79** and **101**) or imidazole (**88**) combined with the pyridinyl-4-CF_3 in the benzyl position.

Pyrrole Methyl Replacements Including 3,5-Disubstituted Analogues. The potential for modifications on the pyrrole ring to improve potency and/or metabolic stability was assessed by replacing either the C3 methyl (R1) with more polar groups or by adding Me or Cl substituents to the C5 methyl (R) in the presence of either C3 Me or C3 CN (Table 6 and Supporting Information Table S4A). These compounds were made to complete the SAR analysis of modifiable positions in the system and extensive FEP+ analysis was not performed, though a good correlation between predicted and tested activity was observed for the one example that was modeled (**119**) (Table S2). Compounds were made in the context of a selection of the best performing amides. Compounds **103**−**123** were synthesized as described in Scheme 6 and Supporting Information Schemes S7−S9. Replacement of the C3 methyl with $COOCH_3$ (**103**), $CONHCH_3$ (**104**), or $CONH_2$ (**105**) all led to a substantial loss of potency for the active enantiomer ranging from 250−800-fold against *Pf*DHODH and 70−150-fold against *Pf*3D7 when compared to the matched methyl containing analogue **2**. Cyano **106** was considerably better tolerated but still led to a 10-fold drop in potency against these key parameters when compared to **2**, although similar metabolic stability was observed. The addition of Me or Cl to C5 did not have a big impact on potency, while, in general, the addition of CN to C3 led to reduced activity in most cases. For compounds with the triazole as the chiral amide, the addition of Me at C3 **107** (C3 Me, C5 Me) led to a 2-fold reduction in potency against *Pf*3D7, while inserting Cl at C5 led to 1.5-fold improvement **121** (Cl, Me) versus **30** (H, Me) and maintained good metabolic stability and solubility (Supporting Information Table S4A). In contrast, within the context of the bridging cyclopropyl, adding the Cl resulted in a 10-fold drop in potency for **123** (Cl, Me) versus **79** (H, Me). The pyrazole **109** (Me, Me) and methylpyrazole **114** (Me, Me) C5 methyl derivatives showed similar potency and comparable solubility/metabolic stability to **33** (H, Me) and **36** (H, Me), respectively, while replacement of the C5 Me with CN in the context of the C3 Me **118** (Me, CN) resulted in a 40-fold loss of potency compared to **33**, mirroring the effects of the CN observed for **106**. Similar results were observed for the isoxazole, where **111** (Me, Me) was similarly potent to **26** (H, Me), and **116** (Me, CN) was 6-fold less potent, or for the cyclopropyl amides where the *Pf*3D7 EC_{50} of **119** was within 2-fold of **2** (H, Me).

Removal of the Bridging Carbon. A final set of compounds explored the effects of removing the bridging methyl altogether on DHODH and *Pf*3D7 potency and metabolic stability. The decision to synthesize this set of compounds was driven by the goal of reducing metabolism at a potentially susceptible position (the bridging carbon). Aryl groups most likely to provide potent binding to Plasmodium DHODHs were identified by computational modeling and compounds (**124**−**163**) were synthesized for a selection of the best previously identified amides, as shown in Schemes 7 and 8

https://doi.org/10.1021/acs.jmedchem.1c00173
J. Med. Chem. 2021, 64, 6085−6136

Table 6. Pyrrole Methyl Replacements, Including Disubstituted Analogues

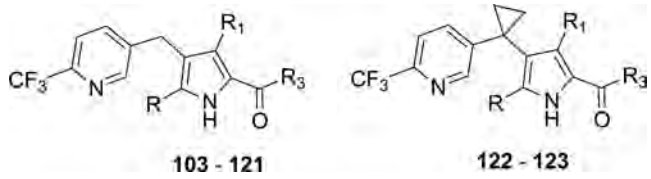

Cmpd	Cmpd ID	stereo chem	R	R1	R3	IC_{50} (μM)			EC_{50} (μM)
						*Pf*DHODH	*Pv*DHODH	*h*DHODH	*Pf*3D7
103	DSM609	NA	H	$COOCH_3$	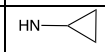	6.4	nd	nd	1.4 ± 0.57 (2)
104	DSM610	NA	H	$CONHCH_3$	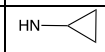	16	nd	nd	3.4 ± 2.8 (2)
105	DSM615	NA	H	$CONH_2$	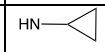	4.9	nd	nd	2.1 ± 0.47 (3)
106	DSM616	NA	H	CN	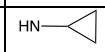	0.41	0.43	>100	0.25
107	DSM638	*ent1*	CH_3	CH_3	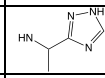	0.29	0.14	>100	0.14
108	DSM639	*ent2*	CH_3	CH_3	As above	43	nd	nd	0.75
109	DSM655	*ent1*	CH_3	CH_3	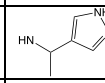	0.087 ± 0.018 (2)	0.088	>100	0.0068 ± 0.0054 (3)
110	DSM656	*ent2*	CH_3	CH_3	As above	11	nd	nd	0.19
111	DSM699	*ent1*	CH_3	CH_3	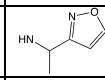	0.065	0.030	>100	0.012 ± 0.0032 (3)
112	DSM700	*ent2*	CH_3	CH_3	As above	53	nd	nd	>1
113	DSM702	*ent1*	CH_3	CH_3	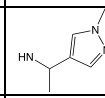	>30	nd	nd	>10
114	DSM703	*ent2*	CH_3	CH_3	As above	0.088	0.076	>100	0.017
115	DSM674	*ent1*	CH_3	CN	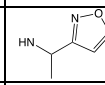	3.2	nd	nd	1.8
116	DSM675	*ent2*	CH_3	CN	As above	0.095	0.099	>100	0.064
117	DSM677	*ent1*	CH_3	CN	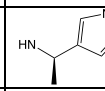	42	nd	nd	>1
118	DSM678	*ent2*	CH_3	CN	As above	0.66	0.44	>100	0.17
119	DSM753	*NA*	Cl	CH_3	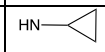	0.12	0.017	>100	0.032 ± 0.021 (4)
120	DSM775	*ent1*	Cl	CH_3	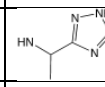	>100	nd	nd	>10
121	DSM776	*ent2*	Cl	CH_3	As above	0.20	0.063	>100	0.040 ± 0.017 (3)
122	DSM786*	*ent1*	Cl	CH_3	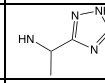	64	nd	nd	nd
123	DSM787*	*ent2*	Cl	CH_3	As above	0.29	0.10	>100	0.13 ± 0.0071 (2)

*With cyclopropyl on bridge. Rac, racemic; ent1, enantiomer 1; and ent2, enantiomer 2. See Table 1 footnote for other abbreviations and error analysis information.

and Supporting Information Schemes S9 and S10 (Table 7). Of the five aryl groups that were synthesized, all of those containing an NH group in the 5-membered ring showed activity with at least one active enantiomer from each series showing

https://doi.org/10.1021/acs.jmedchem.1c00173
J. Med. Chem. 2021, 64, 6085−6136

Scheme 6

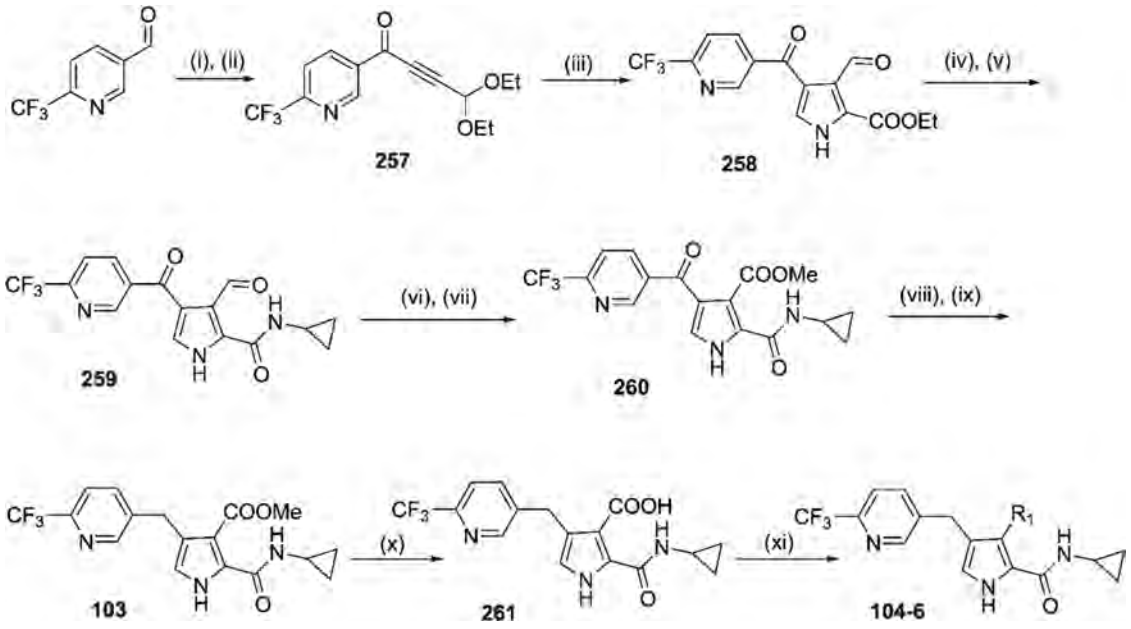

[a]Reagents and conditions: (i) 3,3-diethoxyprop-1-yne, n-BuLi, THF, −78 °C, 1.25 h; (ii) Dess−Martin, CH_2CI_2, RT, 0.5−1 h; (iii) ethyl isocyanoacetate, Ag_2CO_3, NMP, 85°C, 2 h; (iv) NaOH, EtOH, 70 °C, 2 h; (v) HATU, CH_2CI_2, Et_3N, RT, 4 h; (vi) $NaClO_2$, sulfamic acid, HzO, 0 °C−RT, 2 h; (vii) $SOCI_2$, MeOH, 0 °C−RT, 16 h; (viii) $NaBH_4$, EtOH, 0 °C−RT, 1 h; (ix) Et_3SiH, TFA, RT, −85 °C; (x) NaOH, EtOH, H_2O, RT, 80 °C, 2 h; and (xi) R_1 = CONHMe: $MeNH_2$, HATU, Et_3N, THF, 0 °C−RT, 4 h; R_1 = $CONH_2$: CDI, MeCN, RT−80 °C, 2 h, then NH_4OH, RT−80 °C, 4 h; R_1 = CN (from R_1 = $CONH_2$): $POCI_3$, MeCN, pyridine, RT, 80 °C, 2 h.

Scheme 7

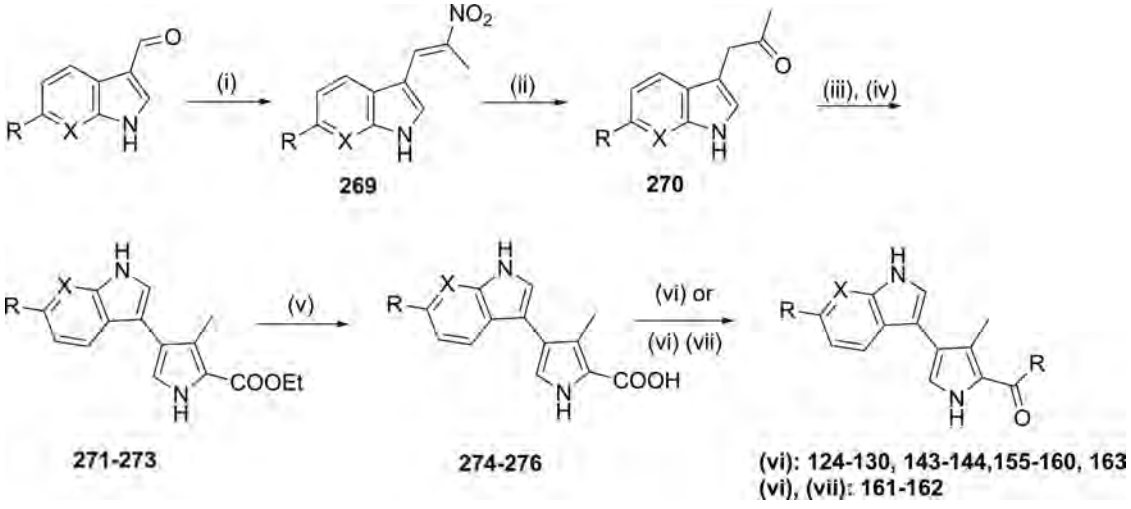

[a]Reagents and conditions: (i) nitroethane, NH_4OAc, RT−100 °C, 1−3 h; (ii) Fe, 4 N HCI, acetone, RT−50/60 °C, 3h; (iii) DMF, DMA, MW, 120 °C, 1 h; (iv) ethyi-2-(hydroxyimino)-3-oxobutanoate, Zn, NaOAc, AcOH, RT−100 °C, 3 h; (v) NaOH, EtOH/H_2O, RT, 2 h; (vi) amine, HATU, Et_3N, CH_2CI_2, RT, 3−4 h; (vii) Et_3SiH, TFA, CH_2CI_2, RT, 1 h.

*Pf*DHODH and *Pf*3D7 activity of <0.1 μM, but in general, the molecular modeling was less predictive of activity for compounds in this set (Table S2). These aryl ring systems included indole (**124**−**130**), indazole (**131**−**142**), pyrazolopyridine (**149**−**154**), and pyrrolopyridine (**155**−**163**). Methylation of the NH within the indazole series led to complete loss of activity (**145**, **146**), while replacement of NH with oxygen (**147**, **148**) also led to poorly active compounds demonstrating that the free NH was an important driver of potent binding. Each of the most active aryl groups also contained a CF_3 at C6. Replacement of CF_3 with F in the indole series led to 10-fold lower activity (**144** vs **135**). Within each series, the most active amide was in all cases the active enantiomer of the isoxazole (**127**, **135**, **154**, and **159**), with the best being the pyrrolopyridine analogue **159** (*Pf*3D7 EC_{50} = 0.0049 μM), followed by pyrazolopyridine **154**. Indole **127** and indazole **135** were 3-fold less active than **154** and 10−12-fold less active than **159**.

Compounds without the bridging carbon (**127**, **135**, **154**, **155**, **156**, **159**, and **163**) were poorly soluble, regardless of the nature of the amide group. Isoxazoles **127** and **154** showed good metabolic stability in HLM (Supporting Information Table

https://doi.org/10.1021/acs.jmedchem.1c00173
J. Med. Chem. 2021, 64, 6085−6136

Scheme 8

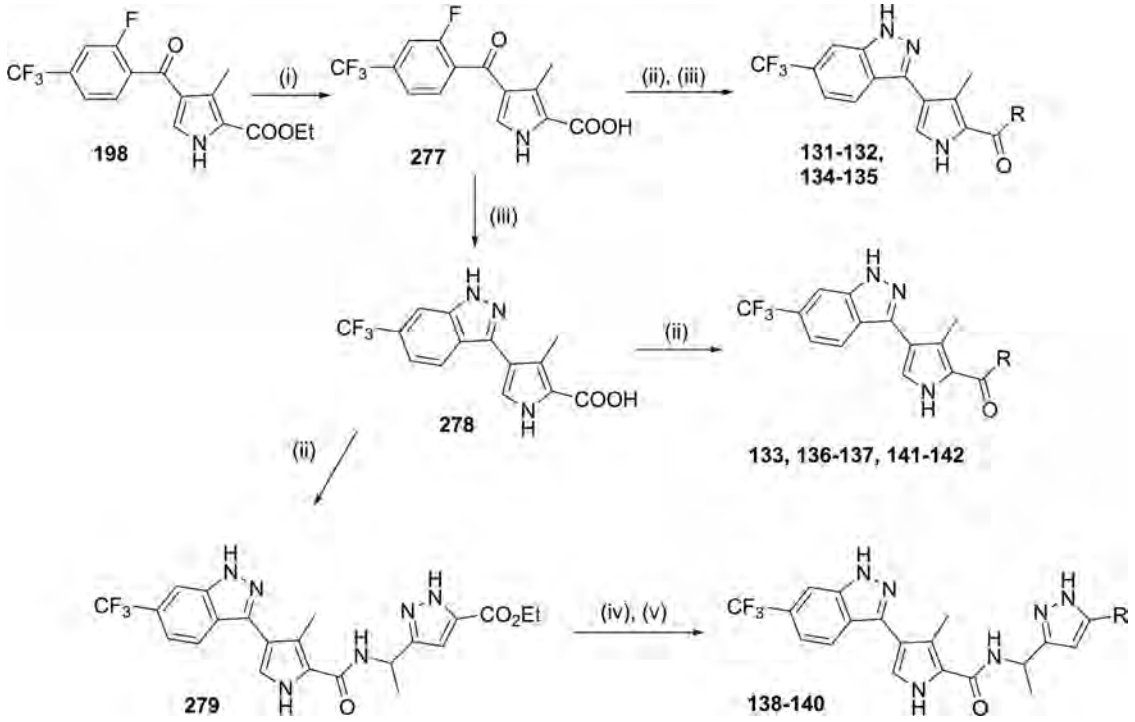

[a]Reagents and conditions: (i) NaOH, EtOH/H_2O, RT, −80 °C, 2 h; (ii) amine, HATU, Et_3N, CH_2Cl_2, RT, 2−4 h; (iii) $NH_2NH_2{\cdot}H_2O$, DMSO, RT, −100 °C, 2 h; (iv) R = $CONH_2$: aq. NH_3, MeOH, RT, −100 °C, 24 h; (v) R = CN: T_3P, DIPEA, CH_2Cl_2, RT, 2 h.

S4A), and while both met our objective (CL_{int} < 10 μL/min/mg), neither was as potent against *Pf*3D7-infected cells as desired. Both of these compounds had better metabolic stability than isoxazole derivatives with the bridging carbon (**127**, **154** vs **26**). The most potent of the compounds lacking the bridging carbon (isoxazole **159**) had a CL_{int} of 22 μL/min/mg but was unlikely to have the required pharmacokinetic (PK) properties needed for advancement. Thus, combined with the poor solubility, compounds lacking the bridging carbon did not meet our objectives to be advanced.

SAR Summary. We analyzed a wide array of pyrrole-based DHODH inhibitors, with the most potent compounds tending to come from a set of chiral amides (Tables 3 and 5) that were suggested based on molecular modeling. Within these, and where tested, the racemate tended to be 2-fold less potent throughout as expected, and the active enantiomer maintained >100-fold better potency against both *Pf*DHODH and the parasite across the tested compounds, although the difference at the enzyme level tended to be greater than for the parasite.

Throughout the series, we observed a good correlation between (1) the FEP+ predicted values and inhibitory activity against *Pf*DHODH (Figure 2A and Supporting Information Figures S3) and (2) between *Pf*DHODH and antiplasmodial activity against *Pf*3D7 asexual blood stage (Figure 2B). For a handful of the most potent antimalarial compounds (e.g., **79**), the activity against *Pf*3D7 was better than would have been expected based on *Pf*DHODH inhibitory activity (discussed below). We assessed species selectivity of compounds against other parasite enzymes and against human DHODH (Tables 1−7). Inhibitory activity against *Pv*DHODH paralleled trends that were observed for *Pf*DHODH, although most compounds show better potency against *Pv*DHODH than *Pf*DHODH, suggesting that efficacy against *P. falciparum* should translate to good efficacy against *P. vivax*. No activity against human DHODH was observed for any analogue; thus, this series would not be expected to show on-target toxicity in humans.

Determination of the Binding Mode of Select Pyrrole Analogues by X-ray Structure Analysis. To assess the contribution of binding interactions to inhibitor potency, we solved the X-ray structures of select compounds that contained variable substituents expected to interact with either the chiral amide binding pocket (**79**, **47**, **56**, **86**, **81**) or the aryl binding pocket (**18**, **127**). Compounds were cocrystallized with *Pf*DHODH and X-ray structures were solved as described (Experimental Section). Data collection and refinement statistics are presented in Supporting Information Table S3. Structures were solved to high resolution and diffracted over a range of 1.6 Å (**86**) to 2.4 Å (**56**). The refinement statistics (R_{work} and R_{free}) demonstrated that all structures were well refined (Table S3) and strong electron density was observed for all inhibitors (Supporting Information Figure S1).

Binding modes were similar to what we observed previously for **3**[20] (Figure 3 and Supporting Information Figure S2). Inhibitors that contained an amide bond (**79**, **47**, **56**, **81**, **86**, and **127**) formed a bifurcated hydrogen (H)-bond between H185 and the pyrrole and amide NH, whereas the ester **18** was only able to form a single H-bond. All compounds also formed a H-bond interaction between their carbonyl and R265. The chiral methyl in all 6 amide-bound structures was orientated in the same direction and pointed toward I272, making its closest contact to **127** at a distance of 3.9 Å (Figure 3C). This orientation establishes the *R*-enantiomers as the active configuration, allowing us to assign the stereochemistry of these compounds. The aromatic 5-membered rings of the chiral amides were bound near flavin mononucleotide (FMN) in a pocket that contains several potential H-bond interactions,

https://doi.org/10.1021/acs.jmedchem.1c00173
J. Med. Chem. 2021, 64, 6085−6136

Table 7. Removal of the Bridging Carbon

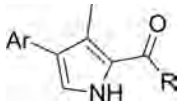

Cmpd	Cmpd ID	Stereo chem	Ar	R	IC_{50} (μM)			EC_{50} (μM)
					*Pf*DHODH	*Pv*DHODH	*h*DHODH	*Pf*3D7
124	DSM693	NA			1.6 ± 0.32 (3)	nd	nd	0.19 ± 0.049 (2)
125	DSM694	NA	As above		16	nd	nd	0.62 ± 0.021 (2)
126	DSM696	*ent1*	As above	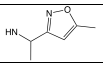	>100	nd	nd	>1
127	DSM697	*ent2*	As above	As above	0.66 ± 0.25 (5)	0.058	>100	0.085 ± 0.035 (2)
128	DSM826	NA	As above	$NHCH_2CF_3$	18	nd	nd	1.2
129	DSM828	*ent1*	As above	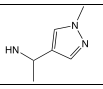	>100	nd	nd	>5
130	DSM829	*ent2*	As above	As above	54	nd	nd	3.4
131	DSM742	NA			4.1	nd	nd	0.25 ± 0.3 (5)
132	DSM743	NA	As above		3.6 ± 0.99 (4)	nd	nd	0.48 ± 0.26 (3)
133	DSM814	NA	As above	NHCH2CF3	22	nd	nd	0.61
134	DSM746	*ent1*	As above		>100	nd	nd	>10 (2)
135	DSM747	*ent2*	As above	As above	0.56 ± 0.32 (2)	0.069	>100	0.062 ± 0.023 (4)
136	DSM794	*ent1*	As above	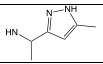	>100	nd	nd	nd
137	DSM795	*ent2*	As above	As above	3.6	nd	nd	nd
138	DSM800	*rac*	As above	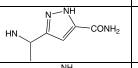	32	nd	nd	2.7
139	DSM802	*ent1*	As above	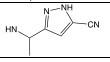	>100	nd	nd	4.5
140	DSM803	*ent2*	As above	As above	11	nd	nd	0.50
141	DSM816	*ent1*	As above		>30	nd	nd	>10
142	DSM817	*ent2*	As above	As above	24	nd	nd	4.1
143	DSM750	*ent1*		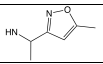	>100	nd	nd	>10 (3)
144	DSM751	*ent2*	As above	As above	0.70 ± 0.0 (2)	0.084	>100	0.72 ± 0.54 (3)
145	DSM769	*ent1*		As above	>30	nd	nd	>10
146	DSM770	*ent2*	As above	As above	>100	nd	nd	>10
147	DSM772	*ent1*		As above	>100	nd	nd	>10
148	DSM773	*ent2*	As above	As above	20	nd	nd	1.9 ± 0.42 (2)
149	DSM804	NA		$NHCH_2CF_3$	3.9	nd	nd	0.35
150	DSM819	NA	As above		2.1	nd	nd	0.20
151	DSM821	*ent1*	As above		>100	nd	nd	>10

https://doi.org/10.1021/acs.jmedchem.1c00173
J. Med. Chem. 2021, 64, 6085−6136

Table 7. continued

Cmpd	Cmpd ID	Stereo chem	Ar	R	IC_{50} (μM)			EC_{50} (μM)
147	DSM772	*ent1*	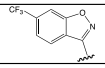	As above	>100	nd	nd	>10
148	DSM773	*ent2*	As above	As above	20	nd	nd	1.9 ± 0.42 (2)
149	DSM804	NA	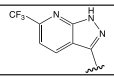	$NHCH_2CF_3$	3.9	nd	nd	0.35
150	DSM819	NA	As above		2.1	nd	nd	0.20
151	DSM821	*ent1*	As above	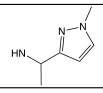	>100	nd	nd	>10
152	DSM822	*ent2*	As above	As above	6.8	nd	nd	2.6
153	DSM824	*ent1*	As above	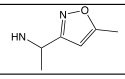	32	nd	nd	5.4
154	DSM825	*ent2*	As above	As above	0.12 ± 0.029 (2)	0.023	>100	0.024 ± 0.0 (2)
155	DSM839	NA	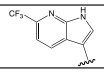	$NHCH_2CF_3$	0.5	nd	nd	0.050
156	DSM840	NA	As above		0.11	nd	nd	0.032
157	DSM842	*ent1*	As above	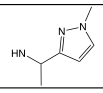	>100	nd	nd	>10
158	DSM843	*ent2*	As above	As above	1.0	nd	nd	0.16
159	DSM869	*ent1*	As above	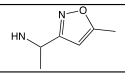	0.071 ± 0.011 (2)	0.015	>100	0.0049 ± 0.0025 (4)
160	DSM870	*ent2*	As above	As above	>100 (2)	nd	nd	3.2
161	DSM871	*ent1*	As above	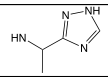	0.51	nd	nd	0.053
162	DSM872	*ent2*	As above	As above	25	nd	nd	2.0
163	DSM879	NA	As above		0.12 ± 0.082 (2)	0.010	>100	0.013 ±0.0080 (4)

whereas the aryl binding pocket was formed by a largely hydrophobic cleft between the two N-terminal helices (helix 1, residues F166-Y176; helix 2, residues G181-Y194). Compounds containing 4-CF_3-pyridinyl (**79**, **47**, **81**, and **86**) in the aryl position formed a H-bond between the pyridinyl nitrogen and an ordered water molecule (Figure 3A,B and Supporting Information Figure S1B,C). Similarly, the indole NH of **127** formed a H-bond with an ordered water molecule in the same area of the pocket (Figure 3C).

Additionally, we observed a set of novel interactions between the aromatic 5-membered rings of the chiral amides and previously unexplored areas of the binding pocket. These groups bound deeper into the pocket than previously explored functionalities (e.g., cyclopropylamide of **3**,[20] the CF_2CH_3 of **1**,[15] or the OEt of **18**, Supporting Information Figure S2D) and, in several cases, these rings were able to make H-bonds with residues in this region of the pocket. These interactions included H-bonds between the Y528 OH and the N of triazole **79** (Figure 3A) and pyrazole **47** (Figure 3B), and as predicted, a H-bond between the NH_2 portion of the carboxamide of **47** and E182. Additionally, the carbonyl oxygen of the **47** carboxamide formed a H-bond with K229, a residue we had not previously observed to form binding interactions with inhibitors in other cocrystal structures. Finally, the isoxazole N of **56** formed a H-bond with the backbone NH of E182 (Figure S2A), whereas in **127** the isoxazole N formed close contacts with both the NH of E182 and the carbonyl O of G181 (3.5 Å in both cases) (Figure 3C).

Identification of Potential Late Lead Compounds. Compounds were prioritized for further studies based on the combined potency, metabolic stability, and solubility data, with an EC_{50} < 0.015 μM against *Pf* 3D7-infected human red blood cells and a human CL_{int} < 10 μL/min/mg being key requirements for advancement. Compounds meeting these objectives included **33**, **36**, and **47** (Table 2) and **79**, **84**, **88**, and **99** (Table 5). **26** was also included to represent the best of the isoxazoles with respect to a combination of potency and metabolic stability, although the *in vitro* human CL_{int} suggested that it would not be sufficiently stable to meet our objectives. The carboxamide pyrazoles **47** and **84** were quickly ruled out, despite their superior metabolic stability. Their structures suggested that they might have poor permeability, which was confirmed by Caco-2 cell monolayer studies and by a mouse

https://doi.org/10.1021/acs.jmedchem.1c00173
J. Med. Chem. 2021, 64, 6085−6136

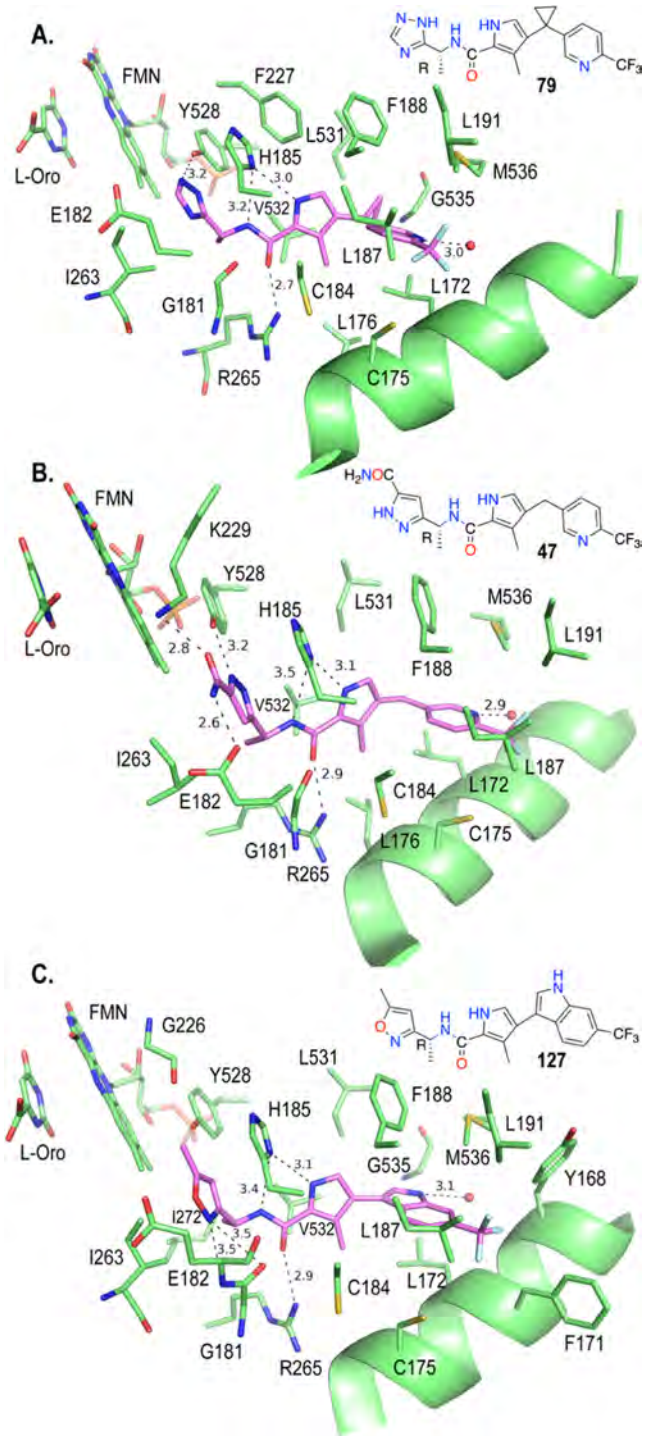

Figure 3. X-ray structures of pyrrole-based inhibitors bound to *Pf*DHODH (green). The 4 Å shell around the bound inhibitor (pink) is shown for (A) **79** (PDB 7KZ4), (B) **47** (PDB 7LOK), and (C) **127** (PDB 7KYY). Hydrogen bonds are depicted by dashed lines with distances given in Å. Structures were displayed with PyMol and chemical structures are shown in each panel as rendered by Chemdraw.

pharmacokinetic (PK) study for **84** in which bioavailability was only 18% (Supporting Information Tables S4B and S5). Compound **88** was synthesized to test the hypothesis that an imidazole group in the chiral amide position would lead to potent CYP inhibition and might reduce metabolism through autoinhibition. As predicted, **88** was a potent inhibitor of the five major CYP isoforms tested (see below); however, this property did not translate to good metabolic stability *in vitro* (Supporting Information Table S4A) or to reduced clearance in a mouse *in vivo* study (Supporting Information Table S5); therefore, this compound was not profiled further. The remaining compounds (**26, 33, 36, 79, 99**) were profiled in additional ADME studies and *in vivo* in mice and rats, and in parasitology studies to evaluate their potential to advance as late-lead candidates.

Assessing Species Selectivity and Safety Pharmacology. Compounds (**26, 33, 36, 79,** and **99**) were profiled to determine if any inhibited mammalian enzymes from species that are commonly used in toxicology studies (Supporting Information Table S6). As was observed for human DHODH, none of the compounds inhibited mouse, rat, or dog DHODH up to the highest tested concentration (100 μM). The lack of mammalian DHODH inhibition by these compounds provides a point of clear superiority over **1** that should make the assessment of the mechanisms of toxicity during the development of compounds in this series more straightforward. Compounds were also tested for cytotoxicity, and none showed growth inhibition of mouse L1210 or human HepG2 cell lines (CC_{50}'s > 20 μM; Supporting Information Table S6).

Preliminary safety pharmacology studies included characterization of effects on the hERG channel (a measure of potential cardiac toxicity), AMES (a measure of mutagenicity potential), and a human receptor panel. The hERG channel was not inhibited by **26, 33, 36,** and **79**, while **99** showed weak inhibition (IC_{50} = 20.4 μM) that would need to be de-risked based on the free fraction safety margin relative to predicted human plasma concentrations at the efficacious dose. Both **79** and **99** were AMES negative in a 5-strain assay with and without metabolic activation. When tested against a panel of human receptors (CEREP panel), both showed inhibition of NK_1, and additionally, **99** had activity against 5-HT_{2A}, A3, and GABA-gated chloride channel receptors (Supporting Information Table S6). However, IC_{50} studies to measure the effect of **99** as an antagonist indicated that only NK1 was significantly inhibited (IC_{50} = 2 μM), whereas the IC_{50} for the other receptors were not considered to be evidence of significant inhibition (IC_{50} of 35, 34, and >30 μM, receptively).

Cytochrome P450 inhibition studies were performed using a substrate-specific interaction approach[20] and both direct and time-dependent inhibition were assessed. Apart from **88**, **33** showed the most significant direct CYP inhibition, with IC_{50} values below 2 μM for CYP2C9 and CYP2D6 (Table 8). Compound **36** showed no inhibition against any isoform with

Table 8. Direct CYP Inhibition

	IC_{50} (μM)				
CYP	**88**	**33**	**36**	**79**	**99**
1A2	<0.25	>20	>20	>20	>20
2B6	nd	>20	20	>20	nd
2C8	nd	18.3	>20	>20	nd
2C9	<0.25	1.7	19.0	12	2.9
2C19	<0.25	4.0	>20	6.3	4.2
2D6	0.32	0.75	12.7	17	17
3A4 (tes/mid)	1.7/ 0.86	>20/c.n.c	8.5/ c.n.c	>20/ >20	>20/ >20
3A4 time-dependent inhibition	nd	possibly	yes	no	no

[a]nd, not determined. c.n.c. could not calculate as there was an apparent increase in the probe metabolite formation during incubations conducted in the presence of the test compound.

https://doi.org/10.1021/acs.jmedchem.1c00173
J. Med. Chem. 2021, 64, 6085−6136

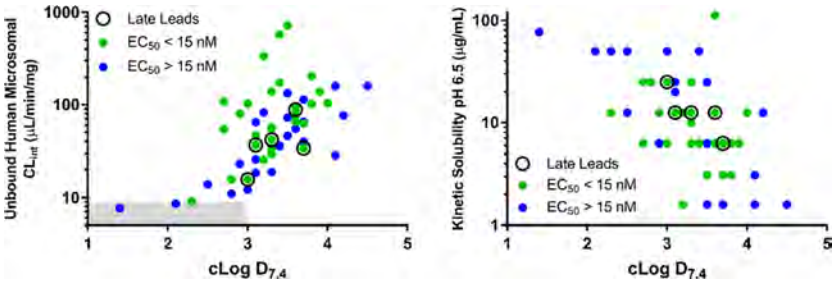

Figure 4. Correlation of Log $D_{7.4}$ with (A) unbound intrinsic clearance and (B) kinetic solubility at pH 6.5. Compound *Pf* 3D7 potency is indicated as depicted in the figure legend.

Table 9. Physicochemical Properties, *In Vitro* Binding and Metabolism

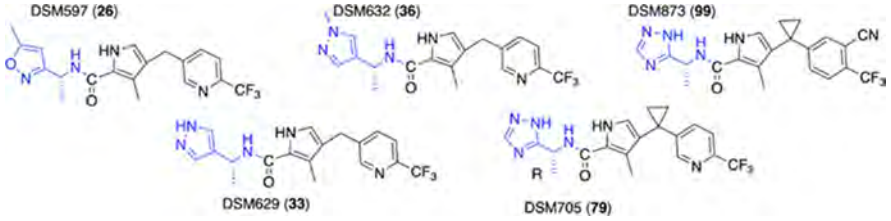

cmpd	1[a]	26	33	36	79	99
MW	415	392	377	391	404	428
cLog $D_{7.4}$	4.0	3.3	2.4	2.8	3.1	3.7
solubility (μg/mL)[b]						
FaSSGF (pH 1.6, 1 h)	6.8	35.1	81	113	1025	185
FaSSIF (pH 6.5, 5 h)	5.1	9.9	34	60	890	261
FeSSIF (pH 5.8, 5 h)	27.6	47.8	81	158	>2000	>2000
PBS (pH 7.4, 5 h)	2.0	5.9	23	49	493	85±10
H/R/M plasma protein binding (% bound)[b]	99.8/97.5/97.0	94.7/93.7/92.2	84.0/91.4/92.1	83.0/95.1/93.6	92.8/94.3/92.1	98.5/98.2/97.9
H/R/M blood-to-plasma ratio	0.54/0.8/0.7	0.7/0.9/0.8[d]	1.1/1.3/1.4	0.8/0.9/0.9	0.7/0.9/0.7	0.7/0.6/0.7
Albumax binding (% bound)[b]	83.1	75.0	49.5	49.5	71.9	89.5
microsome binding (% bound)[b]	71.7	43.3	40.5	44.8	34.2	66.1
H/R/M microsomal CL_{int} (μL/min/mg)	<7/<7/<7	34/29/63	20/28/31	20/21/41	9/12/11	12/15/16
H/R/M unbound microsomal CL_{int} (μL/min/mg)	<25/<25/<25	60/51/111	33/47/52	36/38/75	14/18/17	35/44/47
microsome predicted H/R/M plasma clearance (mL/min/kg)	<0.05/<1.1/<2.8	2.9/5.2/nd	4.9/6.6/14	4.9/3.2/15	1.1/1.8/4.8	0.6/1.4/3.7
Caco-2 permeability A−B/B−A Papp (10^{-6} cm/s)[c]	54, 60/49 ± 5.1	48, 59/57, 66	nd	17 ± 0.3/70 ± 0.6	22, 25/45, 50	

[a]Data for **1** were taken from ref 15 with the exception of plasma protein binding data, which were remeasured using the rapid equilibrium dialysis (RED) method, biorelevant solubility, human B/P, and Caco-2 permeability; each of these were taken from our previous report.[28] [b]Data represent the average of 3−4 measurements; the relative SD (RSD) of solubility measurements was <10% and RSD of fraction unbound values was <15% in all cases. [c]Caco-2 apparent permeability in the apical to basolateral (A−B) or B−A direction; mass balance. [d]Mouse B/P for **26** estimated using the average of the human and rat values >80% in all cases; data represent duplicate measurements or the average of 3 measurements ± SD nd, not determined.

the exception of minor inhibition of CYP2D6 (IC_{50} 12.7 μM), **79** and **99** showed modest inhibition of CYP2C19 (IC_{50} 6.3 and 4.2 μM, respectively) and **99** showed slightly more inhibition of CYP2C9 (IC_{50} 2.9 μM). Time-dependent inhibition studies were conducted using an "IC_{50} shift" protocol, as described previously.[20] There was no evidence of time-dependent inhibition of any isoform, except for CYP3A4/5, for which there was a marginal increase in inhibition for **33** with preincubation in the presence of NADPH (but IC_{50} values were still >20 μM) and an IC_{50} shift from >20 to 5.7 μM for **36** when the preincubation was conducted in the absence or presence of NADPH, respectively. These results are similar to what was observed for **2** in our previous studies.[20] In contrast, no evidence for time-dependent inhibition was observed for **79** or **99**.

Assessment of *In Vitro* ADME Properties. In general, pH 6.5 kinetic solubility and metabolic stability decreased for compounds with higher LogP/$D_{7.4}$ values (Figure 4). The target kinetic solubility was >25 μg/mL, recognizing that studies in physiological media indicated that the kinetic solubility significantly underestimated the solubility under more biorelevant conditions. To facilitate a more accurate comparison between the compounds of different Log $P/D_{7.4}$ that might show different binding to microsomal proteins, CL_{int} values were corrected for the microsomal binding (calculated as described previously[26]). Maintaining Log $D_{7.4}$ within a range of approximately 2 to 3.5 was therefore a goal of the medicinal chemistry program to achieve the best balance of solubility and microsomal stability and avoid issues associated with poor membrane permeability and transporter interactions that can occur for highly polar, low Log $D_{7.4}$ compounds.[27]

https://doi.org/10.1021/acs.jmedchem.1c00173
J. Med. Chem. 2021, 64, 6085−6136

Table 10. Pharmacokinetic Properties after Single IV and PO Doses to Swiss Outbred Mice

cmpd	1	26	33	36	79	99
dose (mg/kg)	IV:1.0 PO:10[a]	IV:2.8 PO:20	IV:nd PO:20	IV:nd PO:20	IV:2.3 PO:2.6/24	IV:0.91 PO:2.4
CL_{plasma} (mL/min/kg)	8.2	7.7	nd	nd	2.8	3.6
$V_{ss\ plasma}$ (L/kg)	2.3	1.4	nd	nd	1.3	1.0
PO $t_{1/2}$ (h)	2.5	2.3	4.4	3.5	3.4/4.5	3.2
PO T_{max} (h)	1-2	1.0	1.0	1.0	4.0/7.5	4.0
PO C_{max} (μM)	3.1	13	6.4	36	2.6/20	2.1
PO $AUC_{0-\infty}$ (μM·h)	22.8	66	65	217	29/250	18.3
bioavailability (%)	46	61	nd	nd	74/70	70

[a]Data are taken from ref 15 and represent the average of the two described studies. Data for **1** are based on the average from two mice per time point, whereas all other data are based on the average of three mice per time point. nd, not determined.

Table 11. Plasma Pharmacokinetic Parameters after a Single IV or PO Dose to Sprague Dawley Rats

cmpd	1[a]	26	33	36	79	99
IV dose (mg/kg)	**2.6**	**1.9**	**2.9**	**2.8**	**1.8**	**1.9**
CL_{plasma} (mL/min/kg)	6.5	3.2 ± 0.40	6.2 ± 1.2	2.4 ± 0.50	6.8 ± 0.70	7.0 ± 0.67
$V_{ss\ plasma}$ (L/kg)	5.9	1.0 ± 0.060	1.7 ± 0.11	0.87 ± 0.034	2.1 ± 0.17	2.1 ± 0.21
PO dose (mg/kg)	**19**	**28**	**31**	**32**	**17/10**	**10**
apparent $t_{1/2}$ (h)	16	4.1 ± 2.9	3.4 ± 0.58	3.7 ± 1.7	3.7 ± 0.40/5.9 ± 1.5	3.8 ± 0.1
PO T_{max} (h)	7	4.3 ± 0.60	3.0 ± 0.87	3.5 ± 0.87	2.5 ± 0.0/0.70 ± 0.30	1.0 ± 0.0
C_{max} (μM)	4.0	16 ± 2.5	2.4 ± 0.38	35 ± 9.7	14 ± 2.1/6.0 ± 0.12	6.2 ± 0.95
AUC_{∞} (μM·h)	120	160 ± 24	22 ± 6.3	360 ± 28	120 ± 14/47 ± 11	42 ± 5.7
bioavailability (%)	57	43 ± 6.2	10 ± 2.8	61 ± 4.3Ta	110 ± 13/77 ± 19	73 ± 10

[a]Data are taken from ref 15. Data for **1** represents the average of two rats; all other data represent mean ± standard deviation for 3 rats.

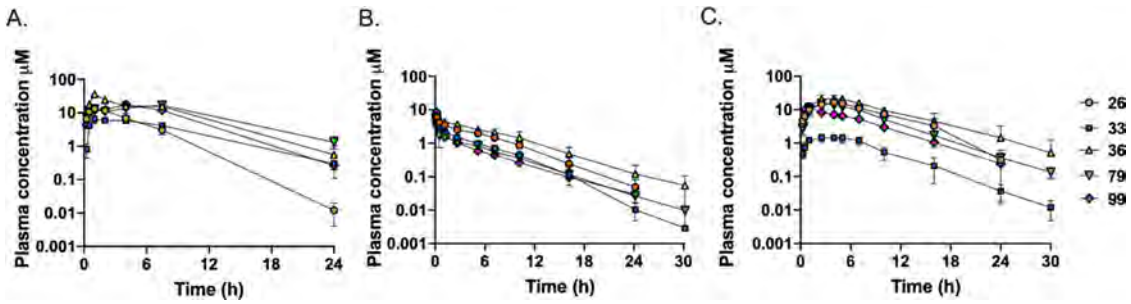

Figure 5. Plasma concentration versus time profiles in mice and rats. To allow easy comparison, data were scaled to a common dose level assuming linear kinetics over the dose range. (A) Mouse profiles following oral administration of 20 mg/kg (scaled). Actual administered doses were **26**:20 mg/kg (n = 2), **33**:20 mg/kg (n = 2), **36**:20 mg/kg (n = 2), **79**:24 mg/kg (n = 3), and **99**:2.4 mg/kg (n = 3). Error bars show the range for multiple measurements in n = 2−3 individual mice at each time point. (B) Rat profiles following intravenous (IV) (scaled to 2 mg/kg) and (C) oral administration (scaled to 20 mg/kg). Actual rat IV/PO doses were **26**:1.9/28 mg/kg; **33**:2.9/31 mg/kg; **36**:2.8/32 mg/kg; **79**:1.8/17 mg/kg; and **99**:1.9/10 mg/kg. Data represent the mean ± standard deviation (SD) for n = 3 rats. Measured doses and pharmacokinetic (PK) parameters deriving from these studies are provided in Tables 10 and 11 (data are not scaled in the tables).

Advanced ADME Studies on Identified Late Leads. The physicochemical and ADME properties of key compounds (**26**, **33**, **36**, **79**, **99**) were further profiled by assessing solubility in physiological buffers and plasma protein binding and to extend *in vitro* metabolism studies to additional mammalian species. The solubility of both **79** and **99** in fasted state simulated gastric fluid (FaSSGF), fasted and fed state simulated intestinal fluid (FaSSIF and FeSSIF, respectively), and pH 7.4 phosphate buffer (PBS) was excellent (Table 9), with both compounds showing very significant improvements over **1**, which suggest that they could be formulated using simple approaches without the need for solubilizing excipients. Of the two compounds, **79** showed superiority over **99**, but both compounds were significantly more soluble than **26**, **33**, or **36**.

Plasma protein binding was determined by ultracentrifugation or rapid equilibrium dialysis (RED) (Table 9) and was lowest for **33** and **36** (ranging from 83 to 95% bound across the species) and highest for **99** (~98% bound for all species). All five tested compounds showed lower protein binding than **1**, which was reassessed using rapid equilibrium dialysis (RED) methods that included a presaturation of the dialysis membrane to improve accuracy for highly protein-bound compounds of this type.[29] This approach yielded similar values for **1** with human and rat plasma, but lower binding for mouse (Table 9) compared to previous methods.[15] Binding for the pyrrole series compounds in Albumax-based media (used for *P. falciparum in vitro* efficacy assays) and in microsome preparations was lower in all cases than for plasma due to the lower protein concentrations. Very little variation between species was observed for *in vitro* metabolism studies across species, although overall, compounds were more stable in human than mouse or rat microsomes (Table 9). Correcting for microsomal binding (measured for this subset of compounds) indicated that **79** had the lowest unbound CL_{int} across all species. **33**, **36**, and **99** all had

https://doi.org/10.1021/acs.jmedchem.1c00173
J. Med. Chem. 2021, 64, 6085−6136

Table 12. Cross-Resistance, Target Validation, and Liver-Stage Activity

	26	33	36	79	99
P. falciparum Asexual Blood Stage (EC_{50} μM)					
*Pf*Dd2[a]	0.0087 ± 0.0015 (13)	0.0024 ± 0.00060 (2)	0.0070 ± 0.0021 (3)	0.018 ± 0.0022 (9)	0.0058 ± 0.0012 (8)
*Pf*D10_Yeast DHODH[b]					
no PG	nd	nd	>10	>10 (3)	>20, >10
+3 μM PG	nd	nd	>10	>10 (3)	>20, >10
Plasmodium berghei Liver Stage (EC_{50} μM)					
	0.0083 ± 0.00064 (2)	nd	nd	0.013±0.0044 (3)	0.0022 ± 0.0016 (2)

[a]Data show the mean ± standard error of the mean with the number of independent replicates in parenthesis. [b]Atovaquone control >20 μM minus proguanil (PG), 0.00016 ± 0.000051 μM plus PG. Additionally, **42**, **44**, **62**, **127**, and **135** were also tested versus the yeast DHODH line and all showed IC_{50} > 10 μM ± PG. nd, not determined.

comparable unbound CL_{int} values, and **26** was the least stable. Compounds **79** and **99** were also profiled in human and rat hepatocytes where data suggested that there were no additional clearance pathways not accounted for by the studies in liver microsomes. Permeability across confluent Caco-2 cell monolayers suggested that permeability was high with no evidence of efflux for **26**, whereas both **79** and **99** showed some efflux (efflux ratios of 4 and 2, respectively), indicating a possible transporter involvement.

Pharmacokinetic (PK) Properties in Mice and Rats. The PK properties of **26**, **33**, **36**, **79**, and **99** were assessed in mice and rats using intravenous (IV) and oral (PO) dosing routes (Tables 10 and 11, Figure 5 and Supporting Information Figure S4). After IV dosing to mice (**26**, **79**, and **9**), plasma clearance of **26** was similar to **1**, while both **79** and **99** showed values that were 2−3-fold lower. IV clearance in mice for all three compounds was lower than for **2** (CL_{plasma} = 26),[20] representing an improvement over the earlier compound from the series. Compared to the clearance values predicted from the *in vitro* microsome data (Table 9), **26**, **79**, and **99** had measured values (Table 10) within approximately 3-fold of the predicted values. Bioavailability of **26**, **79**, and **99** was similar, ranging from 61 to 74%, and all 5 compounds showed good exposure after PO dosing, with **36** showing the highest C_{max}, while **79** demonstrated the highest AUC after oral administration. Assuming dose-proportional kinetics, **99** would be expected to have a similar AUC compared to **79** if administered at a similar dose.

After IV dosing in rats, clearance was relatively low for all 5 compounds, representing a significant improvement over **2** (CL_{plasma} = 29)[20] (Table 11 and Figure 5). The lowest clearance was observed for **26** and **36**, which showed values **2** and **3**-fold lower than for **1**, whereas clearance values for **33**, **79**, and **99** were similar to **1**. Microsome predicted clearance values for **26**, **33**, and **36** (Table 9) were similar to the measured values (Table 11), but predicted values were about 4−5-fold lower than the measured values for **1**, **79**, and **99**. The basis for this is not known (note that *in vitro* studies using cryopreserved hepatocytes predicted even lower clearance than microsomes). None of the compounds were significantly eliminated in urine. All 5 compounds showed similar volumes of distribution, which were 3−5-fold lower than for **1** accounting for the lower half-lives. After PO dosing, bioavailability was poor for **33**, but was otherwise good (42−100%). As was observed after dosing in mice, **36** showed the highest exposure (C_{max} and AUC), but **26**, **79**, and **99** also showed good exposure, and all three showed higher C_{max} compared to **1** (assuming linear kinetics and factoring in the differences in dose). Interestingly, in both mice and rats, a major metabolite of **36** was **33** (Supporting Information Figure S4).

Combining the ADME and PK data with the *in vitro* potency data against both *Pf*DHODH and *Pf*3D7-infected cells suggested that **79** and **99** were the best candidates from the series for advancement. Both showed considerable improvements over the early pyrrole lead **2**,[20] including the finding that they were not irreversible CYP inhibitors. Both compounds showed high solubility in physiologically relevant buffers, were superior to the other pyrrole analogues, and also represented a substantial improvement over **1**. These results suggested that **79** and **99** will be formulated much more readily without the need for complicated solubilizing agents. Predicted clearance values from in vitro microsome (and hepatocyte) studies were lowest for these compounds across all species, and both also had good PK properties in mice and rats. Of the two, **79** had better ADME properties, while **99** was more potent. Neither compound matched the PO half-life observed for **1**, suggesting that they will likely have shorter half-lives in humans. We next turned to parasitology assays to screen for additional factors that might distinguish which compound was the most appropriate for advancement.

Additional Parasitology. Key compounds were profiled on a wider range of *Plasmodium* strains, species, and stages to ensure that they would be effective if used clinically against both drug-sensitive and drug-resistant *P. falciparum* strains, to confirm that like **1** they have liver-stage activity, and to ensure that unlike **1** they would show good *P. vivax* activity. Resistance selections were undertaken for **26** and **79**, and compounds were assessed for cross-resistance with **1**. Finally, *in vivo* efficacy was profiled versus *P. falciparum* in the SCID mouse model. The blood-stage model was chosen for efficacy assessment for several reasons. First, the existing liver-stage models have not yet been fully developed for use in pharmacokinetic/pharmacodynamic (PK/PD) modeling. Second, the blood-stage model was very useful in defining the plasma exposure required for efficacy in either treatment or prophylactic clinical studies for **1**. Finally, there is extensive experience working with this model for human dose predictions, whereas there is little precedence for the current *in vivo* liver-stage models.

Cross-Resistance Data and Proof of Target Killing Mechanism. Compounds were tested for activity against the chloroquine- and pyrimethamine-resistant *P. falciparum* strain Dd2 (Table 12). All 5 profiled compounds (**26**, **33**, **36**, **79**, and **99**) showed similar activity against Dd2, as had been observed with the drug-sensitive strain 3D7 (Tables 2 and 5). Several demonstrated IC_{50} values against *Pf*DHODH that were higher than expected based on their antiplasmodial activity, and that were high enough that they should not be affected by tight-

https://doi.org/10.1021/acs.jmedchem.1c00173
J. Med. Chem. 2021, 64, 6085−6136

Table 13. *Ex Vivo* Studies of *P. falciparum* and *P. vivax* Patient Isolates

	lab strains EC_{50} (μM)		*Pf* field isolates EC_{50} (μM)			*Pv* field isolates EC_{50} (μM)		
cmpd	3D7	Dd2	N	median (range)	median unbound	N	median (range)	median unbound
			Uganda					
1	0.0029 ± 0.0020 (35)	0.0029 ± 0.0016 (36)	483	0.0037 (0.00017−0.019)	0.00077*	NA	NA	NA
36	0.0062 ± 0.0031 (33)	0.0059 ± 0.0023 (32)	414	0.0098 (0.00023−0.040)	0.0020*	NA	NA	NA
79	0.0075 ± 0.0040 (9)	0.0069 ± 0.0026 (9)	182	0.011 (0.0011−0.028)	0.0031*	NA	NA	NA
			Brazilian Western Amazon Schizont maturation (SM)					
79	0.052 (0.015) SG, 0.086 (0.024) SM	NA	8	0.12 (0.077−0.25)	0.055**	6	0.12 (0.078−0.29)	0.033**
99	0.0080 (0.00084) SG, 0.020 (0.0021) SM	NA	5	0.060 (0.032−0.092)	0.0064**	11	0.044 (0.021−0.098)	0.0024**

[a]Median EC_{50} data are shown in micromolar with the range in parenthesis. For lab strains, the number of independent replicates is shown in parenthesis. For field isolates, *N* = number of patient samples studied. *Pf* Uganda lab strain and field isolates were assessed by standard SYBR Green (SG) assays using Albumax-based media.[32,34] Lab strains from the Brazilian study were assessed by either the standard SG assay or by the schizont maturation (SM) assay with lab strain parasites cultured in standard Albumax media and field isolates were cultured in 20% human serum-based media (see the Experimental Methods); unbound values are in parenthesis. Unbound values were calculated using the protein binding data from for *Albumax-based media (Table 9) or based on **McCoys or RPMI human serum-based media binding (Supporting Information Table S4C).

binding kinetics (e.g., **79**, *Pf*DHODH= 0.095 μM, *Pf*3D7 = 0.013 μM). To demonstrate that parasite killing was the result of on-target DHODH inhibition, we profiled compounds versus a *P. falciparum* D10 strain that has been transfected with yeast DHODH. This strain was previously reported to be resistant to both DHODH and cytochrome bc1 inhibitors; however, the two activities can be distinguished by restoration of sensitivity to bc1 inhibitors in the presence of proguanil.[30,31] Parasites expressing yeast DHODH were resistant to all tested compounds with or without proguanil, demonstrating that killing by **36**, **79**, and **99** was driven by DHODH inhibition (Table 12).

***P. berghei* Liver-Stage Activity.** *P. berghei* liver-stage assays were performed to test whether compounds could block the establishment of HepG2 liver-stage infection by sporozoites. All three tested compounds (**26**, **79**, and **99**) showed activity on *P. berghei* liver stage similar to that observed against *P. falciparum* asexual blood stages (Table 12). Importantly, as expected, these data confirm the good liver-stage activity of these compounds and the suitability of the DHODH target for the development of compounds for malaria prophylaxis.

***P. vivax*/*P. falciparum* Field Isolates.** Compound efficacy was assessed against *P. falciparum* and *P. vivax* field isolates in *ex vivo* studies. Compounds were tested against fresh *P. falciparum* parasite isolates collected from malaria patients in Uganda.[32] Using standard Albumax media and a 72 h SYBR Green microplate assay, compounds **36** and **79** showed potency similar to that observed for laboratory strains. Median EC_{50} values in the study were ~3-fold higher than those observed for **1** over a large sample size (Table 13 and Supporting Information Figure S5A), demonstrating that both DHODH inhibitors showed good activity against African isolates from the collection region. A good correlation in results was observed between DHODH inhibitors across the sample set, including for the **1** analogue DSM421,[33] with the exception that results for **1** and **36** showed a lower correlation than those for other pairs (Supporting Information Figure S5B).

A second series of studies compared efficacy against *P. falciparum* versus *P. vivax* field isolates. Because *P. vivax* cannot be cultured continuously, the alternative schizont maturation assay was used to determine compound potency. Field isolates were collected from patients in the Brazilian Amazon. The tested pyrrole-based compounds (**79**, **99**) showed equal activity against both *P. vivax* and *P. falciparum* field isolates (Table 13). These results predicted that, unlike **1**, pyrroles **79** and **99** would be expected to be equally effective for the treatment of either *P. falciparum* and *P. vivax* infections. EC_{50} values in this study were higher than those determined in Albumax-based media. When corrected for protein binding, similar potency was observed between the two assays in the study (Table 13). However, values for **79** were 3−7 higher for both lab strains and clinical isolates in this study than observed in other studies, e.g., *P. falciparum* lab strains (Table 5) or African field isolates (Table 13) using the SYBR Green assay, and were still higher in the schizont maturation assay. The reason for these differences is not understood.

Selection of Drug-Resistant Parasites. *In vitro* selections were performed to generate *P. falciparum* parasites resistant to **26** and **79**. These studies evaluated both the frequency by which resistance develops (minimum inoculum for resistance (MIR)) and the mechanism of resistance. **1** was used as a control in the selections to provide a comparator. In the first study, selections were performed with **26** and **1** versus Dd2 parasites at a range of starting inocula (10^6−10^9) and a dose of 4 × EC_{50} (0.030 μM for **1** and 0.025 μM for **26**). For **26** selections, recrudescent parasites were observed in all three wells or flasks that were cultured at each starting inoculum, whereas for **1**, only inoculum sizes of 10^7 or greater demonstrated recrudescence. In the past few studies, the MIR for **1** was between 10^6 and 10^7; therefore, the results from these current selections show a similar resistance propensity for both compounds.[15,35]

We proceeded to clone parasites by limiting dilution from nine bulk cultures and then PCR amplified and sequenced the *dhodh* gene. In total, 9 SNPs were found among the analyzed clones (Supporting Information Table S7A). Three of the four-point mutations that were selected by **1** have been previously reported (E182D, C276Y, and L531F[15,35−37]), while I272N was novel to this study. Notably, C276Y also emerged in a clinical efficacy study after treatment with **1**.[22] A distinct set of mutations were identified in the **26** selections (L172F, I272F, G535C, V532A, and F188I) consistent with the different binding modes of the two inhibitors (Figure 6A).

https://doi.org/10.1021/acs.jmedchem.1c00173
J. Med. Chem. 2021, 64, 6085−6136

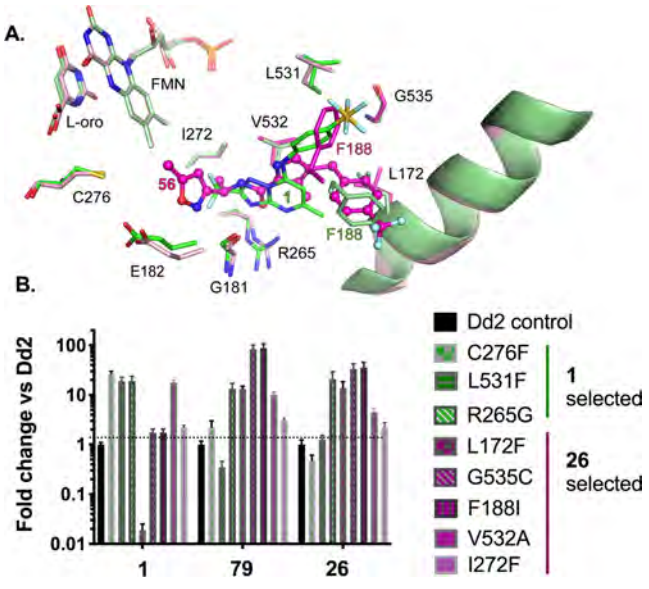

Figure 6. (A) Superimposed X-ray structure of **56** (PDB 7KYV) (pink) and **1** (PDB 4RX0) (green) showing residues involved in resistance mutations. The **56** ligand is displayed in ball and stick (bright pink), and **1** is displayed in sticks (bright green). (B) Differential effects of pyrrole (**26**) versus triazolopyrimidine (**1**) selected mutations in *Pf*DHODH on parasite EC_{50}. The plot shows a bar graph of the fold change (mean ± standard error of the mean (SEM)) in EC_{50} for mutant strains versus wild-type Dd2 parasites. Compounds used for EC_{50} determination are shown on the *X*-axis. The results for mutant lines that were selected using **1** are shown in green and those selected with **26** are shown in pink. Identified *Pf*DHODH mutations are defined in the figure legend. Data were taken from Supporting Information Table S7A. Data for C276F, L531F, and R265 were taken from the previously selected clone data, but were in good agreement with the newer clones showing the same mutations (e.g., F1B9 L531F).

Resistant clones were profiled to determine the EC_{50} shift for **1**, **26**, **79** and to test for cross-resistance to atovaquone (ATQ; Figure 6B and Supporting Information Table S7A). We also profiled previously reported[15,35] **1**-selected mutant Dd2 lines and C276F and C276Y CRISPR/Cas9-edited lines[35] (Figure 6B and Supporting Information Table S7A). Overall, we saw minimal cross-resistance between parasites selected for resistance to the triazolopyrimidine **1** versus the pyrroles **26** and **79**. Exceptions were the R265G and V532A mutations, both showing ∼10−30-fold higher EC_{50} values for all three compounds (Figure 6B and Supporting Information Table S7A). These findings are consistent with observations that R265 forms a key H-bond to all three inhibitors and that V532 is found in both the triazolopyrimidine and pyrrole binding pockets (Figures 3, 6A, and Supporting Information Figure S2). Increased sensitivity of mutant parasites to DHODH inhibitors was also observed when resistance was selected by the opposite scaffold. C276F/Y mutant parasites were 2−10-fold more sensitive to **26**, the L531F mutant was 3−4-fold more sensitive to **79**, and, most strikingly, the L172F mutant was 50-fold more sensitive to **1** (Figure 6B and Supporting Information Table S7A).

A tolerance phenotype was also observed for C276F versus **26** and **79**, and for C276Y versus **79** in some but not all experiments (Supporting Information Table S7 and Figure S6). Tolerance was defined by the observation of only a partial dose-response, with a fraction of cells (20−50%) remaining refractory to inhibition, leading to a plateau of incomplete inhibition at higher concentrations. The reason for the variability of this effect between studies is not understood. The EC_{50} values for **26** and **79** versus these mutants remained similar to wild-type, as determined in the studies where tolerance was not observed, or by fitting the data from the fraction of cells that remained sensitive in the case of tolerance (Supporting Information Figure S6). These results suggested that C276F/Y mutations do not directly impact binding of **26** and **79** to DHODH and that tolerance derives from a different mechanism. This hypothesis was supported by analysis of the effects of these mutations on recombinant *Pf*DHODH. The IC_{50} values for **26** and **79** measured on the C276F and C276Y *Pf*DHODH mutant enzymes were found to be similar to wild-type for C276Y and 2−3-fold lower (more potent) for C276F, whereas the IC_{50} values for **1** increased by 10−20-fold, similar to our previous report[35] (Supporting Information Table S7B).

In prior studies, we showed that DHODH **1**-selected resistant lines harboring point mutations showed full sensitivity to ATQ (previously reported clones, including C276F).[35] However, we also found that high-level amplification (∼12-fold) of the *dhodh* gene and surrounding regions was associated not only with resistance to DHODH inhibitors but with a tolerance phenotype toward ATQ.[38,39] For these reasons, we extended the analysis of ATQ sensitivity to our new **1** and **26**-selected parasite lines and to our CRISPR-edited C276F and C276Y lines. All of the **1** and **26**-selected lines, as well as the CRISPR-edited C276F and C276Y lines, retained full sensitivity to ATQ (Supporting Information Table S7A). A recent study also found that a CRISPR-edited C276F line retained sensitivity to ATQ.[40] However, this study also reported that a combination of *dhodh* gene amplification and the C176F mutation led to tolerance toward both ATQ and the triazolopyrimidine analogue DSM1. Thus, our studies and those of others have uncovered resistance mechanisms related to genetic changes at the *dhodh* locus that have unexpected consequences, for which a mechanistic understanding remains incomplete.

Mapping the selected mutations onto the X-ray structures bound to **1** and the **26**-analogue **56** shows that **1**-selected mutations with the exception of L531F are found primarily near the FMN-side of the pocket near the triazolopyrimidine and CF_2CH_3 portion of **1** (Figure 6A). In contrast, **26**-selected mutations tend to map to the aromatic-binding pocket of the pyrroles, although V532 is closest to the pyrrole/triazolopyrimidine ring pockets, explaining why it impacts both chemical series. On the pyrrole series, L172 forms a close interaction with the bridging carbon and or the cyclopropyl on the bridge and it is also within van der Waals interaction of the 6-position methyl on the triazolopyrimidine ring of **1**. Based on their positions, the L172F and F188I mutations could impact binding directly. Alternatively, these mutations may impact the dynamics of the mobile F188 residue that flips conformation when bound to **1**-series compounds compared to when bound to the pyrroles. F172 may stabilize F188 in the down position through extending the network of aromatic edge-to-face interactions, thus favoring binding of the triazolopyrimidines, while disfavoring the binding of the pyrroles and explaining the greater potency of **1** against cells harboring this mutation. Likewise, the F188I mutation may disrupt this dynamic equilibrium favoring the down position, thus disrupting the binding of the pyrrole-series compounds, while not impacting the binding of **1**.

In a second study, selections were performed to assess the **79** resistance profile. Selections with Dd2 parasites were performed across a range of starting inocula (10^6−10^9) at 4 × EC_{50} (EC_{50} =

https://doi.org/10.1021/acs.jmedchem.1c00173
J. Med. Chem. 2021, 64, 6085−6136

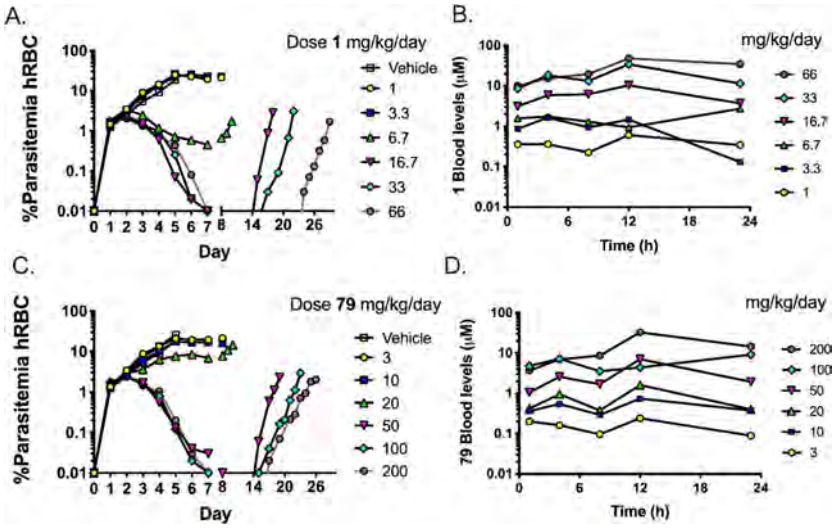

Figure 7. SCID mouse efficacy study of **1** (A, B) and **79** (C, D). Compounds were dosed orally twice a day (BID) for 6 days. Dose levels are expressed as mg/kg/day in the panel legends. **1** was dosed as the spray-dried dispersion formulation (SDD 25% drug load), but dose levels are reported as the free base equivalent. Panels (A) and (C) show %parasitemia of human infected red blood cells (hRBCs) versus time and panels (B) and (D) show compound blood concentrations versus time. One mouse was dosed per dose group for **1** and **79** and 2 mice were dosed for each vehicle control group. Efficacy parameters are reported in Table 14 and SCID pharmacokinetic parameters are reported in Supporting Information Table S10.

Table 14. Comparison of *In Vitro* Potency (3D7 Parasites) and (mg/kg/day) Mouse Efficacy Data for *Pf*DHODH Inhibitors

cmpd	3D7 EC_{50} (μM)	unbound 3D7 EC_{50} (μM)[¥]	ED_{90} (mg/kg/day)	blood AUC_{ED90} (μM·h)	^unbound AUC (μM·h)	blood C_{ED90} (μM)	unbound C_{ED90} (μM)
1	0.0060	0.0010	5.6 (5.4−5.9)	35	0.85	1.48	0.035
79	0.012	0.0034	26 (24−28)	36	4.1	1.48	0.17
99	0.0053	0.00056	<20	<16	<0.47	<0.67	<0.020

[a]Dosing was BID using a 6-day dosing model. Parasite levels, 24 h after the final dose, were used to determine the ED_{90}. For **1** and **79**, data in parentheses represent the 95% confidence interval of the fit. ^Unbound values were estimated based on measured mouse blood concentrations, mouse B/P, and normal mouse plasma protein binding data, with the exception of **1** where the B/P and binding were measured in infected SCID mouse blood and plasma, respectively, and found to be 1.8 and 98.3%. [¥]Unbound EC_{50} was determined using the Albumax binding data from Table 9. C_{ED90} is the average concentration (Cave) at the predicted dose that provides 90% parasite clearance.

0.013 μM). Parasites recrudesced in all flasks by day 30, similar to the results obtained for **26**. The **79**-selected parasites, however, showed only modest EC_{50} shifts (3−7-fold; Supporting Information Table S8A), and targeted sequencing of the *dhodh* gene revealed no SNPs. Whole-genome sequencing (WGS) of two bulk cultures identified a 2-fold amplification of a chromosomal segment harboring the *dhodh* locus (Supporting Information Table S8B), explaining the modest level of resistance. Selections were also performed with 3D7 parasites. Drug assays with two separately pressured bulk cultures (starting inocula 10^5−10^7 at 3 × EC_{50} (EC_{50} = 0.0088 nM)) showed 9−13-fold shifts in EC_{50} (Supporting Information Tables S8A). Parasites were cloned from both flasks, and three clonal lines were sent for WGS. This analysis identified a 4- or 5-fold amplification in the *dhodh* locus but no SNPs in the *dhodh* gene (Supporting Information Tables S8C). Both Dd2 and 3D7 parasites showed amplifications of nonidentical yet overlapping segments that in all cases included *dhodh*. We observed no SNPs common to Dd2 and 3D7 selections, arguing that the only causal resistance mediator was the *dhodh* amplification. These data were generated from Illumina sequencing with a 29- to 57-fold depth of genome sequence coverage for all clones and parental lines (Supporting Information Table S8D). The differing behavior of **79** in these selections compared to other DHODH inhibitors may suggest that it is harder to select for point mutations with **79**, resulting in smaller EC_{50} shifts when resistance does develop. Additional studies would be needed to confirm this result.

SCID Mouse Efficacy Studies. *In vivo* efficacy of **33**, **36**, **79**, and **99** was assessed using the previously reported *P. falciparum* SCID mouse model.[41] Early work on **33** and **36** used the published 4-dose once daily (QD) model, with efficacy parameters assessed one day after the final dose (Day 7). Later work on **79** and **99** used newer models that allowed parasitemia to be monitored for 60 days so that the day of recrudescence (DOR) could be determined. In this model, 6 days of twice daily (BID) dosing was employed to better mimic the human clinical setting where 8 days above the minimum inhibitory concentration (MIC) is the target to enable once weekly dosing of a prophylactic drug. Then, **79** was dosed in parallel to **1** as a comparator over an extensive dose range to establish the parameters with this newer model.

In the 4-day model, **33** and **36** were dosed at 10 and 50 mg/kg and both led to a reduction in parasitemia at both dose levels, although in no case were parasites cleared to below detectable limits (Supporting Information Figure S7 and Table S9A). Based on the limited dose levels, an ED_{90} (dose that clears 90% of parasites) could not be determined, but for **33**, the 10 mg/kg dose reduced parasitemia by 85%. Both the total and free AUC at this dose were similar to the AUCs measured for **2** in a prior study[20] at the approximate ED_{90}, although a dose of 50 mg/kg was required to achieve the same level of exposure as for **2**

https://doi.org/10.1021/acs.jmedchem.1c00173
J. Med. Chem. 2021, 64, 6085−6136

(Supporting Information Tables S9A,B). Thus, **33** appeared to have similar efficacy to **2**, while **36** performed less well.

The 6-day BID dosing study for **1** and **79** was performed at 5 dose levels to allow efficacy parameters to be fully delineated. Doses were selected for **1** based on previous studies and for **79** based on preliminary data showing that exposure in the SCID mouse was 3−5-fold lower than in wild-type mice. Both parasite clearance and the DOR were dose dependent (Figure 7 and Supporting Information Tables S10). Doses of 16.7 mg/kg/day for **1** and of 50 mg/kg/day for **79** provided the maximum rate of parasite killing and fully suppressed parasitemia by days 7−8 (Figure 7 and Supporting Information Table S10). The DOR ranged from 17 to 28 days across these same dose levels. PK sampling was taken throughout the 6 days of dosing and data were used to calculate efficacy parameters. The ED_{90} ranged from 5.6 mg/kg/day for **1** to 25.6 mg/kg/day for **79**, while the AUC_{ED90} and C_{ED90} (average blood concentration that prevents net parasite growth) were similar for the two compounds (AUC_{ED90} = 35 μM·h/day and C_{ED90} = 1.5 μM), but when comparing free concentrations, **1** was 5-fold more potent than **79** (Table 14). For **1**, both the AUC_{ED90} and ED_{90} were similar to the values obtained in our previous 4 dose BID study (AUC_{ED90} = 26 μM·h/day and ED_{90} = 3 mg/kg/day).[15]

In a separate study, the *in vivo* efficacy of **99** was assessed in this model at three dose levels (20, 50, and 100 mg/kg/day administered as 10, 25, or 50 mg/kg BID). **99** showed similar efficacy at 50 and 100 mg/kg/day compared to **79**, although it was superior at the lowest tested dose of 20 mg/kg/day (Supporting Information Figure S8 and Table S10). Because all three doses led to full parasite clearance during the 6 days of dosing, we were only able to estimate efficacy parameters. One caveat was that the parasite clearance rate observed for the 20 mg/kg/day dose of **99** was higher than for the other dose levels, and the reason for this difference is not currently understood (Supporting Information Figure S8).

Unbound AUC and Cave values were estimated based on normal mouse plasma protein binding data (Table 14), with the exception of **1** for which binding data were available for SCID mouse plasma. The most potent of the pyrroles **99** showed *in vivo* efficacy in the same concentration range as **1** (unbound C_{ED90} of <0.02 vs 0.035 μM), while **79** is about 10-fold less active based on this analysis (Table 14). The remaining compounds (**2**, **33**, and **36**) were assessed in a QD model but the data suggest that **2** and **33** have similar efficacy to **79**, while **36** was least effective (Table 14 and Supporting Information Table S9B). Generally, the rank order of potency based on the *in vivo* data mirrors that of the *in vitro Pf*3D7 data when corrected for protein binding (Table 14).

Significant differences in plasma exposure were observed for the pyrroles when dosed in the SCID mouse model versus wild-type Swiss OB mice (Supporting Information Table S11). Blood concentrations (as evaluated by average C_{max}/dose) in infected SCID mice were 3−5-fold lower than observed in the normal mouse (with the exception of **33**), with **79** showing the largest difference. These differences account for why the dose required to achieve ED_{90} for **79** in the SCID mouse model was nearly 5-fold higher than for **1**, despite showing a similar AUC_{ED90}. These observations suggest that clearance could be higher in the SCID mouse than in wild-type mice or that the bioavailability could be lower, but emphasize the importance of comparing effective concentrations rather than effective dose levels.

DISCUSSION

We have conducted an extensive lead optimization program to identify pyrrole-based inhibitors of *Pf*DHODH to deliver candidate drugs that could advance to preclinical development. Using a structure-based computational approach we explored modifications to all regions of the scaffold, allowing identification of a number of compounds with high potency against the *Plasmodium* enzymes and *P. falciparum* asexual blood stages. These compounds also showed species selectivity versus all tested mammalian enzymes, thus improving the properties of **1**. An additional seven coinhibitor DHODH structures were solved that supported the modeling effort. FEP+ calculations to predict potency and prioritize compounds for synthesis showed a good correlation with the measured values, validating the approach. Key compounds from the series were also tested against field isolates and unlike **1**, were shown to have equal efficacy against both *P. falciparum* and *P. vivax* isolates, representing an additional point of superiority over **1**. Finally, the frontrunners **79** and **99** had equivalent efficacy on *P. berghei* liver stages designed to assess effects on the formation of the schizont in liver cells after incubation with sporozoites, supporting their use for malaria prophylaxis.

Resistance studies were performed with **26** and **79** to evaluate both the propensity for resistance to develop and to determine if resistant mutations would share overlapping resistance profiles with **1**. The MIR was similar for **26**, **79**, and **1**, however, while selections to both **26** and **1** led to 20−40-fold shifts in EC_{50} driven by binding site mutations, selections with **79** led to only modest levels of resistance, attributed to gene amplification events. Interestingly, the set of point mutations that was selected by pressure with **26** was different compared to those selected by **1** and most mutations did not lead to cross-resistance between the two different scaffolds, reflective of their different binding modes. One **26**-derived mutation actually led to significantly increased sensitivity to **1**, in a mechanism that may involve stabilization of a normally dynamic and flexible residue (F188) into the conformation that promotes binding of **1** over **26**.

Compounds that showed good *in vitro* potency against *Pf*DHODH, *Pf*3D7 asexual blood stages, and *P. berghei* liver stages were evaluated to determine if they had the properties that would support good *in vivo* efficacy. Physicochemical properties and *in vitro* metabolic stability were evaluated first and potent analogues with good properties in these assays were advanced to further *in vitro* and *in vivo* studies, including mouse and rat PK and SCID mouse efficacy studies. Five compounds were extensively profiled and of these, three showed the liability of time-dependent CYP inhibition (**26**, **33**, and **36**), which was an issue that had previously been identified for **2**. However, two compounds were identified without this liability (**79** and **99**). The addition of the cyclopropyl on the bridging carbon was likely a factor in eliminating time-dependent CYP inhibition. Both **79** and **99** also had superior physicochemical properties and both showed good exposure *in vivo* in mice and rats. Both compounds had similar clearance in rats compared to **1** but had a lower volume of distribution, and therefore a shorter half-life, which likely suggests that they will also have a shorter half-life than **1** in humans. Further studies in other species (e.g., dogs) are needed to address this issue. **79** and **99** exhibited good solubility in simulated gastric and intestinal fluids, which represented another key superiority over **1**. This would be expected to translate to simplified formulation approaches compared to **1**. Finally, the *in vivo* SCID mouse efficacy studies

https://doi.org/10.1021/acs.jmedchem.1c00173
J. Med. Chem. 2021, 64, 6085−6136

also demonstrated that **79** and **99** had good *in vivo* antiparasitic activity with **99**, showing effectiveness similar to that of **1**. While **79** was less potent *in vivo*, it has a lower Log *P* and better physicochemical properties, and so also remains a promising compound.

CONCLUSIONS

Lead optimization of a pyrrole-based series of DHODH inhibitors identified initially by target-based screening was performed using a structure-based approach with a significant computational design. Potent analogues with good activity against parasite enzymes and parasites *in vitro* and *in vivo* were identified. These compounds also had very good species selectivity, illustrated by activity against all *Plasmodium* strains and DHODH enzymes, while not showing activity against mammalian enzymes. Additionally, no significant safety signals were identified in preliminary studies. Two compounds (**79** and **99**) showed particular promise in having improved ADME and PK properties compared to earlier compounds in the series. The overall properties of these new *Plasmodium* DHODH inhibitors support progression into advanced stages of late-lead development to assess preliminary safety and human dose predictions for prophylaxis. These data would be key to determining whether one or both have preclinical candidate quality and might move forward into preclinical development for the prevention of malaria.

EXPERIMENTAL SECTION

Materials. Routine chemicals were sourced from Sigma-Aldrich unless otherwise stated.

DHODH Protein Expression and Purification. BL21-DE3 *E. coli* phage-resistant cells were used to express and purify the various DHODH proteins described in the study. Expression constructs encoding the soluble DHODH domain have been previously described: *Pf*DHODH[42,43] and *Pv*DHODH[14] (N-terminal His_6-tagged DHODH-pRSETb), human DHODH (pET22b C-terminal tag)[43] and rat/mouse/dog DHODHs[15,44] (pET28b C-terminal tag). *Pf*DHODH mutant enzymes C276F and C276Y were previously described.[35] Proteins were purified by HisTrap HP column chromatography, followed by gel-filtration chromatography on a Pharmacia HiLoad 16/600 Superdex 200 column, as previously described,[20] yielding purity >95% based on sodium dodecyl sulfate polyacrylamide gel electrophoresis (SDS-PAGE) analysis. Absorbance at 280 nm was used to determine DHODH concentration based on the ProtParam in ExPASy calculated extinction coefficients as previously described.[45]

Kinetic Analysis of DHODH Inhibition. DHODH activity was monitored in a steady-state assay using the 2,6-dichloroindophenol (DCIP) method at 25 °C in an assay buffer (100 mM HEPES, pH 8.0, 150 mM NaCl, 10% glycerol, 0.1% Triton X-100 reduced, 20 μM CoQD, 200 μM L-DHO, 120 μM DCIP, and 5−20 nM enzyme) as described[45] with the exception of the mutant enzyme analysis which was done using the direct assay as described.[35] The 50% inhibitory concentration (IC_{50}) for each compound was determined over a concentration range of 0.001−100 μM in a 3-fold dilution series. A 100X dilution series was first prepared in dimethyl sulfoxide (DMSO) from an initial 100 mM stock yielding a final DMSO concentration in the assay of 1%. Triplicate rate data were collected at each inhibitor concentration. IC_{50} values were determined by fitting the data to log (inhibitor) vs response equation $Y = \text{bottom} + (\text{top} - \text{bottom})/(1 + 10 \text{ ^ } ((X - \text{Log IC}_{50})))$ in GraphPad Prism.

P. falciparum Growth and Inhibition Assays. P. falciparum cells were maintained in continuous culture using human blood type O+ or A+ erythrocytes (Valley Biomedical or Interstate Blood Bank, TN) at 2% hematocrit and culture media constituting of RPMI 1640 medium (Gibco-R4130) 1640+HEPES and 0.5% Albumax-I (Gibco), supplemented with sodium bicarbonate (23 mM) and hypoxanthine (92 μM). For drug-resistant *P. falciparum* lines in the Fidock lab, the drug was used during selections but was not added for routine maintenance of clonal lines after that point. In the Rathod lab, **1**-resistant parasite lines were maintained in the presence of **1** at the concentration of its selection and **1** was removed 4 days (2 culture passages) prior to the EC_{50} study. For EC_{50} determination, cultures were diluted to 0.5% starting parasitemia at 2% hematocrit. Compound stocks were made in DMSO (30−100 mM) and these were used to generate DMSO dilution series in triplicate for dispensing onto assay plates (either 96 or 384 well plate format), resulting in a final constant DMSO concentration of 0.2% over a range of inhibitor concentrations (0.0003−30 μM depending on the compound) in the final well. Plates were incubated for 72 h at 37 °C in 5% CO_2, 5% O_2, 90% N_2 in 80% humidity, sealed in aluminum foil, and stored at −80 °C for 24 h. Parasite growth was assessed using the SYBR Green method,[34,46] which measures fluorescence (ex./em. 485/535nm) as the output or alternatively by labeling parasites with SYBR Green I and MitoTracker Deep Red and measuring parasitemia using an Accuri C6 flow cytometer.[47] Data were fitted to the log(inhibitor) vs response—Variable slope (four parameters) equation model to determine the 50% effective concentration (EC_{50}) values for parasite growth inhibition.

Growth Assays on P. falciparum and P. vivax Clinical Isolates. Uganda Field Isolates. Field isolates were collected and analyzed for *ex vivo* drug sensitivity using a standard 72 h SYBR Green microplate assay in Albumax-based media, as previously described.[32]

Human Subjects Approval. The study was approved by the Makerere University Research and Ethics Committee, the Uganda National Council for Science and Technology, and the University of California, San Francisco Committee on Human Research. Informed consent was obtained from patients and/or primary caregivers (depending on age).

Sample Collection. Participants over 6 months of age presenting at the outpatient clinics of Tororo District Hospital, Tororo District or Masafu General Hospital, Busia District with clinical suspicion for malaria and a positive Giemsa-stained blood film for *P. falciparum* and without signs of severe disease were enrolled after written informed consent, from December 2015 through October 2020. Parents or guardians of children provided written consent on their behalf. Assent was sought from children 8−17 years old. Patients expressing the use of antimalarial treatment within the previous 30 days were excluded. Second, from December 2015−January 2018, children enrolled in a clinical trial (registered at ClinicalTrials.gov [NCT02163447]) comparing monthly versus every 3-month intermittent therapy with dihydroartemisinin-piperaquine to prevent malaria provided samples if they presented to the study clinic at the Tororo District Hospital with uncomplicated malaria. Blood was collected in a heparinized tube before initiation of therapy. Subjects were treated with artemether-lumefantrine, following national guidelines, after sample collection.

Center of Malaria Control from Rondônia, Brazilian Amazon (CEPEM): Ethical approval. The study received approval from the Ethics Committee from the Centro de Pesquisa em Medicina Tropical-CEPEM-Rondônia (CAAE 61442416.7.0000.0011) dated March 21st, 2017. All participants signed a written informed consent before blood collection.

Sample Collection. P. falciparum and *P. vivax* isolates were collected in February and July 2019 from patients recruited at the Center of Malaria Control (CEPEM) in the city of Porto Velho, state of Rondônia, in the Brazilian Western Amazon. Only monoinfected patients with either *P. falciparum* or *P. vivax*, with parasitemia between 2000 and 80 000 parasites/μL and with at least 70% of ring-stage parasites were recruited. Patients who used any antimalarial drug in the previous month and/or presented severe symptoms of malaria were excluded from this study.

Schizont Maturation (SM) Assay. For the maturation of parasites, rings to schizonts, plates containing parasites and compounds in the concentration tests were maintained in a hypoxia incubator chamber (containing 5% O_2, 5% CO_2, and 90% N_2) at 37 °C for different incubation times (40−52 h for *P. vivax* and 40−56 h for *P. falciparum*) and assays were conducted as described.[48] Briefly, compound stocks

https://doi.org/10.1021/acs.jmedchem.1c00173
J. Med. Chem. 2021, 64, 6085−6136

were made in DMSO (20 mM) and used to generate DMSO dilution series for dispensing onto 96 wells assay plates in a range of concentrations (0.048−1 μM, depending on the compound) in the well. Purified parasites from patient isolates were maturated in complete medium RPMI 1640 medium plus 20% AB human serum for *P. falciparum* samples or McCoy's 5A medium plus 20% AB human serum for *P. vivax* samples. Incubations were stopped when 40% of rings reached the schizont stage (at least three distinct nuclei per parasite) in inhibitor-free control wells. The number of schizonts per 200 asexual stage parasites was determined by thick blood films (stained with 5% Giemsa solution for 30 min) for each inhibitor concentration and then normalized to inhibitor-free control wells (considered as 100%). Half-maximal drug inhibitory response (EC_{50}) was determined by curve fitting using software (OriginLab Corporation, Northampton, MA). As controls, EC_{50}'s were also determined in standard SYBR Green assays or in the above SM assay for *P. falciparum* parasites cultured in Albumax-supplement RPMI 1640 media (described above).

P. berghei Liver-Stage Assays. *P. berghei* liver-stage assays were performed by the Winzeler lab, as previously described.[10,49] Briefly, *P. berghei*-ANKA-GFP-Luc-SMCON (Pb-Luc) sporozoites were used to infect HepG2-A16-CD81EGFP cells for this assay. Assay media (DMEM without phenol Red (Life Technology, CA) supplemented with 5% FBS, 1.45 mg/mL glutamine, 500 units of penicillin, and 500 μg/mL streptomycin) was used for the *Pbluc* and *HepG2tox* assays.

*Selection of **1**, **26**, and **79** Resistant Parasites.* The propensity for Dd2 *P. falciparum* parasites to develop resistance to **26** was evaluated by the selection of resistant parasites under continuous drug pressure at 4 × EC_{50}, as described previously.[15,50] Starting parasite inoculums from 10^6−10^9 were used to allow determination of the minimum inoculum for resistance (MIR) versus **1** as a control with n = 3 flasks per condition. Parasites recrudesced between day 20 and 30, except for parasites seeded at 10^6 inoculum that took longer to come back. All flasks selected for resistance to **26** recrudesced, whereas for **1**, recrudescence was only observed with inoculum sizes of $>10^7$ recrudesced. From a total of 21 resistant bulk cultures to **1** and **26**, 9 were selected for cloning. Clones were profiled to determine the EC_{50} shift for **1**, **26**, and **79** and to test for cross-resistance to atovaquone (ATQ). The *dhodh* gene was sequenced by PCR as described,[9] and 9 SNPs were found among the analyzed clones (Table S6).

Selections for 79 resistant parasites were performed similarly to above on both *P. falciparum* Dd2-B2 (EC_{50} = 0.013 μM) and 3D7 (EC_{50} = 0.0088 μM) cells using starting parasite inoculums Dd2 (10^6−10^8) and 3D7 (10^5−10^7) and drug concentrations of 0.055 and 0.036 μM, respectively. With the Dd2 selections, the parasites cleared by day 14 at all inocula and recrudesced in all flasks by day 30. In 3D7 selections, parasites cleared from the **1** selections in both inocula but recrudescence was only observed for the 10^7 inocula. For the **79** selections, 0.036 μM **79** was not sufficient to clear parasites; therefore, the concentration was increased in 20% increments until 0.11 μM was reached. Targeted Sanger sequencing of the *dhodh* gene was performed as described above but as this did not identify mutations, we performed whole-genome sequencing (WGS) to evaluate both gene copy numbers and to identify other SNPs that might contribute to the resistance phenotype. To generate these WGS data, the samples were pooled and sequenced on an Illumina MiSeq to obtain 300 bp paired-end reads.[51] These reads were aligned to the *P. falciparum* 3D7 genome (PlasmoDB version 36) using BWA (Burrow-Wheeler Alignment). PCR duplicates and unmapped reads were filtered out using Samtools and Picard. The reads were realigned around indels using the GATK RealignerTargetCreator and base quality scores were recalibrated using GATK Table-Recalibration. The GATK HaplotypeCaller (version 4.1.7) was used to identify all possible single nucleotide variants (SNVs) in clones, which were filtered based on quality scores (variant quality as a function of depth QD > 1.5, mapping quality > 40, min base quality score > 18), read depth (depth of read > 5) to obtain high-quality SNPs that were annotated using snpEFF. IGV was used to visually verify the SNP's presence in the clones. BicSeq was used to discover copy number variants (CNVs). Gene IDs are provided from PlasmoDB (https://plasmodb.org/plasmo/).

X-ray Crystallography. Loop truncated *Pf*DHODH (pET28b-TEV- *Pf*$DHOD_{\Delta 384\text{-}413}$) was used for crystallization based on prior findings that the truncation improves crystallization.[52,53] *Pf*$DHOD_{\Delta 384\text{-}413}$ was expressed and purified from *E. coli* BL21 phage-resistant cells (NEB, C252H) transfected with the expression vector. The protein was purified by Ni^{+2}-column chromatography and Gel-filtration as described above. Purified protein was concentrated to 20 mg/mL in buffer containing a detergent (20 mM HEPES pH 7.8, 20 mM NaCl, and 2 mM *n*-dodecyl-*N*,*N*-dimethylamine-*N*-oxide (LDAO, Anatrace), and 10 mM DTT), and stored at −80 °C.

*Crystallization and Data Collection of Pf$DHODH_{\Delta 384\text{-}413}$ Cocrystallized with **18**, **56**, **127**, **79**, **81**, **86**, and **47**.* Preliminary crystallization conditions were found using random crystallization screen *Cryos* suite (Qiagen), Crystal screen 2 (Hampton Research). Hit conditions were then optimized by variation of pH, precipitant, and protein concentrations. Crystals grew in the following conditions: **18** from 0.17 M ammonium acetate, 0.085 M sodium citrate pH 5.6, 25.5% v/v PEG4000, and 15% v/v glycerol; **56** from 0.16 M Ammonium sulfate, 18% v/v PEG4000, 0.1 M sodium acetate pH 5.1, and 24% v/v glycerol; **127** from 0.085 M HEPES pH 7.5, 8.5% 2-propanol, 17% v/v PEG4000, and 15% v/v glycerol; and, **79**, **81**, **86**, and **47** from 0.05 M $MgCl_2$, 28% v/v PEG4000, and 0.1 M Tris-HCl, pH 8.8. The later four crystals were first obtained as clusters and single crystals of these inhibitors in complex with *Pf*$DHODH_{\Delta 384\text{-}413}$ grew only after seeding. All crystallizations were setup using hanging drop vapor diffusion at 20 °C from an equal volume mixture of reservoir solution and *Pf*$DHODH_{\Delta 384\text{-}413}$ (20 mg/mL) pre-equilibrated with 1 mM inhibitor and 2 mM dihydroorotate (DHO).

Diffraction data were collected at 100 K on beamline 19ID at Advanced Photon Source (APS) using an ADSC Q315 detector. For the *Pf*$DHODH_{\Delta 384\text{-}413}$-**18** crystal, 540 images (0.3°/image) were collected and the crystal diffracted to 2.15 Å in a space group of $P2_12_12_1$ with the cell dimension of a = 92.2, b = 97.5, and c = 186.3. For *Pf*$DHODH_{\Delta 384\text{-}413}$-**56**, 360 images (0.5°/image) were collected and the crystal diffracted to 2.4 Å in space group P64 with the cell dimension of $a = b$ = 85.3, and c = 139.2. For *Pf*$DHODH_{\Delta 384\text{-}413}$-**127**, 400 images (0.5°/image) were collected and the crystal diffracted to 2.0 Å in space group $P2_12_12_1$ with the cell dimension of a = 93.1 b = 97.3, and c = 186.9. For *Pf*$DHODH_{\Delta 384\text{-}413}$-**79**, 500 images (0.5°/image) were collected and the crystal diffracted to 1.75 Å in space group $P2_1$ with the cell dimension of a = 51.9, b = 158.0, and c = 63.2. For *Pf*$DHODH_{\Delta 384\text{-}413}$-**81**, 400 images (0.5°/image) were collected and the crystal diffracted to 1.75 Å in space group $P2_1$ with the cell dimension of a = 51.4, b = 158.2, and c = 62.6. For *Pf*$DHODH_{\Delta 384\text{-}413}$-**86**, 400 images (0.5°/image) were collected and the crystal diffracted to 1.60 Å in space group $P2_1$ with the cell dimension of a = 50.1, b = 158.0, and c = 61.1. For *Pf*$DHODH_{\Delta 384\text{-}413}$-**47**, 400 images (0.5°/image) were collected and the crystal diffracted to 1.97 Å in space group $P2_1$ with the cell dimension of a = 52.1, b = 158.3, and c = 62.8. Diffraction data were integrated and intensities were scaled with the HKL2000 package.[54]

Structure Determination and Refinement. Crystallographic phases for *Pf*DHODH inhibitor complexes were solved by molecular replacement with Phaser[55] using PDB ID 3I65[53] as the search model. Structures were rebuilt with COOT[56] and refined with phenix.refine.[57] Refinement statistics are provided in Supporting Information Table S3. For all structures, all amino acid residues were within the allowed section of the Ramachandran plot as defined by MolProbity.[58]

Pf$DHODH_{\Delta 384\text{-}413}$-**18** was refined to R_{work} and R_{free} of 0.182 and 0.224, respectively. Four molecules were found in an asymmetric unit. Electron density was observed for the following residues: Chain A: 158−378, 414−566, and 2 amino acids (Asp and Pro) from the N-terminal-His tag linker, Chain B: 160−378 and 414−566, Chain C: 163−378 and 414−566, and Chain D: 161−377 and 414−566. Three hundred and thirty-five water molecules were modeled into the structure using phenix.refine.

Pf$DHODH_{\Delta 384\text{-}413}$-**56** was refined to R_{work} and R_{free} of 0.180 and 0.199, respectively. A twinning operator (*h*,-*h*-*k*, -*l*) was applied during the refinement. One molecule was found in the asymmetric unit and the refined structure contains amino acid residues 162−383 and 414−566.

https://doi.org/10.1021/acs.jmedchem.1c00173
J. Med. Chem. 2021, 64, 6085−6136

Forty-two water molecules were modeled into the structure using phenix.refine.

*Pf*DHODH$_{\Delta 384\text{-}413}$-**127** was refined to R_{work} and R_{free} of 0.163and 0.207, respectively, with 4 molecules in an asymmetric unit. Electron density was observed for: Chain A: 158−377, 414−566, and 2 amino acids (Asp and Pro) from the N-terminal-His tag linker, Chain B: 167−377 and 414−566, Chain C: 160−377 and 414−566, and Chain D: 161−378 and 414−566. Four hundred and eighty-six water molecules were modeled into the structure using phenix.refine.

*Pf*DHODH$_{\Delta 384\text{-}413}$-**79** was refined to R_{work} and R_{free} of 0.172 and 0.207, respectively, with 2 molecules in an asymmetric unit. Electron density was observed for: Chain A: 159−383 and 414−566 and Chain B: 159−376, 414−566, and 7 amino acids (His, His, His, Ala, Glu, Asn, and Leu) from the N-terminal His tag linker. Four hundred and fifty-five water molecules were modeled into the structure using phenix.refine.

*Pf*DHODH$_{\Delta 384\text{-}413}$-**81** was refined to R_{work} and R_{free} of 0.165 and 0.204, respectively, with 2 molecules in an asymmetric unit. Electron density was observed for: Chain A: 159−383, 414−566, and 6 amino acids (His, His, His, Ala, Glu, and Asn) from the N-terminal His tag linker. Chain B: 159−377, 414−566, and 6 amino acids (His, His, His, Ala, Glu, and Asn) from the N-terminal His tag linker. Four hundred and seventy-two water molecules were modeled into the structure using phenix.refine.

*Pf*DHODH$_{\Delta 384\text{-}413}$-**86** was refined to R_{work} and R_{free} of 0.164 and 0.188, respectively. There are 2 molecules in an asymmetric unit. Electron density was observed for: Chain A: 159−377 and 414−566 and Chain B: 159−383, 414−566, and 6 amino acids (His, His, His, Ala, Glu, and Asn) from the N-terminal His tag linker. Six hundred and sixteen water molecules were modeled into the structure using phenix.refine.

*Pf*DHODH$_{\Delta 384\text{-}413}$-**47** was refined to R_{work} and R_{free} of 0.179 and 0.213, respectively, with 2 molecules in an asymmetric unit. Electron density was observed for: Chain A: 159−383, 414−566, and one amino acid (Pro) from the N-terminal His tag linker. Three hundred and sixteen water molecules were modeled into the structure using phenix.refine.

Computational Modeling. Compound Structure Preparation. Compound ideas considered in this work were built with Seurat, LiveDesign, Maestro (Maestro, Schrödinger, LLC, New York, NY, 2020), or generated by reaction-based enumeration scripts; tautomer enumeration and protonation state assignment at experimental pH was performed using LigPrep. When enumeration produced many candidate compounds, compounds were triaged with WScore docking, before moving to FEP+ simulations.

Protein Structure Preparation. Published in-house *Pf*DHODH structures in complex with inhibitors[14,15,20,33,44,52,53,59] were used as the starting point for computational studies. We hypothesized that the distinctive orientation F188 side chain observed in the **3** (6VTN) cocrystal[20] was a feature attributed to the pyrrole series that we were targeting for optimization and, thus, we biased WScore protein structure selection to proteins with that conformation (PDB files: 6VTY, 6VTN, and 3O8A). Initial studies and most FEP+ modeling were performed with 6VTY, bound to an ester pyrrole analogue of **3**. The structure of **3** (6VTN) and other analogues bound to *Pf*DHODH were used as they became available to evaluate pose "fit" plausibility. As we added to the catalog of crystal structures in this series, the structure bound to **18** was considered for larger membrane-side perturbations. Protein coordinates were prepared for computational studies with the Protein Preparation Wizard. This involved adding hydrogen atoms, filling in missing side chains, assigning the proper ionization state for both the amino acids and cocrystallized ligand at physiological pH.

WaterMap. WaterMap[60−62] was used to profile the location and thermodynamics of waters within *Pf*DHODH complexes. Proteins were prepared with the Protein Preparation Wizard. WaterMap was run in the default mode; the cocrystallized ligands associated with each protein were used to define the binding site area and were removed during the MD simulations of the water structure. WaterMap results were used to rationalize previously generated SAR and hypothesize new opportunities against which to design, score, and synthesize new compound ideas.

WScore. WScore is a docking and scoring methodology[63,64] that was used to incorporate the water structure from WaterMap to provide an atomic-level description of ligand and protein desolvation. The scoring function also integrates and MM-GBSA score component. An ensemble of receptors is used to take into account receptor conformation and protein reorganization. WScore ensemble docking and score were used to triage enumerated compounds and choose compounds to profile with FEP+.

FEP+ Calculations. FEP+, free-energy perturbation (FEP+) methodology, from Schrödinger Suite was used to predict relative binding free energies of *Pf*DHODH ligand complexes as described.[60,65−70] Briefly, a series/set/ensemble of molecular dynamics simulations were performed, as implemented in Desmond[71] (Desmond Molecular Dynamics System, D. E. Shaw Research, New York, NY, 2020. Maestro-Desmond Interoperability Tools, Schrödinger, New York, NY, 2020) and running on GPU to ensure speed and accuracy. The atoms of the small molecule perturbed undergo replica exchange with solute tempering (REST) to ensure good sampling and a cycle closure correction is applied to calculate free-energy estimates relative to one or more reference compounds. Retrospective studies were used to establish baseline protocols for the simulation time and the number of lambda windows used to profile new ideas. Typically, the length of the simulation was increased to 20 ns per lambda window to improve sampling.

Software Version. Schrödinger Release 2015-3, Schrödinger, LLC, New York, NY, 2015, was the starting point, but we used new releases as they became available.

Structure Display and Analysis. MacPyMOL: PyMOL v2.1 enhanced for Mac OS X (Schrödinger LLC) was used to display and render structures and the align command was used to generate structural alignments.

Protein Binding and Physicochemical Measurements. Methods used to assess solubility in biorelevant media (FaSSIF, FeSSIF, and FaSSGF), binding to proteins in various media (plasma, microsomes, and *in vitro* assay media), and whole blood-to-plasma partitioning ratios were performed as described previously.[28] Log $D_{7.4}$ values were calculated using the Chem Axon chemistry cartridge via JChem for Excel software (version 16.4.11).

In Vitro Metabolism. Compounds (1 μM) were incubated for up to 60 min at 37 °C with human, mouse, or rat liver microsomes (Xenotech LLC, Kansas City, KS) at a protein concentration of 0.4 mg/mL with an NADPH regenerating buffer system as described previously.[20] Selected compounds (1 μM) were also incubated with cryopreserved hepatocytes (Xenotech) suspended in Krebs−Henseleit buffer at a cell density of 0.5×10^6 viable cells/mL for up to 4 h. Cell count and viability were determined using the Trypan Blue exclusion method at the start and end of the incubation. The samples were taken from both the microsome and hepatocyte incubations periodically and quenched with acetonitrile containing internal standard and loss of substrate was monitored by liquid chromatography−mass spectrometry (LC-MS) (Waters Xevo G2QTOF coupled to a Waters Acquity UPLC operating in positive electrospray ionization under MS^E mode). Degradation half-life and *in vitro* intrinsic clearance values were calculated from the apparent first-order degradation rate constants.

Caco-2 Permeability Assays. Permeability of compounds across confluent Caco-2 cell monolayers was conducted as described previously.[28] Briefly, experiments were performed using pH 7.4 Hanks balanced salt solution containing 20 mM HEPES in both the apical and basolateral chambers. Donor solutions were prepared by spiking a DMSO stock solution into transport buffer (10 μM) with the final DMSO concentration maintained at 0.1% v/v. Compound flux was assessed in both the apical to basolateral (A−B) and B−A directions over 120 minutes, with samples taken from the donor chamber at the start and end of the experiment and from the acceptor chamber at multiple time points. Compound concentrations were assessed by LC/MS and control compounds were included to confirm monolayer integrity, passive permeation, and Pgp functionality. The apparent permeability coefficient was calculated from the linear slope of the flux

https://doi.org/10.1021/acs.jmedchem.1c00173
J. Med. Chem. 2021, 64, 6085−6136

profile, taking into account the initial donor concentration and the surface area.

Cytochrome P450 Inhibition and Time-Dependent Inhibition Studies. CYP inhibition assays were performed utilizing a substrate-specific interaction approach as described previously.[20] The "IC_{50} shift"-method was used to assess whether compounds showed time-dependent CYP inhibition in human liver microsomes also as previously described.[20]

Animal Studies. Ethical review of all animal studies was undertaken in accordance with either the Australian Code of Practice for the Care and Use of Animals for Scientific Purposes (mouse and rat PK studies) or European Directive 2010/63/EEC (SCID mouse efficacy studies). Human blood samples for the SCID mouse studies were sourced ethically and their research use was in accord with the terms of the informed consents under an IRB/EC approved protocol. Animal experiments performed at the Swiss Tropical and Public Health Institute (Basel, Switzerland) adhered to local and national regulations of laboratory animal welfare in Switzerland (awarded permission no. 2303). Protocols are regularly reviewed and revised following approval by the local authority (Veterinäramt Basel Stadt). Animal experiments were performed at The Art of Discovery (TAD) were approved by The Art of Discovery Institutional Animal Care and Use Committee (TAD-IACUC). This Committee is certified by the Biscay County Government (Bizkaiko Foru Aldundia, Basque Country, Spain) to evaluate animal research projects from Spanish institutions according to point 43.3 from Royal Decree 53/2013, from the 1st of February (BOE-A-2013-1337).

Mouse and Rat Pharmacokinetic (PK) Studies. PK studies were performed in male Sprague Dawley rats and male Swiss outbred mice. Studies were reviewed and approved by the Monash Institute of Pharmaceutical Sciences Animal Ethics Committee. Intravenous dosing (IV) to rats was administered in a saline vehicle containing 5−10% (v/v) DMSO and 2−4% (v/v) Solutol HS 15 administered at a volume of 1 mL as a 10 min infusion into the jugular vein via a surgically implanted catheter. In mice, the IV dose was administered as a bolus injection (2 mL/kg) into the tail vein using the same vehicle. Oral doses to rats and mice were administered by gavage in an aqueous suspension vehicle (0.5% (w/v) carboxymethyl cellulose, 0.4% (v/v) Tween-80 and 0.5% (v/v) benzyl alcohol (10 mL/kg)). Blood was collected up to 24 h postdose into heparin-containing tubes. A maximum of three blood samples was collected from each mouse, with 2−3 mice per time point. For rats, sequential sampling over the complete time period was conducted with 3 rats per dosing group. Following centrifugation, the plasma fraction was transferred to clean tubes after centrifugation and protein was precipitated with acetonitrile (2:1 volume ratio). The supernatant was analyzed to determine plasma drug concentrations by LC-MS against calibration standards prepared in blank rat or mouse plasma and extracted in the same way. Diazepam was added as an internal standard for all plasma samples and calibration standards (prior to protein precipitation). Analysis was performed on a Waters Xevo TQ mass spectrometer coupled to a Waters Acquity UPLC operating in a positive electrospray ionization multiple-reaction monitoring mode using a Supelco Ascentis Express RP amide column (50 mm × 2.1 mm, 2.7 μm) with a mobile phase that consisted of an acetonitrile−water gradient with 0.05% formic acid, a gradient cycle of 4 min, and a flow rate of 0.4 mL/min.

For mice, noncompartmental PK data analysis was based on the mean concentration versus time profile for each dose route, given that sequential sampling (i.e., a complete concentration vs time profile) was not conducted in each animal. For rats, sequential sampling in each animal was conducted and the profile for each rat was assessed using noncompartmental analysis. Rat PK parameters were then averaged for each dosing group to provide a mean and standard deviation.

SCID Mouse *P. falciparum In Vivo* Efficacy Studies. *Studies Conducted at Swiss TPH.* Compound efficacy *in vivo* was evaluated in the murine *P. falciparum* SCID model essentially as described.[41] **33** and **36** were formulated in a vehicle (70% Tween-80 and 30% ethanol, followed by a 10-fold dilution in water) and administered to age-matched female immunodeficient NOD-scidIL2Rγnull mice (NSG) (The Jackson Laboratory, Bar Harbor, ME) (20−22 g) that had been engrafted for 11 days with human erythrocytes (generously provided by the Blood Bank in Zürich, Switzerland). Mice were infected intravenously on day 0 with *P. falciparum* Pf3D70087/N9-infected erythrocytes (2×10^7). On day 3 postinfection parasitemia was 0.75−1.5%, and mice ($n = 2$) were randomly distributed to treatment groups and administered compound or vehicle control once a day for 4 consecutive days by oral gavage (10 mL/kg). Parasitemia was measured by flow cytometry and the %parasitemia is expressed as the %infected human erythrocytes as determined using the previously described methods.[72,73] Efficacy parameters (ED_{90} and AUC_{ED90}) were determined on Day 7, one day after the last dose.

Studies Conducted at the Art of Drug Discovery (TAD). NSG mice engrafted with human erythrocytes (>40% of human erythrocytes in peripheral blood) as described above but sourced from Charles River (France) were intravenously infected with Pf3D70087/N9-parasitized red blood cells 72 h before drug treatment. On study day 1, mice had between 1−2% parasitemia on average and were randomly allocated to selected treatments. **1** and **79** were administered orally BID at six dose levels for 6 days (**1**: 0.5, 1.67, 3.3, 8.3, 16.7, and 33 mg/kg and **79**: 1.5, 5, 10, 25, 50, and 100 mg/kg). **99** was administered at three dose levels BID, 10, 25, and 50 mg/kg for 6 days. **1** was administered as an amorphous spray-dried dispersion formulation (25% DSM265 load)[15] and formulated in 1% methylcellulose (w/v), 0.1% Tween-80 (v/v) in water. Dose levels are expressed as the free base equivalent. **79** and **99** were formulated in 0.5% (w/v) carboxymethyl cellulose, 0.5% (v/v) benzyl alcohol, and 0.4% (v/v) Polysorbate 80 in water and administered at 10 mL/kg. The effect of treatment on parasitemia was assessed by measuring the percentage of infected erythrocytes in peripheral blood every 24 h until parasitemia was below the selected limit of quantitation (usually 0.01%). During the study, samples of peripheral blood were taken from mice to measure drug concentration by LC/MS/MS. Parasitemia was monitored up to day 60 or until parasitemia reached levels requiring euthanasia.

Quantitative pharmacodynamic (PD) response to treatment in each individual of the study was assessed by measuring their (a) parasite net growth inhibition during three cycles of parasite replication (90% of growth inhibition at Day 7 in this study representing one day after the final dose), and (b) parasite killing (day of recrudescence, DoR). The primary PK explanatory variable of efficacy endpoints was the AUC, calculated from the drug concentrations in peripheral blood. To determine parameters of efficacy (ED_{90} and AUC_{ED90}), log parasitemia versus log dose and log parasitemia versus log AUC data were fitted to log (inhibitor) vs response equation in GraphPad Prism. To allow robust calculation of parameters the hillslope was fixed to −5 or −3.5, respectively, and the bottom was fixed to −2 (representing the lower limit of detection of parasitemia). These values are based on the average of data accumulated over the years for drugs with the same mechanism of action, including **1**, for which large data sets were available (at least 8 individuals per curve), in the same *in vivo* system and assay.

Chemistry Experimental. All reagents and starting materials were obtained from commercial suppliers and used without further purification unless otherwise stated. General chemistry experimental conditions were as reported by Kokkonda et al.[20] Chiral purification was carried out by supercritical fluid chromatography (SFC) using a prepacked Lux A1, Chiralpak, Chiralcel, or YMC Amylose column, CO_2 as the mobile phase and cosolvent as specified. Yields from SFC resolution are based on the racemate, i.e., 50% maximum. Optical rotations were $\lambda = 589$, temp = 25.5 °C, concentration = 0.5, cell length = 50 mm. The purity of all tested compounds was >95% based on high-performance liquid chromatography (HPLC), ^{1}H NMR, LC-MS, and SFC purification unless stated otherwise.

Chemistry Synthetic Methods. The reported pyrrole analogues were synthesized as shown in Schemes 1−8 and Supporting Information Schemes S1−S10 using the following methods, which built on learnings from previous work.[20,74,75]

Chemistry Synthetic Methods. *General Procedure A: Propynyl Grignard Reaction.* 1-Propynylmagnesium bromide (0.5 M in THF) (1.1 equiv) was added to the corresponding aryl aldehyde (1 equiv) in THF at 0 °C and stirred for 4 h at RT. The reaction mixture was quenched with 1.5 N HCl solution and extracted with ethyl acetate

https://doi.org/10.1021/acs.jmedchem.1c00173
J. Med. Chem. 2021, 64, 6085−6136

(2×). The resulting organic layer was washed with brine, dried over Na_2SO_4, and concentrated to afford the product (84−94%) as a colorless liquid. Compounds **164**−**167** were prepared using this procedure.

*1-(6-(Trifluoromethyl)pyridin-3-yl)but-2-yn-1-ol (**164**).* Title compound **164** was prepared from 6-(trifluoromethyl)pyridine-3-carboxaledehyde (94%). ^{1}H NMR (400 MHz, DMSO-d_6) δ (ppm): 8.96 (s, 1H), 8.26−8.31 (m, 1H), 8.02 (d, 1H, J = 8.1 Hz), 3.57 (s, 3H); ESIMS m/z (M + 1): 216.0.

*1-(2-Fluoro-6-(trifluoromethyl)pyridin-3-yl)but-2-yn-1-ol (**164a**).* **164a** was prepared from 2-fluoro-6-(trifluoromethyl)pyridine-3-carboxaldehyde (88%). ESIMS m/z (M + 1): 234.2. The product was used without further characterization.

*1-(Benzo[d]oxazol-7-yl)but-2-yn-1-ol (**165**).* **165** was prepared from benzo[d]oxazole-7-carbaldehyde (91%) and used without characterization.

*1-(Benzo[d]oxazol-2-yl)but-2-yn-1-ol (**166**).* **166** was prepared from benzo[d]oxazole-2-carbaldehyde (84%). ESIMS m/z (M + 1): 188.2. The product was used without further characterization.

*1-(4-(Trifluoromethyl)phenyl)but-2-yn-1-ol (**167**).* **167** was prepared from 4-(trifluoromethyl)benzaldehyde (94%). ESIMS m/z (M + 1): 215.2. The product was used without further characterization.

General Procedure B: Hydroxyl Oxidation. Dess−Martin (1.5 equiv) was added to a stirred solution of but-2-yn-1-ol intermediate (1 equiv) in CH_2Cl_2 (150 mL) at RT and maintained for 2 h. The reaction mixture was quenched with saturated $NaHCO_3$ solution and extracted with CH_2Cl_2. The combined organic layers were dried (Na_2SO_4), filtered, and concentrated. The concentrated product was purified by flash chromatography (silica gel, eluting with hexane:EtOAc mixtures from 100 to 80:20%) to afford the product (57−83%) as an off-white solid. Compounds **168**−**172** were prepared using this procedure and **257** by a modified procedure as described.

*1-(6-(Trifluoromethyl)pyridin-3-yl)but-2-yn-1-one (**168**).* **168** was prepared from **164** (83%). ^{1}H NMR (300 MHz, DMSO-d_6) δ (ppm): 10.21 (s, 1H), 8.66 (d, 1H, J = 8.2 Hz), 8.14 (d, 1H, J = 8.2 Hz), 2.21 (s, 3H). ESIMS m/z (M + 1): 214.2.

*1-(2-Fluoro-6-(trifluoromethyl)pyridin-3-yl)but-2-yn-1-one (**169**).* **169** was prepared from **164a** (75%). ^{1}H NMR (400 MHz, DMSO-d_6) δ (ppm): 8.61 (d, 1H, J = 8.0 Hz), 7.72 (d, 1H, J = 8.0 Hz), 2.20 (s, 3H); ESIMS m/z (M + 1): 232.2.

*1-(Benzo[d]oxazol-7-yl)but-2-yn-1-one (**170**).* **170** was prepared from **165** (57%). ^{1}H NMR (400 MHz, $CDCl_3$) δ (ppm): 8.27 (s, 1H), 8.20−8.24 (dd, J = 1.1 Hz & 7.7 Hz, 1H), 8.05−8.08 (dd, J = 1.2 Hz & 7.8 Hz, 1H), 7.50−7.54 (m, 1H), 2.22 (s, 3H); ESIMS m/z (M + 1): 186.2.

*1-(Benzo[d]oxazol-2-yl)but-2-yn-1-one (**171**).* **171** was prepared from **166** (78%). ^{1}H NMR (400 MHz, DMSO-d_6) δ (ppm): 8.02 (d, 1H, J = 8.0 Hz), 7.89−7.92 (m, 1H), 7.63−7.67 (m, 1H), 7.54 (d, 1H, J = 8.0 Hz), 2.27 (s, 3H). ESIMS m/z (M + 1): 186.2.

*1-(4-(Trifluoromethyl)phenyl)but-2-yn-1-one (**172**).* **172** was prepared from **167** (83%). ^{1}H NMR (300 MHz, DMSO-d_6) δ (ppm): 8.25 (d, 2H, J = 8.0 Hz), 7.98 (d, 2H, J = 8.0 Hz), 2.25 (s, 3H). ESIMS m/z (M + 1): 213.2.

*4,4-Diethoxy-1-(6-(trifluoromethyl)pyridin-3-yl)but-2-yn-1-one (**257**).* n-BuLi (1.6 M in hexane) (15.3 mL, 24.60 mmol) was added to a stirred solution of 3,3-diethoxyprop-1-yne (3 g, 23.40 mmol) in THF (40 mL) at −78 °C and maintained for 40 min. Then, 6-(trifluoromethyl)pyridine-3-carboxaldehyde was added (3.70 g, 21.06 mmol) at the same temperature and stirring was continued for 30 min. The reaction mixture was quenched with saturated NH_4Cl solution and extracted with ethyl acetate (2 × 200 mL). The combined organic layers were dried (Na_2SO_4), filtered, and concentrated. The resulting product was stirred in CH_2Cl_2 (50 mL), Dess−Martin reagent was added (14.7 g, 36.1 mmol), and the reaction was maintained for 1 h at RT. The reaction mixture was filtered through Celite and the filtrate was concentrated. The resulting concentrated product was purified by column chromatography using 0−10% ethyl acetate in petroleum ether to afford the product as a pale yellow liquid (2.5 g, 36%). ^{1}H NMR (400 MHz, $CDCl_3$) δ (ppm): 9.44 (brs, 1H), 8.55−8.58 (m, 1H), 7.88 (d, 1H, J = 8.0 Hz), 5.56 (s, 1H), 3.83 (q, 2H, J = 7.1 Hz), 3.73 (q, 2H, J = 7.1 Hz), 1.31 (m, 6H, J = 7.1 Hz); ESIMS m/z (M + 1): 302.2.

General Procedure C: Pyrrole Formation. But-2-yn-1-one intermediate (1 equiv) was added to a stirred solution of Ag_2CO_3 (0.1−0.2 equiv) in NMP at RT. Ethyl isocyanoacetate (1.5 equiv) was added at room temperature and stirred for 2−4 h at 80−85 °C. The reaction mixture was cooled to RT, quenched with water, and extracted with ethyl acetate (2×). The combined organic layers were dried (Na_2SO_4), filtered, and concentrated. The concentrated product was purified by flash chromatography (silica gel, eluting with hexane:EtOAc mixtures from 100 to 60:40%) to afford compounds (27−66%) as an off-white solid. Compounds **173**−**177, 187, 197**−**201, 233**−**235, 258**, and **281** were prepared using this procedure.

*Ethyl 3-Methyl-4-(6-(trifluoromethyl)pyridine-3-carbonyl)-1H-pyrrole-2-carboxylate (**173**).* **173** was prepared from **168** (44%). ^{1}H NMR (300 MHz, DMSO-d_6) δ (ppm): 12.43 (s, 1H), 9.00 (s, 1H), 8.33 (d, 1H, J = 8.1 Hz), 8.05 (d, 1H, J = 8.1 Hz), 7.45 (s, 1H), 4.30 (q, 2H, J = 7.1 Hz), 2.51 (s, 3H), 1.31 (t, 3H, J = 7.1 Hz); ESIMS m/z (M + 1): 327.2.

*Ethyl 4-(2-Fluoro-6-(trifluoromethyl)pyridine-3-carbonyl)-3-methyl-1H-pyrrole-2-carboxylate (**174**).* **174** was prepared from **169** (34%). ^{1}H NMR (300 MHz, DMSO-d_6) δ (ppm): 12.46 (s, 1H), 8.39 (d, 1H, J = 7.8 Hz), 8.01 (d, 1H, J = 7.8 Hz), 7.51 (s, 1H), 4.29 (q, 2H, J = 7.2 Hz), 2.60 (s, 3H), 1.32 (t, 3H, J = 7.2 Hz); ESIMS m/z (M + 1): 345.2.

*Ethyl 4-(Benzo[d]oxazole-7-carbonyl)-3-methyl-1H-pyrrole-2-carboxylate (**175**).* **175** was prepared from **170** (52%). ESIMS m/z (M + 1): 299.2. The product was used without further characterization.

*Ethyl 4-(Benzo[d]oxazole-2-carbonyl)-3-methyl-1H-pyrrole-2-carboxylate (**176**).* **176** was prepared from **171** (27%). ^{1}H NMR (400 MHz, DMSO-d_6) δ (ppm): 12.51 (s, 1H), 8.44 (s, 1H), 8.02 (d, 1H, J = 8.0 Hz), 7.91 (d, 1H, J = 8.0 Hz), 7.60−7.63 (m, 1H), 7.52−7.56 (m, 1H), 4.32 (q, 2H, J = 7.0 Hz), 2.61 (s, 3H), 1.34 (t, 3H, J = 7.0 Hz). ESIMS m/z (M + 1): 299.2.

*Ethyl 3-Methyl-4-((4-(trifluoromethyl)phenyl)carbonyl)-1H-pyrrole-2-carboxylate (**177**).* **177** was prepared from **172** (44%). ^{1}H NMR (300 MHz, DMSO-d_6) δ (ppm): 12.33 (s, 1H), 7.88 (bs, 4H), 7.30 (s, 1H), 4.28 (q, 2H, J = 6.8 Hz), 2.57 (s, 3H), 1.32 (t, 3H, J = 6.8 Hz); ESIMS (M + 1) m/z: 326.2.

*Ethyl 4-((2-Hydroxy-3-nitro-4-(trifluoromethyl)phenyl)carbonyl)-3-methyl-1H-pyrrole-2-carboxylate (**187**).* **187** was prepared from **186** (24%). ESIMS m/z (M + 1): 387.1. Product was used directly without further characterization.

*Ethyl 4-(5-Fluoroisoquinoline-8-carbonyl)-3-methyl-1H-pyrrole-2-carboxylate (**197**).* **197** was prepared from **194** as a brown solid (40%). ESIMS m/z (M + 1): 327.2. The product was used without further characterization.

*Ethyl 4-((2-Fluoro-4-(trifluoromethyl)phenyl)carbonyl)-3-methyl-1H-pyrrole-2-carboxylate (**198**).* **198** was prepared from **192** (64%). ^{1}H NMR (400 MHz, DMSO-d_6) δ (ppm): 12.41 (s, 1H), 7.83−7.85 (m, 1H), 7.69−7.75 (m, 2H), 7.26 (brs, 1H), 4.28 (q, 2H, J = 7.1 Hz), 2.67 (s, 3H), 1.32 (t, 3H, J = 7.1 Hz); ESIMS m/z (M − 1): 342.1.

*Ethyl 4-((2-Bromo-4-(trifluoromethyl)phenyl)carbonyl)-3-methyl-1H-pyrrole-2-carboxylate (**199**).* **199** was prepared from **193** (50%). ^{1}H NMR (400 MHz, DMSO-d_6) δ (ppm): 12.38 (s, 1H), 8.11 (s, 1H), 7.86 (d, 1H, J = 8.0 Hz), 7.64 (d, 1H, J = 8.0 Hz), 7.08 (s, 1H), 4.28 (q, 2H, J = 7.2 Hz), 2.68 (s. 3H), 1.31 (t, 3H, J = 7.2 Hz); ESIMS m/z (M, M + 2): 404.2, 406.2.

*Ethyl 4-(2-Bromo-6-(trifluoromethyl)pyridine-3-carbonyl)-3-methyl-1H-pyrrole-2-carboxylate (**200**).* **200** was prepared from **195** (47%). ESIMS m/z (M, M + 2): 405.3, 407.3. The product was used without further characterization.

*Ethyl 4-((3,4-Difluorophenyl)carbonyl)-3-methyl-1H-pyrrole-2-carboxylate (**201**).* **201** was prepared from **196** (50%). ESIMS m/z (M + 1): 294.0. The product was used without further characterization.

*Ethyl 4-(3-Fluoro-4-(trifluoromethyl)phenylcarbonyl)-3-methyl-1H-pyrrole-2-carboxylate (**233**).* **233** was prepared from **230** (51%). ^{1}H NMR (400 MHz, DMSO-d_6) δ (ppm): 12.38 (brs, 1H), 7.90−7.95 (m, 1H), 7.66−7.77 (m, 2H), 7.40 (d, 1H, J = 4.8 Hz), 4.29 (q, 2H, J = 7.2 Hz), 2.58 (s, 3H), 1.33(t, 3H, J = 7.2 Hz); ESIMS m/z (M − 1): 342.2.

https://doi.org/10.1021/acs.jmedchem.1c00173
J. Med. Chem. 2021, 64, 6085−6136

*Ethyl 3-Methyl-4-(3-(trifluoromethyl)phenylcarbonyl)-1H-pyrrole-2-carboxylate (**234**).* **234** was prepared from **231** (66%). The product was used without further characterization.

*Ethyl 4-(6-(Difluoromethyl)pyridine-3-carbonyl)-3-methyl-1H-pyrrole-2-carboxylate (**235**).* **235** was prepared from **232** (47%). ^{1}H NMR (400 MHz, DMSO-d_6) δ (ppm): 8.93 (d, 1H, J = 1.2 Hz), 8.30 (dd, 1H, J = 1.2 Hz & 8.4 Hz), 7.85 (d, 1H, J = 8.4 Hz), 7.34 (s, 1H), 6.69−6.97 (m, 1H), 4.34 (2H, q, J = 7.2 Hz), 2.66 (s, 3H), 1. 45 (t, 3H, J = 7.2 Hz). ESIMS m/z (M + 1): 309.2.

*3-Formyl-4-(6-(trifluoromethyl)pyridine-3-carbonyl)-1H-pyrrole-2-carboxylate (**258**).* **258** was prepared from **257** (54%). ^{1}H NMR (400 MHz, $CDCl_3$) δ (ppm): 10.44 (s, 1H), 9.78 (brs, 1H), 9.00 (s, 1H), 8.55−8.58 (m, 1H), 7.80 (d, 1H, J = 8.0 Hz), 7.45 (s, 1H), 4.52 (q, 2H, J = 7.1 Hz), 1.51 (t, 3H, J = 7.1 Hz); ESIMS m/z (M + 1): 341.2.

*Ethyl 4-(2-Bromo-6-(trifluoromethyl)pyridine-3-carbonyl)-3-methyl-1H-pyrrole-2-carboxylate (**281**).* **281** was prepared from **280** (47%). ^{1}H NMR (400 MHz, DMSO-d_6) δ (ppm): 12.46 (s, 1H), 8.15 (d, 1H, J = 7.7 Hz), 8.07 (d, 1H, J = 7.7 Hz), 7.37 (s, 1H), 4.28 (q, 2H, J = 6.8 Hz), 2.61 (s, 3H), 1.33 (t, 3H, J = 6.8 Hz); ESIMS m/z (M, M + 2): 405.2, 407.2.

General Procedure D1: Carbonyl to Methylene Reduction. Sodium borohydride (2 equiv) was added portionwise to a stirred solution of carbonyl pyrrole intermediate (1 equiv) in ethanol at 0 °C. The reaction mixture was stirred for 1 h at RT and then concentrated under reduced pressure, dissolved in water, and extracted with ethyl acetate (2×). The resulting combined organic layers were washed with brine, dried over Na_2SO_4, and concentrated to afford an intermediate hydroxyl compound. The intermediate hydroxyl product was used in the next step without characterization. To a stirred solution of hydroxyl intermediate (1 equiv) in trifluoroacetic acid (TFA, 6 equiv) was added triethylsilane (3−4 equiv) at RT and stirred at 85 °C for 1 h. Then, saturated $NaHCO_3$ was added dropwise at 0 °C and the mixture was extracted with ethyl acetate (3×, with careful venting). The combined organic layers were dried (Na_2SO_4), filtered, and concentrated. The resulting concentrated product was triturated with petroleum ether to afford the compound as a white solid (11−77%). Compounds **19**−**20**, **103**, **178**−**180**, **188**, **205**, and **216**−**219** were prepared using this procedure.

*Ethyl 4-(Benzo[d]oxazol-7-ylmethyl)-3-methyl-1H-pyrrole-2-carboxylate (**19**).* **19** was prepared from **175** (11%). ^{1}H NMR (400 MHz, DMSO-d_6) δ (ppm):11.35 (s, 1H), 8.74 (s, 1H), 7.62 (d, 1H, J = 7.2 Hz), 7.29−7.32 (m, 1H), 7.14 (d, 1H, J = 7.1 Hz), 6.72 (d, 1H, J = 3.2 Hz), 4.21 (q, 2H, J = 7.1 Hz), 4.00 (s, 2H), 2.18 (s, 3H), 1.27 (t, 3H, J = 7.1 Hz); ESIMS m/z (M + 1): 285.0; LCMS: 97.99%; HPLC purity: 99.07%.

*Ethyl 4-(Benzo[d]oxazol-2-ylmethyl)-3-methyl-1H-pyrrole-2-carboxylate (**20**).* **20** was prepared from **176** (48%). ^{1}H NMR (400 MHz, DMSO-d_6) δ (ppm): 11.45 (s, 1H), 7.64−7.68 (m, 2H), 7.32−7.36 (m, 2H), 6.94 (s, 1H), 4.23 (q, 2H, J = 6.8 Hz), 4.10 (s, 2H), 2.23 (s, 3H), 1.28 (t, 3H, J = 6.8 Hz); ESIMS m/z (M + 1): 285.0; LCMS: 96.07%; HPLC purity: 95.33%.

*Methyl 2-(Cyclopropylcarbamoyl)-4-((6-(trifluoromethyl)pyridin-3-yl)methyl)-1H-pyrrole-3-carboxylate (**103**).* **103** was prepared from **260** (52%). ^{1}H NMR (400 MHz, DMSO-d_6) δ (ppm): 9.76 (d, 1H, J = 4.0 Hz), 8.61 (brs, 1H), 7.79 (brs, 2H), 6.88 (d, 1H, J = 2.8 Hz), 4.09 (s, 2H), 3.69 (s, 3H), 2.82−2.86 (m, 1H), 0.73−0.77 (m, 2H), 0.46−0.50 (m, 2H); ESIMS m/z (M + 1): 367.8; LCMS:95.59%; HPLC purity:98.27%

*Ethyl 3-Methyl-4-((6-(trifluoromethyl) pyridin-3-yl) methyl)-1H-pyrrole-2-carboxylate (**178**).* **178** was prepared from **173** (77%). ^{1}H NMR (300 MHz, DMSO-d_6) δ (ppm): 11.41 (s, 1H), 8.64 (s, 1H), 7.81 (brs, 2H), 6.81 (s, 1H), 4.21 (q, 2H, J = 7.1 Hz), 3.87 (s, 2H), 2.15 (s, 3H), 1.27 (t, 3H, J = 7.1 Hz); ESIMS m/z: 312.2

*Ethyl 4-((2-Fluoro-6-(trifluoromethyl)pyridin-3-yl)methyl)-3-methyl-1H-pyrrole-2-carboxylate (**179**).* **179** was prepared from **174** (71%). ^{1}H NMR (400 MHz, $CDCl_3$) δ (ppm): 8.89 (s, 1H), 7.63 (d, 1H, J = 8.0 Hz), 7.48 (d, 1H, J = 8.0 Hz), 6.73 (s, 1H), 4.34 (q, 2H, J = 7.1 Hz), 3.87 (s, 2H), 2.24 (s, 3H), 1.37 (t, 3H, J = 7.1 Hz); ESIMS m/z (M + 1): 331.2.

*Ethyl 3-Methyl-4-((4-(trifluoromethyl)phenyl)methyl)-1H-pyrrole-2-carboxylate (**180**).* **180** was prepared from **177** (72%). ^{1}H NMR (300 MHz, DMSO-d_6) δ (ppm): 11.36 (s, 1H), 7.63 (d, 2H, J = 8.0 Hz), 7.38 (s, 2H, J = 8.0 Hz), 6.77 (s, 1H), 4.22 (q, 2H, J = 7.2 Hz), 3.83 (s, 2H), 2.13 (s, 3H), 1.23 (t, 3H, J = 7.2 Hz); ESIMS m/z (M + 1): 312.2.

*Ethyl 4-(2-Hydroxy-3-nitro-(4-(trifluoromethyl)phenyl)methyl)-3-methyl-1H-pyrrole-2-carboxylate (**188**).* **188** was prepared from **187** (35%). ESIMS m/z (M + 1): 373.2. The product was used without further characterization.

*Ethyl 4-((2-Bromo-6-(trifluoromethyl)pyridin-3-yl)methyl)-3-methyl-1H-pyrrole-2-carboxylate (**205**).* **205** was prepared from **200** (68%). ^{1}H NMR (400 MHz, DMSO-d_6) δ (ppm): 11.47 (s, 1H), 7.88 (d, 1H, J = 7.8 Hz), 7.70 (d, 1H, J = 7.8 Hz), 6.73 (s, 1H), 4.20 (q, 2H, J = 7.1 Hz), 3.87 (s, 2H), 2.14 (s, 3H), 1.27 (t, 3H, J = 7.1 Hz); ESIMS m/z (M, M + 2): 391.3, 393.3.

*Ethyl 4-(4-(N,N-Dimethylsulfamoyl)benzyl)-3-methyl-1H-pyrrole-2-carboxylate (**216**).* **216** was prepared from **212** (45%). The product was used without further characterization.

*Ethyl 4-(isoquinolin-8-ylmethyl)-3-methyl-1H-pyrrole-2-carboxylate (**217**).* **217** was prepared from **213** (50%). ESIMS m/z (M + 1): 295.4. The product was used without further characterization.

*Ethyl 4-((5-Methoxyisoquinolin-8-yl)methyl)-3-methyl-1H-pyrrole-2-carboxylate (**218**).* **218** was prepared from **214** (45%). ESIMS m/z (M + 1): 325.4. The product was used without further characterization.

*Ethyl 4-((3-Fluoro-2-iodophenyl)methyl)-3-methyl-1H-pyrrole-2-carboxylate (**219**).* **219** was prepared from **215** (0.6 g, 62%) as a white solid. ^{1}H NMR (300 MHz, DMSO-d_6) δ (ppm): 11.36 (s, 1H), 7.29−7.35 (m, 1H), 7.06−7.11 (m, 1H), 6.90−6.97 (m, 1H), 6.54 (s, 1H), 4.23 (q, 2H, J = 7.2 Hz), 3.74 (s, 2H), 2.13 (s, 3H), 1.28 (t, 3H, J = 7.2 Hz); ESIMS m/z (M + 1): 388.2.

General Procedure D2: Carbonyl to Methylene Reduction. Sodium borohydride (2 equiv) was added portionwise to a stirred solution of carbonyl pyrrole intermediate (1 equiv) in ethanol at 0 °C. The reaction mixture was stirred for 1 h at room temperature and then concentrated, dissolved in water, and extracted with ethyl acetate (2). The resulting combined organic layers were washed with brine, dried over Na_2SO_4, and concentrated to afford an intermediate hydroxyl compound. The product was used in the next step without characterization. To a stirred solution of hydroxyl intermediate (1 equiv) in TFA (6 equiv) and CH_2Cl_2 was added triethylsilane (3−4 equiv) at 0 °C and maintained at RT for 1 h. Then, saturated $NaHCO_3$ was added dropwise at 0 °C and extracted with ethyl acetate (3×, with careful venting). The combined organic layers were dried (Na_2SO_4), filtered, and concentrated. The resulting concentrated product was triturated with petroleum ether to afford the compound as a white solid (42-56%). Compounds **202**−**204**, **206** were prepared by this method.

*Ethyl 4-((5-Fluoroisoquinolin-8-yl)methyl)-3-methyl-1H-pyrrole-2-carboxylate (**202**).* The title compound was prepared from **197** (63%). ^{1}H NMR (400 MHz, DMSO-d_6) δ (ppm): 11.35 (s, 1H), 9.60 (s, 1H), 8.64 (d, 1H. J = 5.8 Hz), 7.97 (d, 1H, J = 5.8 Hz), 7.54−7.59 (m, 1H), 7.33−7.37 (s, 1H), 6.75 (s, 1H), 4.30 (s, 2H), 4.22 (q, 2H, J = 7.2 Hz), 2.21 (s, 3H), 1.27 (t, 3H, J = 7.2 Hz); ESIMS m/z (M + 1): 313.1; LCMS: 93.68%; HPLC purity: 95.07%.

*Ethyl 4-((2-Fluoro-4-(trifluoromethyl)phenyl)methyl)-3-methyl-1H-pyrrole-2-carboxylate (**203**).* **203** was prepared from **198** (42%). ^{1}H NMR (400 MHz, DMSO-d_6) δ (ppm): 11.40 (s, 1H), 7.62 (d, 1H, J = 7.6 Hz), 7.51 (d, 1H, J = 7.6 Hz), 7.34−7.38 (m, 1H), 6.73 (s, 1H), 4.21 (q, 2H, J = 7.1 Hz), 3.82 (s, 2H), 2.15 (s, 3H), 1.27 (t, 3H, J = 7.1 Hz); ESIMS m/z (M + 1): 330.1.

*Ethyl 4-((2-Bromo-4-(trifluoromethyl)phenyl)methyl)-3-methyl-1H-pyrrole-2-carboxylate (**204**).* The title compound was prepared from **199** (42%). ^{1}H NMR (400 MHz, DMSO-d_6) δ (ppm): 11.43 (s, 1H), 7.98 (s, 1H), 7.69 (d, 1H, J = 8.0 Hz), 7.29 (d, 1H, J = 8.0 Hz), 6.68 (s, 1H), 4.24 (q, 2H, J = 7.2 Hz), 3.87 (s, 2H), 2.15 (s. 3H), 1.27 (t, 3H, J = 7.2 Hz); ESIMS m/z (M, M + 2): 390.1, 392.2.

*Ethyl 4-((3,4-Difluorophenyl)methyl)-3-methyl-1H-pyrrole-2-carboxylate (**206**).* **206** was prepared from **201** (58%). ESIMS m/z (M + 1): 280.1. The product was used without further purification.

General Procedure E: Ester Hydrolysis. Sodium hydroxide (2 equiv) was added to a stirred solution of arylmethyl-1*H*-pyrrole-2-carboxylate intermediate (1 equiv) in EtOH:H_2O (4:1) at RT and heated to 80 °C

https://doi.org/10.1021/acs.jmedchem.1c00173
J. Med. Chem. 2021, 64, 6085−6136

for 2 h. The resulting reaction mixture was concentrated, quenched with water, and then acidified with 10% citric acid solution. The solid obtained was filtered, washed with water, and dried to afford the compound as an off-white solid (60-95%). Compounds **181**−**183**, **207**−**209**, **211**, **220**−**223**, **223**, **251**−**255**, **261**, **274**−**277**, and **283** were prepared using this procedure and **210** by an extended procedure as described.

*3-Methyl-4-((6-(trifluoromethyl)pyridin-3-yl)methyl)-1H-pyrrole-2-carboxylic Acid (**181**).* **181** was prepared from **178** (88%). ^{1}H NMR (300 MHz, DMSO-d_6) δ (ppm): 12.15 (s, 1H), 11.29 (s, 1H), 8.64 (s, 1H), 7.81 (brs, 2H), 6.75 (s, 1H), 3.86 (s, 2H), 2.14 (s, 3H); ESIMS m/z (M + 1): 285.2.

*4-(Benzo[d]oxazol-2-ylmethyl)-3-methyl-1H-pyrrole-2-carboxylic Acid (**182**).* **182** was prepared from **20** (67%). ESIMS m/z (M + 1): 257.2. The product was used without further purification.

*3-Methyl-4-(4-(trifluoromethyl)benzyl)-1H-pyrrole-2-carboxylic Acid (**183**).* **183** was prepared from **180** (88%). ESIMS m/z (M + 1): 284.2. The product was used without further characterization.

*4-((5-Fluoroisoquinolin-8-yl)methyl)-3-methyl-1H-pyrrole-2-carboxylic Acid (**207**).* **207** was prepared from **202** (95%). ESIMS m/z (M + 1):285.2. The product was used without further characterization.

*4-(2-Fluoro-4-(trifluoromethyl)benzyl)-3-methyl-1H-pyrrole-2-carboxylic Acid (**208**).* **208** was prepared from **203** (82%). ^{1}H NMR (400 MHz, DMSO-d_6) δ (ppm): 12.11 (s, 1H), 11.27 (s, 1H), 7.62 (s, 1H), 7.50 (s, 1H), 7.35−7.38 (m, 1H), 6.69 (s, 1H), 3.80 (s, 2H), 2.14 (s, 3H); ESIMS m/z (M−1): 300.1; LCMS: 99.45%; HPLC purity: 90.57%.

*4-(2-Bromo-4-(trifluoromethyl)benzyl)-3-methyl-1H-pyrrole-2-carboxylic Acid (**209**).* **209** was prepared from **204** (86%). ESIMS m/z (M, M + 2): 362.2, 364.2. The product was used without further characterization.

*4-((2-Carbamoyl-6-(trifluoromethyl)pyridine-3-yl)methyl)-3-methyl-1H-pyrrole-2-carboxylic Acid (**210**).* Zinc cyanide (0.72 g, 6.14 mmol) was added to a degassed solution of **205** (1.2 g, 3.067 mmol), Pd(dppf)Cl_2 (125 mg, 0.15 mmol), and $Pd_2(dba)_3$ (140 mg, 0.15 mmol) in DMA (20 mL) at RT and stirring was continued for 16 h at 115 °C. The reaction mixture was poured into water (100 mL) and extracted with ethyl acetate (2 × 100 mL). The combined organic layers were dried (Na_2SO_4), filtered, and concentrated. The resulting concentrated product was purified by flash chromatography (silica gel, eluting with the hexane:EtOAc mixture from 100 to 60:40%) to afford ethyl 4-((2-cyano-6-(trifluoromethyl)pyridine-3-yl)methyl)-3-methyl-1*H*-pyrrole-2-carboxylate (0.8 g, 78%) as an off-white solid. ^{1}H NMR (400 MHz, DMSO-d_6) δ (ppm): 11.52 (s, 1H), 8.17 (d, 1H, J = 8.3 Hz), 8.04 (d, 1H, J = 8.3 Hz), 6.79 (s, 1H), 4.23 (q, 2H, J = 6.8 Hz), 4.07 (s, 2H), 2.19 (s, 3H), 1.28 (t, 3H, J = 6.8 Hz); ESIMS m/z (M + 1): 338.0; LCMS: 99.70%; HPLC purity: 99.52%.

Ethyl 4-((2-cyano-6-(trifluoromethyl)pyridine-3-yl)methyl)-3-methyl-1*H*-pyrrole-2-carboxylate was subjected to general procedure E to afford the title compound (21%).

ESIMS m/z (M + 1): 328.2. The product was used without further characterization.

*4-((3,4-Difluorophenyl)methyl)-3-methyl-1H-pyrrole-2-carboxylic Acid (**211**).* **211** was prepared from **206** (72%). ^{1}H NMR (400 MHz, DMSO-d_6) δ (ppm): 12.10 (s, 1H), 11.22 (s, 1H), 7.27−7.34 (m, 1H), 7.16−7.21 (m, 1H), 7.00 (brs, 1H), 6.70 (s, 1H), 3.71 (s, 2H), 2.12 (s, 3H); ESIMS m/z (M − 1): 249.9; LCMS: 97.02%; HPLC purity: 98.60%.

*4-(4-(N,N-Dimethylsulfamoyl)benzyl)-3-methyl-1H-pyrrole-2-carboxylic Acid (**220**).* **220** was prepared from **216** (70%). ESIMS m/z (M + 1): 322.9. The product was used without further characterization.

*4-(Isoquinolin-8-ylmethyl)-3-methyl-1H-pyrrole-2-carboxylic Acid (**221**).* **221** was prepared from **217** (75%). ESIMS m/z (M + 1): 267.0. The product was used without further characterization.

*4-((5-Methoxyisoquinolin-8-yl)methyl)-3-methyl-1H-pyrrole-2-carboxylic Acid (**222**).* **222** was prepared from **218** (80%). The product was used without further characterization.

*4-((3-Fluoro-2-iodophenyl)methyl)-3-methyl-1H-pyrrole-2-carboxylic Acid (**223**).* **223** was prepared from **219** (92%). ^{1}H NMR (300 MHz, DMSO-d_6) δ (ppm): 12.12 (brs, 1H), 11.23 (s, 1H), 7.28−7.35 (m, 1H), 7.06−7.11 (m, 1H), 6.89−6.97 (m, 1H), 6.54 (s, 1H), 3.80 (s, 2H), 2.14 (s, 3H); ESIMS m/z (M − 1): 358.2.

*3-Methyl-4-(1-(6-(trifluoromethyl)pyridin-3-yl)cyclopropyl)-1H-pyrrole-2-carboxylic Acid (**251**).* **251** was prepared from **246** (89%) as an off-white solid. ^{1}H NMR (400 MHz, DMSO-d_6) δ (ppm): 11.36 (s, 1H), 8.40 (s, 1H), 7.74 (d, 1H, J = 8.4 Hz), 7.63 (d, 1H, J = 8.4 Hz), 6.91 (s, 1H), 2.09 (s, 3H), 1.40 (brs, 2H), 1.28 (brs, 2H); ESIMS m/z: 311.2; LCMS: 98.02%; HPLC purity: 94.73%.

*4-((2-Fluoro-4-(trifluoromethyl)phenylmethyl)cyclopropyl)-3-methyl-1H-pyrrole-2-carboxylic Acid (**252**).* **252** was prepared from **247** (78%). ^{1}H NMR (400 MHz, DMSO-d_6) δ (ppm): 12.07 (s, 1H), 11.22 (s, 1H), 7.68−7.73 (m, 1H), 7.47−7.53 (m, 2H), 6.88 (s, 1H), 2.19 (s, 3H), 1.16−1.18 (m, 2H), 1.10−1.11 (m, 2H); ESIMS m/z (M − 1): 325.9; LCMS: 95.59%; HPLC purity: 95.80%.

*4-((3-Fluoro-4-(trifluoromethyl)phenylmethyl)cyclopropyl)-3-methyl-1H-pyrrole-2-carboxylic Acid (**253**).* **253** was prepared from **248** (84%). ^{1}H NMR (400 MHz, DMSO-d_6) δ (ppm): 11.04 (brs, 1H), 7.57−7.61 (m, 1H), 6.98−7.03 (m, 2H), 6.74 (s, 1H), 2.08 (s, 3H), 1.30−1.32 (m, 2H),1.22−1.24 (m, 2H); ESIMS m/z (M − 1): 326.1.

*3-Methyl-4-(1-(3-(trifluoromethyl)phenyl)cyclopropyl)-1H-pyrrole-2-carboxylic Acid (**254**).* **254** was prepared from **249** (60%). The product was used without further characterization.

*4-(1-(6-(Difluoromethyl)pyridin-3-yl)cyclopropyl)-3-methyl-1H-pyrrole-2-carboxylic Acid (**255**).* **255** was prepared from **250** (68%). ESIMS (M + 1)m/z: 293.2. The product was used without further characterization.

*2-(Cyclopropylcarbamoyl)-4-((6-(trifluoromethyl)pyridin-3-yl)-methyl)-1H-pyrrole-3-carboxylic Acid (**261**).* **261** was prepared from **103** (78%). ESIMS m/z (M + 1): 354.2. The product was used without further characterization.

*3-Methyl-4-(6-(trifluoromethyl)-1H-indol-3-yl)-1H-pyrrole-2-carboxylic Acid (**274**).* **274** was prepared from **271** (65%). The product was used without characterization.

*4-(6-Fluoro-1H-indol-3-yl)-3-methyl-1H-pyrrole-2-carboxylic Acid (**275**).* **275** was prepared from **272** (83%). The product was used without characterization.

*4-(6-(Trifluoromethyl)-1H-pyrrolo[2,3-b]pyridin-3-yl)-3-methyl-1H-pyrrole-2-carboxylic Acid (**276**).* **276** was prepared from **273** (92%). ^{1}H NMR (300 MHz, DMSO-d_6) δ (ppm): 12.25 (s, 1H), 11.6 (s, 1H), 8.20 (d, 1H, J = 8.0 Hz); 7.75 (s, 1H), 7.52 (d, 1H, J = 8.0 Hz), 7.14 (s, 1H), 2.33 (s, 3H); ESIMS m/z: 309.9.

*4-(2-Fluoro-4-(trifluoromethyl)benzoyl)-3-methyl-1H-pyrrole-2-carboxylic Acid (**277**).* **277** was prepared from **198** (95%). The product was used without characterization.

*3-Methyl-4-(6-(trifluoromethyl)-1H-pyrazolo[3,4-b]pyridin-3-yl)-1H-pyrrole-2-carboxylic Acid (**283**).* **283** was prepared from **282** (94%). ^{1}H NMR (400 MHz, DMSO-d_6) δ (ppm): 13.99 (s, 1H), 12.43 (s, 1H), 11.88 (s, 1H), 8.69 (d, 1H, J = 8.4 Hz), 7.63 (d, 1H, J = 8.4 Hz), 7.57 (d, 1H, J = 3.2 Hz), 2.56 (s, 3H); ESIMS m/z (M + 1): 311.1; LCMS: 94.77%; HPLC purity: 97.34%.

General Procedure F1: Amide Formation. Amine (1.1 equiv) and triethylamine (2 equiv) were added to pyrrole carboxylic acid intermediate (1 equiv) in CH_2Cl_2 and stirred for 5 min at RT. Then, HATU (1.5 equiv) was added to the reaction mixture and stirring was maintained at RT for 4 h. After completion of the reaction (monitored by thin-layer chromatography (TLC)), water was added to the reaction mixture and crude product was extracted with CH_2Cl_2 (2×). The combined organic layer was dried over Na_2SO_4 and concentrated. The resulting concentrated product was purified by column chromatography using 10−70% ethyl acetate in petroleum ether to afford compound (10−68%) as an off-white solid. Compounds **4**−**7**, **11**−**17**, **21**−**22**, **24**−**28**, **35**−**39**, **51**−**53**, **56**−**58**, **73**−**76**, **81**−**82**, **104**, **111**−**114**, **124**−**130**, **133**, **137**, **141**−**144**, **149**−**160**, **163**, **189**, **256**, and **279** were prepared using this procedure. Compounds **23** and **259** were prepared using procedure F1 with an additional step as described.

*3-Methyl-N-(oxetan-3-yl)-4-((6-(trifluoromethyl)pyridin-3-yl)-methyl)-1H-pyrrole-2-carboxamide (**4**).* **4** was prepared from 3-oxetanamine and **181** (61%). ^{1}H NMR (400 MHz, DMSO-d_6) δ 10.97 (s, 1H), 8.04 (d, 1H, J = 6.4 Hz), 7.80 (s, 2H), 6.72 (s, 1H), 4.90−4.92 (m, 1H), 4.74 (t, 2H, J = 6.4 Hz), 4.49 (t, 2H, J = 6.4 Hz), 3.84 (s, 2H),

https://doi.org/10.1021/acs.jmedchem.1c00173
J. Med. Chem. 2021, 64, 6085−6136

2.12 (s, 3H). ESIMS *m/z* (M + 1); 340.0; LCMS: 97.95%; HPLC purity: 98.13%.

*N-(4-Hydroxytetrahydrofuran-3-yl)-3-methyl-4-((6-(trifluoromethyl)pyridin-3-yl)methyl)-H-pyrrole-2-carboxamide (**5**).* **5** was prepared from 4-aminotetrahydro-3-furanol and **181** (31%). ^{1}H NMR (400 MHz, DMSO-d_6) δ 10.82 (s, 1H, D_2O exch), 8.64 (s, 1H), 7.82 (brs, 2H), 7.45 (d, 1H, D_2O exch), 6.62 (brs, 1H), 5.27 (d, 1H, *J* = 4.0 Hz, D_2O exch), 4.11−4.12 (m, 2H), 3.93−3.97 (m, 1H), 3.88−3.86 (m, 1H), 3.85 (s, 2H), 3.57 (d, 1H, *J* = 9.2 Hz) 3.56 (d, 1H, *J* = 9.2 Hz), 2.13 (s, 3H); ESIMS *m/z* (M + 1); 370.0; LC-MS: 99.11%. HPLC purity: 99.90%.

*N-(4-Methoxytetrahydrofuran-3-yl)-3-methyl-4-((6-(trifluoromethyl)pyridin-3-yl)methyl)-1H-pyrrole-2-carboxamide (**6**).* **6** was prepared from 4-methoxytetrahydro-3-furanamine and **181** (34%). ^{1}H NMR (400 MHz, DMSO-d_6) δ 11.02 (s, 1H, D_2O exch), 8.63 (s, 1H), 7.81 (brs, 2H), 7.56 (d, 1H, D_2O exch), 6.72 (s, 1H), 4.30 (brs, 1H), 3.81−3.91 (m, 5H), 3.59−3.66 (m, 2H), 3.34 (s, 3H), 2.14 (s, 3H); ESIMS *m/z* (M + 1); 384.0; LCMS: 99.45%; HPLC purity: 99.57%.

*N-((1H-Pyrazol-3-yl)methyl)-3-methyl-4-((6-(trifluoromethyl)-pyridin-3-yl)methyl)-1H-pyrrole-2-carboxamide (**7**).* **7** was prepared from 1H-pyrazole-4-methanamine and **181** (24%). ^{1}H NMR (400 MHz, CD_3OD) δ 8.56 (s, 1H), 7.82 (d, 1H, *J* = 8.0 Hz), 7.73 (d, 1H, *J* = 8.0 Hz), 7.58 (s, 1H), 6.73 (s, 1H), 6.31 (s, 1H), 4.58 (s, 2H), 3.95 (s, 2H), 2.21 (s, 3H); ESIMS *m/z* (M + 1); 364.2; LCMS: 99.86%; HPLC purity: 97.24.

*N-Cyclopropyl-4-(4-(N,N-dimethylsulfamoyl)benzyl)-3-methyl-1H-pyrrole-2-carboxamide (**11**).* **11**was prepared from cyclopropanamine and **220** (23%). ^{1}H NMR (300 MHz, MeOD) δ 7.68 (d, *J* = 7.8 Hz, 2H), 7.42 (d, *J* = 8.0 Hz, 2H), 6.67 (s, 1H), 3.90 (s, 2H), 2.81−2.71 (m, 1H), 2.67 (s, 6H), 2.16 (s, 3H), 0.90−0.70 (m, 2H), 0.66−0.46 (m, 2H). ESIMS *m/z* (M + 1): 362.2; LCMS: 96.52%.

*N-Cyclopropyl-4-(isoquinolin-8-ylmethyl)-3-methyl-1H-pyrrole-2-carboxamide (**12**).* **12** was prepared from cyclopropanamine and **221** (25%). ^{1}H NMR (300 MHz, MeOD) δ (ppm): 9.47 (brs, 1H), 8.44 (brs, 1H), 7.83 (d, *J* = 8.0 Hz, 2H), 7.74−7.67 (m, 2H), 7.45 (d, *J* = 6.9 Hz, 2H), 6.41 (s, 1H), 4.35 (s, 2H), 2.89−2.71 (m, 1H), 2.27 (s, 3H), 0.89−0.73 (m, 2H), 0.71−0.53 (m, 2H). ESIMS *m/z* (M + 1): 306.0; LCMS: 97.85%.

*(3,3-Difluoroazetidin-1-yl)(4-(isoquinolin-8-ylmethyl)-3-methyl-1H-pyrrol-2-yl)methanone (**13**).* **13** was prepared from 3,3-difluoroazetidine and **221** (28%). ^{1}H NMR (300 MHz, $CDCl_3$) δ (ppm): 9.43 (s, 1H), 9.11 (brs, 1H), 8.42 (d, *J* = 5.7 Hz, 1H), 7.71−7.48 (m, 2H), 7.42−7.22 (m, 2H), 6.41 (s, 1H), 4.41 (t, *J* = 12.2 Hz, 4H), 4.21 (s, 2H), 2.12 (s, 3H). ESIMS *m/z* (M + 1): 342.2; LCMS: 97.45%.

*4-(Isoquinolin-8-ylmethyl)-3-methyl-N-(2,2,2-trifluoroethyl)-1H-pyrrole-2-carboxamide (**14**).* **14** was prepared from 2,2,2-trifluoroethylamine and **221** (35%). ^{1}H NMR (300 MHz, MeOD) δ (ppm): 9.46 (brs, 1H), 8.46 (brs, 1H), 7.96−7.80 (m, 2H), 7.80−7.67 (m, 2H), 7.59−7.39 (m, 2H), 6.46 (s, 1H), 4.37 (s, 2H), 4.08 (q, *J* = 9.4 Hz, 2H), 2.32 (s, 3H). ESIMS *m/z* (M + 1): 348.2; LCMS: 98.24%.

*N-Cyclopropyl-4-((5-methoxyisoquinolin-8-yl)methyl)-3-methyl-1H-pyrrole-2-carboxamide (**15**).* **15** was prepared from cyclopropylamine and **222** (30%). ^{1}H NMR (300 MHz, $CDCl_3$) δ (ppm): 9.44 (brs, 1H), 9.33 (brs, 1H), 8.54 (d, *J* = 5.5 Hz, 1H), 8.12 (d, *J* = 5.8 Hz, 1H), 7.23 (d, *J* = 7.9 Hz, 1H), 6.94 (d, *J* = 7.9 Hz, 1H), 6.44 (d, *J* = 2.4 Hz, 1H), 6.01 (s, 1H), 4.22 (s, 2H), 4.01 (s, 3H), 2.93−2.83 (m, 1H), 2.24 (s, 3H), 0.93−0.82 (m, 2H), 0.66−0.57 (m, 2H). ESIMS *m/z* (M + 1): 336.2; LCMS: 98.44%.

*N-Cyclopropyl-4-((5-fluoroisoquinolin-8-yl)methyl)-3-methyl-1H-pyrrole-2-carboxamide (**16**).* **16** was prepared from cyclopropylamine and **207** (25%). ^{1}H NMR (500 MHz, DMSO-d_6) δ (ppm): 10.82 (s, 1H), 9.57 (s, 1H), 8.63 (s, 1H), 7.93 (d, *J* = 4.9 Hz, 1H), 7.53 (d, *J* = 9.7 Hz, 1H), 7.49 (s, 1H), 7.36 (s, 1H), 6.46 (s, 1H), 4.27 (s, 2H), 2.83−2.61 (m, 1H), 2.19 (s, 3H), 0.73−0.55 (m, 2H), 0.51−0.38 (m, 2H). ESIMS *m/z* (M + 1): 324.2; LCMS: 97.73%.

*(3,3-Difluoroazetidin-1-yl)(4-((5-fluoroisoquinolin-8-yl)methyl)-3-methyl-1H-pyrrol-2-yl)methanone (**17**).* **17** was prepared from 3,3-difluoroazetidine and **207** (30%). ^{1}H NMR (300 MHz, $CDCl_3$) δ (ppm): 9.58 (s, 1H), 9.34 (brs, 1H), 8.68 (d, *J* = 5.8 Hz, 1H), 8.04 (d, *J* = 5.8 Hz, 1H), 7.55−7.37 (m, 2H), 6.57 (d, *J* = 2.8 Hz, 1H), 4.59 (t, *J* = 12.1 Hz, 4H), 4.34 (s, 2H), 2.28 (s, 3H). ESIMS *m/z* (M + 1): 360.3; LCMS: 98.65%.

4-(Benzo[d]oxazol-2-ylmethyl)-N-cyclopropyl-3-methyl-1H-pyrrole-2-carboxamide (21). **21** was prepared from cyclopropanamine and **182** (22%). ^{1}H NMR (400 MHz, $CDCl_3$) δ (ppm): 9.20 (brs, 1H), 7.69−7.71 (m, 1H), 7.48−7.50 (s, 1H), 7.29−7.33 (m, 2H), 6.93 (s, 1H), 5.88 (brs, 1H), 4.13 (s, 2H), 2.84−2.88 (m, 1H), 2.10 (s, 3H), 0.85-0.89 (m, 2H), 0.58-0.61 (m, 2H); ESIMS *m/z* (M + 1): 296.2; LCMS: 98.13%; HPLC purity: 97.44%.

*(S)-N-(1-Hydroxypropan-2-yl)-3-methyl-4-((6-(trifluoromethyl)-pyridin-3-yl)methyl)-1H-pyrrole-2-carboxamide (**22**).* **22** was prepared from (2*S*)-2-amino-propan-1-ol and **181** (15%). ^{1}H NMR (400 MHz, DMSO-d_6) δ 11.01 (s, 1H), 8.63 (s, 1H), 7.80 (s, 2H), 7.05 (d, 1H), 6.69 (d, 1H), 4.73−4.75 (m, 1H), 3.91−3.95 (m, 1H), 3.85 (s, 2H), 3.38−3.44 (m, 1H), 2.13 (s, 3H), 1.08−1.13 (d, 3H); ESIMS *m/z* (M + 1); 342.2; LCMS: 92.21%; HPLC purity: 97.44%.

*(S)-3-Methyl-N-(1-(methylamino)-1-oxopropan-2-yl)-4-((6-(trifluoromethyl)pyridin-3-yl)methyl)-1H-pyrrole-2-carboxamide (**23**).* (*S*)-Alanine methyl ester and **181** were coupled using general procedure **F1**. After purification, the intermediate methyl ester product in THF was added directly to $MeNH_2$ in methanol solution (2 M, 2 equiv), followed by the addition of Me_3Al (1.0 M in toluene, 3 equiv). The reaction mixture was heated to 100 °C for 1 h in a microwave. The reaction mixture was quenched with 1.5 N HCl solution and extracted with CH_2Cl_2. The combined organic layer was dried over Na_2SO_4 and concentrated under reduced pressure. The resulting concentrated product was purified by column chromatography using 10−50% ethyl acetate in petroleum ether to afford the title compound as an off-white solid (19%). ^{1}H NMR (400 MHz, CD_3OD) δ 8.55 (s, 1H), 8.02 (brs, 1H), 7.81 (d, 1H, *J* = 8.0 Hz), 7.72 (d, 1H, *J* = 8.0 Hz), 6.74 (s, 1H), 4.49 (q, 1H, *J* = 6.8 Hz), 3.95 (s, 2H), 2.76 (d, 3H, *J* = 4.0 Hz), 2.21 (s, 3H), 1.43 (d, 3H, *J* = 6.8 Hz). ESIMS *m/z* (M + 1); 369.2; LC-MS: 98.91%. HPLC purity: 96.76%.

*(S)-N-(1-Amino-1-oxopropan-2-yl)-3-methyl-4-((6-(trifluoromethyl)pyridin-3-yl)methyl)-1H-pyrrole-2-carboxamide (**24**).* **24** was prepared from (*S*)-2-aminopropanamide and **181** (24%). ^{1}H NMR (400 MHz, CD_3OD) δ 8.57 (s, 1H), 7.82 (d, 1H, *J* = 8.0 Hz), 7.27 (d, 1H, *J* = 8.0 Hz), 6.75 (s, 1H), 4.54 (q, 1H, *J* = 8.0), 3.96 (s, 2H), 2.22 (s, 3H), 1.46 (d, 3H, *J* = 8.0); ESIMS *m/z* (M + 1); 355.2; LC-MS: 99.74%. HPLC purity: 96.32%.

*3-Methyl-N-(1-(5-methylisoxazol-3-yl) ethyl)-4-((6-(trifluoromethyl)pyridin-3-yl)methyl)-1H-pyrrole-2-carboxamide (**25**).* **25** was prepared from 1-(5-methyl-isoxazol-3-yl)-ethylamine and **181** (55%). ^{1}H NMR (400 MHz, DMSO-d_6) δ (ppm): 11.02 (s, 1H), 8.63 (s, 1H), 7.81 (s, 2H), 7.80 (d, 1H), 6.73 (s, 1H), 6.18 (s, 1H), 5.13−5.17 (m, 1H), 3.86 (s, 2H), 2.34 (s, 3H), 2.14 (s, 3H), 1.44 (d, 3H); ESIMS *m/z*: 393.2; LCMS: 97.21%; HPLC purity: 98.59%.

*3-Methyl-N-(1-(5-methylisoxazol-3-yl)ethyl)-4-((6-(trifluoromethyl)pyridin-3-yl)methyl)-1H-pyrrole-2-carboxamide, Enantiomer I (**26**).* Racemic (**25**) was resolved by SFC purification using a Lux C4 column and 0.5% DEA in methanol as a cosolvent (30%) to afford the product (retention time 3.13) as an off-white solid (18%). Optical rotation (methanol): −14.797. 1H NMR (400 MHz, DMSO-d_6) δ (ppm): 11.02 (s, 1H), 8.63 (s, 1H), 7.81 (s, 2H), 7.80 (d, 1H), 6.73 (s, 1H), 6.18 (s, 1H), 5.13−5.17 (m, 1H), 3.86 (s, 2H), 2.34 (s, 3H), 2.14 (s, 3H), 1.44 (d, 3H); ESIMS *m/z*: 393.2; HPLC purity: 98.57%; SFC purity: 100%.

*3-Methyl-N-(1-(5-methylisoxazol-3-yl)ethyl)-4-((6-(trifluoromethyl)pyridin-3-yl)methyl)-1H-pyrrole-2-carboxamide, Enantiomer II (**27**).* The product was obtained as for (**26**) above, (retention time 4.0) as an off-white solid (14%). ^{1}H NMR (400 MHz, DMSO-d_6) δ (ppm): 11.02 (s, 1H), 8.63 (s, 1H), 7.81 (s, 2H), 7.80 (d, 1H), 6.73 (s, 1H), 6.18 (s, 1H), 5.13−5.17 (m, 1H), 3.86 (s, 2H), 2.34 (s, 3H), 2.14 (s, 3H), 1.44 (d, 3H); ESIMS *m/z* (M + 1): 393.2; HPLC purity: 98.96%; SFC purity: 100%.

*3-Methyl-N-(1-(1H-pyrazol-3-yl)ethyl)-4-((6-(trifluoromethyl)-pyridin-3-yl)methyl)-1H-pyrrole-2-carboxamide (**28**).* **28** was prepared from **1-(1*H*-pyrazol-3-yl)ethan-1-amine** and **181** as a white solid (15%). ^{1}H NMR (400 MHz, CD_3OD) δ (ppm): 8.56 (s, 1H), 7.82 (d, 1H), 7.72 (d, 1H), 7.60 (brs, 1H), 6.72 (s, 1H), 6.29 (s, 1H), 5.31−5.33 (m, 1H), 3.95 (s, 2H), 2.20 (s, 3H), 1.58 (m, 3H, *J* = 6.8

https://doi.org/10.1021/acs.jmedchem.1c00173
J. Med. Chem. 2021, 64, 6085−6136

Hz); ESIMS *m/z (M + 1)*: 378.2; LCMS: 99.58%; HPLC purity: 94.56%.

*3-Methyl-N-(1-(1-methyl-1H-pyrazol-4-yl)ethyl)-4-((6-(trifluoromethyl)pyridin-3-yl)methyl)-1H-pyrrole-2-carboxamide (**35**).* **35** was obtained from 1-(1-methyl-1*H*-pyrazol-4-yl)ethan-1-amine and **181** (58%). ^{1}H NMR (400 MHz, $CDCl_3$) δ (ppm): 9.19 (bs, 1H), 8.60 (s, 1H), 7.61 (m, 2H), 7.48 (s, 1H), 7.37 (s, 1H), 6.67 (s, 1H), 5.78−5.80 (m, 1H), 5.30−5.34 (m, 1 H), 3.90 (m, 5H), 2.14 (s, 3H), 1.59 (d, 3H); ESIMS *m/z* (M + 1): 392; LCMS: 99.89%; HPLC purity: 97.61%.

*3-Methyl-N-(1-(1-methyl-1H-pyrazol-4-yl)ethyl)-4-((6-(trifluoromethyl)pyridin-3-yl)methyl)-1H-pyrrole-2-carboxamide Enantiomer I (**36**).* Racemic product (**35**) was separated by SFC purification using a Lux A1 column and methanol cosolvent (30%) to afford enantiomer I (retention time 3.13) as an off-white solid (19%). Mp 150−153 °C. Optical rotation (ethanol): 9.997. ^{1}H NMR (400 MHz, $CDCl_3$) δ (ppm): 9.15 (bs, 1H), 8.60 (s, 1H), 7.61 (m, 2H), 7.51 (s, 1H), 7.29 (s, 1H), 6.67 (s, 1H), 5.81 (m, 1H), 5.32 (m, 1 H), 3.92−3.90 (m, 5H), 2.14 (s, 3H), 1.59 (d, 3H); ESIMS *m/z* (M + 1): 392.2; HPLC purity: 97.58%, SFC purity: 99.19%.

*3-Methyl-N-(1-(1-methyl-1H-pyrazol-4-yl)ethyl)-4-((6-(trifluoromethyl)pyridin-3-yl)methyl)-1H-pyrrole-2-carboxamide Enantiomer II (**37**).* The product was obtained as for (**36**) above (retention time 5.07) as an off-white solid (19%). ^{1}H NMR (400 MHz, $CDCl_3$) δ (ppm): 9.23 (bs, 1H), 8.60 (s, 1H), 7.61 (m, 2H), 7.51 (s, 1H), 7.41 (s, 1H), 6.67 (s, 1H), 5.82 (m, 1H), 5.32 (m, 1 H), 3.90 (m, 5H), 2.14 (s, 3H), 1.59 (d, 3H); ESIMS *m/z* (M + 1): 392.2; HPLC purity: 99.00%, SFC purity: 98.75%.

*3-Methyl-N-(1-(1-methyl-1H-1,2,4-triazol-3-yl)ethyl)-4-((6-(trifluoromethyl)pyridin-3-yl)methyl)-1H-pyrrole-2-carboxamide (**38**).* The compound was prepared from 1-(1-methyl-1*H*-1,2,4-triazol-3-yl)ethan-1-amine and **181** as (22%). ^{1}H NMR (400 MHz, CD_3OD) δ (ppm): 8.56 (s, 1H), 8.34 (s, 1H), 7.72−7.80 (m, 2H), 6.74 (s, 1H), 5.29−5.31 (m, 1H), 3.96 (s, 2H), 3.91 (s, 3H), 2.22 (s, 3H), 1.60 (d, 3H, *J* = 7.2 Hz); ESIMS *m/z* (M + 1): 393.0; LCMS: 89.09%; HPLC purity: 80.56%.

*3-Methyl-N-(1-(5-methyl-1,2,4-oxadiazol-3-yl)ethyl)-4-((6-(trifluoromethyl)pyridin-3-yl)methyl)-1H-pyrrole-2-carboxamide (**39**).* **39** was prepared from 1-(5-methyl-1,2,4-oxadiazol-3-yl)ethan-1-amine and **181** (15%). ^{1}H NMR (400 MHz, DMSO-d_6) δ (ppm): 11.06 (s, 1H), 8.63 (s, 1H), 7.88 (d, 1H), 7.81 (s, 2H), 6.74 (s, 1H), 5.17−5.24 (m, 1H), 3.86 (s, 2H), 2.57 (s, 3H), 2.14 (s, 3H), 1.48 (d, 3H, *J* = 6.8 Hz); ESIMS *m/z* (M + 1): 394.1; LCMS: 99.69%; HPLC purity: 98.36%.

*N-(1-(3-Bromoisoxazol-5-yl)ethyl)-3-methyl-4-((6-(trifluoromethyl)pyridin-3-yl)methyl)-1H-pyrrole-2-carboxamide (**51**).* **51** was obtained from 1-(3-bromoisoxazol-5-yl)ethan-1-amine and **181** (25%). ^{1}H NMR (400 MHz, DMSO-d_6) δ (ppm): 11.03 (s, 1H), 8.64 (s, 1H), 7.94 (d, 1H, *J* = 8.4 Hz), 7.81 (s, 1H), 7.80 (s, 1H), 6.73−6.76 (m, 2H), 5.25−5.29 (m, 1H), 3.86 (s, 2H), 2.14 (s, 3H), 1.49 (d, 3H, *J* = 7.0 Hz); ESIMS *m/z* (M + 2): 459.0; LCMS: 94.80%; HPLC purity: 94.87%.

*4-(Isoquinolin-8-ylmethyl)-3-methyl-N-(1-(5-methylisoxazol-3-yl)ethyl)-1H-pyrrole-2-carboxamide (**52**).* The compound was obtained from 1-(5-methylisoxazol-3-yl)ethanamine and **221** (25%). ^{1}H NMR (300 MHz, $CDCl_3$) δ (ppm): 9.53 (s, 1H), 9.36 (brs, 1H), 8.54 (d, *J* = 5.7 Hz, 1H), 7.77−7.56 (m, 3H), 7.34 (d, *J* = 7.0 Hz, 1H), 6.51 (s, 1H), 5.99 (s, 1H), 4.35 (s, 2H), 3.10−2.77 (m, 1H), 2.42 (s, 3H), 2.34 (s, 3H), 1.63 (d, *J* = 6.9 Hz, 3H). ESIMS *m/z* (M + 1): 375.0; LCMS: 96.70%.

*4-((5-Fluoroisoquinolin-8-yl)methyl)-3-methyl-N-(1-(5-methylisoxazol-3-yl)ethyl)-1H-pyrrole-2-carboxamide (**53**).* The compound was obtained from 1-(5-methylisoxazol-3-yl)ethanamine and **207** (28%). ^{1}H NMR (300 MHz, $CDCl_3$) δ 9.51 (s, 1H), 9.44 (brs, 1H), 8.60 (s, 1H), 7.95 (d, *J* = 5 Hz, 1H) 7.27 (d, *J* = 4.4 Hz 1H), 6.58 (d, *J* = 7.1 Hz, 1H), 6.47 (s, 1H), 5.95 (s, 1H), 5.50−5.23 (m, 1H), 4.29 (s, 2H), 2.40 (s, 3H), 2.32 (s, 3H), 1.62 (d, *J* = 6.4 Hz, 3H). ESIMS *m/z* (M + 1): 393.1; LCMS: 97.65%.

*3-Methyl-N-(1-(5-methylisoxazol-3-yl)ethyl)-4-(4-(trifluoromethyl)phenylmethyl)-1H-pyrrole-2-carboxamide Enantiomer I (**56**).* Racemic **56** was obtained from 1-(5-methylisoxazol-3-yl)ethan-1-amine and **183** (55%). The racemic product was separated by SFC purification using a Lux A1 column and methanol cosolvent (40%) to afford enantiomer I (retention time: 2.62) as an off-white solid (24%). 1H NMR (400 MHz, DMSO-d_6) δ (ppm): 11.05 (s, 1H), 7.80 (d, 1H, *J* = 8.0 Hz), 7.61 (s, 2H, *J* = 8.0 Hz), 7.37 (d, 2H, *J* = 8.0 Hz), 6.70 (s, 1H), 6.17 (s, 1H), 5.14−5.17 (m, 1H), 3.81 (s, 2H), 2.36 (s, 3H), 2.12 (s, 3H), 1.44 (d, 3H, *J* = 6.8 Hz); ESIMS *m/z* (M + 1): 392.2. HPLC purity: 98.86%. SFC purity: 100%.

*3-Methyl-N-(1-(5-methylisoxazol-3-yl)ethyl)-4-(4-(trifluoromethyl)phenylmethyl)-1H-pyrrole-2-carboxamide Enantiomer II (**57**).* The product was obtained as for **56** above, (retention time: 5.04) as an off-white solid (26%). ^{1}H NMR (400 MHz, DMSO-d_6) δ (ppm): 11.05 (s, 1H), 7.80 (d, 1H, *J* = 7.6 Hz), 7.61 (s, 2H, *J* = 8.0 Hz), 7.37 (d, 2H, *J* = 8.0 Hz), 6.70 (d, 1H, *J* = 2.4 Hz), 6.18 (s, 1H), 5.14−5.17 (m, 1H), 3.81 (s, 2H), 2.36 (s, 3H), 2.12 (s, 3H), 1.44 (d, 3H, *J* = 6.8 Hz); ESIMS *m/z* (M + 1): 392.2. HPLC purity: 97.54%; SFC purity: 100%.

*N-(1-(3-Bromoisoxazol-5-yl)ethyl)-3-methyl-4-(4-(trifluoromethyl)phenylmethyl)-1H-pyrrole-2-carboxamide (**58**).* Racemic **58** was obtained from 1-(3-bromoisoxazol-5-yl)ethan-1-amine and **183** as an off-white solid (24%). ^{1}H NMR (400 MHz, DMSO-d_6) δ (ppm):10.98, (s, 1H), 7.93 (d, 1H, *J* = 8.4 Hz), 7.62 (d, 2H, *J* = 8.4 Hz), 7.38 (d, 2H, *J* = 8.4 Hz), 6.73 (m, 2H), 5.28 (q, 1H, *J* = 7.2 Hz), 3.81 (s, 2H), 2.12 (s, 3H), 1.49 (d, 3H, *J* = 7.2 Hz); ESIMS *m/z*: 456.0; LCMS: 96.46%; HPLC purity: 93.86%.

*N-Cyclopropyl-3-methyl-4-(1-(6-(trifluoromethyl)pyridin-3-yl)-cyclopropyl)-1H-pyrrole-2-carboxamide (**73**).* **73** was prepared from cyclopropylamine and **251** (50%). ^{1}H NMR (400 MHz, DMSO-d_6) δ (ppm): 10.95 (s, 1H), 8.39 (s, 1H), 7.73 (d, 1H, *J* = 8.4 Hz), 7.63 (d, 1H, *J* = 8.4 Hz), 7.45 (s, 1H), 6.87 (s, 1H), 2.72−2.74 (m, 1H), 2.06 (s, 3H), 1.37−1.40 (m, 2H), 1.23−1.26 (m, 2H), 0.65−0.69 (m, 2H), 0.46−0.49 (m, 2H); ESIMS *m/z*: 350.2; LCMS: 96.67%; HPLC purity: 96.52%.

*(3,3-Difluoroazetidin-1-yl)-(3-methyl-4-(1-(6-(trifluoromethyl)-pyridin-3-yl)cyclopropyl)-1H-pyrrol-2-yl)methanone (**74**).* **74** was prepared from 3,3-difluoroazetidine hydrochloride and **251** (48%). ^{1}H NMR (400 MHz, DMSO-d_6) δ (ppm): 11.06 (s, 1H), 8.41 (s, 1H), 7.73 (d, 1H, *J* = 8.0 Hz), 7.64 (d, 1H, *J* = 8.0 Hz), 6.96 (s, 1H), 4.50−4.57 (m, 4H), 2.03 (s, 3H), 1.40 (brs, 2H), 1.27 (brs, 2H); ESIMS *m/z*: 386.1; LCMS: 99.78%; HPLC purity: 99.67%.

*3-Methyl-N-(1-(5-methylisoxazol-3-yl)ethyl)-4-(1-(6-(trifluoromethyl)pyridin-3-yl) cyclopropyl)-1H-pyrrole-2-carboxamide Enantiomer I (**75**).* Racemic **75** was prepared from 1-(5-methylisoxazol-3-yl)ethan-1-amine and **251** (56%). The racemic product was separated by SFC purification using a Chiralpak 1A column and methanol cosolvent (20%) to afford enantiomer I (retention time: 3.86) as an off-white solid (17%). ^{1}H NMR (400 MHz, DMSO-d_6) δ (ppm): 11.14 (s, 1H), 8.41 (s, 1H), 7.82 (d, 1H), 7.74 (d, 1H), 7.65 (m, 1H), 6.92 (s, 1H), 6.20 (s, 1H), 5.17 (m, 1H), 2.37 (s, 3H), 2.09 (s, 3H), 1.46 (d, 3H, *J* = 8.0 Hz), 1.41 (m, 2H), 1.26 (m, 2H); ESIMS *m/z* (M + 1): 419.0; HPLC purity: 99.59%; SFC purity: 100%.

*3-Methyl-N-(1-(5-methylisoxazol-3-yl)ethyl)-4-(1-(6-(trifluoromethyl)pyridin-3-yl)cyclopropyl)-1H-pyrrole-2-carboxamide Enantiomer II (**76**).* **76** was prepared as for **75** above to afford enantiomer II (retention time: 5.97) as an off-white solid (25%). ^{1}H NMR (400 MHz, DMSO-d_6) δ (ppm): 11.15 (s, 1H), 8.41 (s, 1H), 7.82 (d, 1H), 7.74 (d, 1H), 7.65 (m, 1H), 6.93 (s, 1H), 6.20 (s, 1H), 5.17 (m, 1H), 2.37 (s, 3H), 2.09 (s, 3H), 1.46 (d, 3H, *J* = 8.0 Hz), 1.41 (m, 2H), 1.26 (m, 2H); ESIMS *m/z* (M + 1): 419.1; HPLC purity: 99.78%; SFC purity: 100%.

*3-Methyl-N-[1-(5-methyl-1H-pyrazol-3-yl)ethyl]-4-(1-[6-(trifluoromethyl) pyridine-3-yl]cyclopropyl)-1H-pyrrole-2-carboxamide Enantiomer I (**81**).* Racemic **81** was prepared from 1-(5-methyl-1*H*-pyrazol-3-yl)ethan-1-amine and **251** (52%). The racemic product was separated by SFC purification using a YMC Amylose-C column and methanol cosolvent (40%) to afford enantiomer I (retention time: 2.27) as an off-white solid (17%). ^{1}H NMR (400 MHz, DMSO-d_6) δ (ppm): 12.21 (s, 1H), 11.11 (s, 1H), 8.39 (s, 1H), 7.71 (d, 1H, *J* = 8.3 Hz), 7.62 (d, 1H, *J* = 8.3 Hz), 7.52 (s, 1H), 6.89 (s, 1H), 5.93 (s, 1H), 5.09 (m, 1H), 2.17 (s, 3H), 2.09 (s, 3H), 1.39−1.41 (m, 5H), 1.20−

https://doi.org/10.1021/acs.jmedchem.1c00173
J. Med. Chem. 2021, 64, 6085−6136

1.25 (m, 2H); ESIMS m/z: 418.2; HPLC purity: 98.63%; SFC purity: 98.96%.

*3-Methyl-N-[1-(5-methyl-1H-pyrazol-3-yl)ethyl]-4-(1-[6-(trifluoromethyl) pyridine-3-yl]cyclopropyl)-1H-pyrrole-2-carboxamide Enantiomer II (**82**).* **82** was prepared as for **75** above to afford enantiomer II (retention time: 4.07) as an off-white solid (24%). ^{1}H NMR (400 MHz, DMSO-d_6) δ (ppm): 12.21 (s, 1H), 11.14 (s, 1H), 8.39 (s, 1H), 7.71 (d, 1H, J = 8.3 Hz), 7.62 (d, 1H, J = 8.3 Hz), 7.52 (s, 1H), 6.89 (s, 1H), 5.93 (s, 1H), 5.08 (m, 1H), 2.17 (s, 3H), 2.09 (s, 3H), 1.39−1.41 (m, 5H), 1.20−1.25 (m, 2H); ESIMS m/z: 418.2; HPLC purity: 98.56%; SFC purity: 100%.

*N2-Cyclopropyl-N3-methyl-4-((6-(trifluoromethyl)pyridin-3-yl)-methyl)-1H-pyrrole-2,3-dicarboxamide (**104**).* **104** was prepared from **261** and methylamine (2 M in THF) (38%). ^{1}H NMR (400 MHz, DMSO-d_6) δ (ppm): 11.71 (s, 1H), 9.26 (d, 1H, J = 3.6 Hz), 8.53 (d, 2H, J = 6.0 Hz), 7.73−7.80 (m, 2H), 6.72 (s, 1H), 4.12 (s, 2H), 2.75−2.78 (m, 1H), 2.67 (s, 3H), 0.69−0.73 (m, 2H), 0.42−0.45 (m, 2H); ESIMS m/z (M + 1): 367.0; LCMS:96.88%; HPLC purity: 94.41%.

*3,5-Dimethyl-N-(1-(5-methylisoxazol-3-yl) ethyl)-4-((6-(trifluoromethyl)pyridin-3-yl) methyl)-1H-pyrrole-2-carboxamide Enantiomer I (**111**).* Racemic **111** was prepared from 1-(5-methylisoxazol-3-yl)ethan-1-amine and **262**[20] (48%). The racemic product was separated by SFC purification using a Lux A1 column and methanol cosolvent (30%) to afford enantiomer I (retention time: 2.73) as an off-white solid (19%). ^{1}H NMR (400 MHz, DMSO-d_6) δ (ppm): 10.87 (s, 1H), 8.56 (s, 1H), 7.77 (d, 1H), 7.68 (d, 1H), 7.61 (s, 1H), 6.16 (d, 1H, J = 8.4 Hz), 5.12−5.16 (m, 1H), 3.82 (s, 2H), 2.36 (s, 3H), 2.15 (s, 3H), 2.11 (s, 3H), 1.43 (d, 3H); ESIMS m/z (M + 1): 407.1; HPLC purity: 98.31%; SFC purity: 98.42%.

*3,5-Dimethyl-N-(1-(5-methylisoxazol-3-yl) ethyl)-4-((6-(trifluoromethyl)pyridin-3-yl) methyl)-1H-pyrrole-2-carboxamide Enantiomer II (**112**).* **112** was prepared as for **111** above to afford the product (retention time: 5.02) as an off-white solid (18%). ^{1}H NMR (400 MHz, DMSO-d_6) δ (ppm): 10.87 (s, 1H), 8.56 (s, 1H), 7.77 (d, 1H), 7.68 (d, 1H), 7.61 (s, 1H), 6.16 (d, 1H, J = 8.4 Hz), 5.12−5.16 (m, 1H), 3.82 (s, 2H), 2.36 (s, 3H), 2.15 (s, 3H), 2.11 (s, 3H), 1.43 (d, 3H); ESIMS m/z (M + 1): 407.1; HPLC purity: 96.72%; SFC purity: 100%.

*3,5-Dimethyl-N-(1-(1-methyl-1H-pyrazol-4-yl)ethyl)-4-((6-(trifluoromethyl)pyridin-3-yl)methyl)-1H-pyrrole-2-carboxamide Enantiomer I (**113**).* Racemic **113** was obtained from 1-(1-methyl-1*H*-pyrazol-4-yl)ethan-1-amine and **262**[20] (37%). The racemic product was resolved by SFC purification using a YMC cellulose-SC column and methanol cosolvent (40%) to afford enantiomer I (retention time: 2.12) as an off-white solid (37%). ^{1}H NMR (400 MHz, DMSO-d_6) δ (ppm): 10.82 (s, 1H), 8.56 (s, 1H), 7.77 (d, 1H, J = 8.0 Hz), 7.68 (d, 1H, J = 8.0 Hz), 7.58 (s, 1H), 7.35 (s, 1H), 7.33 (bs, 1H), 5.01−5.03 (m, 1H), 3.81 (s, 2H), 3.78 (s, 3H), 2.14 (s, 3H), 2.11 (s, 3H), 1.39 (d, 3H, J = 6.8 Hz); ESIMS m/z (M + 1): 406.2; HPLC purity: 98.25%; SFC purity: 100%.

*3,5-Dimethyl-N-(1-(1-methyl-1H-pyrazol-4-yl)ethyl)-4-((6-(trifluoromethyl)pyridin-3-yl)methyl)-1H-pyrrole-2-carboxamide Enantiomer II (**114**).* **114** was prepared as for **111** above to afford the product (retention time: 2.5) as an off-white solid (24%). ^{1}H NMR (400 MHz, DMSO-d_6) δ (ppm): 10.83 (s, 1H), 8.56 (s, 1H), 7.77 (d, 1H, J = 8.0 Hz), 7.68 (d, 1H, J = 8.0 Hz), 7.58 (s, 1H), 7.35 (s, 1H), 7.33 (s, 1H), 5.01−5.04 (m, 1H), 3.81 (s, 2H), 3.78 (s, 3H), 2.14 (s, 3H), 2.11 (s, 3H), 1.39 (d, 3H, J = 6.8 Hz); ESIMS m/z (M + 1): 406.2; HPLC purity: 98.14%; SFC purity: 97.69%.

*N-Cyclopropyl-3-methyl-4-(6-(trifluoromethyl)-1H-indol-3-yl)-1H-pyrrole-2-carboxamide (**124**).* **124** was prepared from cyclopropylamine and **274** (38%). ^{1}H NMR (400 MHz, DMSO-d_6) δ (ppm): 11.55 (s, 1H), 11.11 (s, 1H), 7.74 (s, 1H), 7.72−7.74 (d, 1H), 7.55 (m, 2H), 7.30 (d, 1H, J = 8.4 Hz), 7.06 (s, 1H, J = 2.8 Hz), 2.76−2.81 (m, 1H), 2.30 (s, 3H), 0.68−0.73 (m, 2H), 0.51−0.53 (m, 2H); ESIMS m/z (M + 1): 348.1; LCMS: 94.32%; HPLC purity: 95.14%.

*(3,3-Difluoroazetidin-1-yl)(3-methyl-4-(6-(trifluoromethyl)-1H-indol-3-yl)-1H-pyrrol-2-yl)methanone (**125**).* **125** was prepared from 3,3-difluoroazetidine hydrochloride and **274** with 1 extra equiv of Et_3N, as a white solid (45%). ^{1}H NMR (400 MHz, DMSO-d_6) δ (ppm): 11.60 (s, 1H), 11.26 (s, 1H), 7.76−7.78 (d, 1H), 7.76 (s, 1H), 7.61 (s, 1H), 7.31 (d, 1H, J = 8.2 Hz), 7.16 (s, 1H), 4.56−4.62 (m, 4H), 2.27 (s, 3H); ESIMS m/z (M + 1): 384.0; LCMS: 96.23%; HPLC purity: 96.24%.

*3-Methyl-N-(1-(5-methylisoxazol-3-yl)ethyl)-4-(6-(trifluoromethyl)-1H-indol-3-yl)-1H-pyrrole-2-carboxamide Enantiomer I (**126**).* **126** was prepared from 1-(5-methylisoxazol-3-yl)ethan-1-amine and **274** as a pale yellow solid (37%). The racemic product was resolved by SFC purification using a Chiralcel OJ-H column and methanol cosolvent (40%) to afford enantiomer I (retention time: 2.58) as an off-white solid (21%). ^{1}H NMR (400 MHz, DMSO-d_6) δ (ppm): 11.55 (s, 1H), 11.26 (s, 1H), 7.87 (d, 1H, J = 8.0 Hz), 7.74 (s, 1H), 7.73 (s, 1H), 7.56 (s, 1H), 7.30 (d, 1H, J = 8.0 Hz), 7.11 (s, 1H), 6.22 (s, 1H), 5.20−5.23 (m, 1H), 2.38 (s, 3H), 2.32 (s, 3H), 1.49 (d, 3H); ESIMS m/z (M + 1): 417.1; HPLC purity: 96.65%; SFC purity: 100%.

*3-Methyl-N-(1-(5-methylisoxazol-3-yl)ethyl)-4-(6-(trifluoromethyl)-1H-indol-3-yl)-1H-pyrrole-2-carboxamide Enantiomer II (**127**).* **127** was prepared as for **126** above to afford the product (retention time: 3.18) as an off-white solid (24%). ^{1}H NMR (400 MHz, DMSO-d_6) δ (ppm): 11.57 (s, 1H), 11.27 (s, 1H), 7.88 (d, 1H, J = 8.0 Hz), 7.75 (s, 1H), 7.74 (s, 1H), 7.56 (s, 1H), 7.30 (d, 1H, J = 8.0 Hz), 7.12 (s, 1H), 6.23 (s, 1H), 5.19−5.26 (m, 1H), 2.39 (s, 3H), 2.33 (s, 3H), 1.50 (d, 3H); ESIMS m/z (M + 1): 417.1; HPLC purity: 98.81%; SFC purity: 100%.

*3-Methyl-N-(2,2,2-trifluoroethyl)-4-(6-(trifluoromethyl)-1H-indol-3-yl)-1H-pyrrole-2-carboxamide (**128**).* **128** was prepared from 2,2,2-trifluoroethan-1-amine hydrochloride and **274** with 1 extra equiv of Et_3N, as an off-white solid (25%). ^{1}H NMR (400 MHz, CD_3OD) δ (ppm): 7.71−7.72 (m, 1H), 7.68 (d, 1H, J = 8.4 Hz), 7.41 (s, 1H), 7.30 (d, 1H, J = 8.4 Hz), 7.08 (s, 1H), 4.11 (d, 2H, J = 9.2 Hz), 2.36 (s, 3H); ESIMS; m/z (M − 1): 388.1; LCMS: 92.96%; HPLC purity: 96.90%.

*3-Methyl-N-(1-(1-methyl-1H-pyrazol-3-yl)ethyl)-4-(6-(trifluoromethyl)-1H-indol-3-yl)-1H-pyrrole-2-carboxamide Enantiomer I (**129**).* Racemic **129** was prepared from 1-(1-methyl-1*H*-pyrazol-3-yl)ethan-1-amine·HCl and **274** (50%). The racemic product was resolved by SFC purification using a Chiralcel OZ-H column and IPA cosolvent (40%) to afford enantiomer I (retention time: 1.96) as an off-white solid (32%). ^{1}H NMR (400 MHz, CD_3OD) δ (ppm): 7.72 (s, 1H), 7.70 (d, 1H, J = 8.4 Hz), 7.53 (d, 1H, J = 2.2 Hz), 7.42 (s, 1H), 7.29 (d, 1H, J = 8.4 Hz), 7.05 (s, 1H), 6.28 (d, 1H, J = 2.2 Hz), 5.30 (q, 1H, J = 6.8 Hz), 3.89 (s, 3H), 2.38 (s, 3H), 1.60 (d, 3H, J = 6.8 Hz); ESIMS m/z (M + 1): 416.1; HPLC purity: 99.95%; SFC purity: 99.60%.

*3-Methyl-N-(1-(1-methyl-1H-pyrazol-3-yl)ethyl)-4-(6-(trifluoromethyl)-1H-indol-3-yl)-1H- pyrrole-2-carboxamide Enantiomer II (**130**).* **130** was prepared as for **129** above to afford the product (retention time: 2.71) as an off-white solid (20%). ^{1}H NMR (400 MHz, CD_3OD) δ (ppm): 7.72 (s, 1H), 7.70 (d, 1H, J = 8.4 Hz), 7.53 (d, 1H, J = 2.2 Hz), 7.42 (s, 1H), 7.29 (d, 1H, J = 8.4 Hz), 7.05 (s, 1H), 6.28 (d, 1H, J = 2.2 Hz), 5.31 (q, 1H, J = 6.8 Hz), 3.89 (s, 3H), 2.38 (s, 3H), 1.60 (d, 3H, J = 6.8 Hz); ESIMS m/z (M + 1): 416.1; HPLC purity: 99.70%; SFC purity: 100%.

*3-Methyl-N-(2,2,2-trifluoroethyl)-4-(6-(trifluoromethyl)-1H-indazol-3-yl)-1H-pyrrole-2-carboxamide (**133**).* **133** was prepared from 2,2,2-trifluoroethan-1-amine hydrochloride and **278** as an off-white solid (44%). ^{1}H NMR (400 MHz, CD_3OD) δ (ppm): 7.98 (d, 1H, J = 8.4 Hz), 7.89 (s, 1H), 7.42 (d, 1H, J = 8.4 Hz), 7.36 (s, 1H), 4.10−4.17 (m, 2H), 2.52 (s, 3H); ESIMS m/z (M + 1): 391.1; LCMS: 97.86%; HPLC purity: 98.42%.

*3-Methyl-N-(1-(5-methyl-1H-pyrazol-3-yl)ethyl)-4-(6-(trifluoromethyl)-1H-indazol-3-yl)-1H-pyrrole-2-carboxamide Enantiomer I (**136**).* Racemic **136** was prepared from 1-(5-methyl-1*H*-pyrazol-3-yl)ethan-1-amine and **278** (43%). The racemic product was resolved by SFC purification using a Chiralcel OD-H column and methanol cosolvent (40%) to afford enantiomer I (retention time: 1.72) as an off-white solid (24%). ^{1}H NMR (400 MHz, MeOD) δ (ppm): 7.96 (d, 1H), 7.88 (s, 1H), 7.41 (d, 1H), 7.31 (s, 1H), 6.08 (s, 1H), 5.27−5.30 (m, 1H), 2.51 (s, 3H), 2.28 (s, 3H), 1.59 (d, 3H); ESIMS; m/z (M + 1): 417.3; HPLC purity: 99.05; SFC purity: 100%.

3-Methyl-N-(1-(5-methyl-1H-pyrazol-3-yl)ethyl)-4-(6-(trifluoromethyl)-1H-indazol-3-yl)-1H-pyrrole-2-carboxamide Enantiomer II

https://doi.org/10.1021/acs.jmedchem.1c00173
J. Med. Chem. 2021, 64, 6085−6136

*(**137**).* **137** was prepared as for **136** above to afford the product (retention time: 2.36) as an off-white solid (21%). ^{1}H NMR (400 MHz, MeOD) δ (ppm): 7.96 (d, 1H), 7.88 (s, 1H), 7.41 (d, 1H), 7.31 (s, 1H), 6.08 (s, 1H), 5.29−5.30 (m, 1H), 2.51 (s, 3H), 2.28 (s, 3H), 1.59 (d, 3H); ESIMS; m/z (M + 1): 417.2; HPLC purity: 99.02; SFC purity: 100%.

*3-Methyl-N-(1-(1-methyl-1H-pyrazol-3-yl)ethyl)-4-(6-(trifluoromethyl)-1H-indazol-3-yl)-1H-pyrrole-2-carboxamide Enantiomer I (**141**).* Racemic **141** was prepared from 1-(1-methyl-1*H*-pyrazol-3-yl)ethan-1-amine·HCl and **278** (45%). The racemic product was resolved by SFC purification using a Chiralcel OZ-H column and methanol cosolvent (40%) to afford enantiomer I (retention time: 2.11) as a white solid (19%). ^{1}H NMR (400 MHz, DMSO-d_6) δ (ppm): 13.34 (s, 1H), 11.52 (s, 1H), 8.07 (d, 1H, J = 8.4 Hz), 7.89 (s, 1H), 7.74 (d, 1H), 7.60 (s, 1H), 7.37−7.43 (m, 2H), 6.19 (s, 1H), 5.16−5.20 (q, 1H, J = 6.8 Hz), 3.80 (s, 3H), 2.50 (s, 3H), 1.46 (d, 3H, J = 6.8 Hz); ESIMS; m/z (M + 1): 417.1; HPLC purity: 98.06%; SFC purity: 100%.

3-Methyl-N-(1-(1-methyl-1H-pyrazol-3-yl)ethyl)-4-(6-(trifluoromethyl)-1H-indazol-3-yl)-1H-pyrrole-2-carboxamide Enantiomer II (142). **142** was prepared as for **141** above to afford product (retention time: 2.83) as a white solid (19%). ^{1}H NMR (400 MHz, DMSO-d_6) δ (ppm): 13.34 (s, 1H), 11.52 (s, 1H), 8.07 (d, 1H, J = 8.4 Hz), 7.89 (s, 1H), 7.74 (d, 1H), 7.60 (s, 1H), 7.37−7.43 (m, 2H), 6.19 (s, 1H), 5.16−5.20 (q, 1H, J = 6.8 Hz), 3.80 (s, 3H), 2.50 (s, 3H), 1.46 (d, 3H, J = 6.8 Hz); ESIMS; m/z (M + 1): 417.2; HPLC purity: 99.66%; SFC purity: 100%.

*4-(6-Fluoro-1H-indol-3-yl)-3-methyl-N-(1-(5-methylisoxazol-3-yl)ethyl)-1H-pyrrole-2-carboxamide Enantiomer I (**143**).* Racemic **143** was prepared from 1-(5-methylisoxazol-3-yl)ethan-1-amine and **275** as a pale yellow solid (57%). The racemic product was resolved by SFC purification using a Chiralcel OJ-H column and methanol cosolvent (40%) to afford enantiomer I (retention time: 4.62) as a pale yellow solid (19%). ^{1}H NMR (400 MHz, DMSO-d_6) δ (ppm): 11.23 (s, 1H), 11.18 (s, 1H), 7.88 (d, 1H, J = 8.0 Hz), 7.52−7.56 (m, 1H), 7.30 (s, 1H), 7.15−7.18 (d, 1H), 7.09 (s, 1H), 6.85−6.90 (m, 1H), 6.22 (s, 1H), 5.19−5.23 (m, 1H), 2.39 (s, 3H), 2.33 (s, 3H), 1.49 (d, 3H, J = 7.0 Hz); ESIMS m/z (M + 1): 367.1; HPLC purity: 97.79%; SFC purity: 100%.

*4-(6-Fluoro-1H-indol-3-yl)-3-methyl-N-(1-(5-methylisoxazol-3-yl)ethyl)-1H-pyrrole-2-carboxamide Enantiomer II (**144**).* **144** was prepared as for **143** above to afford the product (retention time: 6.26) as a pale yellow solid (25%). ^{1}H NMR (400 MHz, DMSO-d_6) δ (ppm): 11.27 (s, 1H), 11.17 (s, 1H), 7.90 (d, 1H, J = 8.0 Hz), 7.52−7.56 (m, 1H), 7.30 (s, 1H), 7.15−7.18 (d, 1H), 7.09 (s, 1H), 6.85−6.90 (m, 1H), 6.22 (s, 1H), 5.19−5.23 (m, 1H), 2.38 (s, 3H), 2.33 (s, 3H), 1.49 (d, 3H, J = 7.0 Hz); ESIMS m/z (M + 1): 367.1; HPLC purity: 96.20%; SFC purity: 100%.

*3-Methyl-N-(2,2,2-trifluoroethyl)-4-(6-(trifluoromethyl)-1H-pyrazolo[3,4-b]pyridin-3-yl)-1H-pyrrole-2-carboxamide (**149**).* **149** was prepared from 2,2,2-trifluoroethan-1-amine hydrochloride and **283** as an off-white solid (32%). ^{1}H NMR (400 MHz, DMSO-d_6) δ (ppm): 13.99 (s, 1H), 11.68 (s, 1H), 8.69 (d, 1H, J = 8.4 Hz), 8.14−8.17 (m, 1H), 7.66 (d, 1H, J = 8.4 Hz),7.63 (d, 1H, J = 3.2 Hz), 4.10−4.14 (m, 2H), 2.67 (s, 3H); ESIMS m/z (M + 1): 392.1; LCMS: 96.30%; HPLC purity: 98.02%.

*(3,3-Difluoroazetidin-1-yl)-(3-methyl-4-(6-(trifluoromethyl)-1H-pyrazolo[3,4-b]pyridin-3-yl)-1H-pyrrol-2-yl)methanone (**150**).* **150** was prepared from 3,3-difluoroazetidine hydrochloride and **283** as an off-white solid (28%). ^{1}H NMR (400 MHz, DMSO-d_6) δ (ppm): 13.99 (s, 1H), 11.58 (s, 1H), 8.72 (d, 1H, J = 8.0 Hz), 7.66 (s, 1H), 7.63 (d, 1H, J = 3.2 Hz), 4.56−4.62 (m, 4H), 2.48 (s, 3H); ESIMS m/z (M + 1): 386.0; LCMS: 99.16%; HPLC purity: 99.76%.

*3-Methyl-N-(1-(1-methyl-1H-pyrazol-3-yl)ethyl)-4-(6-(trifluoromethyl)-1H-pyrazolo[3,4-b]pyridin-3-yl)-1H-pyrrole-2-carboxamide Enantiomer I (**151**).* **151** was prepared from 1-(1-methyl-1*H*-pyrazol-3-yl)ethan-1-amine, HCl, and **283** to afford the racemic title compound (45%). The racemic product was resolved by SFC purification using a Chiralcel OX-H column and IPA cosolvent (40%) to afford the title compound (retention time 2.4) as an off-white solid (26%). ^{1}H NMR (400 MHz, CD_3OD) δ (ppm): 8.51 (d, 1H, J = 8.4 Hz), 7.61 (d, 1H, J = 8.4 Hz), 7.54 (d, 1H, J = 2.0 Hz), 7.40 (s, 1H), 6.29 (d, 1H, J = 2.0 Hz), 5.29−5.34 (q, 1H, J = 6.8 Hz), 3.89 (s, 3H), 2.58 (s, 3H), 1.61 (d, 3H, J = 6.8 Hz); ESIMS m/z (M + 1): 418.2; HPLC purity: 98.86%; SFC purity: 100%.

*3-Methyl-N-(1-(1-methyl-1H-pyrazol-3-yl)ethyl)-4-(6-(trifluoromethyl)-1H-pyrazolo[3,4-b]pyridin-3-yl)-1H-pyrrole-2-carboxamide Enantiomer II (**152**).* **152** was prepared as for **151** above to afford the product (retention time: 3.23) as an off-white solid (33%). ^{1}H NMR (400 MHz, CD_3OD) δ (ppm): 8.51 (d, 1H, J = 8.4 Hz), 7.61 (d, 1H, J = 8.4 Hz), 7.54 (d, 1H, J = 2.0 Hz), 7.40 (s, 1H), 6.29 (d, 1H, J = 2.0 Hz), 5.31−5.32 (q, 1H, J = 6.8 Hz), 3.89 (s, 3H), 2.58 (s, 3H), 1.61 (d, 3H, J = 6.8 Hz); ESIMS m/z (M + 1): 418.1; HPLC purity: 99.93%; SFC purity: 98.74%.

*3-Methyl-N-(1-(5-methylisoxazol-3-yl)ethyl)-4-(6-(trifluoromethyl)-1H-pyrazolo[3,4-b]pyridin-3-yl)-1H-pyrrole-2-carboxamide Enantiomer I (**153**).* Racemic **153** was prepared from 1-(5-methylisoxazol-3-yl)ethan-1-amine and **283** as a white solid (52%). The racemic product was resolved by SFC purification using a Chiralcel OD-H column and methanol cosolvent (20%) to afford the title compound (retention time 5.21) as a white solid (15%). ^{1}H NMR (400 MHz, DMSO-d_6) δ (ppm): 13.94 (s, 1H), 11.58 (s, 1H), 8.67 (d, 1H, J = 8.0 Hz), 7.98 (d, 1H, J = 8.0 Hz), 7.58−7.65 (m, 2H), 6.22 (s, 1H), 5.22−5.24 (m, 1H), 2.56 (s, 3H), 2.38 (s, 3H), 1.50 (d, 3H, J = 6.8 Hz); ESIMS m/z (M + 1): 419.1; HPLC purity: 99.75%; SFC purity: 99.14%.

*3-Methyl-N-(1-(5-methylisoxazol-3-yl)ethyl)-4-(6-(trifluoromethyl)-1H-pyrazolo[3,4-b]pyridin-3-yl)-1H-pyrrole-2-carboxamide Enantiomer II (**154**).* **154** was prepared as for **153** above to afford the product (retention time: 5.90) as a white solid (16%). ^{1}H NMR (400 MHz, DMSO-d_6) δ (ppm): 13.94 (s, 1H), 11.57 (s, 1H), 8.67 (d, 1H, J = 8.0 Hz), 7.98 (d, 1H, J = 8.0 Hz), 7.58−7.64 (m, 2H), 6.22 (s, 1H), 5.19−5.23 (m, 1H), 2.55 (s, 3H), 2.37 (s, 3H), 1.49 (d, 3H, J = 6.8 Hz); ESIMS m/z (M + 1): 419.1; HPLC purity: 99.80%; SFC purity: 100%.

*3-Methyl-N-(2,2,2-trifluoroethyl)-4-(6-(trifluoromethyl)-1H-pyrrolo[2,3-b]pyridin-3-yl)-1H-pyrrole-2-carboxamide (**155**).* **155** was prepared from 2,2,2-trifluoroethan-1-amine hydrochloride and **276** as an off-white solid (16%). ^{1}H NMR (400 MHz, CD_3OD) δ (ppm): 8.15 (d, 1H, J = 8.4 Hz), 7.59 (s, 1H), 7.52 (d, 1H, J = 8.4 Hz), 7.14 (s, 1H), 4.09−4.16 (m, 2 H), 2.40 (s, 3H); ESIMS m/z (M + 1): 391.0; LCMS: 99.39%; HPLC purity: 95.18%.

*(3,3-Difluoroazetidin-1-yl)(3-methyl-4-(6-(trifluoromethyl)-1H-pyrrolo[2,3-b]pyridin-3-yl)-1H-pyrrol-2-yl)methanone (**156**).* **156** was prepared from 3,3-difluoroazetidine hydrochloride and **276** as a white solid (26%). ^{1}H NMR (400 MHz, CD_3OD) δ (ppm): 8.18 (d, 1H, J = 8.0 Hz); 7.61 (s, 1H), 7.52 (d, 1H, J = 8.2 Hz), 7.17 (s, 1H), 4.58−4.64 (m, 4H), 2.34 (s, 3H); ESIMS m/z (M + 1): 385.1; LCMS: 99.53%; HPLC purity: 98.31%.

*3-Methyl-N-(1-(1-methyl-1H-pyrazol-3-yl)ethyl)-4-(6-(trifluoromethyl)-1H-pyrrolo[2,3-b]pyridin-3-yl)-1H-pyrrole-2-carboxamide Enantiomer I (**157**).* **157** was prepared from 1-(1-methyl-1*H*-pyrazol-3-yl)ethan-1-amine, HCl, and **276** to afford the racemic title compound as a pale yellow solid (37%). The racemic product was resolved by SFC purification using a Chiralcel OX-H column and IPA cosolvent (40%) to afford the title compound (retention time 1.75) as an off-white solid (21%). ^{1}H NMR (400 MHz, DMSO-d_6) δ (ppm): 12.21 (s, 1H), 11.35 (s, 1H), 8.22 (d, 1H, J = 8.0 Hz), 7.73 (s, 1H), 7.68 (d, 1H, J = 8.0 Hz), 7.61 (s, 1H), 7.54 (d, 1H, J = 8.0 Hz), 7.15 (s, 1H), 6.19 (s, 1H), 5.16−5.20 (m, 1H), 3.81 (s, 3H), 2.36 (s, 3H), 1.46 (d, 3H, J = 7.2 Hz); ESIMS m/z (M + 1): 417.9; HPLC purity: 98.71%; SFC purity: 100%.

*3-Methyl-N-(1-(1-methyl-1H-pyrazol-3-yl)ethyl)-4-(6-(trifluoromethyl)-1H-pyrrolo[2,3-b]pyridin-3-yl)-1H-pyrrole-2-carboxamide Enantiomer II (**158**).* **158** was prepared as for **157** above to afford the product (retention time: 2.67) as an off-white solid (10%). ^{1}H NMR (400 MHz, DMSO-d_6) δ (ppm): 12.21 (s, 1H), 11.35 (s, 1H), 8.22 (d, 1H, J = 8.0 Hz), 7.73 (s, 1H), 7.68 (d, 1H, J = 8.0 Hz), 7.61 (s, 1H), 7.54 (d, 1H, J = 8.0 Hz), 7.15 (s, 1H), 6.19 (s, 1H), 5.16−5.20 (m, 1H), 3.81 (s, 3H), 2.36 (s, 3H), 1.46 (d, 3H, J = 7.2 Hz); ESIMS m/z (M + 1): 417.9; HPLC purity: 99.55%; SFC purity: 100%.

*3-Methyl-N-(1-(5-methylisoxazol-3-yl)ethyl)-4-(6-(trifluoromethyl)-1H-pyrrolo[2,3-b] pyridin-3-yl)-1H-pyrrole-2-carboxamide Enantiomer I (**159**).* **159** was prepared from 1-(5-methylisoxazol-3-yl)ethan-1-amine and **276** to afford the racemic title compound (45%). The

https://doi.org/10.1021/acs.jmedchem.1c00173
J. Med. Chem. 2021, 64, 6085−6136

racemic product was resolved by SFC purification using a Lux A1 column and methanol cosolvent (50%) to afford the title compound (retention time 1.56) as an off-white solid (17%). ^{1}H NMR (400 MHz, CD_3OD) δ (ppm): 8.12 (d, 1H, J = 8.0 Hz), 7.55 (s, 1H), 7.48 (d, 1H, J = 8.0 Hz), 7.08 (s, 1H), 6.16 (s, 1H), 5.28−5.33 (q, 1H, J = 7.2 Hz), 2.40 (s, 3H), 2.37 (s, 3H), 1.59 (d, 3H, J = 7.2 Hz); ESIMS m/z (M + 1): 418.0; HPLC purity: 99.41%; SFC purity: 99.72%.

*3-Methyl-N-(1-(5-methylisoxazol-3-yl)ethyl)-4-(6-(trifluoromethyl)-1H-pyrrolo[2,3-b] pyridin-3-yl)-1H-pyrrole-2-carboxamide Enantiomer II (**160**).* **160** was prepared as for **159** above to afford the product (retention time: 2.97) as an off-white solid (15%).

^{1}H NMR (400 MHz, CD_3OD) δ (ppm): 8.12 (d, 1H, J = 8.0 Hz), 7.55 (s, 1H), 7.48 (d, 1H, J = 8.0 Hz), 7.08 (s, 1H), 6.16 (s, 1H), 5.30−5.32 (q, 1H, J = 7.2 Hz), 2.40 (s, 3H), 2.37 (s, 3H), 1.59 (d, 3H, J = 7.2 Hz); ESIMS m/z (M + 1): 418.1; HPLC purity: 99.76%; SFC purity: 99.72%.

*N-Cyclopropyl-3-methyl-4-(6-(trifluoromethyl)-1H-pyrrolo[2,3-b]pyridin-3-yl)-1H-pyrrole-2-carboxamide (**163**).* **163** was prepared from cyclopropylamine and **276** as an off-white solid (31%). ^{1}H NMR (400 MHz, DMSO-d_6) δ (ppm): 12.21 (s,1H), 11.17 (s, 1H), 8.21 (d, 1H, J = 8.1 Hz), 7.72 (s, 1H), 7.58 (s, 1H), 7.54 (d, 1H, J = 8.1 Hz), 7.13 (s, 1H), 2.77−2.79 (m, 1H), 2.34 (s, 3H), 0.69−0.73 (m, 2H), 0.50−0.53 (m, 2H); ESIMS m/z (M + 1): 349.1; LCMS: 96.59%; HPLC purity: 96.22%.

*Ethyl 3-(1-(3-Methyl-4-((6-(trifluoromethyl)pyridine-3-yl)methyl)-1H-pyrrole-2-carboxamido)ethyl)-1H-pyrazole-5-carboxylate (**189**).* **189** was prepared from ethyl 3-(1-aminoethyl)-1*H*-pyrazole-5-carboxylate (preparation in Supporting Information Methods) and **181** as a yellow solid (28%). ^{1}H NMR (400 MHz, DMSO-d_6) δ (ppm): 13.38 (s, 1H), 11.01 (s, 1H), 8.61 (s, 1H), 7.77−7.80 (m, 3H), 6.62−6.73 (m, 2H), 5.17−5.19 (m, 1H), 4.18−4.21 (m, 2H), 3.84 (s, 2H), 2.37 (s, 3H), 1.44−1.48 (m, 3H), 1.18−1.21 (m, 3H); ESIMS m/z (M + 1): 450.2.

*Ethyl 3-(1-(3-Methyl-4-(1-(6-(trifluoromethyl)pyridin-3-yl)-cyclopropyl)-1H-pyrrole-2-carboxamido)ethyl)-1H-pyrazole-5-carboxylate (**256**).* **256** was prepared from ethyl 3-(1-aminoethyl)-1*H*-pyrazole-5-carboxylate (preparation in Supporting Information Methods) and **251** as a gummy solid (59%). The product was used directly without further purification.

*N-Cyclopropyl-3-formyl-4-(6-(trifluoromethyl)pyridine-3-carbonyl)-1H-pyrrole-2-carboxamide (**259**).* The title compound was prepared from **258** using general procedure E followed by general procedure F1 with cyclopropylamine to afford the product as an off-white solid (32%). ESIMS m/z (M + 1): 352.2. The product was used without further characterization.

*Ethyl 3-(1-(3-Methyl-4-(6-(trifluoromethyl)-1H-indazol-3-yl)-1H-pyrrole-2-carboxamido)ethyl)-1H-pyrazole-5-carboxylate (**279**).* Racemic **279** was prepared from ethyl 3-(1-aminoethyl)-1*H*-pyrazole-5-carboxylate (preparation in Supporting Information Methods) and **278** as a gummy solid (68%). The product was used directly without purification.

General Procedure F2: Amide Formation. Me_3Al (2.0 M in toluene) (1.5 equiv) was added to a stirred solution of pyrrole ester intermediate (1 equiv) and amine (1.1−1.5 equiv) in THF at RT and heated at 100−120 °C for 1 h in a microwave. After completion of the reaction (monitored by TLC), 1.5 N HCl solution was added to the reaction mixture and extracted with ethyl acetate (2×). The combined organic layer was dried over Na_2SO_4 and concentrated. The resulting concentrated product was purified by column chromatography using 10−60% ethyl acetate in petroleum ether to afford the compound as a white solid (21−37%). Compounds **8**−**10** and **115**−**116** were prepared using this procedure.

*N-Cyclopropyl-4-((2-fluoro-6-(trifluoromethyl)pyridin-3-yl) methyl)-3-methyl-1H-pyrrole-2-carboxamide (**8**).* **8** was prepared from cyclopropamine and **179** (37%). ^{1}H NMR (400 MHz, $CDCl_3$) δ (ppm): 9.23 (brs, 1H), 7.60 (d, 1H, J = 8.0 Hz), 7.50 (d, 1H J = 8.0 Hz), 6.74 (s, 1H), 5.87 (brs, 1H), 3.88 (s, 2H), 2.86−2.90 (m, 1H), 2.14 (s, 3H), 0.87−0.92 (m, 2H), 0.62−0.64 (m, 2H); ESIMS m/z (M + 1): 342.2; LCMS: 93.46%; HPLC purity: 96.21%.

*((2-Fluoro-6-(trifluoromethyl)pyridin-3-yl)methyl)-3-methyl-N-(2,2,2-trifluoroethyl)-1H-pyrrole-2-carboxamide (**9**).* **9** was prepared from 2,2,2-trifluoro-ethanamine and **179** (21%). ^{1}H NMR (400 MHz, $CDCl_3$) δ (ppm): 9.18 (s, 1H), 7.60−7.64 (m, 1H), 7.50 (d, 1H J = 8.0 Hz), 6.78 (s, 1H), 5.90 (brs, 1H), 4.12−4.16 (m, 2H), 3.89 (s, 2H), 2.23 (s, 3H); ESIMS m/z (M − 1): 382.0; LCMS: 95.70%; HPLC purity: 94.43%.

*(3,3-Difluoroazetidin-1-yl)(4-((2-fluoro-6-(trifluoromethyl)-pyridin-3-yl)methyl)-3-methyl-1H-pyrrol-2-yl)methanone (**10**).* **10** was prepared from 3,3-difluoro-azetidine and **179** (26%). ^{1}H NMR (400 MHz, $CDCl_3$) δ (ppm): 8.84 (brs, 1H), 7.63−7.67 (m, 1H), 7.51 (d, 1H J = 7.6 Hz), 6.77 (s, 1H), 4.47−4.54 (m, 4H), 3.87 (s, 2H), 2.13 (s, 3H); ESIMS m/z (M + 1): 378.0; LCMS: 99.59%; HPLC purity: 99.34%.

*3-Cyano-5-methyl-N-(1-(5-methylisoxazol-3-yl)ethyl)-4-((6-(trifluoromethyl)pyridin-3-yl)methyl)-1H-pyrrole-2-carboxamide Enantiomer I (**115**).* **115** was prepared from 1-(5-methylisoxazol-3-yl)ethan-1-amine and **265** to afford the racemic product (40%). The racemic product was separated by SFC purification using a YMC cellulose C column and IPA cosolvent (30%) to afford enantiomer I (retention time: 1.96) as a white solid (27%). ^{1}H NMR (400 MHz, DMSO-d_6) δ (ppm): 12.11 (s, 1H), 8.64 (s, 1H), 8.34 (d, 1H, J = 8. 0 Hz), 7.79−7.86 (m, 2H), 6.21 (s, 1H), 5.14 (q, 1H, J = 7.2 Hz), 3.98 (s, 2H), 2.37 (s, 3H), 2.24 (s, 3H), 1.46 (d, 3H, J = 7.2 Hz); ESIMS m/z (M + 1): 418.1; HPLC purity: 96.69%; SFC purity: 100%.

*3-Cyano-5-methyl-N-(1-(5-methylisoxazol-3-yl)ethyl)-4-((6-(trifluoromethyl)pyridin-3-yl)methyl)-1H-pyrrole-2-carboxamide Enantiomer II (**116**).* **116** was prepared as for **115** above to afford the product (retention time: 4.05) as an off-white solid (30%). ^{1}H NMR (400 MHz, DMSO-d_6) δ (ppm): 12.11 (s, 1H), 8.64 (s, 1H), 8.33 (d, 1H, J = 8. 0 Hz), 7.79−7.86 (m, 2H), 6.21 (s, 1H), 5.14 (q, 1H, J = 7.2 Hz), 3.98 (s, 2H), 2.37 (s, 3H), 2.23 (s, 3H), 1.46 (d, 3H, J = 7.2 Hz); ESIMS m/z (M + 1): 418.1; HPLC purity: 99.28%; SFC purity: 99.34%.

General Procedure G: Amide Coupling followed by Trityl Deprotection. Amide coupling was carried out as described in general procedure F1. The uncharacterized product in CH_2Cl_2, was treated with TFA (4 equiv) and triethylsilane (2 equiv) at RT and stirred for 1 h. After completion of the reaction, the reaction mixture was quenched with sat. $NaHCO_3$ by a dropwise addition at 0 °C and extracted with CH_2Cl_2 (3×). The combined organic layers were dried (Na_2SO_4), filtered, and concentrated. The resulting concentrated product was purified by column chromatography using 0−5% methanol in CH_2Cl_2 to afford the product as an off-white solid (3−38%). Compounds **29**−**34, 40, 42**−**43, 54**−**55, 59**−**60, 62**−**65, 77**−**80, 92**−**97, 101**−**102, 107**−**110, 120**−**123, 161**−**162, and 224** were prepared using this procedure. Examples **61** and **117**−**118** were prepared by a modified procedure as described.

*N-(1-(1H-1,2,4-Triazol-3-yl) ethyl)-3-methyl-4-((6-(trifluoromethyl)pyridin-3-yl)methyl)-1H-pyrrole-2-carboxamide (**29**).* **29** was obtained from 1-(1-(triphenylmethyl)-1*H*-1,2,4-triazol-3-yl)ethan-1-amine (preparation in Supporting Information Methods) and **181** (15%). ^{1}H NMR (400 MHz, DMSO-d_6_D_2O) δ (ppm): 8.59 (s, 1H), 7.78 (s, 2H), 6.73 (s, 1H), 5.20−5.18 (m, 1H), 3.83 (s, 2H), 2.12 (s, 3H), 1.45 (d, J = 7.2 Hz, 3H); ESIMS m/z (M + 1): 379.2; LCMS: 98.44%; HPLC purity: 98.07%.

*N-(1-(1H-1,2,4-Triazol-3-yl) ethyl)-3-methyl-4-((6-(trifluoromethyl)pyridin-3-yl)methyl)-1H-pyrrole-2-carboxamide Enantiomer I (**30**).* The racemic product **29** was separated by SFC purification using a LuxA1 column and methanol cosolvent (30%) to afford Enantiomer I (retention time: 2.89) as an off-white solid (21%). ^{1}H NMR (400 MHz, DMSO-d_6) δ (ppm): 8.63 (s, 1H), 8.14 (bs, 1H), 7.97 (bs, 1H), 7.80 (s, 2H), 6.72 (s, 1H), 5.21−5.26 (m, 1H), 3.86 (s, 2H), 2.16 (s, 3H), 1.49 (d, 3H); ESIMS m/z (M + 1): 379.2; HPLC purity: 97.75%; SFC purity: 100%.

*N-(1-(1H-1,2,4-Triazol-3-yl) ethyl)-3-methyl-4-((6-(trifluoromethyl)pyridin-3-yl)methyl)-1H-pyrrole-2-carboxamide Enantiomer II (**31**).* The product was obtained as for **30** above (retention time: 4.21) to afford enantiomer II as an off-white solid (25%). ^{1}H NMR (400 MHz, DMSO-d_6) δ (ppm): 8.63 (s, 1H), 8.14 (bs, 1H), 7.96 (bs, 1H), 7.80 (s, 2H), 6.72 (s, 1H), 5.22−5.26 (m, 1H), 3.86 (s, 2H), 2.16 (s, 3H), 1.46 (d, J = 7.2 Hz, 3H); ESIMS m/z (M + 1): 379.2; HPLC purity: 99.15%; SFC purity: 100%.

https://doi.org/10.1021/acs.jmedchem.1c00173
J. Med. Chem. 2021, 64, 6085−6136

*3-Methyl-N-(1-(1H-pyrazol-4-yl)ethyl)-4-((6-(trifluoromethyl)-pyridin-3-yl)methyl)-1H-pyrrole-2-carboxamide (**32**).* **32** was obtained from 1-(1-(triphenylmethyl)-1*H*-pyrazol-4-yl)ethan-1-amine (preparation in Supporting Information Methods) and **181** (19%). ^{1}H NMR (400 MHz, CD_3OD) δ (ppm): 8.40 (s, 1H), 7.65 (d, 1H, J = 8.2 Hz), 7.56 (d, 1H, J = 8.2 Hz), 7.46 (brs, 2H), 6.54 (s, 1H), 5.09 (q, 1H, J = 6.8 Hz), 3.79 (s, 2H), 2.04 (s, 3H), 1.41 (d, 3H, J = 6.8 Hz); ESIMS m/z (M + 1): 378; LCMS: 99.90%; HPLC purity: 96.45%.

*3-Methyl-N-(1-(1H-pyrazol-4-yl)ethyl)-4-((6-(trifluoromethyl)-pyridin-3-yl)methyl)-1H-pyrrole-2-carboxamide Enantiomer I (**33**).* The racemic product **32** was separated by SFC purification using a LuxA1 column and methanol cosolvent (30%) to afford Enantiomer I (retention time: 2.94) as an off-white solid (26%). Mp 225−230 °C. Optical rotation (ethanol): 9.198. ^{1}H NMR (400 MHz, CD_3OD) δ (ppm): 8.56 (s, 1H), 7.81 (d, 1H, J = 8.2 Hz), 7.71 (d, 1H, J = 8.2 Hz), 7.61 (brs, 2H), 6.70 (s, 1H), 5.25 (q, 1H, J = 6.8 Hz), 3.94 (s, 2H), 2.19 (s, 3H), 1.57 (d, 3H, J = 6.8 Hz); ESIMS m/z (M + 1): 378.2; HPLC purity: 98.61%; SFC purity: 99.72%.

*3-Methyl-N-(1-(1H-pyrazol-4-yl)ethyl)-4-((6-(trifluoromethyl)-pyridin-3-yl)methyl)-1H-pyrrole-2-carboxamide Enantiomer II (**34**).* The product was obtained as for **33** above (retention time: 4.27) to afford enantiomer II as an off-white solid (26%). ^{1}H NMR (400 MHz, CD_3OD) δ (ppm): 8.56 (s, 1H), 7.81 (d, 1H, J = 8.2 Hz), 7.71 (d, 1H, J = 8.2 Hz), 7.61 (brs, 2H), 6.70 (s, 1H), 5.25 (q, 1H, J = 6.8 Hz), 3.94 (s, 2H), 2.19 (s, 3H), 1.57 (d, 3H, J = 6.8 Hz); ESIMS m/z (M + 1): 378.2; HPLC purity: 98.52%; SFC purity: 99.74%.

*3-Methyl-N-(1-(5-methyl-1H-1,2,4-triazol-3-yl)ethyl)-4-((6-(trifluoromethyl) pyridin-3-yl)methyl)-1H-pyrrole-2-carboxamide (**40**).* **40** was obtained from 1-(5-methyl-1-triphenymethyl-1*H*-1,2,4-triazol-3-yl)ethan-1-amine (preparation in Supporting Information Methods) and **181** (36%). ^{1}H NMR (400 MHz, CD_3OD) δ (ppm): 8.56 (s, 1H), 7.83 (d, J = 8.2 Hz, 1H), 7.73 (d, J = 8.2 Hz, 1 H), 6.75 (s, 1H), 5.27−5.28 (m, 1H), 3.96 (s, 2H), 2.72 (s, 3H), 2.24 (s, 3H), 1.60 (brs, 3H); ESIMS m/z (M + 1): 393.2; LCMS: 94.65%; HPLC purity: 96.64%.

*3-Methyl-N-(1-(5-methyl-1H-pyrazol-3-yl)ethyl)-4-((6-(trifluoromethyl)pyridin-3-yl)methyl)-1H-pyrrole-2-carboxamide Enantiomer I (**42**).* Racemic **42** was prepared from 1-(5-methyl-1*H*-pyrazol-3-yl)ethan-1-amine and **181** (36%). The racemic product was separated by SFC purification using a LuxA1 column and methanol cosolvent (40%) to afford enantiomer I (retention time: 2.44) as an off-white solid (24%). ^{1}H NMR (400 MHz, DMSO-d_6) δ (ppm): 12.22 (s, 1H), 11.04 (s, 1H), 8.63 (s, 1H), 7.80 (s, 2H), 7.53 (bs, 1H), 6.69 (s, 1 H), 5.92 (s, 1H), 5.09 (m, 1H), 3.85 (s, 2H), 2.17 (s, 3H), 2.15 (s, 3H), 1.40 (d, 3H, J = 6.8 Hz); ESIMS m/z (M + 1): 392.1; HPLC purity: 98.86%; SFC purity: 100%.

*3-Methyl-N-(1-(5-methyl-1H-pyrazol-3-yl)ethyl)-4-((6-(trifluoromethyl)pyridin-3-yl)methyl)-1H-pyrrole-2-carboxamide Enantiomer II (**43**).* The product was obtained as for **42** above (retention time: 5.02) as an off-white solid (26%). ^{1}H NMR (400 MHz, DMSO-d_6) δ (ppm): 12.22 (s, 1H), 11.04 (s, 1H), 8.63 (s, 1H), 7.80 (s, 2H), 7.53 (bs, 1H), 6.69 (s, 1 H), 5.92 (s, 1H), 5.09 (m, 1H), 3.85 (s, 2H), 2.17 (s, 3H), 2.15 (s, 3H), 1.40 (d, 3H, J = 6.8 Hz); ESIMS m/z (M + 1): 392.1; HPLC purity: 98.93%; SFC purity: 100%.

*N-(1-(1H-1,2,4-Triazol-3-yl)ethyl)-4-((5-fluoroisoquinolin-8-yl)-methyl)-3-methyl-1H-pyrrole-2-carboxamide Enantiomer I (**54**).* The product was prepared from 1-(1-(triphenylmethyl)-1*H*-1,2,4-triazol-3-yl)ethan-1-amine (preparation in Supporting Information Methods) and **207** (23%). The racemic product was separated by SFC purification using a LuxA1 column and methanol cosolvent (40%) to afford enantiomer I (retention time 3.73) as an off-white solid (29%). ^{1}H NMR (400 MHz, CD_3OD) δ (ppm): 9.49 (s, 1H), 8.54 (d, 1H, J = 5.9 Hz), 8.23 (s, 1H), 8.01 (d, 1H, J = 5.9 Hz), 7.40−7.43 (m, 2H), 6.46 (s, 1H), 5.36 (q, 1H, J = 7.0 Hz), 4.34 (s, 2H), 2.31 (s, 3H), 1.61 (d, 3H, J = 7.0 Hz); ESIMS m/z (M + 1): 379.1; HPLC purity: 98.09%, SFC purity: 100%.

*N-(1-(1H-1,2,4-Triazol-3-yl)ethyl)-4-((5-fluoroisoquinolin-8-yl)-methyl)-3-methyl-1H-pyrrole-2-carboxamide Enantiomer II (**55**).* The product was obtained as for **54** above (retention time: 5.62) as an off-white solid (31%). ^{1}H NMR (400 MHz, CD_3OD) δ (ppm): 9.49 (s, 1H), 8.53 (d, 1H, J = 5.9 Hz), 8.14 (s, 1H), 8.01 (d, 1H, J = 5.9 Hz), 7.40−7.45 (m, 2H), 6.45 (s, 1H), 5.36 (q, 1H, J = 7.0 Hz), 4.34 (s, 2H), 2.30 (s, 3H), 1.61 (d, 3H, J = 7.0 Hz); ESIMS m/z (M + 1): 379.1; HPLC purity: 99.01%, SFC purity: 100%.

*N-(1-(1H-1,2,4-Triazol-3-yl)ethyl)-4-(2-fluoro-4-(trifluoromethyl)-benzyl)-3-methyl-1H-pyrrole-2-carboxamide Enantiomer I (**59**).* Racemic **59** was prepared from 1-(1-triphenylmethyl-1*H*-1,2,4-triazol-3-yl)ethan-1-amine (preparation in Supporting Information Methods) and **208** (30%). The racemic product was separated by SFC purification using a Lux A1 column and methanol cosolvent (30%) to afford enantiomer I (retention time 2.16) as an off-white solid (26%). ^{1}H NMR (400 MHz, DMSO-d_6) δ (ppm): 13.60 (bs, 1H), 11.06 (s, 1H), 8.20 (brs, 1H), 7.76 (s, 1H), 7.60 (d, 1H, J = 8.0 Hz), 7.49 (d, 1H, J = 8.0 Hz), 7.33−7.37 (m, 1H), 6.66 (s, 1H), 5.23 (q, 1H, J = 7.0 Hz), 3.79 (s, 2H), 2.16 (s, 3H), 1.46 (d, 3H, J = 7.0 Hz); ESIMS m/z (M + 1): 396.1; HPLC purity: 97.47%. SFC purity: 100%.

*N-(1-(1H-1,2,4-Triazol-3-yl)ethyl)-4-(2-fluoro-4-(trifluoromethyl)-benzyl)-3-methyl-1H-pyrrole-2-carboxamide Enantiomer II (**60**).* The product was obtained as for **59** above (retention time: 2.79) as an off-white solid (23%). ^{1}H NMR (400 MHz, DMSO-d_6) δ (ppm): 13.82 (bs, 1H), 11.07 (s, 1H), 8.20 (brs, 1H), 7.76 (s, 1H), 7.60 (d, 1H, J = 8.0 Hz), 7.49 (d, 1H, J = 8.0 Hz), 7.34−7.38 (m, 1H), 6.67 (s, 1H), 5.24 (q, 1H, J = 7.0 Hz), 3.80 (s, 2H), 2.17 (s, 3H), 1.47 (d, 3H, J = 7.0 Hz); ESIMS m/z (M + 1): 396.1; HPLC purity: 96.32%. SFC purity: 99.19%.

*N-(1-(1H-1,2,4-Triazol-3-yl) ethyl)-4-((2-fluoro-6-(trifluoromethyl)pyridin-3-yl)methyl)-3-methyl-1H-pyrrole-2-carboxamide (**61**).* Racemic **61** was prepared from 1-(1-triphenylmethyl-1*H*-1,2,4-triazol-3-yl)ethan-1-amine (preparation in Supporting Information Methods) and **179** using general procedure F2 and trityl deprotection as described to afford the product as an off-white solid (3%). ^{1}H NMR (400 MHz, $CDCl_3$) δ (ppm): 10.25 (s, 1H), 8.12 (brs, 1H), 7.61 (d, 1H, J = 8.0 Hz), 7.48 (d, 1H, J = 8.0 Hz), 6.76 (s, 1H), 6.71 (bs, 1H), 5.48−5.52 (m, 1H), 3.87 (s, 2H), 2.24 (s, 3H), 1.77 (d, 3H, J = 6.8 Hz); ESIMS m/z (M + 1): 397.1; LCMS: 94.41%; HPLC purity: 95.36%.

*N-(1-(1H-1,2,4-Triazol-3-yl)ethyl)-4-(2-bromo-4-(trifluoromethyl)benzyl)-3-methyl-1H-pyrrole-2-carboxamide (**62**).* Racemic **62** was prepared from 1-(1-triphenylmethyl-1*H*-1,2,4-triazol-3-yl)ethan-1-amine (preparation in Supporting Information Methods) and **209** (14%). ^{1}H NMR (400 MHz, MeOD) δ (ppm): 8.44 (brs, 1H), 7.86 (s, 1H), 7.54 (d, 1H, J = 8.0 Hz), 7.27 (d, 1H, J = 8.0 Hz), 6.63 (s, 1H), 5.36−5.37 (m, 1H), 3.94 (s, 2H), 2.18 (s, 3H), 1.61 (brs, 3H); ESIMS m/z (M, M + 2): 456.1, 458.1; LCMS: 96.33%; HPLC purity: 95.93%.

*N-(1-(1H-1,2,4-Triazol-3-yl)ethyl)-4-((2-cyano-6-(trifluoromethyl)pyridine-3-yl) methyl)-3-methyl-1H-pyrrole-2-carboxamide (**63**).* Racemic **63** was prepared from 1-(1-triphenylmethyl-1*H*-1,2,4-triazol-3-yl)ethan-1-amine (preparation in Supporting Information Methods) and **210** to afford the product as a white solid (3%). ^{1}H NMR (400 MHz, CD_3OD) δ (ppm): 8.42 (brs, 1H), 7.95 (s, 2H), 6.75 (s, 1H), 5.35 (q, 1H, J = 6.0 Hz), 4.13 (s, 2H), 2.23 (s, 3H), 1.61 (d, 3H, J = 6.0 Hz); ESIMS m/z (M + 1): 404.1; LCMS: 94.79%; HPLC purity: 92.83%.

*N-(1-(1H-1,2,4-Triazol-3-yl) ethyl)-4-((3,4-difluorophenyl)-methyl)-3-methyl-1H-pyrrole-2-carboxamide Enantiomer I (**64**).* Racemic **64** was prepared from 1-(1-triphenylmethyl-1*H*-1,2,4-triazol-3-yl)ethan-1-amine (preparation in Supporting Information Methods) and **211** (14%). The racemic product was separated by SFC purification using a Lux A1 column and methanol cosolvent (40%) to afford enantiomer I (retention time 2.49) as an off-white solid (23%). ^{1}H NMR (400 MHz, DMSO-d_6) δ (ppm): 13.81 (brs, 1H), 11.01 (bs, 1H), 8.44 (bs, 1 h), 7.74 (brs, 1H), 7.27−7.34 (m, 1H), 7.14−7.18 (m, 1H), 7.00 (s, 1H), 6.69 (s, 1H), 5.20−5.27 (m, 1H), 3.71 (s, 2H), 2.13 (s, 3H), 1.47 (d, 3H); ESIMS m/z (M + 1): 346.1; HPLC purity: 99.54%; SFC purity: 100%.

*N-(1-(1H-1,2,4-Triazol-3-yl) ethyl)-4-((3,4-difluorophenyl)-methyl)-3-methyl-1H-pyrrole-2-carboxamide Enantiomer II (**65**).* The product was obtained as for **64** above (retention time: 3.61) as an off-white solid (19%). ^{1}H NMR (400 MHz, DMSO-d_6) δ (ppm): 13.81 (brs, 1H), 11.01 (bs, 1H), 8.48 (bs, 1 h), 7.63−7.85 (brs, 1H), 7.27−7.34 (m, 1H), 7.15−7.20 (m, 1H), 7.00 (s, 1H), 6.69 (s, 1H),

https://doi.org/10.1021/acs.jmedchem.1c00173
J. Med. Chem. 2021, 64, 6085−6136

5.23 (m, 1H), 3.71 (s, 2H), 2.13 (s, 3H), 1.47 (d, 3H); ESIMS *m*/*z* (M + 1): 346.1; HPLC purity: 99.47%; SFC purity: 100%.

*N-(1-(1H-Pyrazol-4-yl)ethyl)-3-methyl-4-(1-(6-(trifluoromethyl)-pyridin-3-yl)cyclopropyl)-1H-pyrrole-2-carboxamide Enantiomer I (**77**).* Racemic **77** was prepared from 1-(1-(triphenylmethyl)-1*H*-pyrazol-4-yl)ethan-1-amine (preparation in Supporting Information Methods) and **251** to afford the racemic product (24%). The racemic product was separated by SFC purification using a Lux A1 column and methanol cosolvent (30%) to afford enantiomer I (retention time 2.41) as an off-white solid (30%). ^{1}H NMR (400 MHz, DMSO-d_6) δ (ppm): 11.07 (s, 1H), 8.39 (s, 1H), 7.72 (d, 1H), 7.64 (s, 1H), 7.62 (brs, 1H), 7.51 (d, 1H), 7.45 (brs, 1H), 6.87 (s, 1H), 5.05−5.11 (m, 1H), 2.09 (s, 3H), 1.39−1.43 (m, 4H), 1.24 (brs, 3H). ESIMS *m*/*z*: 404.2; HPLC purity: 96.93%, SFC purity: 98.61%.

*N-(1-(1H-Pyrazol-4-yl)ethyl)-3-methyl-4-(1-(6-(trifluoromethyl)-pyridin-3-yl)cyclopropyl)-1H-pyrrole-2-carboxamide Enantiomer II (**78**).* The product was obtained as for **77** above (retention time: 3.2) as an off-white solid (19%). ^{1}H NMR (400 MHz, DMSO-d_6) δ (ppm): 11.07 (s, 1H), 8.39 (s, 1H), 7.72 (d, 1H), 7.64 (s, 1H), 7.62 (brs, 1H), 7.51 (d, 1H), 7.45 (brs, 1H), 6.87 (s, 1H), 5.05−5.11 (m, 1H), 2.09 (s, 3H), 1.39−1.43 (m, 4H), 1.24 (brs, 3H). ESIMS *m*/*z* (M + 1): 404.2, HPLC purity: 98.54%, SFC purity: 96.02%.

*3-Methyl-N-(1-(1H-1,2,4-triazol-3-yl)ethyl)-4-(1-(6-(trifluoromethyl) pyridin-3-yl)cyclopropyl)-1H-pyrrole-2-carboxamide Enantiomer I (**79**).* Racemic **79** was prepared from 1-(1-triphenylmethyl-1*H*-1,2,4-triazol-3-yl)ethan-1-amine (preparation in Supporting Information Methods) and **251** to afford the product (43%) as a white solid. The racemic product was separated by SFC purification using a Lux A1 column and isopropanol cosolvent (30%) to afford enantiomer I (retention time 2.07) as an off-white solid (23%). Mp 140−145°C. Optical rotation (ethanol): −15.196. ^{1}H NMR (400 MHz, CD_3OD) δ (ppm): 8.36 (s, 2H), 7.68 (s, 2H), 6.93 (s, 1H), 5.38 (q, 1H, *J* = 6.8 Hz), 2.21 (s, 3H), 1.63 (d, 3H, *J* = 6.8 Hz), 1.42−1.45 (m, 2H), 1.36−1.39 (m, 2H); ESIMS *m*/*z* (M + 1): 405.2; HPLC purity: 99.39%; SFC purity: 100%.

*3-Methyl-N-(1-(1H-1,2,4-triazol-3-yl)ethyl)-4-(1-(6-(trifluoromethyl) pyridin-3-yl)cyclopropyl)-1H-pyrrole-2-carboxamide Enantiomer II (**80**).* The product was obtained as for **79** above (retention time: 3.81) as an off-white solid (20%). Optical rotation (ethanol): 15.596. ^{1}H NMR (400 MHz, CD_3OD) δ (ppm): 8.36 (s, 2H), 7.68 (s, 2H), 6.93 (s, 1H), 5.38 (q, 1H, *J* = 6.8 Hz), 2.21 (s, 3H), 1.63 (d, 3H, *J* = 6.8 Hz), 1.42−1.45 (m, 2H), 1.36−1.39 (m, 2H); ESIMS *m*/*z*: 405.2; HPLC purity: 98.47%; SFC purity: 100%.

*N-(1-(1H-1,2,4-Triazol-3-yl) ethyl)-4-(1-(2-fluoro-4-(trifluoromethyl)phenyl)cyclopropyl)-3-methyl-1H-pyrrole-2-carboxamide Enantiomer I (**92**).* Racemic **92** was prepared from 1-(1-triphenylmethyl-1*H*-1,2,4-triazol-3-yl)ethan-1-amine (preparation in Supporting Information Methods) and **252** (36%). The racemate was resolved by SFC purification using a Lux A1 column and methanol cosolvent (30%) to afford enantiomer I (retention time: 2.1) as an off-white solid (18%). ^{1}H NMR (400 MHz, CD_3OD) δ (ppm): 8.45 (brs, 1H), 7.66−7.70 (m, 1H), 7.40 (d, 1H, *J* = 8.0 Hz), 7.29 (d, 1H, *J* = 8.0 Hz), 6.94 (s, 1H), 5.32 (m, 1H), 2.32 (s, 3H), 1.59 (brs, 3H), 1.28−1.31 (m, 2H), 1.18−1.19 (m, 2H); ESIMS *m*/*z* (M + 1): 422.1; LCMS 97.84%; SFC purity: 98.09%.

*N-(1-(1H-1,2,4-Triazol-3-yl) ethyl)-4-(1-(2-fluoro-4-(trifluoromethyl)phenyl)cyclopropyl)-3-methyl-1H-pyrrole-2-carboxamide Enantiomer II (**93**).* The product was obtained as for **92** above (retention time: 2.87) as an off-white solid (17%). ^{1}H NMR (400 MHz, CD_3OD) δ (ppm): 8.45 (brs, 1H), 7.66−7.70 (m, 1H), 7.40 (d, 1H, *J* = 8.0 Hz), 7.29 (d, 1H, *J* = 8.0 Hz), 6.94 (s, 1H), 5.33 (m, 1H), 2.32 (s, 3H), 1.59 (brs, 3H), 1.27−1.31 (m, 2H), 1.17−1.19 (m, 2H); ESIMS *m*/*z* (M + 1): 422.1; LCMS 98.78%; SFC purity: 100%.

*N-(1-(1H-1,2,4-Triazol-3-yl)ethyl)-4-(1-(3-fluoro-4-(trifluoromethyl)phenyl)cyclopropyl)-3-methyl-1H-pyrrole-2-carboxamide Enantiomer I (**94**).* Racemic **94** was prepared from 1-(1-triphenylmethyl-1*H*-1,2,4-triazol-3-yl)ethan-1-amine (preparation in Supporting Information Methods) and **253** (39%). The racemate was resolved by SFC purification using a Lux A1 column and IPA cosolvent (40%) to afford enantiomer I (retention time: 1.48) as an off-white solid (28%). ^{1}H NMR (400 MHz, CD_3OD) δ (ppm): 8.47 (brs, 1H), 7.48−7.57 (m, 1H), 6.99 (d, 1H), 6.89−6.95 (m, 2H), 5.38 (brs, 1H), 2.20 (s, 3H), 1.59−1.63 (brs, 3H), 1.31−1.42 (m, 4H); ESIMS *m*/*z* (M + 1): 422.1; LCMS: 98.08%; HPLC purity: 92.20%; SFC purity: 96.07%.

*N-(1-(1H-1,2,4-Triazol-3-yl)ethyl)-4-(1-(3-fluoro-4-(trifluoromethyl)phenyl)cyclopropyl)-3-methyl-1H-pyrrole-2-carboxamide Enantiomer II (**95**).* The product was obtained as for **94** above (retention time: 2.45) as an off-white solid (33%). ^{1}H NMR (400 MHz, CD_3OD) δ (ppm): 8.46 (brs, 1H), 7.48−7.53 (t, 1H), 6.99 (d, 1H), 6.90−6.95 (m, 2H), 5.38 (brs, 1H), 2.20 (s, 3H), 1.59−1.64 (brs, 3H), 1.31−1.42 (m, 4H); ESIMS *m*/*z* (M + 1): 422.1; LCMS: 98.53%; HPLC purity: 90.95%; SFC purity: 97.84%.

*N-(1-(1H-1,2,4-Triazol-3-yl) ethyl)-3-methyl-4-(1-(3-(trifluoromethyl)phenyl)cyclopropyl)-1H-pyrrole-2-carboxamide Enantiomer I (**96**).* Racemic **96** was prepared from 1-(1-triphenylmethyl-1*H*-1,2,4-triazol-3-yl)ethan-1-amine (preparation in Supporting Information Methods) and **254** (32%). The racemate was resolved by SFC purification using a Lux A1 column and 0.5% isopropylamine in IPA cosolvent (40%) to afford enantiomer I (retention time: 1.41) as an off-white solid (15%). ^{1}H NMR (400 MHz, CD_3OD) δ (ppm): 8.40 (brs, 1H), 7.40−7.41 (m, 2H), 7.33−7.33 (m, 2H), 6.91 (s, 2H), 5.38 (q, 1H, *J* = 6.8 Hz), 2.19 (s, 3H), 1.65 (d, 3H, *J* = 6.8 Hz), 1.30−1.33 (m, 2H), 1.25−1.27 (m, 2H); ESIMS *m*/*z* (M + 1): 404.1; LCMS: 99.00%; SFC purity: 100%.

*N-(1-(1H-1,2,4-Triazol-3-yl) ethyl)-3-methyl-4-(1-(3-(trifluoromethyl)phenyl)cyclopropyl)-1H-pyrrole-2-carboxamide Enantiomer II (**97**).* The product was obtained as for **96** above (retention time: 2.45) as an off-white solid (10%). ^{1}H NMR (400 MHz, CD_3OD) δ (ppm): 8.43 (brs, 1H), 7.39−7.43 (m, 2H), 7.32−7.34 (m, 2H), 6.91 (s, 2H), 5.38 (q, 1H, *J* = 6.8 Hz), 2.19 (s, 3H), 1.65 (d, 3H, *J* = 6.8 Hz), 1.30−1.33 (m, 2H), 1.25−1.27 (m, 2H); ESIMS; *m*/*z* (M + 1): 404.1; LCMS: 97.74%; SFC purity: 100%.

*4-(1-(6-(Difluoromethyl)pyridin-3-yl)cyclopropyl)-3-methyl-N-(1-(1H-1,2,4-triazol-3-yl)ethyl)-1H-pyrrole-2-carboxamide Enantiomer I (**101**).* Racemic **101** was prepared from 1-(1-triphenylmethyl-1*H*-1,2,4-triazol-3-yl)ethan-1-amine (preparation in Supporting Information Methods) and **255** (36%). The racemate was resolved by SFC purification using a Lux A1 column and IPA cosolvent (40%) to afford enantiomer I (retention time: 1.29) as an off-white solid (23%). ^{1}H NMR (400 MHz, CD_3OD) δ (ppm): 8.30 (d, 1H, *J* = 2.0 Hz), 7.66 (dd, 1H, *J* = 2.0 Hz & 8.4 Hz), 7.56 (d, 1H, *J* = 8.0 Hz), 6.93 (s, 1H), 6.68 (t, 1H, *J* = 55.2 Hz), 5.38 (q, 1H, *J* = 6.8 Hz), 2.21 (s, 3H), 1.64 (d, 3H, *J* = 6.8 Hz), 1.39−1.41 (m, 2H), 1.32−1.34 (m, 2H); ESIMS *m*/*z* (M + 1): 387.2; HPLC purity: 99.50%; SFC purity: 100%.

*4-(1-(6-(Difluoromethyl)pyridin-3-yl)cyclopropyl)-3-methyl-N-(1-(1H-1,2,4-triazol-3-yl)ethyl)-1H-pyrrole-2-carboxamide Enantiomer II (**102**).* The product was obtained as for **101** above (retention time: 1.99) as an off-white solid (42%). ^{1}H NMR (400 MHz, CD_3OD) δ (ppm): 8.30 (d, 1H, *J* = 2.0 Hz), 7.66 (dd, 1H, *J* = 2.0 Hz & 8.4 Hz), 7.56 (d, 1H, *J* = 8.0 Hz), 6.93 (s, 1H), 6.68 (t, 1H, *J* = 55.2 Hz), 5.38 (q, 1H, *J* = 6.8 Hz), 2.21 (s, 3H), 1.64 (d, 3H, *J* = 6.8 Hz), 1.39−1.41 (m, 2H), 1.32−1.34 (m, 2H); ESIMS *m*/*z* (M + 1): 387.2; HPLC purity: 96.03%; SFC purity: 99.16.

*N-(1-(1H-1,2,4-Triazol-3-yl)ethyl)-3,5-dimethyl-4-((6-(trifluoromethyl)pyridin-3-yl)methyl)-1H-pyrrole-2-carboxamide Enantiomer I (**107**).* Racemic **107** was prepared from 1-(1-triphenylmethyl-1*H*-1,2,4-triazol-3-yl)ethan-1-amine (preparation in Supporting Information Methods) and **262**[20] (26%). The racemate was resolved by SFC purification using a YMC cellulose-SC column and methanol cosolvent (30%) to afford enantiomer I (retention time: 2.1) as an off-white solid (29%). ^{1}H NMR (400 MHz, DMSO-d_6) δ (ppm): 13.79 (s, 1H), 10.95 (s, 1H), 8.58 (s, 1H), 8.19 (brs, 1H), 7.78 (d, 1H, *J* = 8.0 Hz), 7.67 (d, 1H, *J* = 8.0 Hz), 7.62 (brs, 1H), 5.21−5.25 (m, 1H), 3.83 (s, 2H), 2.16 (s, 3H), 2.13 (s, 3H), 1.42 (d, 3H, *J* = 6.8 Hz); ESIMS *m*/*z* (M + 1): 393.2; HPLC purity: 99.46%; SFC purity: 99.94%.

*N-(1-(1H-1,2,4-Triazol-3-yl)ethyl)-3,5-dimethyl-4-((6-(trifluoromethyl)pyridin-3-yl)methyl)-1H-pyrrole-2-carboxamide Enantiomer II (**108**).* The product was obtained as for **107** above (retention time: 3.37) as an off-white solid (27%). ^{1}H NMR (400 MHz, DMSO-d_6) δ (ppm): 13.81 (s, 1H), 10.95 (s, 1H), 8.58 (s, 1H), 8.19 (brs, 1H), 7.78 (d, 1H, *J* = 8.0 Hz), 7.68 (d, 1H, *J* = 8.0 Hz), 7.61 (brs,

https://doi.org/10.1021/acs.jmedchem.1c00173
J. Med. Chem. 2021, 64, 6085−6136

1H), 5.21−5.25 (m, 1H), 3.83 (s, 2H), 2.16 (s, 3H), 2.13 (s, 3H), 1.47 (d, 3H, J = 6.8 Hz); ESIMS m/z (M + 1): 393.2; HPLC purity: 97.96%; SFC purity: 99.44%.

*N-(1-(1H-Pyrazol-4-yl)ethyl)-3,5-dimethyl-4-((6-(trifluoromethyl)-pyridin-3-yl)methyl)-1H-pyrrole-2-carboxamide Enantiomer I (**109**).* Racemic **109** was prepared from 1-(1-trityl-1*H*-pyrazol-4-yl)ethan-1-amine (preparation in Supporting Information Methods) and **262**[20] (27%). The racemate was resolved by SFC purification using a Lux A1 column and methanol cosolvent (30%) to afford enantiomer I (retention time: 2.48) as an off-white solid (44%). ^{1}H NMR (400 MHz, DMSO-d_6) δ (ppm): 12.66 (bs, 1H), 10.90 (s, 1H), 8.58 (s, 1H), 7.78 (d, 1H), 7.68 (d, 1H), 7.43−7.58 (m, 2H), 7.38 (d, 1H), 5.04−5.10 (m, 1H), 3.82 (s, 2H), 2.15 (s, 3H), 2.12 (s, 3H), 1.42 (d, 3H); ESIMS m/z (M + 1): 392.1; HPLC purity: 95.37%; SFC purity: 100%.

*N-(1-(1H-Pyrazol-4-yl)ethyl)-3,5-dimethyl-4-((6-(trifluoromethyl)-pyridin-3-yl)methyl)-1H-pyrrole-2-carboxamide Enantiomer II (**110**).* The product was obtained as for **109** above (retention time: 3.15) as an off-white solid (35%). ^{1}H NMR (400 MHz, DMSO-d_6) δ (ppm): 12.66 (bs, 1H), 10.86 (s, 1H), 8.58 (s, 1H), 7.78 (d, 1H), 7.68 (d, 1H), 7.44−7.64 (m, 2H), 7.39 (d, 1H), 5.06−5.11 (m, 1H), 3.82 (s, 2H), 2.15 (s, 3H), 2.12 (s, 3H), 1.42 (d, 3H); ESIMS m/z (M + 1): 392.2; HPLC purity: 94.45%; SFC purity: 100%.

*N-(1-(1H-Pyrazol-4-yl)ethyl)-3-cyano-5-methyl-4-((6-(trifluoromethyl)pyridin-3-yl)methyl)-1H-pyrrole-2-carboxamide Enantiomer I (**117**).* Racemic **117** was prepared from 1-(1-triphenylmethyl-1*H*-pyrazol-4-yl)ethan-1-amine (preparation in Supporting Information Methods) and **265** using general procedure F2 and trityl deprotection to afford the product as a white solid (25%). The racemate was resolved by SFC purification using a YMC cellulose C column and IPA cosolvent (30%) to afford enantiomer I (retention time: 2.6) as a white solid (19%). ^{1}H NMR (400 MHz, DMSO-d_6) δ (ppm) 12.69 (s, 1H), 12.06 (brs,1H), 8.64 (s, 1H), 8.02 (d, 1H, J = 7.2 Hz), 7.79−7.85 (m, 2H), 7.58 (brs, 2H), 5.07 (q, 1H, J = 7.2 Hz), 3.97 (s, 2H), 2.21 (s, 3H), 1.44 (d, 3H, J = 7.2 Hz); ESIMS m/z (M + 1): 403.2; HPLC purity: 99.23%; SFC purity: 100%.

*N-(1-(1H-Pyrazol-4-yl)ethyl)-3-cyano-5-methyl-4-((6-(trifluoromethyl)pyridin-3-yl)methyl)-1H-pyrrole-2-carboxamide Enantiomer II (**118**).* The product was obtained as for **117** above (retention time: 3.09) as a white solid (30%). ^{1}H NMR (400 MHz, DMSO-d_6) δ (ppm) 12.69 (s, 1H), 12.08 (brs,1H), 8.63 (s, 1H), 8.02 (d, 1H, J = 7.2 Hz), 7.78−7.85 (m, 2H), 7.58 (brs, 2H), 5.07 (q, 1H, J = 7.2 Hz), 3.97 (s, 2H), 2.21 (s, 3H), 1.44 (d, 3H, J = 7.2 Hz); ESIMS m/z (M + 1): 403.1; HPLC purity: 98.47%; SFC purity: 100%.

*N-(1-(1H-1,2,4-Triazol-3-yl)ethyl)-5-chloro-3-methyl-4-((6-(trifluoromethyl)pyridin-3-yl)methyl)-1H-pyrrole-2-carboxamide Enantiomer I (**120**).* Racemic **120** was prepared from 1-(1-triphenylmethyl-1*H*-triazol-3-yl)ethan-1-amine (preparation in Supporting Information Methods) and **266** (32%). The racemate was resolved by SFC purification using a Chiralcel OX-H column and 0.5% DEA in methanol cosolvent (30%) to afford enantiomer I (retention time: 2.05) as an off-white solid (34%). ^{1}H NMR (400 MHz, CD_3OD) δ (ppm): 8.55 (s, 1H), 8.47 (s, 1H), 7.78 (d, 1H, J = 8.8 Hz), 7.73 (d, 1H, J = 8.8 Hz), 5.36 (q, 1H, J = 6.9 Hz), 3.95 (s, 2H), 2.23 (s, 3H), 1.62 (brs, 3H); ESIMS m/z: 412.9; HPLC purity: 98.42%; SFC purity: 100%.

*N-(1-(1H-1,2,4-Triazol-3-yl)ethyl)-5-chloro-3-methyl-4-((6-(trifluoromethyl)pyridin-3-yl)methyl)-1H-pyrrole-2-carboxamide Enantiomer II (**121**).* The product was obtained as for **120** above (retention time: 3.38) as an off-white solid (26%). ^{1}H NMR (400 MHz, CD_3OD) δ (ppm): 8.55 (s, 1H), 8.46 (bs, 1H), 7.78 (d, 1H, J = 8.8 Hz), 7.73 (d, 1H, J = 8.8 Hz), 5.36 (q, 1H, J = 6.9 Hz), 3.95 (s, 2H), 2.23 (s, 3H), 1.62 (brs, 3H); ESIMS m/z: 412.9; HPLC purity: 98.13%; SFC purity: 100%.

*N-(1-(1H-1,2,4-Triazol-3-yl) ethyl)-5-chloro-3-methyl-4-(1-(6-(trifluoromethyl)pyridin-3-yl)cyclopropyl)-1H-pyrrole-2-carboxamide Enantiomer I (**122**).* Racemic **122** was prepared from 1-(1-triphenylmethyl-1*H*-pyrazol-4-yl)ethan-1-amine (preparation in Supporting Information Methods) and **267** (23%). The racemate was resolved by SFC purification using a YMC cellulose-SC column and methanol cosolvent (30%) to afford enantiomer I (retention time: 1.82) as an off-white solid (27%). ^{1}H NMR (400 MHz, CD_3OD) δ (ppm): 8.48 (s, 1H), 8.34 (s, 1H), 7.65−7.71 (m, 2H), 5.37 (brs, 1H), 2.29 (s, 3H), 1.62 (m, 3H), 1.53−1.55 (m, 2H), 1.43−1.47 (m, 2H). ESIMS m/z (M + 1): 439.1; HPLC purity: 98.38%; SFC purity: 100%.

*N-(1-(1H-1,2,4-Triazol-3-yl) ethyl)-5-chloro-3-methyl-4-(1-(6-(trifluoromethyl)pyridin-3-yl)cyclopropyl)-1H-pyrrole-2-carboxamide Enantiomer II (**123**).* The product was obtained as for **122** above (retention time: 2.43) as an off-white solid (34%). ^{1}H NMR (400 MHz, CD_3OD) δ (ppm): 8.47 (s, 1H), 8.34 (s, 1H), 7.65−7.71 (m, 2H), 5.37 (brs, 1H), 2.29 (s, 3H), 1.63 (m, 3H), 1.52−1.55 (m, 2H), 1.43−1.47 (m, 2H). ESIMS m/z (M + 1): 439.1; HPLC purity: 95.08%; SFC purity: 95.61%.

*3-Methyl-N-(1-(5-methylisoxazol-3-yl)ethyl)-4-(6-(trifluoromethyl)-1H-pyrrolo[2,3-b] pyridin-3-yl)-1H-pyrrole-2-carboxamide Enantiomer I (**161**).* Racemic **161** was prepared from 1-(1-triphenylmethyl-1*H*-triazol-3-yl)ethan-1-amine (preparation in Supporting Information Methods) and **276** (44%). The racemate was resolved by SFC purification using a Lux A1 column and methanol cosolvent (40%) to afford enantiomer I (retention time: 1.53) as an off-white solid (42%). ^{1}H NMR (400 MHz, CD_3OD) δ (ppm): 8.45 (brs, 1H), 8.12 (d, 1H, J = 8.0 Hz), 7.54 (s, 1H), 7.48 (d, 1H, J = 8.0 Hz), 7.08 (s, 1H), 5.37−5.42 (q, 1H, J = 6.8 Hz), 2.37 (s, 3H), 1.64 (d, 3H, J = 6.8 Hz); ESIMS m/z (M + 1): 404.1; HPLC purity: 93.70%; SFC purity: 95.48%.

*3-Methyl-N-(1-(5-methylisoxazol-3-yl)ethyl)-4-(6-(trifluoromethyl)-1H-pyrrolo[2,3-b] pyridin-3-yl)-1H-pyrrole-2-carboxamide Enantiomer II (**162**).* The product was obtained as for **161** above (retention time: 2.37) as an off-white solid (30%). ^{1}H NMR (400 MHz, CD_3OD) δ (ppm): 8.26 (brs, 1H), 8.12 (d, 1H, J = 8.0 Hz), 7.54 (s, 1H), 7.48 (d, 1H, J = 8.0 Hz), 7.08 (s, 1H), 5.37−5.42 (q, 1H, J = 6.8 Hz), 2.37 (s, 3H), 1.64 (d, 3H, J = 6.8 Hz); ESIMS m/z (M + 1): 404.1; HPLC purity: 99.74%; SFC purity: 99.21%.

*N-(1-(1H-1,2,4-Triazol-3-yl) ethyl)-4-((3-fluoro-2-iodophenyl)-methyl)-3-methyl-1H-pyrrole-2-carboxamide (**224**).* **224** was prepared from 1-(1-triphenylmethyl-1*H*-1,2,4-triazol-3-yl)ethan-1-amine (preparation in Supporting Information Methods) and **223** (38%). ^{1}H NMR (400 MHz, CD_3OD) δ (ppm): 8.26 (s, 1H), 7.23−7.29 (m, 1H), 6.69−6.99 (m, 2H), 6.55 (s, 1H), 5.36−5.39 (m, 1H), 3.89 (s, 2H), 2.18 (s, 3H), 1.27−1.31 (d, 3H, J = 7.0 Hz); ESIMS m/z (M + 1): 454.4.

General Procedure H: Amide Coupling followed by Tosyl Deprotection. Amide coupling was carried out as described in general procedure F1. The uncharacterized product in THF was treated with TBAF (1.0 M THF) (2 equiv) at RT and continued for 2 h. After completion of the reaction, the reaction mixture was quenched with sat· $NaHCO_3$ and extracted with CH_2Cl_2 (3×). The combined organic layers were dried (Na_2SO_4), filtered, and concentrated. The resulting concentrated product was purified by column chromatography using 0−5% methanol in CH_2Cl_2 to afford the product (35%). Compounds **41** and **88**−**89** were prepared by this method.

*3-Methyl-N-(1-(2-methyl-1H-imidazol-4-yl)ethyl)-4-((6-(trifluoromethyl)pyridin-3-yl)methyl)-1H-pyrrole-2-carboxamide (**41**).* The title compound was prepared using 1-(2-methyl-1-(4-methylbenzene-1-sulphonyl)-1*H*-imidazol-4-yl)ethan-1-amine (preparation in Supporting Information Methods) and **181** as an off-white solid (35%). ^{1}H NMR (400 MHz, DMSO-d_6) δ (ppm): 11.55 (s, 1H), 11.06 (s, 1H), 8.63 (s, 1H), 7.80 (s, 2H), 7.44 (d, 1 H, J = 6.0 Hz), 6.75 (s, 1H), 6.68 (s, 1H), 5.01−5.03 (m, 1H), 3.85 (s, 2H), 2.23 (s, 3H), 2.15 (s, 3H), 1.38 (d, 3H, J = 6.4 Hz); ESIMS m/z: 392.2; LCMS: 98.37%; HPLC purity: 98.67%.

*N-(1-(1H-Imidazol-4-yl)ethyl)-3-methyl-4-(1-(6-(trifluoromethyl)-pyridin-3-yl)cyclopropyl)-1H-pyrrole-2-carboxamide Enantiomer I (**88**).* Racemic **88** was prepared from general procedure H (but heating to 50 °C for 2 h) using 1-(2-methyl-1-(4-methylbenzene-1-sulphonyl)-1*H*-imidazol-4-yl)ethan-1-amine (preparation in Supporting Information Methods) and **251** (36%). Racemic **88** was resolved by SFC purification using a Lux A1 column and IPA cosolvent (30%) to afford the product (retention time: 2.34) as a white solid (29%). ^{1}H NMR (400 MHz, CD_3OD) δ (ppm): 8.35 (s, 1H), 7.67 (brs, 3H), 7.03 (s, 1H), 6.90 (s, 1H), 5.27 (q, 1H, J = 6.6 Hz), 2.19 (s, 3H), 1.58 (d, 3H, J = 6.6 Hz), 1.42−1.43 (m, 2H), 1.37−1.38 (m, 2H); ESIMS m/z (M + 1): 404.2; HPLC purity: 99.37%; SFC purity: 100%.

https://doi.org/10.1021/acs.jmedchem.1c00173
J. Med. Chem. 2021, 64, 6085−6136

*N-(1-(1H-Imidazol-4-yl)ethyl)-3-methyl-4-(1-(6-(trifluoromethyl)-pyridin-3-yl)cyclopropyl)-1H-pyrrole-2-carboxamide Enantiomer II (**89**).* The compound was prepared as for **88** to afford the product (retention time: 3.94) as a white solid (36%). ^{1}H NMR (400 MHz, CD_3OD) δ (ppm): 8.35 (s, 1H), 7.67 (brs, 3H), 7.03 (s, 1 H), 6.90 (s, 1H), 5.26 (q, 1H, J = 6.6 Hz), 2.19 (s, 3H), 1.58 (d, 3H, J = 6.6 Hz), 1.43 (m, 2H), 1.37 (m, 2H); ESIMS m/z (M + 1): 404.1; HPLC purity: 99.24%; SFC purity: 100%.

General Procedure I1: Weinreb Amide Formation. 1,1′-Carbonyldiimidazole (1.2 equiv) was added to a stirred solution of the aryl/heteroaryl carboxylic acid (1 equiv) in DMF at RT for 1 h. Then, *N,O*-dimethylhydroxylamine hydrochloride (2.5 equiv) was added to the reaction mixture at RT and stirring continued for 4 h. The reaction mixture was poured into water and extracted with ethyl acetate (2×). The combined organic layers were dried (Na_2SO_4), filtered, and concentrated. The concentrated product was purified by flash chromatography (silica gel, eluting with hexane:EtOAc mixtures from 100 to 70:30%) to afford product as a yellow liquid (91−94%). Compounds **190**−**191** were prepared by this method. Compound **229** was prepared by an alternative procedure as described.

*2-Fluoro-N-methoxy-N-methyl-4-(trifluoromethyl)benzamide (**190**).* The compound was prepared from 2-fluoro-4-(trifluoromethyl)-benzoic acid (94%). ^{1}H NMR (400 MHz, DMSO-d_6) δ (ppm): 7.83 (d, 1H, J = 8.0 Hz), 7.73−7.76 (m, 1H), 7.68 (d, 1H, J = 8.0 Hz), 3.48 (s, 3H), 3.32 (s, 3H); ESIMS m/z (M + 1): 252.1

*2-Bromo-N-methoxy-N-methyl-4-(trifluoromethyl)benzamide (**191**).* The compound was prepared from 2-bromo-4-(trifluoromethyl)benzoic acid (91%). ^{1}H NMR (400 MHz, CD_3OD) δ (ppm): 8.09 (s, 1H), 7.80−7.87 (s, 1H), 7.69−7.72 (m, 1H), 3.46 (s, 3H), 3.31 (s, 3H); ESIMS m/z (M, M + 2): 312.2, 314.2.

*6-(Difuoromethyl)-N-methoxy-N-methylpyridine-3-carboxamide (**229**).* $Pd(OAc)_2$ (0.16 g, 0.72 mmol) and 4,5-bis-(diphenylphosphino)-9, 9-dimethylxanthene (0.70 g, 1.2 mmol) were added to a purged solution of 5-bromo-2-(difluoromethyl)pyridine (5 g, 24.03 mmol), K3PO4 (15.3 g, 72.07 mmol), and *N,O*-dimethylhydroxylamine hydrochloride (3.52 g, 36.09 mmol) in *m*-xylene (70 mL) at RT. The reaction was heated to 100 °C for 16 h under CO gas. The reaction mixture was cooled to RT, 10% $NaHCO_3$ was added, and the mixture extracted with ethyl acetate (3 × 100 mL). The concentrated product was purified by flash chromatography (silica gel, eluting with hexane:EtOAc mixtures from 100 to 60:40%) to afford product (2.5 g, 48%) as a white solid. ^{1}H NMR (400 MHz, DMSO-d_6) δ (ppm): 8.91 (s, 1H), 8.26 (dd, 1H, J = 2.0 Hz & 8.0 Hz), 7.81 (d, 1H, J = 8.0 Hz), 6.79 (t, 1H, J = 55.2 Hz), 3.62 (s, 3H), 3.33 (s, 3H); ESIMS m/z (M + 1): 217.1.

General Procedure J: Propynyl Grignard on Weinreb Amide. 1-Propynylmagnesium bromide (0.5 M in THF) (1.2 equiv) was added to the aryl/heteroaryl amide in THF at 0 °C and stirred for 4 h at RT. The reaction mixture was quenched with 1.5 N HCl solution and extracted with ethyl acetate (2×). The combined organic layer was washed with brine, dried over Na_2SO_4, and concentrated to afford the product as a yellow liquid (82−93%). Compounds **192**−**193** and **232** were prepared by this method.

*1-(2-Fluoro-4-(trifluoromethyl)phenyl)but-2-yn-1-one (**192**).* **192** was prepared from **190** (89%). ^{1}H NMR (400 MHz, DMSO-d_6) δ (ppm): 8.20−8.24 (m, 1H), 7.89−7.92 (m, 1H), 7.78 (d, 1H, J = 8.0 Hz), 2.22 (s, 3H).

*1-(2-Bromo-4-(trifluoromethyl)phenyl)but-2-yn-1-one (**193**).* **193** was prepared from **191** as a yellow solid (82%). ESIMS m/z (M, M + 2): 291.2, 293.2. The product was used without further characterization.

*1-(6-(Difluoromethyl)pyridin-3-yl)but-2-yn-1-one (**232**).* The title compound was prepared from **229** (2.1 g, 93%). ^{1}H NMR (400 MHz, DMSO-d_6) δ (ppm): 9.31 (s, 1H), 8.62 (dd, 1H, J = 2.0 Hz & 8.4 Hz), 7.88 (d, 1H, J = 8.4 Hz), 6.83 (t,1H, J = 55.2), 2.25 (s, 3H); ESIMS m/z (M + 1): 196.0.

General Procedure I2: Weinreb Amide Formation followed by Propynyl Grignard. 1,1′-Carbonyldiimidazole (1.2 equiv) was added to a stirred solution of the aryl/heteroaryl carboxylic acid (1 equiv) in DMF at RT for 1 h. Then, *N,O*-dimethylhydroxylamine hydrochloride (2.5 equiv) was added to the reaction mixture at RT and stirring was continued for 4 h. The reaction mixture was poured into water and extracted with ethyl acetate (2×). The combined organic layers were dried (Na_2SO_4), filtered, and concentrated. The concentrated product was purified by flash chromatography (silica gel, eluting with hexane:EtOAc mixtures from 100 to 70:30%). Then, 1-propynylmagnesium bromide (0.5 M in THF) (1.2 equiv) was added to the amide product in THF at 0 °C and stirred for 4 h at RT. The reaction mixture was quenched with 1.5 N HCl solution and extracted with ethyl acetate (2×). The combined organic layer was washed with brine, dried over Na_2SO_4, and concentrated to afford the product as an off-white solid (54-89%). Compounds **194**−**196**, **230**−**231**, and **280** were prepared by this method.

*1-(5-Fluoroisoquinolin-8-yl)but-2-yn-1-one (**194**).* **194** was prepared from 5-fluoroisoquinoline-8-carboxylic acid (54%). ESIMS m/z (M + 1): 214.2. The product was used without further characterization.

*1-(2-Bromo-6-(trifluoromethyl)pyridin-3-yl) but-2-yn-1-ol (**195**).* **195** was prepared from 2-bromo-6-(trifluoromethyl)-3-pyridinecarboxylic acid (68%). ^{1}H NMR (400 MHz, $CDCl_3$) δ (ppm): 8.29 (d, 1H, J = 7.8 Hz), 8.09 (d, 1H, J = 7.8 Hz), 3.48 (s, 3H); ESIMS m/z: (M, M + 2): 291.2, 293.2.

*1-(3,4-Difluorophenyl)but-2-yn-1-one (**196**).* **196** was prepared from 3,4-difluorobenzoic acid (1.6 g, 89%). ESIMS m/z (M + 1): 181.0. The product was used without further characterization.

*1-(3-Fluoro-4-(trifluoromethyl)phenyl)but-2-yn-1-one (**230**).* **230** was prepared from 3-fluoro-4-(trifluoromethyl)benzoic acid as a yellow liquid (62%). ^{1}H NMR (400 MHz, DMSO-d_6) δ (ppm): 8.01−8.10 (m, 3H), 2.26 (s, 3H); ESIMS m/z (M + 1): 230.9.

*1-(3-(Trifluoromethyl)phenyl)but-2-yn-1-one (**231**).* **231** was prepared from 3-(trifluoromethyl)benzoic acid (83%). The product was used without characterization.

*1-(2-Bromo-6-(trifluoromethyl)pyridin-3-yl)but-2-yn-1-one (**280**).* **280** was prepared from 2-bromo-6-(trifluoromethyl)-3-pyridinecarboxylic acid (68%). ESIMS m/z (M, M + 2): 292.2, 294.2. The product was used without further characterization.

General Procedure K: N-Tosylation of Pyrrole Carboxylate. Sodium hydride (1.5 equiv) was added to a stirred solution of pyrrole carboxylate intermediate (1 equiv) in DMF at 0 °C for 30 min. Tosyl chloride (1.5 equiv) was added at 0 °C and the reaction mixture was stirred at RT for 4 h. Water was added and the reaction mixture was then extracted with ethyl acetate (2×). The resulting combined organic layer was washed with brine, dried over Na_2SO_4, and concentrated. The concentrated product was purified by flash chromatography (silica gel, eluting with hexane:EtOAc mixtures from 100 to 60:40%) to afford the product as an off-white solid (55−81%). Compounds **236**−**239** were prepared using this procedure, compound **240** was prepared by a modified procedure.

*Ethyl 3-Methyl-1-(4-methylbenzenesulfonyl)-4-(6-(trifluoromethyl)pyridine-3-carbonyl)-1H-pyrrole-2-carboxylate (**236**).* **236** was prepared from **173** (55%). ^{1}H NMR (300 MHz, DMSO-d_6) δ (ppm): 9.12 (s, 1H), 8.45 (d, 1H, J = 8.1 Hz), 8.23 (s, 1H), 8.13 (d, 1H, J = 8.1 Hz), 7.98 (d, 2H, J = 8.4 Hz), 7.50 (d, 2H, J = 8.4 Hz), 4.25 (q, 2H, J = 7.2 Hz), 2,43 (s, 3H), 2.40 (s, 3H), 1.22 (t, 3H, J = 7.2 Hz); ESIMS m/z (M + 1): 480.9.

*Ethyl 4-(2-Fluoro-4-(trifluoromethyl)benzoyl)-3-methyl-1-(4-methylbenzenesulfonyl)-1H-pyrrole-2-carboxylate (**237**).* **237** was prepared from **198** (81%). The product was used without characterization.

*Ethyl 4-(3-Fluoro-4-(trifluoromethyl)benzoyl)-3-methyl-1-(4-methylbenzene-1-sulfonyl)-1H-pyrrole-2-carboxylate (**238**).* **238** was prepared from **233** (78%). ^{1}H NMR (400 MHz, DMSO-d_6) δ (ppm): 8.16 (s, 1H), 7.92−8.09 (m, 3H), 7.79−7.90 (m, 2H), 7.49−7.51 (m, 2H), 4.24 (q, 2H, J = 9.2 Hz), 2.43 (s, 3 H), 2.38 (s, 3H), 1.22 (t, 3H, J = 9.2 Hz); ESIMS m/z (M − 1): 496.2.

*Ethyl 3-Methyl-1-(4-methylbenzene-1-sulfonyl)-4-(3-(trifluoromethyl)benzoyl)-1H-pyrrole-2-carboxylate (**239**).* The title compound was prepared from **234** (81%). The product was used without characterization.

*Ethyl 4-(6-(Difluoromethyl)pyridine-3-carbonyl)-3-methyl-1-(4-methylbenzene-1-sulfonyl)-1H-pyrrole-2-carboxylate (**240**).* 4-Di-

https://doi.org/10.1021/acs.jmedchem.1c00173
J. Med. Chem. 2021, 64, 6085−6136

methylaminopyridine (DMAP, 56 mg, 0.49 mmol) was added to a stirred solution of **235** (1.5 g, 4.87 mmol) and Et_3N (1.3 mL, 9.74 mmol) in CH_2Cl_2 (20 mL) at 0 °C for 10 min. Tosyl chloride (1.1 g, 5.84 mmol) was added at 0 °C and the reaction mixture was stirred for 2 h at room temperature. Then, 1.5 N HCl (100 mL) was added and the reaction mixture was extracted with ethyl acetate (2 × 100 mL). The resulting combined organic layer was washed with brine, dried over Na_2SO_4, and concentrated. The concentrated product was purified by flash chromatography (silica gel, eluting with hexane:EtOAc mixtures from 100 to 80:20%) to afford the product (2.0 g, 89%). ^{1}H NMR (400 MHz, CD_3OD) δ (ppm): 9.03 (s, 1H), 8.39 (dd, 1H, J = 1.6 Hz & 8.0 Hz), 8.03 (s, 1H), 7.89−7.94 (m, 3H), 7.46 (d, 2H, J = 8.4 Hz), 6.72−6.99 (t, 1H, J = 55.2 Hz), 4.31 (q, 2H, J = 7.2 Hz), 2,47 (s, 6H), 1.31 (t, 3H, J = 7.2 Hz); ESIMS m/z (M + 1): 462.9.

General Procedure L: Ethenyl Pyrrole Formation. Methylmagnesium bromide (2.0 M in THF) (1.2−1.5 equiv) was added to the general procedure K tosylated product (1 equiv) in THF at 0 °C and stirred for 4 h at RT. The reaction mixture was quenched with 1.5 N HCl solution and extracted with ethyl acetate (2×). The resulting organic layer was washed with brine, dried over Na_2SO_4, and concentrated to afford the methylated product. Iodine (catalytic, 0.2 equiv) was added to the methylated intermediate in toluene at RT and stirred for 16 h at 115 °C. The reaction mixture was quenched with 10% $Na_2S_2O_3$ solution and extracted with ethyl acetate (2×). The resulting organic layer was washed with brine, dried over Na_2SO_4, and concentrated. The concentrated product was purified by flash chromatography (silica gel, eluting with hexane:EtOAc from 100 to 90:10%) to afford the product as a gray solid (55−73%). Compounds **241**−**245** were prepared using this procedure.

*Ethyl 3-Methyl-1-(4-methylbenzenesulfonyl)-4-(1-(6-(trifluoromethyl)pyridin-3-yl)ethenyl)-1H-pyrrole-2-carboxylate (**241**).* **241** was prepared from **236** (73%). ^{1}H NMR (400 MHz, DMSO-d_6) δ (ppm): 8.79 (s, 1H), 7.88−7.95 (m, 4H), 7.75 (s, 1H), 7.49 (d, 2H, J = 8.2 Hz), 5.99 (s, 1H), 5.66 (s, 1H), 4.19 (q, 2H, J = 7.1 Hz), 2.43 (s, 3H), 1.88 (s, 3H), 1.19 (t, 3H, J = 7.1 Hz); ESIMS m/z (M + 1): 480.0.

*Ethyl 4-(1-(2-Fluoro-4-(trifluoromethyl)phenyl)ethenyl)-3-methyl-1-(4-methylbenzenesulfonyl)-1H-pyrrole-2-carboxylate (**242**).* **242** was prepared from **237** (55%). The product was used without characterization.

*Ethyl 4-(1-(3-Fluoro-4-(trifluoromethyl)phenyl)ethenyl)-3-methyl-1-(4-methylbenzene-1-sulfonyl)-1H-pyrrole-2-carboxylate (**243**).* **243** was prepared from **238** (66%). ^{1}H NMR (400 MHz, DMSO-d_6) δ (ppm): 7.90−7.92 (m, 2H), 7.72−7.79 (m, 2H), 7.47−7.51 (m, 3H), 7.26 (d, 1H, J = 10.8 Hz), 5.96 (s, 1H), 5.59 (s, 1H), 4.20 (q, 2H, J = 9.6 Hz), 2.42 (s, 3 H), 1.84 (s, 3H), 1.18 (t, 3H, J = 9.6 Hz); ESIMS m/z (M + 1): 496.2.

*Ethyl 3-Methyl-1-(4-methylbenzene-1-sulfonyl)-4-(1-(3-(trifluoromethyl)phenyl)ethenyl)-1H-pyrrole-2-carboxylate (**244**).* **244** was prepared from **239** (69%). The product was used without characterization.

*Ethyl 4-(1-(6-(Difluoromethyl)pyridin-3-yl)ethenyl)-3-methyl-1-(4-methylbenzene-1-sufonyl)-1H-pyrrole-2-carboxylate (**245**).* **245** was prepared from **240** (61%). ^{1}H NMR (400 MHz, DMSO-d_6) δ (ppm): 8.60 (d, 1H, J = 1.6 Hz), 7.87−7.92 (m, 3H), 7.71 (d, 1H, J = 8.0 Hz), 7.65 (s, 1H), 7.46 (d, 2H, J = 8.0 Hz), 6.76 (t, 1H, J = 55.2 Hz), 5.88 (s, 1H), 5.58 (s, 1H), 4.26 (q, 2H, J = 7.2 Hz), 2.48 (s, 3H), 1.93 (s, 3H), 1.26 (t, 3H, J = 7.2 Hz); ESIMS m/z (M − 1): 459.2.

General Procedure M: Cyclopropyl Formation. A solution of general procedure L ethenyl product (1 equiv) in THF (10 mL) was added to a stirred solution of trimethylsulfoxonium iodide (2 equiv) and t-BuOK (2 equiv) in DMSO at 0 °C and stirred for 4 h at RT. The reaction mixture was poured into water and extracted with ethyl acetate (2×). The combined organic layers were dried (Na_2SO_4), filtered, and concentrated. The concentrated product was purified by flash chromatography (silica gel, eluting with hexane:EtOAc mixtures from 100 to 60:40%) to afford the product as an off-white solid (49−71%). Compounds **246**−**250** were prepared using this procedure.

*Ethyl 3-Methyl-1-(4-methylbenzenesulfonyl)-4-(1-(6-(trifluoromethyl)pyridin-3-yl)cyclopropyl)-1H-pyrrole-2-carboxylate (**246**).* **246** was prepared from **241** (71%). ^{1}H NMR (400 MHz, DMSO-d_6) δ (ppm): 8.41 (s, 1H), 7.89 (d, 2H, J = 8.3 Hz), 7.80 (s, 1H), 7.77 (d, 1H, J = 8.3 Hz), 7.67−7.69 (m, 1H), 7.48 (d, 2H, J = 8.1 Hz), 4.16 (q, 2H, J = 7.1 Hz), 2.42 (s, 3H), 1.96 (s, 3H), 1.44−1.47 (m, 2H), 1.37−1.40 (m, 2H), 1.17 (t, 3H, J = 7.1 Hz); ESIMS m/z (M + 1): 494.1.

*Ethyl 4-(1-(2-Fluoro-4-(trifluoromethyl)phenyl)cyclopropyl)-3-methyl-1-(4-methylbenzenesulfonyl)-1H-pyrrole-2-carboxylate (**247**).* **247** was prepared from **242** (53%). The product was used without characterization.

*Ethyl 4-(1-(3-Fluoro-4-(trifluoromethyl)phenyl)cyclopropyl)-3-methyl-1-(4-methylbenzene-1-sulfonyl)-1H-pyrrole-2-carboxylate (**248**).* **248** was prepared from **243** (63%). ^{1}H NMR (400 MHz, DMSO-d_6) δ (ppm): 7.86−7.89 (m, 2H), 7.75 (s, 1H), 7.59−7.62 (m, 1H), 7.46−7.49 (m, 2H), 6.96−7.08 (m, 2H), 4.16 (q, 2H, J = 9.6 Hz), 2.28 (s, 3 H), 1.36−1.39 (m, 4H), 1.84 (s, 3H), 1.18 (t, 3H, J = 9.2 Hz); ESIMS m/z (M + 1): 510.0.

*Ethyl 4-(1-(3-(Trifluoromethyl)phenyl)cyclopropyl)-3-methyl-1-(4-methylbenzene-1-sulfonyl)-1H-pyrrole-2-carboxylate (**249**).* **249** was prepared from **244** (49%). The product was used without characterization.

*Ethyl 4-(1-(6-(Difluoromethyl)pyridin-3-yl)cyclopropyl)-3-methyl-1-(4-methylbenzene-1-sufonyl)-1H-pyrrole-2-carboxylate (**250**).* **250** was prepared from **245** (60%). ^{1}H NMR (400 MHz, DMSO-d_6) δ (ppm): 8.28 (d, 1H, J = 7.2 Hz), 7.85 (d, 2H, J = 8.4 Hz), 7.69 (s, 1H), 7.58−7.65 (m, 2H), 7.44 (d, 2H, J = 8.4 Hz), 6.69 (t, 1H, J = 55.2 Hz), 4.23 (q, 2H, J = 7.2 Hz), 2.47 (s, 3H), 1.44−1.45 (m, 2H), 1.38−1.40 (m, 2H), 1.25 (t, 3H, J = 7.2 Hz); ESIMS m/z (M + 1): 475.2.

General Procedure N: Amide Coupling and Indazole Formation. The corresponding amine and pyrrole carboxylic acid intermediate were coupled together using general procedure F1. The intermediate phenylcarbonylpyrrole carboxamide (1 equiv) was used directly, stirred in DMSO, treated with $NH_2NH_2{\cdot}H_2O$ (20 equiv), and then heated to 100 °C for 2 h. After consumption of the starting material, the reaction mixture was poured into water and stirred for 10 min. The solid obtained was filtered, washed with water, and dried to afford the title compound as an off-white solid (13−45%). Title compounds **131**−**132** and **134**−**135** were prepared using this procedure.

*N-Cyclopropyl-3-methyl-4-(6-(trifluoromethyl)-1H-indazol-3-yl)-1H-pyrrole-2-carboxamide (**131**).* Cyclopropylamine and **277** were reacted together to produce the title compound (13%). ^{1}H NMR (400 MHz, CD_3OD) δ (ppm): 7.97 (d, 1H, J = 8.0 Hz), 7.89 (s, 1H), 7.41 (d, 1H, J = 8.0 Hz), 7.30 (s, 1H), 2.82−2.87 (m, 1H), 2.48 (s, 3H), 0.83−0.87 (m, 2H), 0.64−0.68 (m, 2H); ESIMS m/z (M + 1): 349.1; LCMS: 98.36%; HPLC purity: 98.13%.

*(3,3-Difluoroazetidin-1-yl)(3-methyl-4-(6-(trifluoromethyl)-1H-indazol-3-yl)-1H-pyrrol-2-yl)methanone (**132**).* 3,3-Difluoroazetidine hydrochloride and **277** were reacted together to produce the title compound (45%). ^{1}H NMR (400 MHz, DMSO-d_6) δ (ppm): 13.39 (s, 1H), 11.51 (s, 1H), 8.11 (d, 1H, J = 8.0 Hz), 7.91 (s, 1H), 7.50 (s, 1H), 7.40 (d, 1H, J = 8.0 Hz), 4.56−4.63 (m, 4H), 2.42 (s, 3H); ESIMS m/z: 385.1; LCMS: 91.55%; HPLC purity: 93.13%.

*3-Methyl-N-(1-(5-methylisoxazol-3-yl)ethyl)-4-(6-(trifluoromethyl)-1H-indazol-3-yl)-1H-pyrrole-2-carboxamide Enantiomer I (**134**).* 1-(5-Methylisoxazol-3-yl)ethan-1-amine and **277** were reacted together to produce the racemic title compound (32%). The racemic product was resolved by SFC using a YMC Amylose-SA column and 0.5% isopropylamine in methanol cosolvent (40%) to afford the title compound (retention time 2.95) as an off-white solid (27%). ^{1}H NMR (400 MHz, MeOD) δ (ppm): 7.97 (d, 1H, J = 8.0 Hz), 7.89 (s, 1H), 7.41 (d, 1H, J = 8.0 Hz), 7.34 (s, 1H), 6.21 (s, 1H), 5.32−5.38 (q, 1H, J = 7.2 Hz), 2.52 (s, 3H), 2.43 (s, 3H), 1.63 (d, 3H, J = 7.2 Hz); ESIMS m/z: 418.1; HPLC purity: 99.06%; SFC purity: 100%.

*3-Methyl-N-(1-(5-methylisoxazol-3-yl)ethyl)-4-(6-(trifluoromethyl)-1H-indazol-3-yl)-1H-pyrrole-2-carboxamide Enantiomer II (**135**).* **135** was prepared as for **134** above (retention time 4.62) as an off-white solid (24%). ^{1}H NMR (400 MHz, MeOD) δ (ppm): 7.97 (d, 1H, J = 8.0 Hz), 7.89 (s, 1H), 7.41 (d, 1H, J = 8.0 Hz), 7.33 (s, 1H), 6.20 (s, 1H), 5.32−5.38 (q, 1H, J = 7.2 Hz), 2.52 (s, 3H), 2.43 (s, 3H), 1.63 (d, 3H, J = 7.2 Hz); ESIMS m/z: 418.1; HPLC purity: 98.32%; SFC purity: 100%.

https://doi.org/10.1021/acs.jmedchem.1c00173
J. Med. Chem. 2021, 64, 6085−6136

General Procedure O: Friedel–Crafts acetylation of pyrroles. Ethyl 3-methyl-1*H*-pyrrole-2-carboxylate (1 equiv) and 3-fluoro-2-iodobenzoyl chloride (1.5 equiv) were dissolved in anhydrous CH_2Cl_2 (100 mL) under argon and cooled to 0 °C in an ice/water bath. $AlCl_3$ (3 equiv) was added portionwise to the reaction mixture and stirred at 40 °C for 16 h. The reaction mixture was poured into ice water (100 mL) slowly. The resulting reaction mixture was extracted with CH_2Cl_2 (2 × 150 mL). The combined organic layer was washed with saturated sodium bicarbonate solution, dried (Na_2SO_4), and concentrated. The resulting concentrated product was purified by column chromatography using 0−50% ethyl acetate in petroleum ether to afford the product (23−45%). Compounds **212**−**215** were prepared using this procedure.

*Ethyl 4-(4-(N,N-Dimethylsulfamoyl)benzoyl)-3-methyl-1H-pyrrole-2-carboxylate (**212**).* **212** was prepared from ethyl 3-methyl-1*H*-pyrrole-2-carboxylate and 4-(*N*,*N*-dimethylsulfamoyl)benzoyl chloride (30%). ESIMS *m*/*z* (M + 1): 365.2. The product was used without further characterization.

*Ethyl 4-(Isoquinoline-8-carbonyl)-3-methyl-1H-pyrrole-2-carboxylate (**213**).* **213** was prepared from ethyl 3-methyl-1*H*-pyrrole-2-carboxylate and 8-isoquinolinecarbonyl chloride (45%). ESIMS *m*/*z* (M + 1): 309.3. The product was used without further characterization.

*Ethyl 4-(5-Methoxyisoquinoline-8-carbonyl)-3-methyl-1H-pyrrole-2-carboxylate (**214**).* **214** was prepared from ethyl 3-methyl-1*H*-pyrrole-2-carboxylate and 5-methoxy-8-isoquinolinecarbonyl chloride (40%). ESIMS *m*/*z* (M + 1): 339.3. The product was used without further characterization.

*Ethyl 4-((3-Fluoro-2-iodophenyl)carbonyl)-3-methyl-1H-pyrrole-2-carboxylate (**215**).* **215** was prepared from ethyl 3-methyl-1*H*-pyrrole-2-carboxylate and 3-fluoro-2-iodobenzoyl chloride (23%). ^{1}H NMR (300 MHz, DMSO-d_6) δ (ppm): 12.52 (s, 1H), 7.50−7.57 (m, 1H), 7.38−7.43 (m, 1H), 7.24−4.26 (m, 1 H), 6.32 (s, 1H), 4.27 (q, 2H, *J* = 7.2 Hz), 2.22 (s, 3H), 1.32 (t, 3H, *J* = 7.2 Hz); ESIMS *m*/*z* (M + 1): 402.2.

The remaining compounds were prepared as described individually.

*Ethyl 3-Methyl-4-((4-(trifluoromethyl)benzo[d]oxazol-7-yl)methyl)-1H-pyrrole-2-carboxylate (**18**).* $SnCl_2$ (0.14 g, 0.81 mmol) was added to a stirred solution of **188** (0.15 g, 0.40 mmol) in ethanol:water (8:2 mL) at RT and stirred for 4 h at 80 °C. The reaction mixture was concentrated, basified with saturated sodium bicarbonate solution (10 mL), and extracted with ethyl acetate (2 × 30 mL). The combined organic layers were dried (Na_2SO_4), filtered, and concentrated. The resulting concentrated product was dissolved in triethyl orthoformate (1 mL) and heated to 100 °C for 18 h. The reaction mixture was concentrated and purified by flash chromatography (silica gel, eluting with hexane:EtOAc mixtures from 100 to 70:30%) to afford the product (10 mg, 7%) as an off-white solid. ^{1}H NMR (300 MHz, $CDCl_3$) δ (ppm): 8.85 (bs, 1H), 8.25 (s, 1H), 7.58 (d, 1H, *J* = 8.4 Hz), 7.22 (d, 1H, *J* = 8.4 Hz), 6.71 (s, 1H), 4.33 (q, 2H, *J* = 7.1 Hz), 4.14 (s, 2H), 2.29 (s, 3H), 1.36 (t, 3H, *J* = 7.1 Hz); ESIMS *m*/*z* (M + 1): 353.2 LCMS: 96.78%; HPLC purity: 98.59%.

*N-(1-(5-Cyano-1H-pyrazol-3-yl)ethyl)-3-methyl-4-(((6-trifluoromethyl)pyridine-3-yl)methyl)-1H-pyrrole-2-carboxamide Enantiomer I (**44**).* To a stirred solution of racemic **46** (180 mg, 0.43 mmol) in CH_2Cl_2 (10 mL), *N*,*N*-diisopropylethylamine (DIPEA, 0.3 mL, 0.86 mmol) was added followed by T3P in ethyl acetate (50 wt %, 0.5 mL). The reaction mixture was then stirred for 2 h at RT. After completion of the reaction (monitored by TLC), water was added and the reaction mixture was extracted with CH_2Cl_2 (2 × 40 mL). The combined organic layer was dried over Na_2SO_4 and concentrated. The resulting concentrated product was purified by column chromatography using 30−80% ethyl acetate in petroleum ether to afford the racemic product (80 mg, 47%). The racemic product was resolved by SFC purification using a Lux A1 column eluting with methanol cosolvent (40%) to afford the product (retention time: 1.88) as an off-white solid (13 mg, 16%). ^{1}H NMR (400 MHz, DMSO-d_6) δ (ppm): 13.87 (s, 1H), 11.00 (s, 1H), 8.63 (s, 1H), 7.82 (m, 1H), 7.81(s, 2H), 6.85 (s, 1H,), 6.75 (s, 1H), 5.18−5.25 (m, 1H), 3.86 (s, 2H), 2.14 (s, 3H), 1.47 (d, 3H, *J* = 7.0 Hz); ESIMS *m*/*z* (M + 1): 403.1; HPLC purity: 95.30%; SFC purity: 98.59%.

*N-(1-(5-Cyano-1H-pyrazol-3-yl)ethyl)-3-methyl-4-(((6-trifluoromethyl)pyridine-3-yl)methyl)-1H-pyrrole-2-carboxamide Enantiomer II (**45**).* **45** was obtained by the same SFC process as described in **44** above (retention time: 2.96) as an off-white solid (18 mg, 23%). ^{1}H NMR (400 MHz, DMSO-d_6) δ (ppm): 13.87 (s, 1H), 11.00 (s, 1H), 8.63 (s, 1H), 7.83 (m, 1H), 7.81(s, 2H), 6.85 (s, 1H,), 6.75 (s, 1H), 5.18−5.25 (m, 1H), 3.86 (s, 2H), 2.14 (s, 3H), 1.47 (d, 3H, *J* = 7.0 Hz); ESIMS *m*/*z* (M + 1): 403.1; HPLC purity: 99.90%; SFC purity: 98.73%.

*3-(1-(3-Methyl-4-((6-(trifluoromethyl)pyridine-3-yl)methyl)-1H-pyrrole-2-carboxamido)ethyl)-1H-pyrazole-5-carboxamide (**46**).* Aqueous ammonia (10 mL) was added to a stirred solution of **189** (400 mg, 0.90 mmol) in methanol (4 mL), and the reaction mixture was stirred for 24 h at 100 °C in a sealed tube. The reaction mixture was concentrated and purified by preparative HPLC to afford the product as a pale yellow solid (0.18 g, 48%). ^{1}H NMR (400 MHz, MeOD) δ (ppm): 8.56 (s, 1H), 7.82 (d, 1H, *J* = 8.0 Hz), 7.73 (d, 1H, *J* = 8.1 Hz), 6.71−6.74 (bs, 1H), 6.71 (s, 1H), 5.29−5.38 (m, 1H), 3.96 (s, 2H), 2.22 (s, 3H), 1.59−1.63 (d, 3H, *J* = 7.0 Hz); ESIMS *m*/*z* (M + 1): 421.1; LCMS: 99.65%; HPLC purity: 98.47%.

*3-(1-(3-Methyl-4-((6-(trifluoromethyl)pyridine-3-yl)methyl)-1H-pyrrole-2-carboxamido)ethyl)-1H-pyrazole-5-carboxamide Enantiomer I (**47**).* Racemic **46** was resolved by SFC purification using a Chiralcel OD-H column eluting with IPA cosolvent (30%) to afford enantiomer I (retention time 3.37) as an off-white solid (22%). ^{1}H NMR (400 MHz, MeOD) δ (ppm): 8.55 (s, 1H), 7.82 (d, 1H, *J* = 8.0 Hz), 7.73 (d, 1H, *J* = 8.1 Hz), 6.70−6.73 (bs, 1H), 6.73 (s, 1H), 5.33 (m, 1H), 3.95 (s, 2H), 2.22 (s, 3H), 1.60−1.62 (d, 3H, *J* = 7.0 Hz); ESIMS *m*/*z* (M + 1): 421.2; HPLC purity: 97.66%; SFC purity: 100%.

*3-(1-(3-Methyl-4-((6-(trifluoromethyl)pyridine-3-yl)methyl)-1H-pyrrole-2-carboxamido)ethyl)-1H-pyrazole-5-carboxamide Enantiomer II (**48**).* **48** was prepared as described for **47** above (retention time 4.61) as an off-white solid (26%). ^{1}H NMR (400 MHz, MeOD) δ (ppm): 8.56 (s, 1H), 7.83 (d, 1H, *J* = 8.0 Hz), 7.73 (d, 1H, *J* = 8.1 Hz), 6.71−6.74 (bs, 1H), 6.74 (s, 1H), 5.34 (m, 1H), 3.96 (s, 2H), 2.22 (s, 3H), 1.61−1.63 (d, 3H, *J* = 7.0 Hz); ESIMS *m*/*z* (M + 1): 421.2; HPLC purity: 96.01%; SFC purity: 96.71%.

*N-Methyl-3-(1-(3-methyl-4-((6-(trifluoromethyl)pyridin-3-yl)methyl)-1H-pyrrole-2-carboxamido)ethyl)-1H-pyrazole-5-carboxamide Enantiomer I (**49**).* Methylamine (1 M in THF; 0.5 mL, 0.52 mmol) was added to a stirred solution of **189** (200 mg, 0.45 mmol) in THF (4 mL) at RT. Then, Me_3Al (1.0 M in toluene) (1.0 mL, 1.0 mmol) was added and stirred at 100 °C for 1 h in a microwave. The reaction mixture was quenched with 1.5 N HCl solution and extracted with ethyl acetate (2 × 50 mL). The combined organic layer was dried over Na_2SO_4 and concentrated. The resulting concentrated product was purified by column chromatography using 10−50% ethyl acetate in petroleum ether to afford the racemic product (0.12 g, 62%). The racemic product was resolved by SFC purification using a YMC Amylose-SA column eluting with IPA cosolvent (40%) to afford the title compound (retention time: 1.79) as an off-white solid (26 mg, 22%). ^{1}H NMR (400 MHz, CD_3OD) δ (ppm): 8.56 (s, 1H), 7.81 (d, 1H, *J* = 8.0 Hz), 7.72 (d, 1H, *J* = 8.0 Hz), 6.74 (s, 1H), 6.68 (s, 1H), 5.33 (m, 1H) 3.95 (s, 2H), 2.89 (s, 3H), 2.21 (s, 3H), 1.60 (d, 3H, *J* = 6.4 Hz); ESIMS *m*/*z* (M + 1): 435.1; HPLC purity: 95.96%; SFC purity: 100%.

*N-Methyl-3-(1-(3-methyl-4-((6-(trifluoromethyl)pyridin-3-yl)methyl)-1H-pyrrole-2-carboxamido)ethyl)-1H-pyrazole-5-carboxamide Enantiomer II (**50**).* **50** was obtained by the same SFC process as described for **49** above (retention time: 3.1) as an off-white solid (20 mg, 17%). ^{1}H NMR (400 MHz, CD_3OD) δ (ppm): 8.56 (s, 1H), 7.81 (d, 1H, *J* = 8.0 Hz), 7.72 (d, 1H, *J* = 8.0 Hz), 6.74 (s, 1H), 6.68 (s, 1H), 5.32 (m, 1H), 3.95 (s, 2H), 2.90 (s, 3H), 2.21 (s, 3H), 1.61 (d, 3H, *J* = 6.4 Hz); ESIMS *m*/*z* (M + 1): 435.2; HPLC purity: 95.88%; SFC purity: 99.52%.

*N-(1-(1H-1,2,4-Triazol-3-yl) ethyl)-4-((2-cyano-3-fluorophenyl)-methyl)-3-methyl-1H-pyrrole-2-carboxamide (**66**).* To a stirred solution of **224** (0.17 g, 0.38 mmol) in DMA:H_2O (9 mL:1 mL) were added zinc dust (0.05 g, 0.75 mmol), Pd(dppf)Cl_2 (0.015 g, 0.018 mmol), and poly(methyl hydrosiloxane) (1.0 mL) at RT. Then, zinc cyanide (0.13 g, 1.13 mmol) was added and heated to 80 °C for 16 h.

https://doi.org/10.1021/acs.jmedchem.1c00173
J. Med. Chem. 2021, 64, 6085−6136

The reaction mixture was then quenched with water (50 mL) and extracted with ethyl acetate (3 × 50 mL). The combined organic layers were dried (Na_2SO_4), filtered, and concentrated. The resulting concentrated product was purified by preparative HPLC to afford the product as a white solid (25 mg, 19%). ^{1}H NMR (400 MHz, CD_3OD) δ (ppm): 8.26 (s, 1H), 7.57−7.63 (m, 1H), 7.20 (d, 1H, J = 8.8 Hz), 7.15 (d, 1H, J = 8.0 Hz), 6.70 (s, 1H), 5.38 (q, 1H, J = 6.8 Hz), 4.02 (s, 2H), 2.25 (s, 3H), 1.63 (d, 3H, J = 6.8 Hz); ESIMS m/z (M + 1): 353.1; LCMS: 99.77%; HPLC purity: 97.26%.

*3-Methyl-N-(1-(5-methylisoxazol-3-yl)ethyl)-4-(1-(6-(trifluoromethyl)pyridin-3-yl)ethyl)-1H-pyrrole-2-carboxamide (**67**).* Methylmagnesium bromide (2.0 M in THF) (0.37 mL, 0.74 mmol) was added to a stirred solution of **173** (0.20 g, 0.61 mmol) in THF (5 mL) at 0 °C and stirring was continued for 4 h at RT. The reaction mixture was quenched with 1.5 N HCl solution and extracted with ethyl acetate (2 × 10 mL). The resulting organic layer was washed with brine and dried over Na_2SO_4. The resulting concentrated product was purified by column chromatography using 10−50% ethyl acetate in petroleum ether to afford ethyl 4-(1-hydroxy-1-(6-(trifluoromethyl)pyridin-3-yl)ethyl)-3-methyl-1*H*-pyrrole-2-carboxylate (0.15 g, 73%) as a gummy solid. The product was used without purification.

To a stirred solution of the above pyrrole carboxylate intermediate (0.15 g, 0.44 mmol) in TFA (0.19 mL, 2.6 mmol) and CH_2Cl_2 (1 mL) was added triethylsilane (0.26 g, 1.76 mmol) at RT and stirred at 85 °C for 1 h. After completion of the reaction, the reaction mixture was quenched with sat·$NaHCO_3$ (50 mL) by dropwise addition at 0 °C and extracted with ethyl acetate (3 × 10 mL, with careful venting). The combined organic layers were dried (Na_2SO_4), filtered, and concentrated. The resulting concentrated product was triturated with petroleum ether to afford ethyl 3-methyl-4-(1-(6-(trifluoromethyl)-pyridin-3-yl)ethyl)-1*H*-pyrrole-2-carboxylate (**225**) (0.12 g, 83%) as a white solid. The product was used without purification.

Sodium hydroxide (30 mg, 0.74 mmol) was added to a stirred solution of **225** (0.12 g, 0.37 mmol) in EtOH:water (4:1 mL) at RT and heated to 80 °C for 2 h. The resulting reaction mixture was concentrated and quenched with water (2 mL). Then, it was acidified with 10% citric acid solution. The solid obtained was filtered, washed with water, and dried to afford 3-methyl-4-(1-(6-(trifluoromethyl)-pyridin-3-yl)ethyl)-1*H*-pyrrole-2-carboxylic acid (80 mg, 73%) as an off-white solid. The product was used without purification.

1-(5-Methylisoxazol-3-yl)ethan-1-amine (37 mg, 0.29 mmol) and triethylamine (0.07 mL, 0.54 mmol) were added to a stirred solution of the above pyrrole carboxylic acid intermediate (80 mg, 0.27 mmol) in dichloromethane (2 mL) at RT and continued for 5 min. Then, HATU (0.15 g, 0.40 mmol) was added to the reaction mixture and stirred at RT for 3 h. After completion of the reaction (monitored by TLC), water was added to the reaction mixture and extracted with dichloromethane (2 × 10 mL). The combined organic layer was dried over Na_2SO_4 and concentrated. The resulting concentrated product was purified by column chromatography using 10−40% ethyl acetate in petroleum ether to afford the title compound (50 mg, 46%) as an off-white solid. ^{1}H NMR (400 MHz, DMSO-d_6) δ (ppm): 11.07, (s, 1H), 8.66 (s, 1H), 7.77−7.84 (m, 3H), 6.90 (s, 1H), 6.17 (s, 1H), 5.13−5.16 (m, 1H), 4.15 (q, 1H, J = 7.2 Hz), 2.36 (s, 3H), 2.02 (s, 3H), 1.54 (d, 3H, J = 7.2 Hz), 1.44 (d, 3H, J = 7.2 Hz); ESIMS m/z (M − 1): 405; LCMS: 99.74%; HPLC purity: 98.81%.

*4-(Hydroxy(6-(trifluoromethyl)pyridin-3-yl)methyl)-3-methyl-N-(1-(5-methylisoxazol-3-yl)ethyl)-1H-pyrrole-2-carboxamide (**68**).* Sodium hydroxide (112 mg, 3.06 mmol) was added to a stirred solution of **173** (0.50 g, 1.53 mmol) in EtOH:H_2O (9:1 mL) at RT and heated to 80 °C for 4 h. The resulting reaction mixture was concentrated, water was added (4 mL), and then acidified with 10% citric acid solution. The solid obtained was filtered, washed with water, and dried to afford 3-methyl-4-(6-(trifluoromethyl)pyridine-3-carbonyl)-1*H*-pyrrole-2-carboxylic acid as an off-white solid (420 mg, 92%). ESIMS m/z (M + 1): 299.2. The product was used without purification.

1-(5-Methylisoxazol-3-yl)ethan-1-amine (125 mg, 1.61 mmol) and triethylamine (0.4 mL, 2.82 mmol) were added to a stirred solution of the above pyrrole intermediate (420 mg, 1.34 mmol) in (10 mL) at RT and stirring was continued for 5 min. Then, HATU (0.8 g, 2.11 mmol) was added to the reaction mixture and stirring was continued at RT for 16 h. After completion of the reaction (monitored by TLC), water was added to the reaction mixture and extracted with CH_2Cl_2 (2 × 50 mL). The combined organic layer was dried over Na_2SO_4 and concentrated. The resulting concentrated product was purified by column chromatography using 0-40% ethyl acetate in petroleum ether to afford 3-methyl-*N*-(1-(5-methylisoxazol-3-yl)ethyl)-4-(6-(trifluoromethyl)-pyridine-3-carbonyl)-1*H*-pyrrole-2-carboxamide (**227**) (400 mg, 70%) as an off-white solid. ESIMS m/z (M + 1): 407.2. The product was used without further purification.

Sodium borohydride (75 mg, 1.97 mmol) was added portionwise to a stirred solution of **227** (0.4 g, 0.99 mmol) in ethanol (10 mL) at 0 °C. Then, the reaction mixture was stirred for 1 h at room temperature. The reaction mixture was concentrated under reduced pressure. Water (10 mL) was added to the concentrated product and the mixture was extracted with ethyl acetate (2 × 50 mL). The resulting combined organic layer was washed with brine, dried over Na_2SO_4, and concentrated to afford the title compound as an off-white solid (0.4 g, 99%). ^{1}H NMR (400 MHz, DMSO-d_6) δ (ppm): 11.05 (s, 1H), 8.72 (s, 1H), 7.99 (d, 1H, J = 7.6 Hz), 7.86 (d, 1H, J = 8.4 Hz), 7.79 (d, 1H, J = 8.4 Hz), 6.66 (s, 1H), 6.62 (s, 1H), 5.80 (brs, 2H), 5.15−5.17 (m, 1H), 2.36 (s, 3H), 2.18 (s, 3H), 1.43 (d, 3H, J = 7.0 Hz); ESIMS m/z (M + 1): 409.0; LCMS: 99.66%; HPLC purity: 98.34%.

*4-(Methoxy(6-(trifluoromethyl)pyridin-3-yl)methyl)-3-methyl-N-(1-(5-methylisoxazol-3-yl)ethyl)-1H-pyrrole-2-carboxamide (**69**).* MeI (0.21 g, 0.74 mmol) was added to a stirred solution of **68** (0.15 g, 0.37 mmol) and Cs_2CO_3 (0.21 g, 0.74 mmol) in THF (3 mL) at 0 °C. The reaction mixture was stirred for 16 h at room temperature. Water was added and the mixture was extracted with ethyl acetate (2 × 30 mL). The resulting combined organic layer was washed with brine, dried over Na_2SO_4, and concentrated. The crude product was purified by prep. HPLC to afford product (35 mg, 23%) as a white solid. ^{1}H NMR (400 MHz, DMSO-d_6) δ (ppm): 11.17 (s, 1H), 8.72 (s, 1H), 7.98 (d, 1H, J = 8.8 Hz), 7. 89 (d, 1H, J = 8.0 Hz), 7.84 (d, 1H, J = 8.0 Hz), 6.71 (d, 1H, J = 2.0 Hz), 6.18 (d, 1H, J = 3.8 Hz), 5.48 (s, 1H), 5.13−5.16 (m, 1H), 3.27 (s, 3H), 2.36 (brs, 3H), 2.16 (s, 3H), 1.43−1.45 (m, 3H); ESIMS m/z (M + 1): 423.2; LCMS: 99.66%; HPLC purity: 94.67%.

*4-(Cyano(6-(trifluoromethyl)pyridin-3-yl)methyl)-3-methyl-N-(1-(5-methylisoxazol-3-yl) ethyl)-1H-pyrrole-2-carboxamide (**70**).* Boc anhydride (236 mg, 0.108 mmol) was added to a stirred solution of **227** (400 mg, 0.98 mmol), triethylamine (0.2 mL, 1.47 mmol), and DMAP (12 mg, 0.09 mmol) in CH_2Cl_2 (20 mL) at RT and continued for 4 h. After completion of the reaction (monitored by TLC), water was added and the reaction mixture extracted with CH_2Cl_2 (2 × 50 mL). The combined organic layer was dried over Na_2SO_4 and concentrated. The resulting concentrated product was purified by column chromatography using 0−40% ethyl acetate in petroleum ether to afford *tert*-butyl 3-methyl-2-((1-(5-methylisoxazol-3-yl)ethyl)carbamoyl)-4-(6-(trifluoromethyl)pyridine-3-carbonyl)-1*H*-pyrrole-1-carboxylate (450 mg, 90%) as a yellow liquid. ESIMS m/z (M + 1): 507.2. The product was used without purification.

Sodium borohydride (67 mg, 1.78 mmol) was added portionwise to a stirred solution of the above Boc-pyrrole intermediate (0.45 g, 0.89 mmol) in ethanol (10 mL) at 0 °C, and the reaction mixture was stirred for 1 h at RT. The reaction mixture was concentrated under reduced pressure. Water (10 mL) was added to the concentrated product and the mixture was extracted with ethyl acetate (2 × 50 mL). The resulting combined organic layer was washed with brine, dried over Na_2SO_4, and concentrated to afford *tert*-butyl 4-(hydroxy(6-(trifluoromethyl)-pyridin-3-yl)methyl)-3-methyl-2-((1-(5-methylisoxazol-3-yl)ethyl)-carbamoyl)-1*H*-pyrrole-1-carboxylate (**228**) (0.4 g, 89%). ESIMS m/z (M + 1): 509.2. The product was used without further purification.

TMSCN (78 mg, 0.79 mmol) was added to a stirred solution of **228** (400 mg, 0.79 mmol) and tris(pentafluorophenyl)borane (20 mg, 0.04 mmol) in acetonitrile (4 mL) at RT. Stirring was continued for 8 h at RT. After completion of the reaction (by TLC), the reaction mixture was concentrated to afford *tert*-butyl 4-(cyano(6-(trifluoromethyl)-pyridin-3-yl)methyl)-3-methyl-2-((1-(5-methylisoxazol-3-yl)ethyl)

https://doi.org/10.1021/acs.jmedchem.1c00173
J. Med. Chem. 2021, 64, 6085−6136

carbamoyl)-1*H*-pyrrole-1-carboxylate (100 mg, 25%). ESIMS *m/z* (M + 1): 518.2. The product was used without further purification.

HCl (4.5 N) in dioxane (2 mL) was added to a stirred solution of the above Boc cyano pyrrole intermediate (100 mg, 0.19 mmol) in dioxane (2 mL) at 0 °C and stirring was continued for 2 h at RT. After completion of the reaction (monitored by TLC), the reaction mixture was concentrated and then dissolved in ethyl acetate (10 mL) and washed with sodium bicarbonate solution (10 mL). The separated organic layer was dried over Na_2SO_4, concentrated, and purified by column chromatography using 0−60% ethyl acetate in petroleum ether to afford the title compound (20 mg, 25%). ^{1}H NMR (400 MHz, $CDCl_3$) δ (ppm): 9.54 (s, 1H), 8.75 (s, 1H), 7.91 (d, 1H, J = 8.4 Hz), 7.75 (d, 1H, J = 8.4 Hz), 6.87−6.89 (m, 1H), 6.52 (d, 1H, J = 7.6 Hz), 5.97 (s, 1H), 5.34−5.37 (m, 1H), 5.21 (s, 1H), 2.44 (s, 3H), 2.27 (s, 3H), 1.61 (d, 3H, J = 7.2 Hz); ESIMS *m/z* (M + 1): 418.2; LCMS: 98.83%; HPLC purity: 98.24%.

*3-Methyl-N-(1-(5-methylisoxazol-3-yl)ethyl)-4-((6-(trifluoromethyl)pyridin-3-yl)methyl-d2)-1H-pyrrole-2-carboxamide Enantiomer I (**71**).* Sodium borodeuteride (0.51 g, 12.26 mmol) was added portionwise to a stirred solution of **173** (2 g, 6.12 mmol) and trifluoroacetic acid-*d* (10 mL) in chloroform (20 mL) at 0 °C. The reaction mixture was stirred for 16 h at RT. Saturated $NaHCO_3$ (50 mL) was then added dropwise at 0 °C and the mixture was extracted with CH_2Cl_2 (3 × 40 mL). The combined organic layers were dried (Na_2SO_4), filtered, and concentrated. The resulting concentrated product was purified by column chromatography using 0−40% ethyl acetate in petroleum ether to afford ethyl 3-methyl-4-((6-(trifluoromethyl) pyridin-3-yl)methyl-d2)-1*H*-pyrrole-2-carboxylate (**226**) as an off-white solid (0.8 g, 42%). ^{1}H NMR (300 MHz, DMSO-d_6) δ (ppm): 11.39 (s, 1H), 8.63 (s, 1H), 7.77−7.87 (m, 2H), 6.80 (s, 1H), 4.17 (q, 2H, J = 7.1 Hz), 2.14 (s, 3H), 1.26 (t, 3H, J = 7.1 Hz).

Sodium hydroxide (200 mg, 5.09 mmol) was added to a stirred solution of **226** (800 mg, 2.54 mmol) in EtOH:H_2O (16:4 mL) at RT and heated to 80 °C for 2 h. The reaction mixture was acidified using citric acid. The solid obtained was filtered and washed with diethyl ether to afford 3-methyl-4-((6-(trifluoromethyl) pyridin-3-yl)methyl-d2)-1*H*-pyrrole-2-carboxylic acid as a white solid (600 mg, 82%). The product was used without purification.

1-(5-Methylisoxazol-3-yl)ethan-1-amine (97 mg, 0.84 mmol) and triethylamine (0.2 mL, 1.40 mmol) were added to a stirred solution of the above deuterated pyrrole carboxylic acid intermediate (200 mg, 0.70 mmol) in CH_2Cl_2 (4 mL) at RT and stirring continued for 5 min. Then, HATU (400 mg, 1.05 mmol) was added to the reaction mixture and stirring was continued at RT for 4 h. After completion of the reaction (monitored by TLC), water was added and the mixture was extracted with CH_2Cl_2 (2 × 30 mL). The combined organic layer was dried over Na_2SO_4 and concentrated. The resulting concentrated product was purified by column chromatography using 10−50% ethyl acetate in petroleum ether to afford the racemic product as an off-white solid (150 mg, 55%). The racemic product was resolved by SFC using a YMC Amylose-SA column and methanol cosolvent (30%) to afford the title compound as an off-white solid (retention time 2.6) (24 mg, 18%). ^{1}H NMR (400 MHz, DMSO-d_6) δ (ppm): 11.09 (s, 1H), 8.64 (s, 1H), 7.81−7.83 (m, 3H), 6.73 (s, 1H), 6.18 (s, 1H), 5.14−5.18 (m, 1H), 2.34 (s, 3H), 2.14 (s, 3H), 1.45 (d, 3H, J = 7.2 Hz); ESIMS *m/z* (M + 1): 396.2; HPLC purity: 99.49%; SFC purity: 99.35%.

*3-Methyl-N-(1-(5-methylisoxazol-3-yl)ethyl)-4-((6-(trifluoromethyl)pyridin-3-yl)methyl-d2)-1H-pyrrole-2-carboxamide Enantiomer II (**72**).* **72** was prepared as for **71** above to afford the product as an off-white solid (retention time 3.79) (21 mg, 15%). ^{1}H NMR (400 MHz, DMSO-d_6) δ (ppm): 11.13 (s, 1H), 8.63 (s, 1H), 7.85 (m, 1H), 7.80 (s, 2H), 6.72 (s, 1H), 6.17 (s, 1H), 5.13−5.17 (m, 1H), 2.35 (s, 3H), 2.13 (s, 3H), 1.44 (d, 3H, J = 7.2 Hz); ESIMS *m/z* (M + 1): 396.2; HPLC purity: 99.36%; SFC purity: 98.89%.

*3-(1-(3-Methyl-4-(1-(6-(trifluoromethyl)pyridin-3-yl)cyclopropyl)-1H-pyrrole-2-carboxamido)ethyl)-1H-pyrazole-5-carboxamide (**83**).* Aqueous ammonia (10 mL) was added to a stirred solution of **256** (0.45 g, 0.95 mmol) in methanol (2 mL) and the reaction heated to 100 °C for 24 h. The reaction mixture was concentrated and purified by preparative HPLC to afford the racemic title compound as a white solid (150 mg, 36%). ^{1}H NMR (400 MHz, CD_3OD) δ (ppm): 8.35 (s, 1H), 7.67 (s, 2H), 6.91 (s, 1H), 6.71 (s, 1H), 5.34−5.36 (m, 1H), 2.19 (s, 3H), 1.62 (d, 3H), 1.41−1.42 (m, 2H), 1.36−1.37 (m, 2H); ESIMS *m/z* (M + 1): 446.9; LCMS: 99.67%; HPLC purity: 98.46%.

3-(1-(3-Methyl-4-(1-(6-(trifluoromethyl)pyridin-3-yl)cyclopropyl)-1H-pyrrole-2-carboxamido)ethyl)-1H-pyrazole-5-carboxamide Enantiomer I (84). Racemic **83** was resolved by SFC purification using a YMC Amylose-SA column and methanol cosolvent (40%) to afford the product (retention time: 2.14) as a white solid (30%). ^{1}H NMR (400 MHz, CD_3OD) δ (ppm): 8.33 (s, 1H), 7.64 (s, 2H), 6.90 (s, 1H), 6.70 (s, 1H), 5.33−5.34 (m, 1H), 2.17 (s, 3H), 1.60 (d, 3H), 1.39−1.42 (m, 2H), 1.34−1.35 (m, 2H); ESIMS *m/z* (M + 1): 447.1; HPLC purity: 98.93%; SFC purity: 97.76%.

*3-(1-(3-Methyl-4-(1-(6-(trifluoromethyl)pyridin-3-yl)cyclopropyl)-1H-pyrrole-2-carboxamido)ethyl)-1H-pyrazole-5-carboxamide Enantiomer II (**85**).* **85** was prepared as for **84** above to afford the product (retention time: 3.27) as a white solid (19%). ^{1}H NMR (400 MHz, CD_3OD) δ (ppm): 8.33 (s, 1H), 7.64 (s, 2H), 6.90 (s, 1H), 6.70 (s, 1H), 5.33−5.34 (m, 1H), 2.17 (s, 3H), 1.60 (d, 3H), 1.39−1.42 (m, 2H), 1.34−1.35 (m, 2H); ESIMS *m/z* (M + 1): 447.1; HPLC purity: 99.43%; SFC purity: 100%.

*N-(1-(5-Cyano-1H-pyrazol-3-yl)ethyl)-3-methyl-4-(1-(6-(trifluoromethyl) pyridin-3-yl)cyclopropyl)-1H-pyrrole-2-carboxamide Enantiomer I (**86**).* To a stirred solution of **83** (120 mg, 0.27 mmol) in CH_2Cl_2 (3 mL) was added DIPEA (0.25 mL, 1.08 mmol) followed by T3P (50 wt % in ethyl acetate) (0.35 mL, 0.54 mmol). The reaction mixture was then stirred for 2 h at RT. After completion of the reaction (monitored by TLC), water was added to the reaction mixture and the reaction mixture was extracted with dichloromethane (2 × 40 mL). The combined organic layer was dried over Na_2SO_4 and concentrated. The resulting concentrated product was purified by column chromatography using 30−80% ethyl acetate in petroleum ether to afford the product as an off-white solid (70 mg, 61%). The racemic product was resolved by SFC purification using a Lux A1 column and methanol cosolvent (30%) to afford product (retention time: 2.52) as a white solid (17%). ^{1}H NMR (400 MHz, DMSO-d_6) δ (ppm): 13.87 (s, 1H), 11.08 (s, 1H), 8.40 (s, 1H), 7.83 (d, 1H, J = 8.0 Hz), 7.73 (d, 1H, J = 8.0 Hz), 7.63 (d 1H), 6.93 (s, 1H), 6.85 (s, 1H), 5.20−5.23 (m, 1H), 2.09 (s, 3H), 1.48 (d, 3H, J = 6.7 Hz), 1.40 (brs, 2H), 1.24 (brs, 2H); ESIMS *m/z* (M + 1): 429.0; HPLC purity: 98.71%, SFC purity: 99.20%.

*N-(1-(5-Cyano-1H-pyrazol-3-yl)ethyl)-3-methyl-4-(1-(6-(trifluoromethyl) pyridin-3-yl)cyclopropyl)-1H-pyrrole-2-carboxamide Enantiomer II (**87**).* **87** was prepared as for **86** above to afford the product (retention time: 3.51) as a white solid (24%). ^{1}H NMR (400 MHz, DMSO-d_6) δ (ppm): 13.87 (s, 1H), 11.09 (s, 1H), 8.40 (s, 1H), 7.84 (d, 1H, J = 8.0 Hz), 7.73 (d, 1H, J = 8.0 Hz), 7.63 (d 1H), 6.93 (s, 1H), 6.84 (s, 1H), 5.20−5.23 (m, 1H), 2.09 (s, 3H), 1.47 (d, 3H, J = 6.7 Hz), 1.40 (brs, 2H), 1.24 (brs, 2H); ESIMS *m/z* (M + 1): 428.9; HPLC purity: 99.57%, SFC purity: 99.29%.

*N-Methyl-3-(1-(3-methyl-4-(1-(6-(trifluoromethyl)pyridin-3-yl) cyclopropyl)-1H-pyrrole-2-carboxamido)ethyl)-1H-pyrazole-5-carboxamide Enantiomer I (**90**).* Methylamine (1.0 M in THF) (0.5 mL, 0.51 mmol) was added to a stirred solution of **256** (200 mg, 0.42 mmol) in THF (4 mL) at RT. Then, Me_3Al (1.0 M in toluene) (0.8 mL, 0.82 mmol) was added to the reaction mixture and stirred at 100 °C for 2 h in a microwave. The resulting reaction mixture was quenched with 1.5 N HCl solution and extracted with ethyl acetate (2 × 40 mL). The combined organic layer was dried over Na_2SO_4 and concentrated. The resulting concentrated product was purified by column chromatography using 10−50% ethyl acetate in petroleum ether to afford the racemic product as a white solid (0.11 g, 57%). The racemic product was resolved by SFC purification using a YMC Amylose-SA column and 0.5% isopropylamine in IPA cosolvent (30%) to afford the title compound (retention time: 3.03) as a white solid (32%). ^{1}H NMR (400 MHz, CD_3OD) δ (ppm): 8.36 (s, 1H), 7.68 (s, 2H), 6.92 (s, 1H), 6.69 (s, 1H), 5.34 (m, 1H), 2.90 (s, 3H), 2.20 (s, 3H), 1.62 (d, 3H,), 1.37−1.45 (m, 4H); ESIMS *m/z* (M + 1): 461.2; HPLC purity: 97.78%; SFC purity: 100%.

*N-Methyl-3-(1-(3-methyl-4-(1-(6-(trifluoromethyl)pyridin-3-yl) cyclopropyl)-1H-pyrrole-2-carboxamido)ethyl)-1H-pyrazole-5-carboxamide Enantiomer II (**91**).* **91** was prepared as for **90** above to

https://doi.org/10.1021/acs.jmedchem.1c00173
J. Med. Chem. 2021, 64, 6085−6136

afford the product (retention time: 4.33) as a white solid (29%). ^{1}H NMR (400 MHz, CD_3OD) δ (ppm): 8.36 (s, 1H), 7.68 (s, 2H), 6.92 (s, 1H), 6.69 (s, 1H), 5.35 (m, 1H), 2.90 (s, 3H), 2.20 (s, 3H), 1.62 (d, 3H,), 1.37−1.45 (m, 4H); ESIMS m/z (M + 1): 461.2; HPLC purity: 95.88%; SFC purity: 100%.

*4-(1-[3-Cyano-4-(trifluoromethyl)phenyl]cyclopropyl)-3-methyl-N-[1-(1H-1,2,4-triazol-3-yl)ethyl]-1H-pyrrole-2-carboxamide (**98**).* Potassium cyanide (1.16 g, 17.81 mmol) was added to a stirred solution of racemic **94** (3.0 g, 7.13 mmol) in DMSO (20 mL) at RT. Then, the reaction mixture was stirred for 20 h at 130 °C. The starting material was not all consumed but continuation of heating lead to side product formation. Therefore, the reaction mixture was quenched with water (200 mL) and extracted with ethyl acetate (3 × 200 mL). The combined organic layers were dried (Na_2SO_4), filtered, and concentrated. The resulting concentrated product was purified by preparative HPLC to afford the product as a white solid (550 mg, 18%). ^{1}H NMR (400 MHz, CD_3OD) δ (ppm): 8.34 (brs, 1H), 7.71 (d, 1H, J = 8.4 Hz), 7.54 (s, 1H), 7.47 (d, 1H, J = 8.4 Hz), 6.89 (s, 1H), 5.35−5.37 (m, 1H), 2.19 (s, 3H), 1.61 (d, 3H, J = 6.8 Hz), 1.41−1.42 (m, 2H), 1.34−1.36 (m, 2H); ESIMS m/z (M + 1): 429.2; LCMS: 97.67%; HPLC purity: 97.55%.

*4-(1-[3-Cyano-4-(trifluoromethyl)phenyl]cyclopropyl)-3-methyl-N-[1-(1H-1,2,4-triazol-3-yl)ethyl]-1H-pyrrole-2-carboxamide Enantiomer I (**99**).* **98** was resolved by SFC purification using a Lux A1 column and IPA cosolvent (30%) to afford the product (retention time: 1.70) as an off-white solid (40%). Mp 135−140 °C. Optical rotation (ethanol): −12.797. ^{1}H NMR (400 MHz, CD_3OD) δ (ppm): 8.28 (brs, 1H), 7.75 (d, 1H, J = 8.4 Hz), 7.57 (s, 1H), 7.49−7.51 (d, 1H, J = 8.4 Hz), 6.92 (s, 1H), 5.36−5.41 (m, 1H), 2.18 (s, 3H), 1.64 (d, 3H, J = 6.8 Hz), 1.43−1.45 (m, 2H), 1.37−1.40 (m, 2H); ESIMS (m/z) (M + 1): 429.1; HPLC purity: 99.92; SFC purity: 100%.

*4-(1-[3-Cyano-4-(trifluoromethyl)phenyl]cyclopropyl)-3-methyl-N-[1-(1H-1,2,4-triazol-3-yl)ethyl]-1H-pyrrole-2-carboxamide Enantiomer II (**100**).* The title compound was prepared as for **99** above (retention time: 3.15) as an off-white solid (35%). Optical rotation (ethanol): 14.396. ^{1}H NMR (400 MHz, CD_3OD) δ (ppm): 8.28 (brs, 1H), 7.75 (d, 1H, J = 8.4 Hz), 7.57 (s, 1H), 7.49−7.51 (d, 1H, J = 8.4 Hz), 6.92 (s, 1H), 5.38 (m, 1H), 2.19 (s, 3H), 1.64 (d, 3H, J = 6.8 Hz), 1.43−1.46 (m, 2H), 1.37−1.40 (m, 2H); ESIMS (m/z): 429.1; HPLC purity: 99.38%; SFC purity: 100%.

*N2-Cyclopropyl-4-((6-(trifluoromethyl)pyridin-3-yl)methyl)-1H-pyrrole-2,3-dicarboxamide (**105**).* 1,1′-Carbonyldiimidazole (44 mg, 0.27 mmol) was added to a stirred solution of **261** (80 mg, 0.23 mmol) in acetonitrile (3 mL) at RT and stirred at 80 °C for 2 h. Then, NH4OH solution was added at RT and stirred for 4 h at 80 °C. The reaction mixture was concentrated and acidified with 1.5 N HCl solution. The solid obtained was filtered, washed with water, and dried to afford the product as an off-white solid (60 mg, 76%). ^{1}H NMR (400 MHz, DMSO-d_6) δ (ppm): 11.72 (s, 1H), 9.50 (s, 1H), 8.58 (s, 1H), 8.01 (s, 1H), 7.76−7.81 (m, 2H), 7.51 (s, 1H), 6.68 (s, 1H), 4.14 (s, 2H), 2.69−2.74 (m, 1H), 0.70−0.72 (m, 2H), 0.42−0.44 (m, 2H); ESIMS m/z (M + 1): 352.8.

*3-Cyano-N-cyclopropyl-4-((6-(trifluoromethyl)pyridin-3-yl)-methyl)-1H-pyrrole-2-carboxamide (**106**).* $POCl_3$ (22 mg, 0.15 mmol) was added to a stirred solution of **105** (35 mg, 0.10 mmol) in acetonitrile (2 mL) and pyridine (15 mg, 0.20 mmol) at RT and heated to 80 °C for 2 h. The reaction mixture was cooled to RT, then acidified with 1.5 N HCl solution, and extracted with ethyl acetate (2 × 15 mL). The combined organic layer was dried (Na_2SO_4), filtered, and concentrated. The resulting concentrated product was purified by column chromatography using 5−60% ethyl acetate in petroleum ether to afford the product as an off-white solid (12 mg, 36%). ^{1}H NMR (400 MHz, $CDCl_3$) δ (ppm): 9.85 (s, 1H), 8.64 (s, 1H), 7.75 (d, 1H, J = 8.0 Hz), 7.66 (d, 1H, J = 8.0 Hz), 6.74 (s, 1H), 6.52 (s, 1H), 4.04 (s, 2H), 2.89−2.92 (m, 1H), 0.90−0.94 (m, 2H), 0.67−0.71 (m, 2H); ESIMS m/z (M + 1): 334.8; LCMS: 99.31%; HPLC purity: 97.91%.

*5-Chloro-N-cyclopropyl-3-methyl-4-((6-(trifluoromethyl)pyridin-3-yl)methyl)-1H-pyrrole-2-carboxamide (**119**).* *N*-Chlorosuccinamide (20 mg, 0.15 mmol) was added to a stirred solution of **268**[20] (50 mg, 015 mmol) in DMF (2 mL) at room temperature and stirring was continued for 4 h. The reaction mixture was poured into water and extracted with ethyl acetate (2 × 30 mL). The combined organic layer was dried over Na_2SO_4 and concentrated. The resulting concentrated product was purified by column chromatography using 10−50% ethyl acetate in petroleum ether to afford the product as an off-white solid (25 mg, 45%). ^{1}H NMR (400 MHz, DMSO-d_6) δ (ppm): 11.71 (s, 1H), 8.60 (s, 1H), 7.81 (d, 1H, J = 8.2 Hz), 7.72 (d, 1H, J = 8.2 Hz), 7.49 (s, 1H), 3.85 (s, 2H), 2.71−2.73 (m, 1H), 2.12 (s, 3H), 0.65−0.68 (m, 2H), 0.43−0.47 (m, 2H); ESIMS m/z (M + 1): 358.1; LCMS: 96.84%; HPLC purity: 99.78%.

*3-(1-(3-Methyl-4-(6-(trifluoromethyl)-1H-indazol-3-yl)-1H-pyrrole-2-carboxamido)ethyl)-1H-pyrazole-5-carboxamide (**138**).* Aqueous ammonia (10 mL) was added to a stirred solution of **279** (0.52 g, 1.10 mmol) in methanol (3 mL) and heated to 100 °C for 24 h. The reaction mixture was concentrated and purified by preparative HPLC to afford the title compound as an off-white solid (25%). ^{1}H NMR (400 MHz, CD_3OD) δ (ppm): 7.97 (d, 1H, J = 8.8 Hz), 7.89 (s, 1H), 7.41 (d, 1H, J = 8.8 Hz), 7.33 (s, 1H), 6.79 (s, 1H), 5.39−5.41 (m, 1H), 2.52 (s, 3H), 1.67 (d, 3H, J = 6.8 Hz); ESIMS; m/z (M + 1): 446.9; LCMS: 97.36%; HPLC purity: 93.862%.

*N-(1-(5-Cyano-1H-pyrazol-3-yl)ethyl)-3-methyl-4-(6-(trifluoromethyl)-1H-indazol-3-yl)-1H-pyrrole-2-carboxamide Enantiomer I (**139**).* To a stirred solution of **138** (120 mg, 0.27 mmol) in CH_2Cl_2 (3 mL) was added DIPEA (0.25 mL, 1.08 mmol) followed by T3P (50 wt % in ethyl acetate) (0.35 mL, 0.54 mmol). The reaction mixture was stirred for 2 h at RT. After completion of the reaction (monitored by TLC), water was added and the reaction mixture extracted with CH_2Cl_2 (2 × 40 mL). The combined organic layer was dried over Na_2SO_4 and concentrated. The resulting concentrated product was purified by column chromatography using 30−80% ethyl acetate in petroleum ether to afford the racemic product as an off-white solid (52%). The racemic product was resolved by SFC purification using a Chiralcel OJ-H column and methanol cosolvent (30%) to afford the title compound (retention time 3.02) as a white solid (26%). ^{1}H NMR (400 MHz, CD_3OD) δ (ppm): 7.97 (d, 1H, J = 8.4 Hz), 7.89 (s, 1H), 7.41 (d, 1H, J = 8.4 Hz), 7.34 (s, 1H), 6.81 (s, 1H), 5.39−5.44 (q, 1H, J = 6.8 Hz), 2.52 (s, 3H), 1.67 (d, 3H, J = 6.8 Hz); ESIMS; m/z (M + 1): 428.2; HPLC purity: 99.05%; SFC purity: 100%.

*N-(1-(5-Cyano-1H-pyrazol-3-yl)ethyl)-3-methyl-4-(6-(trifluoromethyl)-1H-indazol-3-yl)-1H-pyrrole-2-carboxamide Enantiomer II (**140**).* **140** was prepared as for **139** above (retention time 3.74) as a white solid (23%). ^{1}H NMR (400 MHz, CD_3OD) δ (ppm): 7.97 (d, 1H, J = 8.4 Hz), 7.89 (s, 1H), 7.41 (d, 1H, J = 8.4 Hz), 7.34 (s, 1H), 6.81 (s, 1H), 5.40−5.44 (q, 1H, J = 6.8 Hz), 2.52 (s, 3H), 1.67 (d, 3H, J = 6.8 Hz); ESIMS; m/z (M + 1): 428.1; HPLC purity: 99.22%; SFC purity: 97.91%.

*3-Methyl-4-(1-methyl-6-(trifluoromethyl)-1H-indazol-3-yl)-N-(1-(5-methylisoxazol-3-yl) ethyl)-1H-pyrrole-2-carboxamide Enantiomer I (**145**).* 1-(5-Methylisoxazol-3-yl)ethan-1-amine and **277** were reacted together using general procedure F1 to produce 4-(2-fluoro-4-(trifluoromethyl)benzoyl)-3-methyl-*N*-(1-(5-methylisoxazol-3-yl)ethyl)-1*H*-pyrrole-2-carboxamide as an off-white solid (60%). The intermediate carboxamide (100 mg, 0.24 mmol) was used directly and treated with methyl hydrazine (0.2 mL) with stirring in DMSO (1 mL) at RT and then heated to 100 °C for 2 h. After consumption of the starting material, the reaction mixture was poured into water and stirred for 10 min. The solid obtained was filtered, washed with water, and dried to afford the racemic product (69%). The racemic product was resolved by SFC purification using a Lux A1 column and IPA cosolvent (40%) to afford the title compound (retention time 4.30) as an off-white solid (24%). ^{1}H NMR (400 MHz, MeOD) δ (ppm): 7.94−7.96 (m, 2H), 7.40−7.43 (d, 1H, J = 8.0 Hz), 7.33 (s, 1H), 6.19 (s, 1H), 5.31−5.36 (q, 1H, J = 7.0 Hz), 4.17 (s, 3H), 2.52 (s, 3H), 2.42 (s, 3H), 1.62 (d, 3H, J = 7.0 Hz); ESIMS m/z (M + 1): 432.2; HPLC purity: 99.23%; SFC purity: 99.69%.

*3-Methyl-4-(1-methyl-6-(trifluoromethyl)-1H-indazol-3-yl)-N-(1-(5-methylisoxazol-3-yl) ethyl)-1H-pyrrole-2-carboxamide Enantiomer I (**146**).* **146** was prepared as for **145** above (retention time 5.81) as an off-white solid (20%). ^{1}H NMR (400 MHz, MeOD) δ (ppm): 7.94−7.96 (m, 2H), 7.40−7.43 (d, 1H, J = 8.0 Hz), 7.32 (s, 1H), 6.19 (s, 1H), 5.31−5.36 (q, 1H, J = 7.0 Hz), 4.17 (s, 3H), 2.52 (s,

https://doi.org/10.1021/acs.jmedchem.1c00173
J. Med. Chem. 2021, 64, 6085−6136

3H), 2.42 (s, 3H), 1.62 (d, 3H, J = 7.0 Hz); ESIMS m/z (M + 1): 432.2; HPLC purity: 98.16%; SFC purity: 98.60%.

*3-Methyl-N-(1-(5-methylisoxazol-3-yl)ethyl)-4-(6-(trifluoromethyl)benzo[d]isoxazol-3-yl)-1H-pyrrole-2-carboxamide Enantiomer I (**147**).* The intermediate carboxamide described in **145** above (0.2 g, 0.47 mmol) was treated with $NH_2OH{\cdot}HCl$ (0.13 g, 1.89 mmol) in pyridine (2 mL) at RT and then heated to 100 °C for 16 h. The resulting reaction mixture was concentrated, 1.5 N HCl was added (10 mL), and the mixture was extracted with CH_2Cl_2 (2 × 40 mL). The combined organic layer was dried over Na_2SO_4 and concentrated. The resulting concentrated product was purified by column chromatography using 10−50% ethyl acetate in petroleum ether to afford 4-((2-fluoro-4-(trifluoromethyl)phenyl)(hydroxyimino)methyl)-3-methyl-*N*-(1-(5-methylisoxazol-3-yl)ethyl)-1*H*-pyrrole-2-carboxamide as an off-white solid (0.15 g, 63%). NaOMe (40 mg, 060 mmol) was added to a stirred solution of the intermediate hydroxyimino compound (0.13 g, 0.30 mmol) in THF (4 mL) at RT and heated to 60 °C for 6 h. The resulting reaction mixture was concentrated, water was added (5 mL), and the mixture was extracted with dichloromethane (2 × 40 mL). The combined organic layer was dried over Na_2SO_4 and concentrated. The resulting concentrated product was purified by column chromatography using 10−50% ethyl acetate in petroleum ether to afford the racemic product (80 mg, 56%) as an off-white solid. The racemic product was resolved by SFC purification using a Chiralcel OZ-H column and methanol cosolvent (30%) to afford the title compound (retention time 3.0) as an off-white solid (21%). ^{1}H NMR (400 MHz, MeOD) δ (ppm): 8.17−8.19 (d, 1H), 8.07 (s, 1H), 7.71−7.73 (d, 1H) 7.67(s, 1H), 6.21 (s, 1H), 5.32−5.38 (m, 1H), 2.62 (s, 3H), 2.44 (s, 3H), 1.63 (d, 3H); ESIMS (M + 1) m/z: 419.0; HPLC purity: 98.34%; SFC purity: 99.48%.

*3-Methyl-N-(1-(5-methylisoxazol-3-yl)ethyl)-4-(6-(trifluoromethyl)benzo[d]isoxazol-3-yl)-1H-pyrrole-2-carboxamide Enantiomer II (**148**).* **148** was prepared as for **147** above (retention time 3.44) as an off-white solid (20%). ^{1}H NMR (400 MHz, MeOD) δ (ppm): 8.17−8.19 (d, 1H), 8.07 (s, 1H), 7.71−7.73 (d, 1H) 7.67(s, 1H), 6.21 (s, 1H), 5.32−5.38 (m, 1H), 2.62 (s, 3H), 2.44 (s, 3H), 1.63 (d, 3H); ESIMS (M + 1) m/z: 419.1; HPLC purity: 96.51%; SFC purity: 99.24%.

*2-Hydroxy-N-methoxy-N-methyl-4-(trifluoromethyl)benzamide (**184**).* 1,1′-Carbonyldiimidazole (7.65 g, 54.51 mmol) was added to a stirred solution of 2-hydroxy-4-(trifluoromethyl)benzoic acid (10.0 g, 45.42 mmol) in DMF (50 mL) at RT and stirring continued for 1 h. Then, *N*,*O*-dimethylhydroxylamine hydrochloride (11.13 g, 113.56 mmol) was added to the reaction mixture at RT and stirring was continued for 4 h. The reaction mixture was poured into water and extracted with ethyl acetate (2 × 300 mL). The combined organic layers were dried (Na_2SO_4), filtered, and concentrated. The concentrated product was purified by flash chromatography (silica gel, eluting with hexane:EtOAc mixtures from 100 to 70:30%) to yield the product as a yellow liquid (8.0 g, 71%). ^{1}H NMR (300 MHz, $CDCl_3$) δ (ppm): 11.31 (s, 1H), 8.12 (d, 1H, J = 8.4 Hz), 7.27−7.28 (m, 1H), 7.10−7.12 (dd, 1H, J = 0.8 Hz & 8.4 Hz), 3.67 (s, 3H), 3.45 (s, 3H). ESIMS m/z (M + 1): 250.1.

*1-(2-Hydroxy-4-(trifluoromethyl)phenyl)but-2-yn-1-one (**185**).* 1-Propynylmagnesium bromide (0.5 M in THF) (71 mL, 35.30 mmol) was added to **184** (8 g, 32.10 mmol) in THF (150 mL) at 0 °C and stirred for 4 h at RT. The reaction mixture was quenched with 1.5 N HCl solution and extracted with ethyl acetate (2 × 300 mL). The resulting organic layer was washed with brine, dried over Na_2SO_4, and concentrated to afford the product as a colorless liquid (4 g, 55%). ^{1}H NMR (300 MHz, $CDCl_3$) δ (ppm): 11.75 (s, 1H), 8.16 (d, 1H, J = 8.4 Hz), 7.26 (d, 1H, J = 8.4 Hz), 7.19 (d, 1H), 2.24 (s, 3H). ESIMS m/z (M + 1): 229.1.

*1-(2-Hydroxy-3-nitro-4-(trifluoromethyl)phenyl)but-2-yn-1-one (**186**).* Conc·HNO_3 (4 mL) was added to a stirred solution of **185** (4 g, 17.53 mmol) in acetic acid (20 mL) at 0 °C. Then, conc·H_2SO_4 (4 mL) was added slowly at 0 °C and the reaction mixture was stirred for 4 h at 0 °C. After completion of the reaction (monitored by TLC), the reaction mixture was poured into ice cold water and extracted with ethyl acetate (2 × 100 mL). The combined organic layers were dried (Na_2SO_4), filtered, and concentrated. The concentrated product was purified by flash chromatography (silica gel, eluting with hexane:EtOAc mixtures from 100 to 70:30%) to afford the product as a yellow solid (1.5 g, 31%). ^{1}H NMR (300 MHz, $CDCl_3$) δ (ppm): 12.20 (s, 1H), 8.29 (d, 1H, J = 8.4 Hz), 7.32 (d, 1H, J = 8.2 Hz), 2.29 (s, 3H). ESIMS m/z (M − 1): 272.2.

*Methyl 2-(Cyclopropylcarbamoyl)-4-(6-(trifluoromethyl)pyridine-3-carbonyl)-1H-pyrrole-3-carboxylate (**260**).* Sodium chlorite (0.31 g, 3.42 mmol) was added to a stirred solution of **259** (0.8 g, 2.27 mmol) and sulfamic acid (0.3 g, 3.42 mmol) in methanol (5 mL) and water (2 mL) at 0 °C and stirring continued for 2 h at RT. Water was added to the reaction mixture and extracted with ethyl acetate (2 × 30 mL). The combined organic layer was dried over Na_2SO_4 and concentrated. SOCl2 (0.3 mL, 3.41 mmol) was added to a stirred solution of the concentrated product in methanol (10 mL) at 0 °C and stirring continued for 16 h at RT. The resulting reaction mixture was concentrated, dissolved in ethyl acetate (20 mL), washed with 10% $NaHCO_3$ solution, dried over Na_2SO_4, and evaporated. The resulting concentrated product was purified by column chromatography using 5−30% ethyl acetate in petroleum ether to afford the product as an off-white solid (0.30 g, 35%). ESIMS m/z (M + 1): 382.2. The product was used without further characterization.

*Ethyl 3-Bromo-5-methyl-4-((6-(trifluoromethyl)pyridin-3-yl)-methyl)-1H-pyrrole-2-carboxylate (**264**).* *N*-Bromosuccinimide (NBS, 0.52 g, 2.89 mmol) was added to a stirred solution of **263**[20] (0.9 g, 2.89 mmol) in DMF (10 mL) at 0 °C and stirred at RT for 2 h. The resulting reaction mixture was concentrated and quenched with water (10 mL) and stirred for 10 min. The solid obtained was filtered, washed with water, and dried to afford the product as an off-white solid (0.8 g, 71%). ^{1}H NMR (400 MHz, DMSO-d_6) δ (ppm): 11.99 (s, 1H), 8.60 (s, 1H), 7.79 (d, 1H, J = 8.0 Hz), 7.72 (d, 1H, J = 8.0 Hz), 4.22 (q, 2H, J = 7.0 Hz), 3.87 (s, 2H), 2.20 (s, 3H), 1.27 (t, 3H, J = 7.0 Hz); ESIMS m/z (M, M + 2): 390.8, 391.8.

*Ethyl 3-Cyano-5-methyl-4-((6-(trifluoromethyl)pyridin-3-yl)-methyl)-1H-pyrrole-2-carboxylate (**265**).* CuCN (0.52 g, 2.89 mmol) was added to a stirred solution of **264** (0.8 g, 2.05 mmol) in DMF (10 mL) at RT and stirred at 130 °C for 16 h. Water (20 mL) was added to reaction mixture and extracted with ethyl acetate (2 × 50 mL). The resulting combined organic layer was washed with brine, dried over Na_2SO_4, and concentrated. The resulting concentrated product was purified by column chromatography using 10−50% ethyl acetate in petroleum ether to afford the product as an off-white solid (0.5 g, 72%). ^{1}H NMR (400 MHz, DMSO-d_6) δ (ppm): 12.66 (s, 1H), 8.63 (s, 1H), 7.77−7.83 (m, 2H), 4.27 (q, 2H, J = 7.0 Hz), 3.99 (s, 2H), 2.21 (s, 3H), 1.88 (t, 3H, J = 7.0 Hz); ESIMS m/z (M + 1): 338.0; LCMS: 96.04%; HPLC purity: 97.66%.

*5-Chloro-3-methyl-4-((6-(trifluoromethyl)pyridin-3-yl)methyl)-1H-pyrrole-2-carboxylic Acid (**266**).* *N*-Chlorosuccinimide (NCS, 0.23 g, 1.27 mmol) was added to a stirred solution of **181** (300 mg, 1.05 mmol) in DMF (2 mL) at RT and stirred for 16 h. The reaction mixture was poured into water and extracted with CH_2Cl_2 (2 × 10 mL). The combined organic layer was dried over Na_2SO_4 and concentrated. The crude product was purified by preparative HPLC to afford as a white solid (0.16 g, 48%). ^{1}H NMR (400 MHz, DMSO-d_6) δ (ppm): 12.41 (s, 1H), 12.25 (s, 1H), 8.61 (s, 1H), 7.81 (d, 1H, J = 8.0 Hz), 7.30 (d, 1H, J = 8.0 Hz), 3.87 (s, 2H), 2.09 (s, 3H); ESIMS m/z (M): 319.3

*5-Chloro-3-methyl-4-(1-(6-(trifluoromethyl)pyridin-3-yl)-cyclopropyl)-1H-pyrrole-2-carboxylic Acid (**267**).* NCS (0.23 g, 1.36 mmol) was added to a stirred solution of **251** (350 mg, 1.13 mmol) in DMF (3 mL) at RT and stirred for 6 h. The reaction mixture was poured into water and extracted with CH_2Cl_2 (2 × 30 mL). The combined organic layer was dried over Na_2SO_4 and concentrated. The crude product was purified by preparative HPLC to afford the product as a white solid (0.13 g, 34%). ^{1}H NMR (400 MHz, DMSO-d_6) δ (ppm): 12.42 (s, 1H), 12.28 (s, 1H), 8.63 (s, 1H), 7.83 (d, 1H, J = 8.0 Hz), 7.35 (d, 1H, J = 8.0 Hz), 2.12 (s, 3H), 1.50−1.59 (m, 2H), 1.40−1.49 (m, 2H); ESIMS m/z (M): 345.3.

*(E)-3-(2-Nitroprop-1-en-1-yl)-6-(trifluoromethyl)-1H-pyrrolo [2,3-b]pyridine (**269**).* Ammonium acetate (3.20 g, 42.03 mmol) was added to a stirred solution of 6-(trifluoromethyl)-1*H*-pyrrolo[2,3-*b*]pyridine-

https://doi.org/10.1021/acs.jmedchem.1c00173
J. Med. Chem. 2021, 64, 6085−6136

3-carbaldehyde (3.0 g, 14.01 mmol) in nitroethane (20 mL) at RT and stirred for 1 h at 100 °C. The reaction mixture was poured into ice water (100 mL) and extracted with ethyl acetate (2 × 100 mL). The combined organic layer was dried (Na_2SO_4) and concentrated. The resulting concentrated product was purified by column chromatography using 0−50% ethyl acetate in petroleum ether to afford the product as a yellow solid (3.0 g, 79%). ESIMS m/z (M + 1): 272.2. The product was used without further characterization.

*1-(6-(Trifluoromethyl)-1H-pyrrolo[2,3-b]pyridin-3-yl)propan-2-one (**270**).* Iron powder (3.1 g, 55.35 mmol) was added to a stirred solution of **269** (3.0 g, 11.07 mmol) in acetone (40 mL) at RT and heated to 50 °C with stirring. Then, 4 N HCl solution (20 mL) was added dropwise at the same temperature and stirred for 3 h. The reaction mixture was concentrated under reduced pressure, 4 N HCl solution (30 mL) was poured onto the residue and the mixture extracted with CH_2Cl_2 (2 × 100 mL). The combined organic layer was dried (Na_2SO_4) and concentrated. The concentrated product was purified by column chromatography using 0−40% ethyl acetate in petroleum ether to afford the product as an off-white solid (1.5 g, 56%). ESIMS m/z (M + 1): 243.2. ^{1}H NMR (300 MHz, $CDCl_3$) δ (ppm): 11.26 (brs, 1H), 8.10 (d, 1H, J = 8.1 Hz), 7.55−7.57 (m, 2H), 3.92 (s, 2H), 2.26 (s, 3H); ESIMS m/z (M + 1): 243.6.

*Ethyl 3-Methyl-4-(6-(trifluoromethyl)-1H-indol-3-yl)-pyrrole-2-carboxylate (**271**).* *N*,*N*-Dimethylformamide dimethyl acetal (4.0 mL) was added to 1-(6-(trifluoromethyl)-1*H*-indol-3-yl)propan-2-one (commercial) (0.8 g, 3.31 mmol) and heated to 120 °C in a microwave for 1 h. The reaction mixture was concentrated under reduced pressure to afford (4-dimethylamino)-3-(6-(trifluoromethyl)-1*H*-indol-3-yl)-but-3-en-2-one (1.0 g crude) as a gummy solid that was used directly. To a stirred solution of the intermediate but-en-one (1.0 g, 3.39 mmol) in acetic acid (20 mL) were added ethyl-2-(hydroxyimino)3-oxobutanoate (0.538 g, 3.39 mmol), sodium acetate (0.833 g, 10.16 mmol), and zinc (1.10 g, 16.93 mmol). The reaction mixture was heated to 100 °C for 3 h. The reaction mixture was then concentrated under reduced pressure, the residue was poured into saturated $NaHCO_3$ solution, and extracted with ethyl acetate (2 × 100 mL). The combined organic layer was dried (Na_2SO_4) and concentrated. The resulting concentrated product was purified by column chromatography using 0−40% ethyl acetate in petroleum ether to afford the product as a pale yellow solid (0.7 g, 62%). ^{1}H NMR (400 MHz, DMSO-d_6) δ (ppm): 11.68 (s, 1H), 11.61 (s, 1H), 7.71−7.76 (m, 2H); 7.61 (s, 1H), 7.32 (d, 1H, J = 8.4 Hz), 7.14 (d, 1H, J = 2.0 Hz), 4.28 (q, 2H, J = 6.8 Hz), 2.34 (s, 3H), 1.33 (t, 3H, J = 6.8 Hz); ESIMS m/z (M + 1): 337.0; LCMS: 98.58%; HPLC purity: 98.76%.

*Ethyl 4-(6-Fluoro-1H-indol-3-yl)-3-methyl-1H-pyrrole-2-carboxylate (**272**).* *N*,*N*-Dimethylformamide dimethyl acetal (5.0 mL) was added to 1-(6-fluoro-1*H*-indol-3-yl)propan-2-one (commercial) (1.0 g, 5.23 mmol) and heated to 120 °C in a microwave for 1 h. The reaction mixture was concentrated under reduced pressure to afford 4-(dimethylamino)-3-(6-fluoro-1*H*-indol-3-yl)but-3-en-2-one (1.1 g) as a gummy solid that was used directly. To a stirred solution of intermediate but-en-one (1.1 g, 4.47 mmol) in acetic acid (15 mL) were added ethyl-2-(hydroxyimino)3-oxobutanoate (0.538 g, 4.47 mmol), sodium acetate (1.1 g, 13.41 mmol), and zinc (1.46 g, 22.36 mmol). The reaction mixture was heated to 100 °C for 3 h. The reaction mixture was then concentrated under reduced pressure, the residue was poured into saturated $NaHCO_3$ solution, and extracted with ethyl acetate (2 × 100 mL). The combined organic layer was dried (Na_2SO_4) and concentrated. The resulting concentrated product was purified by column chromatography using 0−40% ethyl acetate in petroleum ether to afford the product as a pale yellow solid (26%). ^{1}H NMR (300 MHz, DMSO-d_6) δ (ppm): 11.61 (s, 1H), 11.20 (s, 1H), 7.48−7.53 (m, 1H); 7.33 (s, 1H), 7.15−7.20 (m, 1H), 7.10 (s, 1H), 6.87−6.90 (m, 1H), 4.28 (q, 2H, J = 7.2 Hz), 2.33 (s, 3H), 1.32 (t, 3H, J = 7.2 Hz); ESIMS m/z: 287.2; LCMS: 99.09%; HPLC purity: 97.03%.

*Ethyl 3-Methyl-4-(6-(trifluoromethyl)-1H-pyrrolo[2,3-b]pyridin-3-yl)-1H-pyrrole-2-carboxylate (**273**).* *N*,*N*-Dimethylformamide dimethyl acetal (5.0 mL) was added to **270** (1.50 g, 6.20 mmol) and heated to 120 °C in a microwave for 1 h. The reaction mixture was concentrated under reduced pressure to afford (*Z*)-4-(dimethylamino)-3-(6-(trifluoromethyl)-1*H*-pyrrolo[2,3-*b*] pyridin-3-yl)but-3-en-2-one (1.85 g, 100%) as a gummy solid. ESIMS m/z (M + 1): 298.2. The product was used without further purification. To a stirred solution of intermediate but-en-one (1.85 g, 6.20 mmol) in acetic acid (20 mL) were added ethyl-2-(hydroxyimino)3-oxobutanoate (0.96 g, 6.20 mmol), sodium acetate (1.50 g, 18.6 mmol), and zinc (2.0 g, 31.0 mmol). The reaction mixture was heated to 100 °C for 3 h. The reaction mixture was then concentrated under reduced pressure, residue was then poured into saturated $NaHCO_3$ solution, and extracted with ethyl acetate (2 × 200 mL). The combined organic layer was dried (Na_2SO_4) and concentrated. The resulting concentrated product was purified by column chromatography using 0−40% ethyl acetate in petroleum ether to afford the product as a pale yellow solid (0.5 g, 29%). ^{1}H NMR (300 MHz, CD_3OD) δ (ppm): 8.15 (d, 1H, J = 8.0 Hz); 7.59 (s, 1H), 7.52 (d, 1H, J = 8.0 Hz), 7.14 (s, 1H), 4.35 (q, 2H, J = 7.2 Hz), 2.41 (s, 3H), 1.41 (t, 3H, J = 7.2 Hz); ESIMS m/z: 337.9; LCMS: 98.79%; HPLC purity: 96.69%.

*3-Methyl-4-(6-(trifluoromethyl)-1H-indazol-3-yl)-1H-pyrrole-2-carboxylic acid (**278**).* $NH_2NH_2{\cdot}H_2O$ (1.5 mL, 2 vol) was added to a stirred solution of **277** (0.75 g, 0.21 mmol) in DMSO (4 mL) and the reaction mixture heated to 100 °C for 1 h. After consumption of the starting material, the reaction mixture was poured into water and acidified with 1.5 N HCl solution. The solid obtained was filtered, washed with water, and dried to afford the product as a white solid (0.6 g, 82%). ^{1}H NMR (400 MHz, DMSO-d_6) δ (ppm): 13.38 (s, 1H), 12.36 (brs, 1H), 11.79 (s, 1H), 8.07 (d, 1H, J = 8.4 Hz), 7.91 (s, 1H), 7.43 (s, 1H), 7.40 (d, 1H, J = 8.4 Hz), 2.52 (s, 3H); ESIMS; m/z (M − 1): 308.0; LCMS: 96.01%; HPLC purity: 92.79%.

*Ethyl 3-Methyl-4-(6-(trifluoromethyl)-1H-pyrazolo[3,4-b]pyridin-3-yl)-1H-pyrrole-2-carboxylate (**282**).* $NH_2NH_2{\cdot}H_2O$ (1.6 mL, 2 vol) was added to a stirred solution of **281** (800 mg, 1.98 mmol) in DMSO (4 mL) was heated to 80 °C for 30 min. After completion of the starting material, the reaction mixture was poured into water and stirred for 10 min. The solid obtained was filtered, washed with water, and dried to afford the product as an off-white solid (500 mg, 75%). ESIMS m/z (M + 1): 339.3. The product was used without further characterization.

■ ASSOCIATED CONTENT

Supporting Information

The Supporting Information is available free of charge at https://pubs.acs.org/doi/10.1021/acs.jmedchem.1c00173.

Supporting information methods; supporting information Schemes S1−S10; FEP+ predictions for previously reported[20] Pyrrole-based DHODH inhibitors (Table S1); FEP+ predictions for compounds reported in this publication (Table S2); X-ray data collection and refinement statistics for the structures of PfDHODH bound to select pyrroles (Table S3); *In vitro* metabolism and kinetic solubility data (Table S4A); Caco-2 permeability studies for carboxamide pyrazoles **47** and **84** (Table S4B); mouse PK data after (IV) and oral (PO) dosing for **84**, **88**, and **154** (Table S5); species selectivity and preliminary safety analysis (Table S6); summary of *P. falciparum* EC_{50} values on Dd2 wild-type and DHODH inhibitor (**1** and **26**) selected resistant cell lines (Table S7A); steady-state kinetic analysis of recombinant C276F and C276Y mutant *Pf*DHODH versus **26** and **79** (Table S7B); EC_{50} determination of 79-resistant Dd2 and 3D7 parasites (Table S8A); list of genes included in the CNV region of **79** Dd2-resistant parasites (Table S8B); list of genes included in the CNV region of **79** 3D7-resistant parasites (Table S8C); metrics of whole-genome sequencing of **79**-resistant parasites and their parental lines (Table S8D); SCID mouse efficacy studies on **33** and **36** (conducted at Swiss TPH) (Table S9); SCID mouse efficacy studies on **1**, **79** and **99** (conducted at

https://doi.org/10.1021/acs.jmedchem.1c00173
J. Med. Chem. 2021, 64, 6085−6136

TAD) (Table S10); comparison of exposure for SCID mouse versus normal mouse (Table S11); electron density for *Pf*DHODH coinhibitor structures showing the Fo-Fc map of the bound inhibitors prior to refinement (Figure S1); X-ray structures of *Pf*DHODH (green) bound to **56**, **86**, **81**, and **18** (Figure S2); FEP+ predictions correlated to measured IC_{50} values on *Pf*DHODH (Figure S3); mouse and rat PK profiles for **36** showing concentrations **33** as a metabolite (Figure S4); Uganda *P. falciparum* field isolates. Scatterplots and Spearman Correlations (Figure S5); tolerance phenotype of C276F and C276Y mutant clones versus **26** and **79** (Figure S6); SCID mouse efficacy study of **33** and **36** showing parasitemia and drug blood concentrations over time (Figure S7); SCID mouse efficacy study of **99** showing parasitemia and drug blood concentrations over time (Figure S8); NMR and LCMS data for key compounds (**26**, **33**, **36**, **79**, and **99**) (PDF)

Molecular Formula Strings Excel Spread sheet (CSV)

Accession Codes

PDB coordinates. The coordinates for the structure of *Pf*DHODH bound to **18, 56, 127, 79, 81, 86**, and **47** have been submitted to the Protein Data Bank (PDB 7KYK, 7KYV, 7KYY, 7KZ4, 7KZY, 7LO1, 7LOK, respectively). The authors will release the atomic coordinates and experimental data upon article publication.

AUTHOR INFORMATION

Corresponding Author

Margaret A. Phillips − *Department of Biochemistry, University of Texas Southwestern Medical Center at Dallas, Dallas, Texas 75390-9135, United States;* orcid.org/0000-0001-5250-5578; Email: margaret.phillips@utsouthwestern.edu

Authors

Michael J. Palmer − *Medicines for Malaria Venture, 1215 Geneva, Switzerland*

Xiaoyi Deng − *Department of Biochemistry, University of Texas Southwestern Medical Center at Dallas, Dallas, Texas 75390-9135, United States*

Shawn Watts − *Schrodinger, Inc., New York, New York 100036-4041, United States*

Goran Krilov − *Schrodinger, Inc., New York, New York 100036-4041, United States*

Aleksey Gerasyuto − *Schrodinger, Inc., New York, New York 100036-4041, United States*

Sreekanth Kokkonda − *Departments of Chemistry and Global Health, University of Washington, Seattle, Washington 98195, United States*

Farah El Mazouni − *Department of Biochemistry, University of Texas Southwestern Medical Center at Dallas, Dallas, Texas 75390-9135, United States*

John White − *Departments of Chemistry and Global Health, University of Washington, Seattle, Washington 98195, United States*

Karen L. White − *Centre for Drug Candidate Optimisation, Monash Institute of Pharmaceutical Sciences, Monash University, Parkville, VIC 3052, Australia*

Josefine Striepen − *Department of Microbiology and Immunology, Columbia University Irving Medical Center, New York 10032, United States*

Jade Bath − *Department of Microbiology and Immunology, Columbia University Irving Medical Center, New York 10032, United States*

Kyra A. Schindler − *Department of Microbiology and Immunology, Columbia University Irving Medical Center, New York 10032, United States*

Tomas Yeo − *Department of Microbiology and Immunology, Columbia University Irving Medical Center, New York 10032, United States*

David M. Shackleford − *Centre for Drug Candidate Optimisation, Monash Institute of Pharmaceutical Sciences, Monash University, Parkville, VIC 3052, Australia*

Sachel Mok − *Department of Microbiology and Immunology, Columbia University Irving Medical Center, New York 10032, United States;* orcid.org/0000-0002-9605-0154

Ioanna Deni − *Department of Microbiology and Immunology, Columbia University Irving Medical Center, New York 10032, United States*

Aloysus Lawong − *Department of Biochemistry, University of Texas Southwestern Medical Center at Dallas, Dallas, Texas 75390-9135, United States*

Ann Huang − *Department of Biochemistry, University of Texas Southwestern Medical Center at Dallas, Dallas, Texas 75390-9135, United States*

Gong Chen − *Centre for Drug Candidate Optimisation, Monash Institute of Pharmaceutical Sciences, Monash University, Parkville, VIC 3052, Australia*

Wen Wang − *Centre for Drug Candidate Optimisation, Monash Institute of Pharmaceutical Sciences, Monash University, Parkville, VIC 3052, Australia*

Jaya Jayaseelan − *Centre for Drug Candidate Optimisation, Monash Institute of Pharmaceutical Sciences, Monash University, Parkville, VIC 3052, Australia*

Kasiram Katneni − *Centre for Drug Candidate Optimisation, Monash Institute of Pharmaceutical Sciences, Monash University, Parkville, VIC 3052, Australia*

Rahul Patil − *Centre for Drug Candidate Optimisation, Monash Institute of Pharmaceutical Sciences, Monash University, Parkville, VIC 3052, Australia*

Jessica Saunders − *Centre for Drug Candidate Optimisation, Monash Institute of Pharmaceutical Sciences, Monash University, Parkville, VIC 3052, Australia*

Shatrughan P. Shahi − *Syngene International Ltd, Bangalore 560099, India*

Rajesh Chittimalla − *Syngene International Ltd, Bangalore 560099, India*

Iñigo Angulo-Barturen − *TAD, Biscay Science and Technology Park, 48160, Bizkaia, Basque Country, Spain*

María Belén Jiménez-Díaz − *TAD, Biscay Science and Technology Park, 48160, Bizkaia, Basque Country, Spain*

Sergio Wittlin − *Swiss Tropical and Public Health Institute, 4002 Basel, Switzerland; University of Basel, 4002 Basel, Switzerland*

Patrick K. Tumwebaze − *Infectious Diseases Research Collaboration, Kampala, Uganda*

Philip J. Rosenthal − *Department of Medicine, University of California, San Francisco, California 94143, United States*

Roland A. Cooper − *Department of Natural Sciences and Mathematics, Dominican University of California, San Rafael, California 94901, United States*

Anna Caroline Campos Aguiar − *University of Sao Paulo, Sao Carlos Institute of Physics, Sáo Carlos, SP 13560-970, Brazil*

https://doi.org/10.1021/acs.jmedchem.1c00173
J. Med. Chem. 2021, 64, 6085−6136

Rafael V. C. Guido − *University of Sao Paulo, Sao Carlos Institute of Physics, Sáo Carlos, SP 13560-970, Brazil*
Dhelio B. Pereira − *Tropical Medicine Research Center of Rondonia, Porto Velho, RO 76812-329, Brazil*
Nimisha Mittal − *Department of Pediatrics, Division of Host-Microbe Systems and Therapeutics, School of Medicine, University of California San Diego, La Jolla, California 92093, United States*
Elizabeth A. Winzeler − *Department of Pediatrics, Division of Host-Microbe Systems and Therapeutics, School of Medicine, University of California San Diego, La Jolla, California 92093, United States;* orcid.org/0000-0002-4049-2113
Diana R. Tomchick − *Department of Biochemistry, University of Texas Southwestern Medical Center at Dallas, Dallas, Texas 75390-9135, United States*
Benoît Laleu − *Medicines for Malaria Venture, 1215 Geneva, Switzerland*
Jeremy N. Burrows − *Medicines for Malaria Venture, 1215 Geneva, Switzerland;* orcid.org/0000-0001-8448-6068
Pradipsinh K. Rathod − *Departments of Chemistry and Global Health, University of Washington, Seattle, Washington 98195, United States*
David A. Fidock − *Department of Microbiology and Immunology and Division of Infectious Diseases, Department of Medicine, Columbia University Irving Medical Center, New York 10032, United States*
Susan A. Charman − *Centre for Drug Candidate Optimisation, Monash Institute of Pharmaceutical Sciences, Monash University, Parkville, VIC 3052, Australia*

Complete contact information is available at: https://pubs.acs.org/10.1021/acs.jmedchem.1c00173

Author Contributions

S.W., G.K., and A.G. performed computational structure-based modeling. M.J.P., S.W., G.K., A.G., M.A.P., and S.A.C. contributed to the compound design and determination of the compound target list. M.J.P. supervised synthetic chemistry, which was carried out by S.K., S.P.S., and R.C.; M.A.P. designed and supervised enzyme kinetic analysis and structural biology was carried out by X.D., F.E.M., and A.H., with X-ray structure determination also supervised by D.T.; M.A.P. and P.K.R. supervised blood-stage parasite assays conducted by A.L. and J.W. S.A.C. supervised all ADME and PK studies carried out by K.L.W., G.C., W.W., J.J., K.K., R.P., D.M.S., and J.S.; D.F supervised the generation of new drug-resistant lines and their analysis carried out by K.S., J.S., J.B., T.Y., S.M., and I.D.; I.A.P., M.B.J.-D., and S.W. were responsible for SCID mouse efficacy studies; A.C.C.A., R.V.C.G., and D.B.P. carried out field studies in Brazil; P.K.T., P.J.R., and R.A.C. carried out field studies in Africa; N.M. an E.W. conducted *P. berghei* liver-stage studies. B.L. and J.N.B. supervised M.M.V. studies and provided chemistry advise. M.J.P., S.A.C., and M.A.P. wrote the paper, which was edited and approved by all authors.

Funding

This work was supported by funds from the United States National Institutes of Health (NIH), R01AI103947 (to M.A.P. and P.K.R.), from Medicines for Malaria Venture (M.M.V.). Schrödinger acknowledges support from the Bill & Melinda Gates Foundation (contract #26296). M.A.P. acknowledges the support of the Welch Foundation (I-1257). MAP holds the Sam G. Winstead and F. Andrew Bell Distinguished Chair in Biochemistry. P.K.R. acknowledges funding support from NIH (AI093380, AI139179, and AI089688), D.A.F. acknowledges funding support the Department of Defense (E01 W81XWH1910086) and the NIH (R01 AI109023).

Notes

The authors declare the following competing financial interest(s): B.L. and J.N.B. are employees of Medicines for Malaria Venture.

■ ACKNOWLEDGMENTS

The authors thank Suraksha Gahalawat for performing melting point and optical rotation measurements on selected compounds (UT Southwestern), Heekuk Park and Anne-Cartin Uhlemann for assistance with genome sequencing (Columbia), and Christoph Fischli for technical assistance with the SCID mouse *P. falciparum in vivo* efficacy studies (Swiss TPH). The results shown in this report are derived from work performed at the Argonne National Laboratory, Structural Biology Center at the Advanced Photon Source. PlasmoDB (Plasmodium genomics resource) was used during analysis of sequencing results during the study of drug-resistant clones.

■ ABBREVIATIONS

DHODH, dihydroorotate dehydrogenase; *Pf*, *Plasmodium falciparum*; *Pv*, *Plasmodium vivax*; *h*DHODH, human DHODH; mDHODH, mouse DHODH; rDHODH, rat DHODH; dDHODH, dog DHODH; *Pf*3D7, *P. falciparum* 3D7 parasites; *Pf*Dd2, *P. falciparum* Dd2 parasites; PG, proguanil; DSM, code name assigned to compounds from our team and stands for Dallas, Seattle, and Melbourne, reflecting the location of the three project groups on the team; ADME, absorption, distribution, metabolism, and excretion; PK, pharmacokinetics

■ REFERENCES

(1) Phillips, M. A.; Burrows, J. N.; Manyando, C.; van Huijsduijnen, R. H.; Van Voorhis, W. C.; Wells, T. N. C. Malaria. *Nat. Rev. Dis. Primers* **2017**, *3*, No. 17050.
(2) World Health Organization. World Malaria Report. https://www.who.int/teams/global-malaria-programme/reports/world-malaria-report-2020 (accessed Dec 15, 2020).
(3) White, N. J.; Pukrittayakamee, S.; Hien, T. T.; Faiz, M. A.; Mokuolu, O. A.; Dondorp, A. M. Malaria. *Lancet* **2014**, *383*, 723−735.
(4) Menard, D.; Dondorp, A. Antimalarial drug resistance: a threat to malaria elimination. *Cold Spring Harbor Perspect. Med.* **2017**, *7*, No. a025619.
(5) Tilley, L.; Straimer, J.; Gnadig, N. F.; Ralph, S. A.; Fidock, D. A. Artemisinin action and resistance in *Plasmodium falciparum*. *Trends Parasitol.* **2016**, *32*, 682−696.
(6) Xie, S. C.; Ralph, S. A.; Tilley, L. K13, the cytostome, and artemisinin resistance. *Trends Parasitol.* **2020**, *36*, 533−544.
(7) van der Pluijm, R. W.; Imwong, M.; Chau, N. H.; Hoa, N. T.; Thuy-Nhien, N. T.; Thanh, N. V.; Jittamala, P.; Hanboonkunupakarn, B.; Chutasmit, K.; Saelow, C.; Runjarern, R.; Kaewmok, W.; Tripura, R.; Peto, T. J.; Yok, S.; Suon, S.; Sreng, S.; Mao, S.; Oun, S.; Yen, S.; Amaratunga, C.; Lek, D.; Huy, R.; Dhorda, M.; Chotivanich, K.; Ashley, E. A.; Mukaka, M.; Waithira, N.; Cheah, P. Y.; Maude, R. J.; Amato, R.; Pearson, R. D.; Goncalves, S.; Jacob, C. G.; Hamilton, W. L.; Fairhurst, R. M.; Tarning, J.; Winterberg, M.; Kwiatkowski, D. P.; Pukrittayakamee, S.; Hien, T. T.; Day, N. P.; Miotto, O.; White, N. J.; Dondorp, A. M. Determinants of dihydroartemisinin-piperaquine treatment failure in *Plasmodium falciparum* malaria in Cambodia, Thailand, and Vietnam: a prospective clinical, pharmacological, and genetic study. *Lancet Infect. Dis.* **2019**, *19*, 952−961.
(8) van der Pluijm, R. W.; Tripura, R.; Hoglund, R. M.; Pyae Phyo, A.; Lek, D.; Ul Islam, A.; Anvikar, A. R.; Satpathi, P.; Satpathi, S.; Behera, P.

K.; Tripura, A.; Baidya, S.; Onyamboko, M.; Chau, N. H.; Sovann, Y.; Suon, S.; Sreng, S.; Mao, S.; Oun, S.; Yen, S.; Amaratunga, C.; Chutasmit, K.; Saelow, C.; Runcharern, R.; Kaewmok, W.; Hoa, N. T.; Thanh, N. V.; Hanboonkunupakarn, B.; Callery, J. J.; Mohanty, A. K.; Heaton, J.; Thant, M.; Gantait, K.; Ghosh, T.; Amato, R.; Pearson, R. D.; Jacob, C. G.; Goncalves, S.; Mukaka, M.; Waithira, N.; Woodrow, C. J.; Grobusch, M. P.; van Vugt, M.; Fairhurst, R. M.; Cheah, P. Y.; Peto, T. J.; von Seidlein, L.; Dhorda, M.; Maude, R. J.; Winterberg, M.; Thuy-Nhien, N. T.; Kwiatkowski, D. P.; Imwong, M.; Jittamala, P.; Lin, K.; Hlaing, T. M.; Chotivanich, K.; Huy, R.; Fanello, C.; Ashley, E.; Mayxay, M.; Newton, P. N.; Hien, T. T.; Valecha, N.; Smithuis, F.; Pukrittayakamee, S.; Faiz, A.; Miotto, O.; Tarning, J.; Day, N. P. J.; White, N. J.; Dondorp, A. M.; et al. Tracking Resistance to Artemisinin, C., Triple artemisinin-based combination therapies versus artemisinin-based combination therapies for uncomplicated *Plasmodium falciparum* malaria: a multicentre, open-label, randomised clinical trial. *Lancet* **2020**, *395*, 1345−1360.

(9) White, N. J. Triple artemisinin-containing combination anti-malarial treatments should be implemented now to delay the emergence of resistance. *Malar. J.* **2019**, *18*, No. 338.

(10) Ashton, T. D.; Devine, S. M.; Mohrle, J. J.; Laleu, B.; Burrows, J. N.; Charman, S. A.; Creek, D. J.; Sleebs, B. E. The Development process for discovery and clinical advancement of modern antimalarials. *J. Med. Chem.* **2019**, *62*, 10526−10562.

(11) Kuhen, K. L.; Chatterjee, A. K.; Rottmann, M.; Gagaring, K.; Borboa, R.; Buenviaje, J.; Chen, Z.; Francek, C.; Wu, T.; Nagle, A.; Barnes, S. W.; Plouffe, D.; Lee, M. C.; Fidock, D. A.; Graumans, W.; van de Vegte-Bolmer, M.; van Gemert, G. J.; Wirjanata, G.; Sebayang, B.; Marfurt, J.; Russell, B.; Suwanarusk, R.; Price, R. N.; Nosten, F.; Tungtaeng, A.; Gettayacamin, M.; Sattabongkot, J.; Taylor, J.; Walker, J. R.; Tully, D.; Patra, K. P.; Flannery, E. L.; Vinetz, J. M.; Renia, L.; Sauerwein, R. W.; Winzeler, E. A.; Glynne, R. J.; Diagana, T. T. KAF156 is an antimalarial clinical candidate with potential for use in prophylaxis, treatment, and prevention of disease transmission. *Antimicrob. Agents Chemother.* **2014**, *58*, 5060−5067.

(12) White, N. J.; Duong, T. T.; Uthaisin, C.; Nosten, F.; Phyo, A. P.; Hanboonkunupakarn, B.; Pukrittayakamee, S.; Jittamala, P.; Chuthasmit, K.; Cheung, M. S.; Feng, Y.; Li, R.; Magnusson, B.; Sultan, M.; Wieser, D.; Xun, X.; Zhao, R.; Diagana, T. T.; Pertel, P.; Leong, F. J. Antimalarial activity of KAF156 in falciparum and vivax Malaria. *N. Engl. J. Med.* **2016**, *375*, 1152−1160.

(13) Rottmann, M.; McNamara, C.; Yeung, B. K.; Lee, M. C.; Zou, B.; Russell, B.; Seitz, P.; Plouffe, D. M.; Dharia, N. V.; Tan, J.; Cohen, S. B.; Spencer, K. R.; Gonzalez-Paez, G. E.; Lakshminarayana, S. B.; Goh, A.; Suwanarusk, R.; Jegla, T.; Schmitt, E. K.; Beck, H. P.; Brun, R.; Nosten, F.; Renia, L.; Dartois, V.; Keller, T. H.; Fidock, D. A.; Winzeler, E. A.; Diagana, T. T. Spiroindolones, a potent compound class for the treatment of malaria. *Science* **2010**, *329*, 1175−1180.

(14) Coteron, J. M.; Marco, M.; Esquivias, J.; Deng, X.; White, K. L.; White, J.; Koltun, M.; El Mazouni, F.; Kokkonda, S.; Katneni, K.; Bhamidipati, R.; Shackleford, D. M.; Angulo-Barturen, I.; Ferrer, S. B.; Jimenez-Diaz, M. B.; Gamo, F. J.; Goldsmith, E. J.; Charman, W. N.; Bathurst, I.; Floyd, D.; Matthews, D.; Burrows, J. N.; Rathod, P. K.; Charman, S. A.; Phillips, M. A. Structure-guided lead optimization of triazolopyrimidine-ring substituents identifies potent *Plasmodium falciparum* dihydroorotate dehydrogenase inhibitors with clinical candidate potential. *J. Med. Chem.* **2011**, *54*, 5540−5561.

(15) Phillips, M. A.; Lotharius, J.; Marsh, K.; White, J.; Dayan, A.; White, K. L.; Njoroge, J. W.; El Mazouni, F.; Lao, Y.; Kokkonda, S.; Tomchick, D. R.; Deng, X.; Laird, T.; Bhatia, S. N.; March, S.; Ng, C. L.; Fidock, D. A.; Wittlin, S.; Lafuente-Monasterio, M.; Benito, F. J.; Alonso, L. M.; Martinez, M. S.; Jimenez-Diaz, M. B.; Bazaga, S. F.; Angulo-Barturen, I.; Haselden, J. N.; Louttit, J.; Cui, Y.; Sridhar, A.; Zeeman, A. M.; Kocken, C.; Sauerwein, R.; Dechering, K.; Avery, V. M.; Duffy, S.; Delves, M.; Sinden, R.; Ruecker, A.; Wickham, K. S.; Rochford, R.; Gahagen, J.; Iyer, L.; Riccio, E.; Mirsalis, J.; Bathhurst, I.; Rueckle, T.; Ding, X.; Campo, B.; Leroy, D.; Rogers, M. J.; Rathod, P. K.; Burrows, J. N.; Charman, S. A. A long-duration dihydroorotate dehydrogenase inhibitor (DSM265) for prevention and treatment of malaria. *Sci. Transl. Med.* **2015**, *7*, No. 296ra111.

(16) Paquet, T.; Le Manach, C.; Cabrera, D. G.; Younis, Y.; Henrich, P. P.; Abraham, T. S.; Lee, M. C. S.; Basak, R.; Ghidelli-Disse, S.; Lafuente-Monasterio, M. J.; Bantscheff, M.; Ruecker, A.; Blagborough, A. M.; Zakutansky, S. E.; Zeeman, A. M.; White, K. L.; Shackleford, D. M.; Mannila, J.; Morizzi, J.; Scheurer, C.; Angulo-Barturen, I.; Martinez, M. S.; Ferrer, S.; Sanz, L. M.; Gamo, F. J.; Reader, J.; Botha, M.; Dechering, K. J.; Sauerwein, R. W.; Tungtaeng, A.; Vanachayangkul, P.; Lim, C. S.; Burrows, J.; Witty, M. J.; Marsh, K. C.; Bodenreider, C.; Rochford, R.; Solapure, S. M.; Jimenez-Diaz, M. B.; Wittlin, S.; Charman, S. A.; Donini, C.; Campo, B.; Birkholtz, L. M.; Hanson, K. K.; Drewes, G.; Kocken, C. H. M.; Delves, M. J.; Leroy, D.; Fidock, D. A.; Waterson, D.; Street, L. J.; Chibale, K. Antimalarial efficacy of MMV390048, an inhibitor of Plasmodium phosphatidylinositol 4-kinase. *Sci. Transl. Med.* **2017**, *9*, No. eaad9735.

(17) Burrows, J. N.; Duparc, S.; Gutteridge, W. E.; Hooft van Huijsduijnen, R.; Kaszubska, W.; Macintyre, F.; Mazzuri, S.; Mohrle, J. J.; Wells, T. N. C. New developments in anti-malarial target candidate and product profiles. *Malar. J.* **2017**, *16*, No. 26.

(18) Lover, A. A.; Baird, J. K.; Gosling, R.; Price, R. N. Malaria Elimination: Time to Target All Species. *Am. J. Trop. Med. Hyg.* **2018**, *99*, 17−23.

(19) Haston, J. C.; Hwang, J.; Tan, K. R. Guidance for Using Tafenoquine for Prevention and Antirelapse Therapy for Malaria — United States. *MMWR. Morb. Mortal. Wkly. Rep.* **2019**, *68*, 1062−1068.

(20) Kokkonda, S.; Deng, X.; White, K. L.; El Mazouni, F.; White, J.; Shackleford, D. M.; Katneni, K.; Chiu, F. C. K.; Barker, H.; McLaren, J.; Crighton, E.; Chen, G.; Angulo-Barturen, I.; Jimenez-Diaz, M. B.; Ferrer, S.; Huertas-Valentin, L.; Martinez-Martinez, M. S.; Lafuente-Monasterio, M. J.; Chittimalla, R.; Shahi, S. P.; Wittlin, S.; Waterson, D.; Burrows, J. N.; Matthews, D.; Tomchick, D.; Rathod, P. K.; Palmer, M. J.; Charman, S. A.; Phillips, M. A. Lead optimization of a pyrrole-based dihydroorotate dehydrogenase inhibitor series for the treatment of malaria. *J. Med. Chem.* **2020**, *63*, 4929−4956.

(21) McCarthy, J. S.; Lotharius, J.; Rückle, T.; Chalon, S.; Phillips, M. A.; Elliott, S.; Sekuloski, S.; Griffin, P.; Ng, C. L.; Fidock, D. A.; Marquart, L.; Williams, N. S.; Gobeau, N.; Bebrevska, L.; Rosario, M.; Marsh, K.; Möhrle, J. J. Safety, tolerability, pharmacokinetics, and activity of the novel long-acting antimalarial DSM265: a two-part first-in-human phase 1a/1b randomised study. *Lancet Infect. Dis.* **2017**, *17*, 626−635.

(22) Llanos-Cuentas, A.; Casapia, M.; Chuquiyauri, R.; Hinojosa, J. C.; Kerr, N.; Rosario, M.; Toovey, S.; Arch, R. H.; Phillips, M. A.; Rozenberg, F. D.; Bath, J.; Ng, C. L.; Cowell, A. N.; Winzeler, E. A.; Fidock, D. A.; Baker, M.; Mohrle, J. J.; Hooft van Huijsduijnen, R.; Gobeau, N.; Araeipour, N.; Andenmatten, N.; Ruckle, T.; Duparc, S. Antimalarial activity of single-dose DSM265, a novel plasmodium dihydroorotate dehydrogenase inhibitor, in patients with uncomplicated *Plasmodium falciparum* or *Plasmodium vivax* malaria infection: a proof-of-concept, open-label, phase 2a study. *Lancet Infect. Dis.* **2018**, *18*, 874−883.

(23) Flannery, E. L.; Foquet, L.; Chuenchob, V.; Fishbaugher, M.; Billman, Z.; Navarro, M. J.; Betz, W.; Olsen, T. M.; Lee, J.; Camargo, N.; Nguyen, T.; Schafer, C.; Sack, B. K.; Wilson, E. M.; Saunders, J.; Bial, J.; Campo, B.; Charman, S. A.; Murphy, S. C.; Phillips, M. A.; Kappe, S. H.; Mikolajczak, S. A. Assessing drug efficacy against *Plasmodium falciparum* liver stages in vivo. *JCI Insight* **2018**, *3*, No. e92587.

(24) Murphy, S. C.; Duke, E. R.; Shipman, K. J.; Jensen, R. L.; Fong, Y.; Ferguson, S.; Janes, H. E.; Gillespie, K.; Seilie, A. M.; Hanron, A. E.; Rinn, L.; Fishbaugher, M.; VonGoedert, T.; Fritzen, E.; Kappe, S. H.; Chang, M.; Sousa, J. C.; Marcsisin, S. R.; Chalon, S.; Duparc, S.; Kerr, N.; Mohrle, J. J.; Andenmatten, N.; Rueckle, T.; Kublin, J. G. A Randomized Trial Evaluating the Prophylactic Activity of DSM265 against preerythrocytic *Plasmodium falciparum* infection during controlled human malarial infection by mosquito bites and direct venous inoculation. *J. Infect. Dis.* **2018**, *217*, 693−702.

(25) Sulyok, M.; Ruckle, T.; Roth, A.; Murbeth, R. E.; Chalon, S.; Kerr, N.; Samec, S. S.; Gobeau, N.; Calle, C. L.; Ibanez, J.; Sulyok, Z.;

https://doi.org/10.1021/acs.jmedchem.1c00173
J. Med. Chem. 2021, 64, 6085−6136

Held, J.; Gebru, T.; Granados, P.; Bruckner, S.; Nguetse, C.; Mengue, J.; Lalremruata, A.; Sim, B. K. L.; Hoffman, S. L.; Mohrle, J. J.; Kremsner, P. G.; Mordmuller, B. DSM265 for *Plasmodium falciparum* chemoprophylaxis: a randomised, double blinded, phase 1 trial with controlled human malaria infection. *Lancet Infect. Dis.* **2017**, *17*, 636−644.
(26) Austin, R. P.; Barton, P.; Cockroft, S. L.; Wenlock, M. C.; Riley, R. J. The influence of nonspecific microsomal binding on apparent intrinsic clearance, and its prediction from physicochemical properties. *Drug Metab. Dispos.* **2002**, *30*, 1497−1503.
(27) Smith, D. A.; Beaumont, K.; Maurer, T. S.; Di, L. Clearance in Drug Design. *J. Med. Chem.* **2019**, *62*, 2245−2255.
(28) Charman, S. A.; Andreu, A.; Barker, H.; Blundell, S.; Campbell, A.; Campbell, M.; Chen, G.; Chiu, F. C. K.; Crighton, E.; Katneni, K.; Morizzi, J.; Patil, R.; Pham, T.; Ryan, E.; Saunders, J.; Shackleford, D. M.; White, K. L.; Almond, L.; Dickins, M.; Smith, D. A.; Moehrle, J. J.; Burrows, J. N.; Abla, N. An in vitro toolbox to accelerate anti-malarial drug discovery and development. *Malar. J.* **2020**, *19*, No. 1.
(29) Di, L.; Breen, C.; Chambers, R.; Eckley, S. T.; Fricke, R.; Ghosh, A.; Harradine, P.; Kalvass, J. C.; Ho, S.; Lee, C. A.; Marathe, P.; Perkins, E. J.; Qian, M.; Tse, S.; Yan, Z.; Zamek-Gliszczynski, M. J. Industry perspective on contemporary protein-binding methodologies: considerations for regulatory drug-drug interaction and related guidelines on highly bound drugs. *J. Pharm. Sci.* **2017**, *106*, 3442−3452.
(30) Ganesan, S. M.; Morrisey, J. M.; Ke, H.; Painter, H. J.; Laroiya, K.; Phillips, M. A.; Rathod, P. K.; Mather, M. W.; Vaidya, A. B. Yeast dihydroorotate dehydrogenase as a new selectable marker for *Plasmodium falciparum* transfection. *Mol. Biochem. Parasitol.* **2011**, *177*, 29−34.
(31) Painter, H. J.; Morrisey, J. M.; Mather, M. W.; Vaidya, A. B. Specific role of mitochondrial electron transport in blood-stage *Plasmodium falciparum*. *Nature* **2007**, *446*, 88−91.
(32) Rasmussen, S. A.; Ceja, F. G.; Conrad, M. D.; Tumwebaze, P. K.; Byaruhanga, O.; Katairo, T.; Nsobya, S. L.; Rosenthal, P. J.; Cooper, R. A. Changing antimalarial drug sensitivities in uganda. *Antimicrob. Agents Chemother.* **2017**, *61*, e01516−17.
(33) Phillips, M. A.; White, K. L.; Kokkonda, S.; Deng, X.; White, J.; El Mazouni, F.; Marsh, K.; Tomchick, D. R.; Manjalanagara, K.; Rudra, K. R.; Wirjanata, G.; Noviyanti, R.; Price, R. N.; Marfurt, J.; Shackleford, D. M.; Chiu, F. C.; Campbell, M.; Jimenez-Diaz, M. B.; Bazaga, S. F.; Angulo-Barturen, I.; Martinez, M. S.; Lafuente-Monasterio, M.; Kaminsky, W.; Silue, K.; Zeeman, A. M.; Kocken, C.; Leroy, D.; Blasco, B.; Rossignol, E.; Rueckle, T.; Matthews, D.; Burrows, J. N.; Waterson, D.; Palmer, M. J.; Rathod, P. K.; Charman, S. A. A Triazolopyrimidine-based dihydroorotate dehydrogenase inhibitor with improved drug-like properties for treatment and prevention of malaria. *ACS Infect. Dis.* **2016**, *2*, 945−957.
(34) Smilkstein, M.; Sriwilaijaroen, N.; Kelly, J. X.; Wilairat, P.; Riscoe, M. Simple and inexpensive fluorescence-based technique for high-throughput antimalarial drug screening. *Antimicrob. Agents Chemother.* **2004**, *48*, 1803−1806.
(35) White, J.; Dhingra, S. K.; Deng, X.; El Mazouni, F.; Lee, M. C. S.; Afanador, G. A.; Lawong, A.; Tomchick, D. R.; Ng, C. L.; Bath, J.; Rathod, P. K.; Fidock, D. A.; Phillips, M. A. Identification and mechanistic understanding of dihydroorotate dehydrogenase point mutations in *Plasmodium falciparum* that confer in vitro resistance to the clinical candidate DSM265. *ACS Infect. Dis.* **2019**, *5*, 90−101.
(36) Mandt, R. E. K.; Lafuente-Monasterio, M. J.; Sakata-Kato, T.; Luth, M. R.; Segura, D.; Pablos-Tanarro, A.; Viera, S.; Magan, N.; Ottilie, S.; Winzeler, E. A.; Lukens, A. K.; Gamo, F. J.; Wirth, D. F. In vitro selection predicts malaria parasite resistance to dihydroorotate dehydrogenase inhibitors in a mouse infection model. *Sci. Transl. Med.* **2019**, *11*, No. eaav1636.
(37) Ross, L. S.; Gamo, F. J.; Lafuente-Monasterio, M. J.; Singh, O. M.; Rowland, P.; Wiegand, R. C.; Wirth, D. F. In vitro resistance selections for *Plasmodium falciparum* dihydroorotate dehydrogenase inhibitors give mutants with multiple point mutations in the drug-binding site and altered growth. *J. Biol. Chem.* **2014**, *289*, 17980−17995.
(38) Guler, J. L.; White, J., 3rd; Phillips, M. A.; Rathod, P. K. Atovaquone tolerance in *Plasmodium falciparum* parasites selected for high-level resistance to a dihydroorotate dehydrogenase inhibitor. *Antimicrob. Agents Chemother.* **2015**, *59*, 686−689.
(39) Guler, J. L.; Freeman, D. L.; Ahyong, V.; Patrapuvich, R.; White, J.; Gujjar, R.; Phillips, M. A.; DeRisi, J.; Rathod, P. K. Asexual populations of the human malaria parasite, *Plasmodium falciparum*, use a two-step genomic strategy to acquire accurate, beneficial DNA amplifications. *PLoS Pathog.* **2013**, *9*, No. e1003375.
(40) Painter, H. J.; Morrisey, J. M.; Mather, M. W.; Orchard, L. M.; Luck, C.; Smilkstein, M. J.; Riscoe, M. K.; Vaidya, A. B.; Llinas, M. Atypical molecular basis for drug resistance to mitochondrial function inhibitors in *Plasmodium falciparum*. *Antimicrob. Agents Chemother.* **2021**, *65*, e02143−20.
(41) Jimenez-Diaz, M. B.; Mulet, T.; Viera, S.; Gomez, V.; Garuti, H.; Ibanez, J.; Alvarez-Doval, A.; Shultz, L. D.; Martinez, A.; Gargallo-Viola, D.; Angulo-Barturen, I. Improved murine model of malaria using *Plasmodium falciparum* competent strains and non-myelodepleted NOD-scid IL2Rgammanull mice engrafted with human erythrocytes. *Antimicrob. Agents Chemother.* **2009**, *53*, 4533−4536.
(42) Hurt, D. E.; Widom, J.; Clardy, J. Structure of *Plasmodium falciparum* dihydroorotate dehydrogenase with a bound inhibitor. *Acta Crystallogr., Sect. D: Biol. Crystallogr.* **2006**, *62*, 312−323.
(43) Baldwin, J.; Farajallah, A. M.; Malmquist, N. A.; Rathod, P. K.; Phillips, M. A. Malarial dihydroorotate dehydrogenase: substrate and inhibitor specificity. *J. Biol. Chem.* **2002**, *277*, 41827−41834.
(44) Deng, X.; Kokkonda, S.; El Mazouni, F.; White, J.; Burrows, J. N.; Kaminsky, W.; Charman, S. A.; Matthews, D.; Rathod, P. K.; Phillips, M. A. Fluorine modulates species selectivity in the triazolopyrimidine class of *Plasmodium falciparum* dihydroorotate dehydrogenase inhibitors. *J. Med. Chem.* **2014**, *57*, 5381−5394.
(45) Malmquist, N. A.; Gujjar, R.; Rathod, P. K.; Phillips, M. A. Analysis of flavin oxidation and electron-transfer inhibition in *Plasmodium falciparum* dihydroorotate dehydrogenase. *Biochemistry* **2008**, *47*, 2466−2475.
(46) Bennett, T. N.; Paguio, M.; Gligorijevic, B.; Seudieu, C.; Kosar, A. D.; Davidson, E.; Roepe, P. D. Novel, rapid, and inexpensive cell-based quantification of antimalarial drug efficacy. *Antimicrob. Agents Chemother.* **2004**, *48*, 1807−1810.
(47) Ekland, E. H.; Schneider, J.; Fidock, D. A. Identifying apicoplast-targeting antimalarials using high-throughput compatible approaches. *FASEB J.* **2011**, *25*, 3583−3593.
(48) Russell, B. M.; Udomsangpetch, R.; Rieckmann, K. H.; Kotecka, B. M.; Coleman, R. E.; Sattabongkot, J. Simple in vitro assay for determining the sensitivity of Plasmodium vivax isolates from fresh human blood to antimalarials in areas where P. vivax is endemic. *Antimicrob. Agents Chemother.* **2003**, *47*, 170−173.
(49) Antonova-Koch, Y.; Meister, S.; Abraham, M.; Luth, M. R.; Ottilie, S.; Lukens, A. K.; Sakata-Kato, T.; Vanaerschot, M.; Owen, E.; Jado, J. C.; Maher, S. P.; Calla, J.; Plouffe, D.; Zhong, Y.; Chen, K.; Chaumeau, V.; Conway, A. J.; McNamara, C. W.; Ibanez, M.; Gagaring, K.; Serrano, F. N.; Eribez, K.; Taggard, C. M.; Cheung, A. L.; Lincoln, C.; Ambachew, B.; Rouillier, M.; Siegel, D.; Nosten, F.; Kyle, D. E.; Gamo, F. J.; Zhou, Y.; Llinas, M.; Fidock, D. A.; Wirth, D. F.; Burrows, J.; Campo, B.; Winzeler, E. A. Open-source discovery of chemical leads for next-generation chemoprotective antimalarials. *Science* **2018**, *362*, No. eaat9446.
(50) Ng, C. L.; Fidock, D. A. *Plasmodium falciparum* In Vitro Drug Resistance Selections and Gene Editing. *Malaria Control and Elimination*; Methods in Molecular Biology; Humana, 2019; Vol. *2013*, pp 123−140.
(51) Vanaerschot, M.; Murithi, J. M.; Pasaje, C. F. A.; Ghidelli-Disse, S.; Dwomoh, L.; Bird, M.; Spottiswoode, N.; Mittal, N.; Arendse, L. B.; Owen, E. S.; Wicht, K. J.; Siciliano, G.; Bosche, M.; Yeo, T.; Kumar, T. R. S.; Mok, S.; Carpenter, E. F.; Giddins, M. J.; Sanz, O.; Ottilie, S.; Alano, P.; Chibale, K.; Llinas, M.; Uhlemann, A. C.; Delves, M.; Tobin, A. B.; Doerig, C.; Winzeler, E. A.; Lee, M. C. S.; Niles, J. C.; Fidock, D. A. Inhibition of resistance-refractory *P. falciparum* kinase pkg delivers prophylactic, blood stage, and transmission-blocking antiplasmodial activity. *Cell Chem. Biol.* **2020**, *27*, 806−816.e8.

https://doi.org/10.1021/acs.jmedchem.1c00173
J. Med. Chem. 2021, 64, 6085−6136

(52) Booker, M. L.; Bastos, C. M.; Kramer, M. L.; Barker, R. H., Jr; Skerlj, R.; Sidhu, A. B.; Deng, X.; Celatka, C.; Cortese, J. F.; Guerrero Bravo, J. E.; Crespo Llado, K. N.; Serrano, A. E.; Angulo-Barturen, I.; Jimenez-Diaz, M. B.; Viera, S.; Garuti, H.; Wittlin, S.; Papastogiannidis, P.; Lin, J. W.; Janse, C. J.; Khan, S. M.; Duraisingh, M.; Coleman, B.; Goldsmith, E. J.; Phillips, M. A.; Munoz, B.; Wirth, D. F.; Klinger, J. D.; Wiegand, R.; Sybertz, E. Novel inhibitors of *Plasmodium falciparum* dihydroorotate dehydrogenase with anti-malarial activity in the mouse model. *J. Biol. Chem.* **2010**, *285*, 33054−33064.

(53) Deng, X.; Gujjar, R.; El Mazouni, F.; Kaminsky, W.; Malmquist, N. A.; Goldsmith, E. J.; Rathod, P. K.; Phillips, M. A. Structural plasticity of malaria dihydroorotate dehydrogenase allows selective binding of diverse chemical scaffolds. *J. Biol. Chem.* **2009**, *284*, 26999−27009.

(54) Otwinowski, Z.; Minor, W. Processing of X-ray diffraction data collected in oscillation mode. In *Methods in Enzymology*; Elsevier Inc., 1997; Vol. *276*, pp 307−326.

(55) McCoy, A.; Grosse-Kunstleve, R.; Adams, P.; Winn, M.; Storoni, L.; Read, R. Phaser crystallographic software. *J. Appl. Crystallogr.* **2007**, *40*, 658−674.

(56) Emsley, P.; Lohkamp, B.; Scott, W. G.; Cowtan, K. Features and development of Coot. *Acta Crystallogr., Sect. D: Biol. Crystallogr.* **2010**, *66*, 486−501.

(57) Adams, P.; Afonine, P.; Bunkóczi, G.; Chen, V.; Davis, I.; Echols, N.; Headd, J.; Hung, L.; Kapral, G.; Grosse-Kunstleve, R.; McCoy, A.; Moriarty, N.; Oeffner, R.; Read, R.; Richardson, D.; Richardson, J.; Terwilliger, T.; Zwart, P. PHENIX: a comprehensive Python-based system for macromolecular structure solution. *Acta Crystallogr., Sect. D: Biol. Crystallogr.* **2010**, *66*, 213−221.

(58) Chen, V. B.; Arendall, W. B.; Headd, J. J.; Keedy, D. A.; Immormino, R. M.; Kapral, G. J.; Murray, L. W.; Richardson, J. S.; Richardson, D. C. MolProbity: all-atom structure validation for macromolecular crystallography. *Acta Crystallogr., Sect. D: Biol. Crystallogr.* **2010**, *66*, 12−21.

(59) Kokkonda, S.; Deng, X.; White, K. L.; Coteron, J. M.; Marco, M.; de Las Heras, L.; White, J.; El Mazouni, F.; Tomchick, D. R.; Manjalanagara, K.; Rudra, K. R.; Chen, G.; Morizzi, J.; Ryan, E.; Kaminsky, W.; Leroy, D.; Martinez-Martinez, M. S.; Jimenez-Diaz, M. B.; Bazaga, S. F.; Angulo-Barturen, I.; Waterson, D.; Burrows, J. N.; Matthews, D.; Charman, S. A.; Phillips, M. A.; Rathod, P. K. Tetrahydro-2-naphthyl and 2-indanyl triazolopyrimidines targeting *Plasmodium falciparum* dihydroorotate dehydrogenase display potent and selective antimalarial activity. *J. Med. Chem.* **2016**, *59*, 5416−5431.

(60) Abel, R.; Wang, L.; Harder, E. D.; Berne, B. J.; Friesner, R. A. Advancing Drug Discovery through Enhanced Free Energy Calculations. *Acc. Chem. Res.* **2017**, *50*, 1625−1632.

(61) Abel, R.; Young, T.; Farid, R.; Berne, B. J.; Friesner, R. A. Role of the active-site solvent in the thermodynamics of factor Xa ligand binding. *J. Am. Chem. Soc.* **2008**, *130*, 2817−2831.

(62) Young, T.; Abel, R.; Kim, B.; Berne, B. J.; Friesner, R. A. Motifs for molecular recognition exploiting hydrophobic enclosure in protein-ligand binding. *Proc. Natl. Acad. Sci. U.S.A.* **2007**, *104*, 808−813.

(63) Murphy, R. B.; Repasky, M. P.; Greenwood, J. R.; Tubert-Brohman, I.; Jerome, S.; Annabhimoju, R.; Boyles, N. A.; Schmitz, C. D.; Abel, R.; Farid, R.; Friesner, R. A. WScore: a flexible and accurate treatment of explicit water molecules in ligand-receptor docking. *J. Med. Chem.* **2016**, *59*, 4364−4384.

(64) Repasky, M. P.; Murphy, R. B.; Banks, J. L.; Greenwood, J. R.; Tubert-Brohman, I.; Bhat, S.; Friesner, R. A. Docking performance of the glide program as evaluated on the Astex and DUD datasets: a complete set of glide SP results and selected results for a new scoring function integrating WaterMap and glide. *J. Comput.-Aided Mol. Des.* **2012**, *26*, 787−799.

(65) Chen, W.; Deng, Y.; Russell, E.; Wu, Y.; Abel, R.; Wang, L. Accurate calculation of relative binding free energies between ligands with different net charges. *J. Chem. Theory Comput.* **2018**, *14*, 6346−6358.

(66) Steinbrecher, T. B.; Dahlgren, M.; Cappel, D.; Lin, T.; Wang, L.; Krilov, G.; Abel, R.; Friesner, R.; Sherman, W. Accurate binding free energy predictions in fragment optimization. *J. Chem. Inf. Model.* **2015**, *55*, 2411−2420.

(67) Wang, L.; Berne, B. J. Efficient sampling of puckering states of monosaccharides through replica exchange with solute tempering and bond softening. *J. Chem. Phys.* **2018**, *149*, No. 072306.

(68) Harder, E.; Damm, W.; Maple, J.; Wu, C.; Reboul, M.; Xiang, J. Y.; Wang, L.; Lupyan, D.; Dahlgren, M. K.; Knight, J. L.; Kaus, J. W.; Cerutti, D. S.; Krilov, G.; Jorgensen, W. L.; Abel, R.; Friesner, R. A. OPLS3: A force field providing broad coverage of drug-like small molecules and proteins. *J. Chem. Theory Comput.* **2016**, *12*, 281−296.

(69) Roos, K.; Wu, C.; Damm, W.; Reboul, M.; Stevenson, J. M.; Lu, C.; Dahlgren, M. K.; Mondal, S.; Chen, W.; Wang, L.; Abel, R.; Friesner, R. A.; Harder, E. D. OPLS3e: Extending force field coverage for drug-like small molecules. *J. Chem. Theory Comput.* **2019**, *15*, 1863−1874.

(70) Wang, L.; Wu, Y.; Deng, Y.; Kim, B.; Pierce, L.; Krilov, G.; Lupyan, D.; Robinson, S.; Dahlgren, M. K.; Greenwood, J.; Romero, D. L.; Masse, C.; Knight, J. L.; Steinbrecher, T.; Beuming, T.; Damm, W.; Harder, E.; Sherman, W.; Brewer, M.; Wester, R.; Murcko, M.; Frye, L.; Farid, R.; Lin, T.; Mobley, D. L.; Jorgensen, W. L.; Berne, B. J.; Friesner, R. A.; Abel, R. Accurate and reliable prediction of relative ligand binding potency in prospective drug discovery by way of a modern free-energy calculation protocol and force field. *J. Am. Chem. Soc.* **2015**, *137*, 2695−2703.

(71) Bowers, K. J.; Chow, E.; Xu, H.; Dror, R. O.; Eastwood, M. P.; Gregersen, B. A.; Klepeis, J. L.; Kolossvary, I.; Moraes, M. A.; Sacerdoti, F. D.; Salmon, J. K.; Shan, Y.; Shaw, D. E. In *Scalable Algorithms for Molecular Dynamics Simulations on Commodity Clusters*, Proceedings of the ACM/IEEE Conference on Supercomputing (SC06), Tampa, Florida, 2006.

(72) Jiménez-Díaz, M. B.; Mulet, T.; Gomez, V.; Viera, S.; Alvarez, A.; Garuti, H.; Vazquez, Y.; Fernandez, A.; Ibanez, J.; Jimenez, M.; Gargallo-Viola, D.; Angulo-Barturen, I. Quantitative measurement of Plasmodium-infected erythrocytes in murine models of malaria by flow cytometry using bidimensional assessment of SYTO-16 fluorescence. *Cytometry, Part A* **2009**, *75A*, 225−235.

(73) Jiménez-Díaz, M. B.; Viera, S.; Ibanez, J.; Mulet, T.; Magan-Marchal, N.; Garuti, H.; Gomez, V.; Cortes-Gil, L.; Martinez, A.; Ferrer, S.; Fraile, M. T.; Calderon, F.; Fernandez, E.; Shultz, L. D.; Leroy, D.; Wilson, D. M.; Garcia-Bustos, J. F.; Gamo, F. J.; Angulo-Barturen, I. A new in vivo screening paradigm to accelerate antimalarial drug discovery. *PLoS One* **2013**, *8*, No. e66967.

(74) Nara, H.; Kaieda, A.; Sato, K.; Naito, T.; Mototani, H.; Oki, H.; Yamamoto, Y.; Kuno, H.; Santou, T.; Kanzaki, N.; Terauchi, J.; Uchikawa, O.; Kori, M. Discovery of novel, highly potent, and selective matrix metalloproteinase (mmp)-13 inhibitors with a 1,2,4-triazol-3-yl moiety as a zinc binding group using a structure-based design approach. *J. Med. Chem.* **2017**, *60*, 608−626.

(75) Kanaya, N. I. T.; Muto, R.; Watanabe, T.; Ochiai, Y. Preparation of 1-(3-pyridyl or 3-pyridazinyl)-5-heterocyclylpyrazole derivatives as platelet aggregation inhibitors. WO2006014005 20060209A1, 2006.

https://doi.org/10.1021/acs.jmedchem.1c00173
J. Med. Chem. 2021, 64, 6085−6136